Development of Methodologies for Improving Thermal Stability of Plant Fibers for Application in Thermoplastic Composites

by

Diogenes Ricardo Lumertz Vedoy

A thesis

presented to the University of Waterloo

in fulfillment of the

thesis requirement for the degree of

Doctor of Philosophy

in

Chemical Engineering

Waterloo, Ontario, Canada, 2012

Author's Declaration

I hereby declare that I am the sole author of this thesis. This is a true copy of the thesis, including any required final revisions, as accepted by my examiners.

I understand that my thesis may be made electronically available to the public.

Abstract

Thermal degradation during composite fabrication is the main impediment for the wide use of agro-based fibers as filler and reinforcement in engineering thermoplastic composites.

Different thermal, chemical and physical techniques (e.g., alkali, steam explosion and retting) aiming to increase the fiber-matrix adhesion or reduce the plant fibers water absorption have been presented in the literature. However, there have been very few attempts to solve the difficulties associated with processing engineering thermoplastics with plant fibers.

Most of these attempts involved the use of additives (such as plasticizers and salts) to lower the polymers processing temperature and plant fibers with inherent higher thermal stability (such as Curaua and cellulose). Despite all these efforts, no important progress has been achieved.

Therefore, to explore the full potential of wheat straw and expand its use in commercial applications, an experimental study was carried out to develop different methodologies to improve the thermal stability of wheat straw fiber. In this thesis, most attention is given to wheat straw because of the relevance and potential of entering the market as commercial filler today.

It is reported here that the thermal stability and chemical composition of wheat straw do not seem to significantly vary with wheat straw type and cultivation region. For example, the main thermal degradation of wheat straw samples starts in a narrow window of temperature which goes from 220.8 to 237.8 °C and from 224.8 to 238.1 °C for air and nitrogen atmospheres, respectively. On the other hand, lignin and inorganic materials are the wheat straw components with the highest relative variation.

In addition, it is showed here that silane modification is an efficient method to increase the temperature of degradation of wheat straw. The highest improvements were achieved with chlorosilane modifiers and combinations of alkoxysilane and chlorosilane modifiers.

In fact, the silane treated samples have lower thermal degradation during the fabrication of composites with polyamide-6. It is observed here that the extruded and injection molded composites containing silane treated wheat straw samples have significant smaller thermal degradation than those utilizing untreated wheat straw samples. Equally important, it seems that the mechanical properties of the composites are not affected by the addition of silane treated samples in comparison with untreated wheat straw.

In addition, another efficient treatment method is presented in this thesis. This method employs ultraviolet light to modify and improve the thermal stability of wheat straw. This method offers important economical and environmental benefits. Significant improvements (e.g., 40 ºC increase on the temperature at 2% of weight loss) were achieved after treatment for short periods of time (up to 15 minutes) and without the use of any pre-treatment or production of toxic by-products. This treatment method represents a novel application for ultraviolet light with potential for industrial use.

Acknowledgements

First, my sincere gratitude to my supervisor, Dr. Leonardo C. Simon, for giving me the opportunity to start my PhD studies, and for all his assistance and guidance along the way.

I would also like to thank to Dr. Ting Tsui for his fruitful collaboration and discussions in this research project, and to my committee members Dr. David Potter, Dr. Elizabeth Weckman, Dr.Ting Tsui, and Dr. Ali Elkamel for taking the time to read my thesis, and their valuable comments and suggestions.

This project would not have been possible without the financial support provided by the Ontario BioCar Initiative (ORF-MRI) grant for which I am very grateful. Thanks to our industrial partners, Ford Motors Company, A. Schulman Inc. and Omtec Inc for their collaboration and in-kind donations.

Special thanks to all my friends for making this journey more enjoyable. I am grateful to Dr. Ravindra Reddy, and Dr. Sang-Young Anthony Shin for all their valuable assistance and very constructive discussions.

Last but not least, I am extremely grateful and blessed for the encouragement and support of my parents Natalicio and Luzia, and my sister Marcia, along my entire life. To my wife and my love, Jazmin. Thanks for your support and for keeping me strong during the difficult hours. Finally, thanks to God for my little angel Laurita, whose shining eyes and big cheeks ("*bochechuda*") keep me happy and going every day.

Dedication

To my parents, Natalicio and Luzia Vedoy.

Table of Contents

List of Figures

List of Tables

Chapter 1 - Introduction

1.1 Motivation

The use of plant fibers as filler and reinforcement materials for thermoplastic composites has attracted considerable attention in different industries such as automotive, construction and packaging. Several plant fibers such as wood, hemp, kenaf, flax jute, oil palm, bamboo, wheat straw and sisal have been investigated for thermoplastic composites.

Most of these fibers have high specific properties (i.e., the ratio of mechanical properties per mass) and low density when compared to glass fiber or other mineral filler that have reinforcing attributes (like talc, mica or wollastonite for example). Therefore, plant fibers are excellent candidates to reduce the weight of thermoplastic composites by replacing glass fiber or mineral fillers. In addition, they are non-toxic, non-abrasive, annually renewable and recyclable.

Contrary to plant fibers cultivated specifically (dedicated) for use in composites, the fibers derived as a by-product of other agricultural activities (also referred to as agro-based fibers) offer additional economical and environmental benefits. Because the original plant was cultivated for food, agro-based fibers such as wheat straw, soy stalk and rice husk do not cause any extra environmental impact associated with cultivation. As another consequence of being agricultural residues or by-products, these agro-based fibers are relatively inexpensive, annually renewable, recyclable and available in abundant quantity in many regions of the world where agriculture is a major economical activity.

Great success has been achieved in compounding wheat straw with thermoplastics that require low processing temperatures such as polypropylene (Hornsby et al., 1997; Panthapulakkal and Sain, 2007; Panthapulakkal et al., 2006; Panthapulakkal and Sain, 2006; Reddy et al., 2010). Due to the contribution of many researchers (Erickson, L.; Fatoni, R.; Kruger, P; Lee, E.; Golbabaie, M.; Ng, Z.; Sardashti, A.; Simon, L.), problems regarding fiber-matrix compatibility have been overcome allowing the utilization of this composite material in automotive products such as the quarter trim bin in the Ford Flex vehicle model 2010 (Media.Ford, 2009).

Despite all this progress, there are some important limitations preventing the exploration of the full potential of the agro-based fibers in thermoplastic composites. Most of the chemical components of wheat straw or any agro-based fibers start to degrade at 200 °C and therefore, these fibers can suffer

severe thermal degradation especially in the case of exposure to the temperatures required to process engineering thermoplastics (temperatures above 220 °C).

Thus, in order to extend the use of wheat straw fiber to other polymers with higher processing temperatures, the lower thermal stability of this agro-based fiber has to be addressed. The major challenge is to create methodologies which can enhance the thermal stability of the wheat straw fiber.

There have been few attempts aimed towards solving the limitations related to processing engineering thermoplastics (such as polyamide-6) with plant fibers (Amintowlieh, Y., 2010; Xu, X., 2008). These attempts have tackled the problem using two main approaches which focus either on the polymer or the fiber.

For one side, researchers have tried to lower the processing temperature of the polymer usually through addition of additives (e.g., plasticizers, salts). The main drawbacks of this approach include the decrease in the composite's mechanical properties and processing difficulties due to the change in the polymer's viscosity.

On the other hand, plant fibers with naturally higher thermal stability such as Curaua and cellulose fibers have been employed in the fabrication of engineering thermoplastics composites (Santos et al., 2007; Xu, X., 2008). Despite the higher thermal stability of these fibers, the results were not promising. Significant thermal degradation occurred during the composite production.

To the best of our knowledge, none of the works in the literature have focused on enhancing the thermal stability of wheat straw. This motivates the current project with the following specific objectives:

1.2 Objectives

1) Provide better understanding of the thermal degradation of wheat straw fiber.
2) Develop methodologies for preparation of wheat straw fiber with enhanced thermal stability.
3) Create knowledge to extend the use of agro-based fibers to engineering thermoplastics.

In order to meet these objectives, this thesis is organized as follows.

1.3 Document Review

In Chapter 2 (Literature Review) relevant works presented in the literature that will support and justify this research are introduced. In this chapter are also described the chemical and structural composition of some plant fibers as well the main methods employed to modify these fibers.

Chapter 3 (Understanding the Thermal Degradation and Chemical Kinetics of Wheat Straw Fiber) provides a better understanding of the thermal degradation of wheat straw under non-isothermal and isothermal conditions utilizing air and nitrogen atmospheres. In this chapter, the thermal stability of several wheat straw samples from different regions is evaluated with the assistance of thermogravimetry analysis (TGA). This study is part of the first main objective of this project.

The second objective and major goal of this thesis, (enhance the thermal stability of wheat straw) is pursued in Chapters 4, 5, and 7.

The performance of all these methodologies developed here is evaluated using parameters ($T_{2\%}$ and Wt250 under air and nitrogen) obtained from TGA analysis. These parameters allow the identification and selection of straw fibers with superior thermal stability For example, Wt250 estimates the residence time, that is, the time that the wheat straw fiber would remain at high temperature inside of an extruder or injection moulding machines during the production of medium or large automotive components (with more than 3 lbs).

In Chapter 4 (Thermochemical Modification of the Wheat Straw Fiber) different thermochemical treatments are applied to wheat straw fiber to improve its thermal stability. The effect of several variables such as time, temperature, and use of pretreatment is evaluated in this chapter.

The second method to enhance the thermal stability of wheat straw is presented in Chapter 5 (Development of Methodology for Silane Modification). This method is based on silane modification. A comprehensive study including different chlorosilane and alkoxysilane modifiers as well as different sets of reaction conditions (e.g., type of solvent, combination of solvents, pH and pre-hydrolysis of silane solution) is carried out in this chapter. The performance of the silane treatment is evaluated with the use of TGA and amount of grafted silane.

In Chapter 6 (Wheat Straw Fiber/Polyamide-6 Composites), the ultimate reason for improving the thermal stability, which is being able to compound wheat straw with engineering thermoplastics, is

explored (third objective of this thesis). This chapter also attempts to evaluate if wheat straw with enhanced thermal stability will suffer less thermal degradation during the compounding process. For that, the thermal stability and the mechanical properties of the silane treated wheat straw/polyamide-6 composites are evaluated.

Chapter 7 (Novel Use of Ultraviolet Irradiation to Improve the Thermal Stability of the Wheat Straw Fiber) presents the third method to enhance the thermal stability. This method relies on the exposure to ultraviolet light during different periods of time to modify the straw fiber. To the best of our knowledge, this is a novel use of ultraviolet light. Chemical composition and FTIR characterization are used here in an attempt to explain the modification caused to the UV treated wheat straw.

Finally, Chapter 8 (Concluding Remarks, Main Contributions and Future Work) presents the concluding remarks, main contributions and recommendations for future work.

Chapter 2 - Literature Review

This chapter presents relevant work regarding the chemical and structural composition of plant fibers as well as the most common methods employed to modify these fibers.

2.1 Chemical Composition of Plant Fibers

The three major components of plant fibers are cellulose (38-50 %), hemicellulose (17-32 %) and lignin (15-30 %). Other components are pectin and inorganic matter, especially silica (Kiran, 1986). The amount of these components in the plant fiber can alter depending on the growing conditions, age and type of the fiber. Different parts of the same plant might have different composition. The percentage of each one of these components and the way they are arranged determine the thermal and physical properties of plant fibers. The importance of knowledge of the chemical composition of these fibers lies in the fact that thermal and physical properties of plant fibers are determined by the chemical composition. For example, it is widely recognized that the presence of hemicellulose, and especially lignin, lead to low thermal stability of the agro-based fibers (Hornsby[1], 1997).

Wheat straw consists of 34-40 % of cellulose, 30-35 % of hemicellulose and 14-15 % of lignin according to Lawther et al. (1996) and Sun et al. (1998). In another study, White and Ansell (1983) reported that the cellulose, hemicellulose and lignin contents of wheat straw were 56.7 %, 28.4 % and 16.6 %, respectively.

The wheat straw stalk consists of sections of stems connected by hard bulbous areas, termed nodes. It can be seen from Figure 1 and Figure 2 that the stem of wheat straw has three different structures: an outer layer, a cellular inner region and a central void. The outer layer or epidermis has its external surface covered by silica and it is comprised of great amounts of cellulose fibrils linked together by lignin. The covering of silica preserves the living cell, while the cellulose rich epidermis is responsible for the stiffness of the straw stalk. In the internal surface of epidermis, between the epidermis and the parenchyma, there is a layer of lignin.

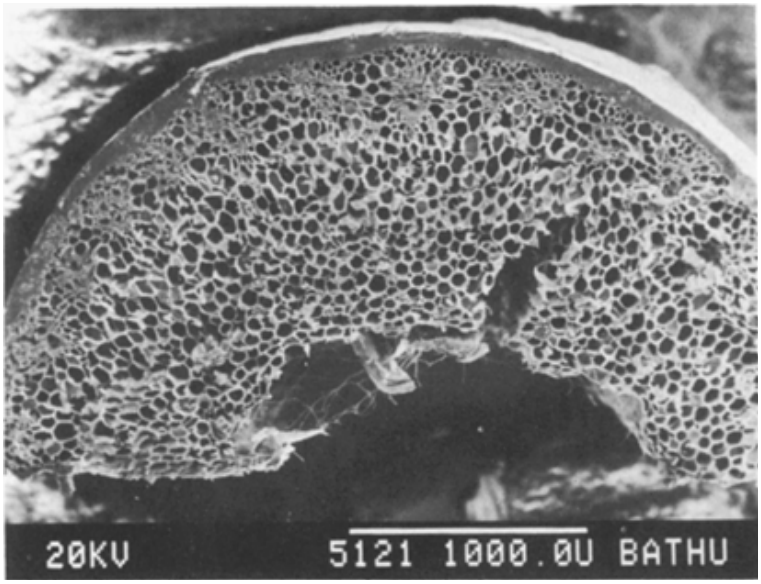

Figure 1: Cross-section of wheat straw stem (White and Ansell, 1983).

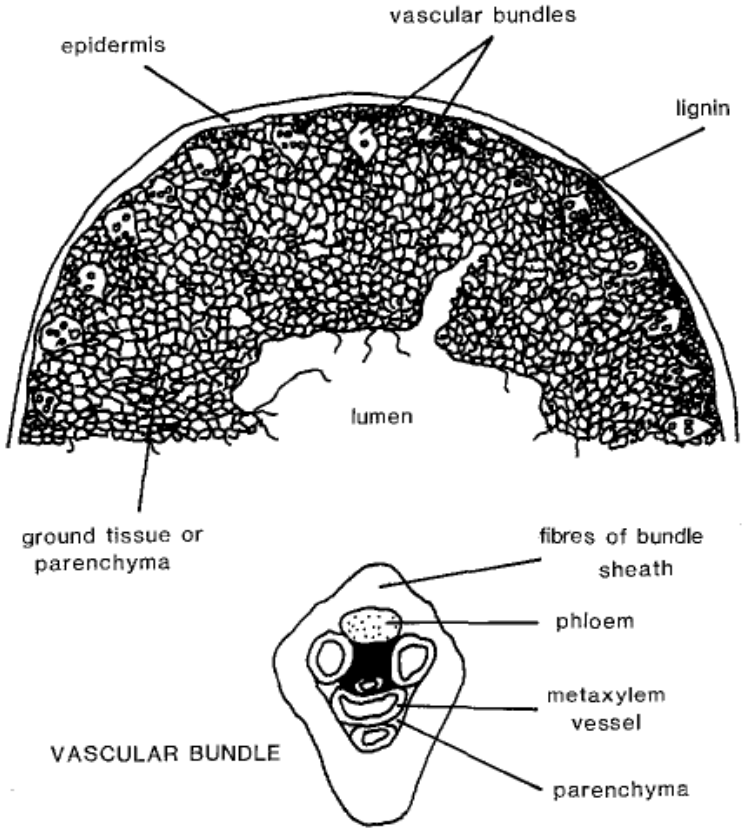

Figure 2: Schematic diagram of the structure of wheat straw (White, and Ansell, 1983).

The cellular inner region has two distinct structures: the ground tissue or parenchyma and the vascular bundles or sclerenchyma. The parenchyma is composed of living cells capable of cell division with thin and flexible cell walls. These cells have different forms depending on their attributes and location in the plant. The main functions of the parenchyma are related to the synthesis and storage of organic food and to gaseous exchange. In contrast, the cells of sclerenchyma tissue have hard and thick walls responsible for the strengthening and the supporting of the plant parts that have ceased elongation. The vascular bundle accounts for about 30 % of the volume occupied by the cellular inner region (Hornsby[1], 1997; Liu et al., 2005; White and Ansell, 1983). It can be seen in Figure 3 that these vascular bundles have cylindrical shape resembling annular rings. They act like a conducting system for transport of water and synthesized organic nutrients.

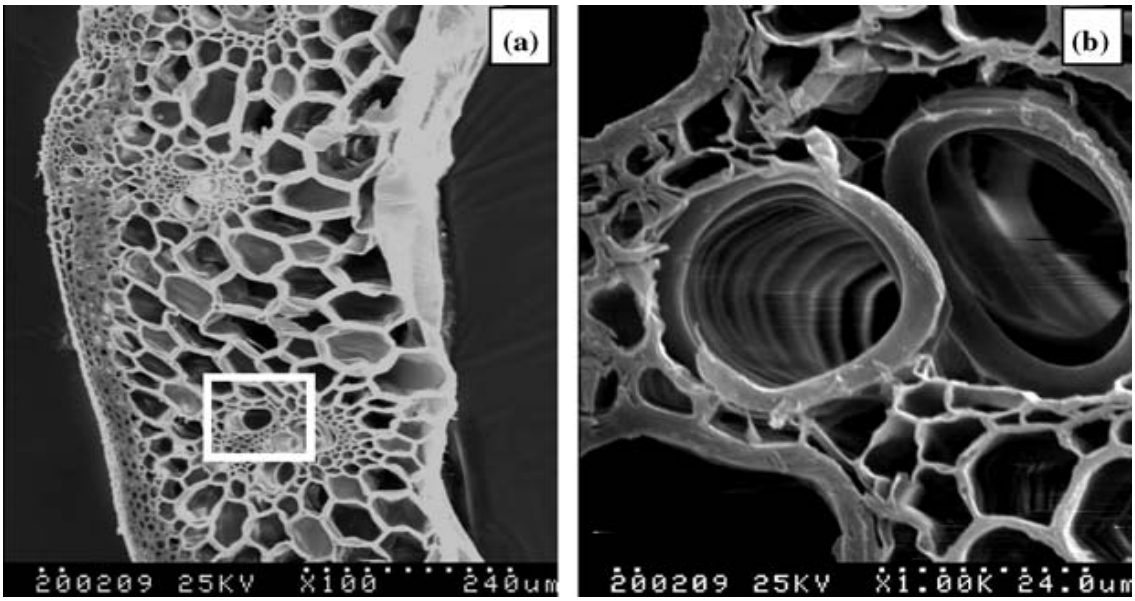

Figure 3: SEM photograph of cross section of wheat straw untreated (Liu et al., 2005).

Liu et al. (2005) studied wheat straw harvested in China. It was found that the amount of silica on the outer surface of the epidermis was about 1 %. After the extraction of lignin and hemicellulose, the authors concluded that the crystallinity of the cellulose obtained from different parts of the wheat straw (leaf sheath, epidermis, parenchyma or node) was similar, see Table 1. That paper further stated

that wheat straw had only the cellulose type I allomorph in the stable cellulose I_β polymorphic crystal structure.

Table 1: Crystallinity index of cellulose from different parts of wheat straw (adapted from Liu et al., 2005).

Sample	Crystallinity
Leaf sheath	47.4
Epidermis	44.4
Parenchyma	44.3
Node	43.2
Hydrolyzed for 10 h	77.2

Hemp fibers are comprised of 67 to 78 % of cellulose, 5.5 to 16.1 % of hemicellulose, and 2.9 to 3.3 % of lignin, 0.8 to 2.5 % of pectin and some fats and waxes. The variation on the amount of each one of these constituents is caused by the species and the test method used (Wang et al., 2003). For example, Mwaikambo and Ansell described the chemical composition of hemp to be 74 % of cellulose, 18% of hemicellulose, only 4 % of lignin and 1 % of pectin (Mwaikambo and Ansell, 2002). However, Feng et al. (2008) reported a different composition for hemp bast fibers obtained from China: 58.17 % of cellulose, 18.16 % of hemicellulose, 6.21 % of lignin, 6.56 % of pectin, 8.24 % of water soluble matter, and 2.66 % of wax. The cellulose is the major constituent of the cell wall structure and it is bonded together by pectin and lignin that are abundant in the primary and secondary wall, respectively, and middle lamella. The hemp bast stalk consists of sections of stems connected by hard bulbous areas, termed nodes. It can be seen from Figure 4 that the stem of hemp has a structure arrangement similar to wheat straw with three different regions: an outer layer, a cellular inner region and a central void.

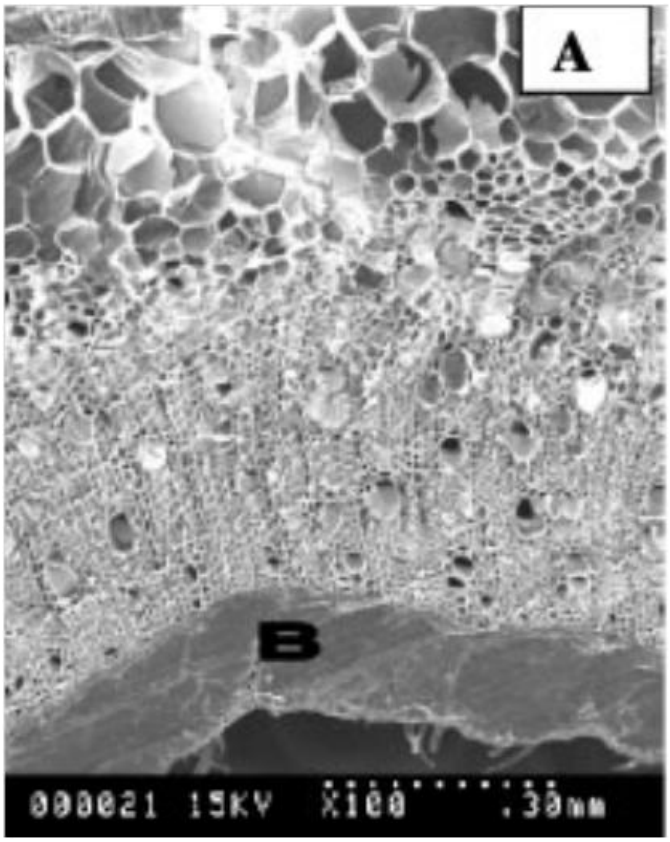

Figure 4: SEM micrograph of hemp stem and (Prasad et al., 2004)

Soybean stem is comprised of 40 % of α-cellulose, 20 % of hemicellulose and 20 % of lignin as reported by Wang and Sain (2007); whereas, Reddy and Yang (2009) found that soybean stem are made up of 44 to 83 % of cellulose, 5 to 14 % of lignin and the remaining composition being hemicellulose. About 90 % of the soybean plant consists of stem material, while the other 10 % corresponds to soy seed.

2.1.1 Lignocellulose

The word lignocellulose designates the structure formed by the association of cellulose, hemicellulose and lignin. In the plant cell wall these three components create a natural composite. In the cell wall long linear chains of cellulose bundled together in a cablelike shape are surrounded by a

matrix of hemicellulose through covalent bonds. Similarly, hemicellulose has a rodlike structure that facilitates a tight assembling with cellulose. Lignin is connected to hemicellulose and cellulose through hydrogen bonds and acts like glue binding together the lignocellulose components. In contrast to Figure 5 (a), Figure 5 (b) clearly depicts the helical fibril of cellulose after removal of the matrix of hemicellulose and lignin.

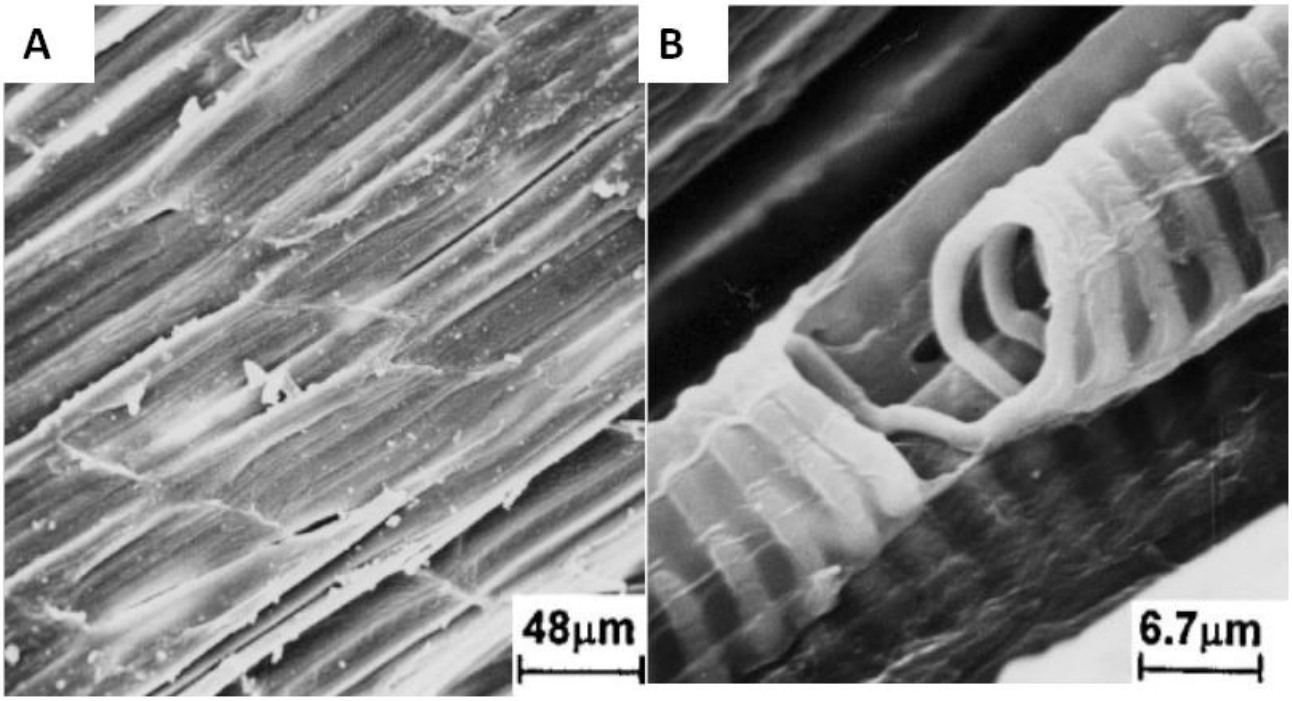

Figure 5: (a) Untreated and (b) alkali treated sisal fiber (adapted from Rong et al., 2001).

The typical length of the repeating unit of the cellulose backbone is 1 nm. The association of several of these basic structural units forms a single elementary fibril (yellow linear structure in the Figure 6) with an average thickness of 3.5 nm and several of these elementary fibrils bundled together will create the cellulose crystallites. A thread-like structure with a typical thickness of 25 nm is obtained by covering four of these cellulose crystallites with a monolayer of hemicellulose, as illustrated in Figure 6 by the yellow and blue structures (Ramos, 2003; Mwaikambo and Ansell, 2002). The result of assembling these complex structures together is a semi-rigid cell wall that

performs a series of functions such as protection against insect invasion, resistance to internal and/or external pressure and regulation of flux of substance between the cell and the environment.

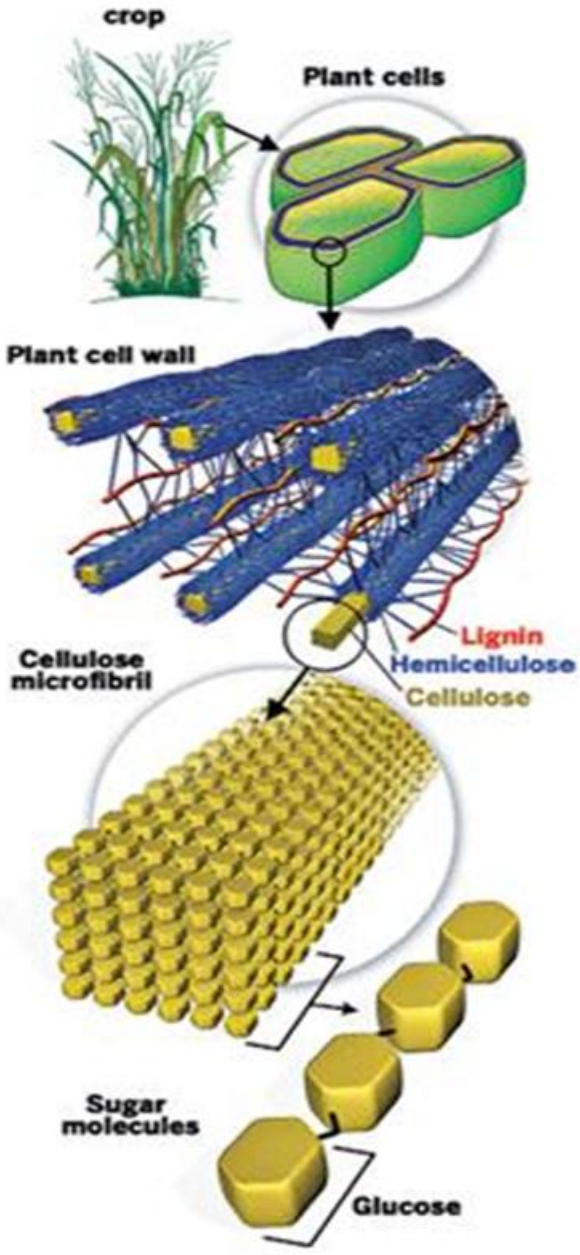

Figure 6: Structure of the cell wall of crop (Adapted from CEN-Chemical and Engineering News, 2008).

2.1.2 Cellulose

Cellulose is a linear and unbranched polysaccharide consisting of a long chain of D-glucopyranose (anhydroglucose) units linked together by β-1,4 bonds (Figure 7). The number of repeating units in a polymer chain of cellulose varies from several hundreds to more than 10,000. Each building block of cellulose presents three hydroxyl groups who are responsible for the lattice forces that keep the crystalline regions. Whereas two of these hydroxyl groups are responsible for the formation of intermolecular hydrogen bonds, the third one forms intramolecular hydrogen bonds (Preston, 1986; Bogan and Brewer, 2002).

During the thermal decomposition of cellulose, various products such as levoglucosan, water, carbon dioxide, carbon monoxide and volatile saturated hydrocarbons are formed (Hornsby[1], 1997). In accordance with that, Yang[1] et al. (2007) found that CO, CO_2, CH_4 and some organics (mixture of acids, aldehydes, alkanes and ethers) are the main gas products evolved during the TGA pyrolysis of cellulose. The authors reported that cellulose suffers an endothermic degradation in the range of temperature between 315 and 400 °C; whereas, Hornsby[1] (1997) argues that α-cellulose starts to thermally decompose around 250 and 300 °C under air and nitrogen atmosphere, respectively.

In comparison with lignin and hemicellulose, the liberation of CO_2 during pyrolysis of cellulose was small, starting at 300 °C. This result is expected, since formation of CO_2 is mainly caused by modification of functional groups such as carboxyl (C=O) and COOH; and these groups are not extensively present in the cellulose structure. In the same way, the decomposition of cellulose into CO was negligible with a small peak at 380 °C. In contrast, cellulose was greatly converted into organic compounds (C=O, C-O-C, etc) between 300 and 450 °C. This is explained by the fact that cellulose structure displayed a high content of OH and C-O organic compounds (Yang[1] et al., 2007).

The cellulose content, degree of polymerization and crystallinity are some of the factors that affect the physical properties of plant fibers. These chemical factors are mostly determined by conditions during growth of the plant and variety of the plant.

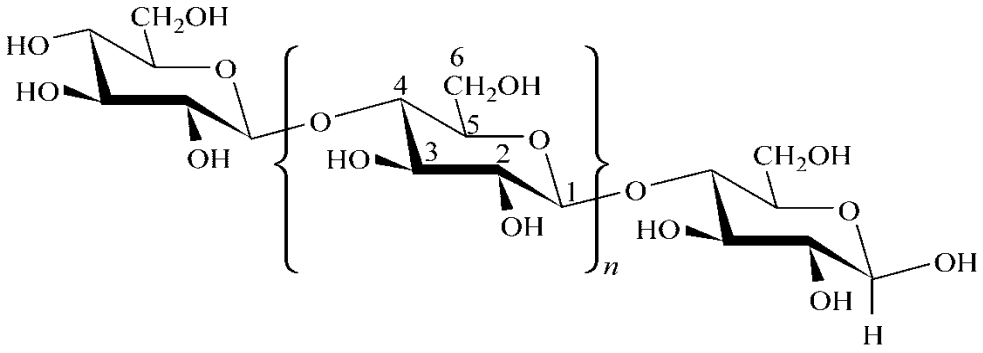

Figure 7: Structure of natural cellulose (Bogan and Brewer, 2002, Encyclopedia of Polymer Science and Technology).

2.1.3 Hemicellulose

Hemicelluloses are fully amorphous and formed by different building blocks in contrast to cellulose. These building blocks include pentoses (xylose, rhamnose and arabinose), hexoses (glucose, mannose and galactose) and uronic acids (Figure 8). Xylose is the major constituent of the backbone of many hemicelluloses, while arabinose and mannose are found in the branch of the chain (Figure 9). Hemicellulose has short chains usually containing 500 to 3,000 monomer units and thus has a significantly lower molecular weight than cellulose.

Hemicelluloses are hydrophilic and suffer exothermal degradation at 220-315 °C. The presence of pentosans makes hemicelluloses less stable than cellulose and favors degradation through hydrolysis and dehydration reactions. These reactions occur in range of temperature from 200 to around 260 °C and are the main mechanism responsible for thermal degradation of hemicelluloses. Rachini et al. (2009) reported that thermal degradation of hemicellulose present in hemp fibers started at 260 °C and 220 °C under argon and air, respectively. In agreement with that, Feng et al. (2008) describes that the first decomposition stage of hemp fibers occurred in the interval of temperature between 200 °C and 270 °C through depolymerization of hemicellulose with a mass loss of 3.33 %. In another study, Sun et al. (2002) investigated how the method of extraction affects the physiochemical properties of the hemicellulose obtained from wheat

straw. The first step of decomposition happens from 90 to 150 °C and is attributed to water evaporation. The second step starts at around 230 °C, where the weight loss was 10 %. The authors suggested that depolymerization of short chains of the hemicellulose occurred during this stage of degradation and the temperature of degradation of the hemicellulose is directly proportional to the molecular weight of the polymer.

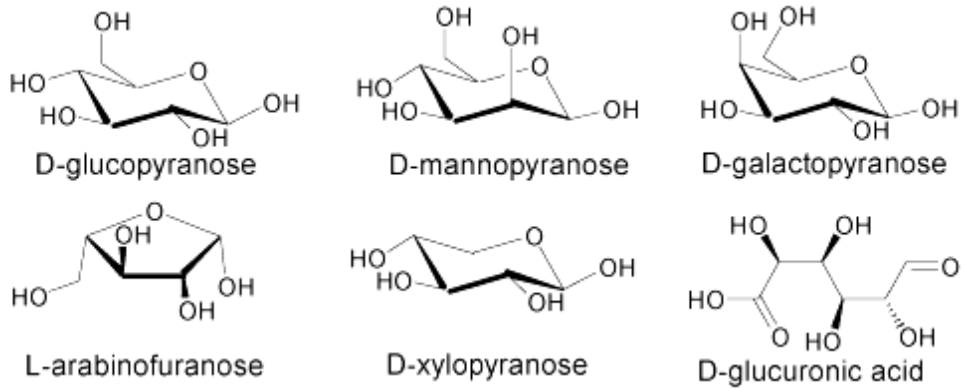

Figure 8: Main constituents of hemicelluloses (Hansen and Plackett, 2008).

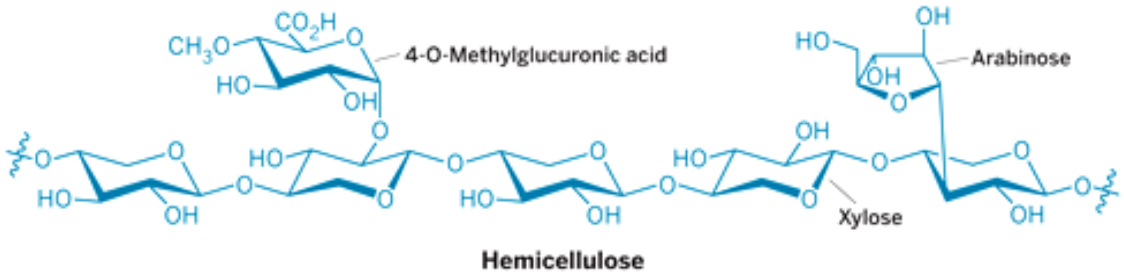

Figure 9: Structural arrangement of the main constituents of hemicelluloses (Adapted from CEN-Chemical and Engineering News, 2008).

2.1.4 Lignin

Lignin is a natural copolymer with a complex structure. The lignin macromolecule contains a variety of functional groups; the mostly common are methoxyl groups, phenolic hydroxyl groups, and

few terminal aldehyde groups. Table 2 presents the frequency of some common functional groups found in lignin.

Table 2: Functional groups in softwood lignin per 100 phenyl propane units.

Functional Group	Abundance per 100 C9 units
Carbonyl	10-15
Benzyl alcohol	15-20
Phenolic hydroxyl (free)	15-30
Methoxyl	92-96

Even though lignin has been studied for more than 100 years, the knowledge of the chemistry of lignin is still insufficient to establish an exact structural formula. The isolation of lignin without changing its chemical composition is the major challenge in the determination of an accurate structural formula for lignin. Therefore, the term lignin does not represent a specific compound but rather a group of high molecular and amorphous compounds which have very similar chemical properties but very different molecular weight (Brauns, F.E., 1952).

More recently, lignin has been described as a random, three-dimensional, highly-branched and interlocking network polymer (Figure 10) comprised of variously linked phenylpropane units (Sjöström, E., 1993). In fact, many lignin chemists agreed that lignin is composed of a mixture of one or more of the following phenolpropane groups which are connected through a variety of different types of linkages: 4-Coumaryl alcohol, Coniferyl alcohol and Sinapyl alcohol. Figure 11 presents a schematic representation of the structure of these compounds. Polymerization of these building blocks will lead to the formation of lignin with different types of chain structures such as Hydroxyphenyl, Guaiacyl and Syringyl (Figure 12). Lignin is covalently bound to the hemicellulose which is bound to cellulose via hydrogen bonding.

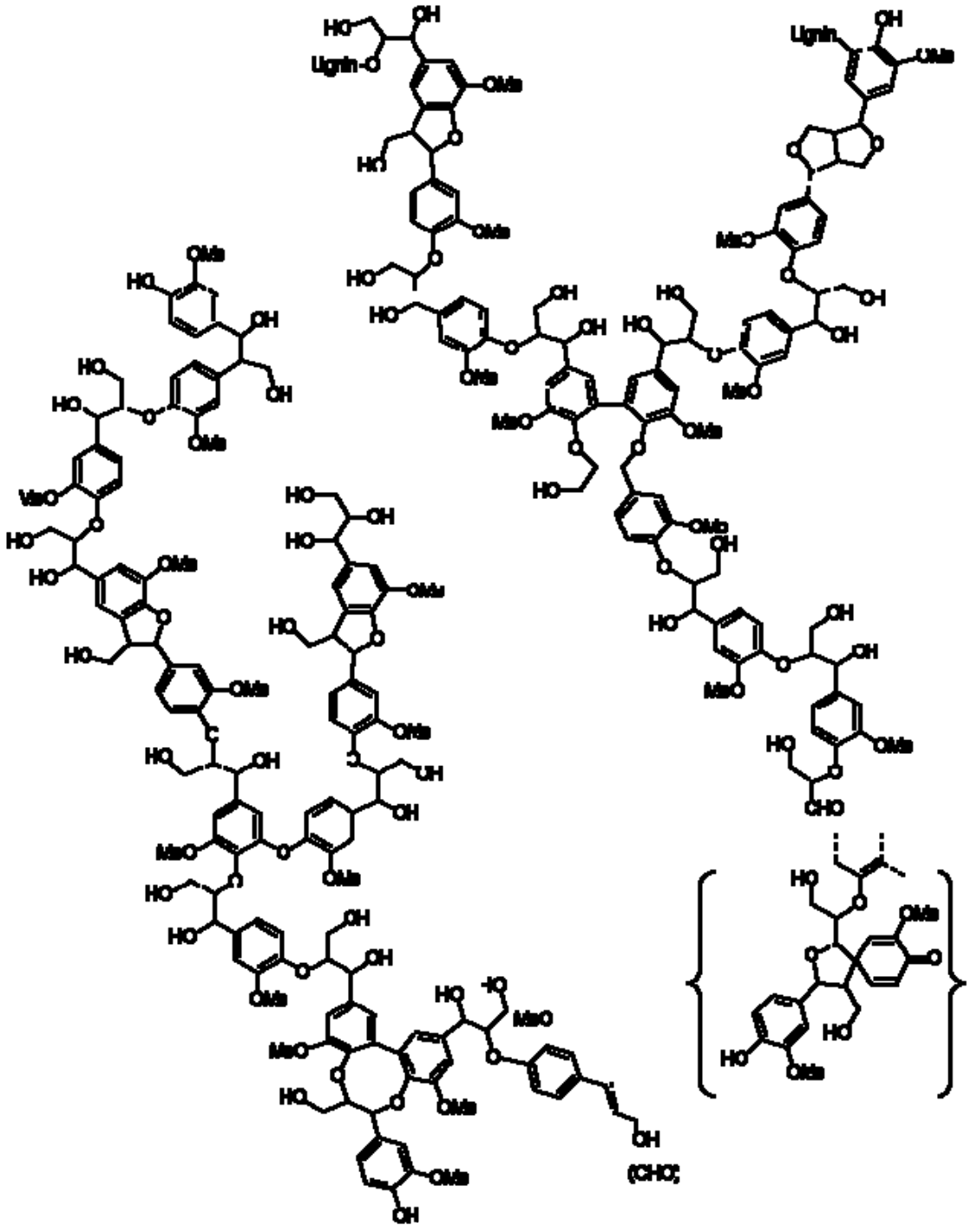

Figure 10: Structural model of softwood lignin (http://helsinki.fi/~orgkm_ww/lignin_structure.html).

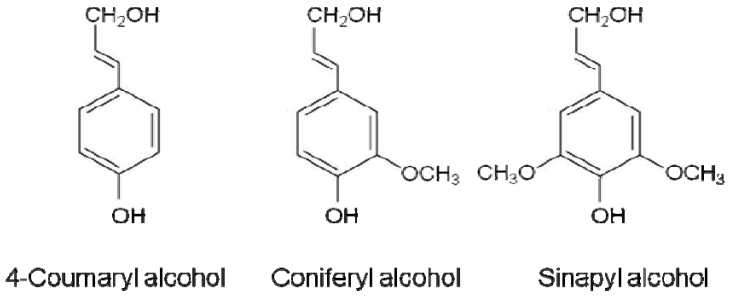

Figure 11: Structural formula of monomers believed to be the major lignin fragments.

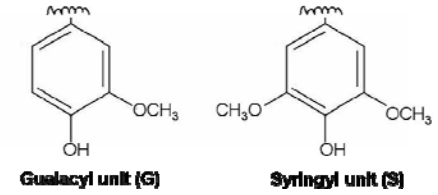

Figure 12: Structural formula of monomers believed to be the major lignin fragments.

Lignin plays a vital role in providing mechanical support by binding cellulose and hemicelluloses in plant fibers. This macromolecule also decreases the permeation of water through the cell walls of the xylem, thereby playing an important role in the transport of water and nutrients. Finally, lignin has an important function in the natural defence against degradation by impeding penetration of destructive enzymes through the cell wall (Sarkanen and Ludwig, 1971; Sjostrom, E., 1993).

2.1.5 How does lignin decompose?

Even though the degradation of lignin prolongs up to 600 °C, the initial temperature of degradation for lignin is the lowest one among the components of plant fibers. For this reason it is important to understand the mechanism of degradation of lignin.

Bartkiwiak and Zakrzewski (2004) studied thermal degradation of lignin isolated from pine and beech wood using Tappi and sulfate methods. They investigated the effect of different degrees of degradation on the chemical composition of the sample. The authors found that lignin isolated by the Tappi method from pinewood presented the maximum rate of degradation at 354 °C and 442 °C when

the heating rates were 1 °C.min^{-1} and 50 °C.min^{-1}, respectively. In contrast, the thermal degradation of beech wood lignin isolated by Tappi method is shown to follow a process with three and two stages under the heating rate of 1 °C.min^{-1} and 50 °C.min^{-1}, respectively. The maximum rate of degradation for the three steps process were 296, 318 and 364 °C, whereas in the two step process 318 and 414 °C are the temperatures at which the maximum rate of degradation takes place.

Neither the sources of lignin nor the rates of temperature increase appeared to have an influence on the total mass loss at 1000 °C, for the case of Tappi method. These data are summarized in Table 3. Concerning the elementary composition, it was found that as the degree of thermal decomposition increases the percentage of hydrogen and methoxy groups significantly decreases for all types of lignin. While the carbon content was constant in the case of Tappi pine lignin and Sulphate beech lignin, the increase of thermal degradation results in a slight increase in the carbon content for the case of Tappi beech lignin and Sulphate pine lignin.

Table 3: Thermal analysis results obtained for pine and beech wood lignin extracted as Tappi method Bartkiwiak and Zakrzewski (2004).

Lignin source	Heating rate (°C/min)	Interval of temperature of degradation (°C)	Main degradation temperature (°C)	Total mass loss at 1000°C (%)
Pine wood	1	254-450	354	47.6
	50	333-539	442	48.8
Beech wood	1	170-310	296	60.4
		---	318	
		---	364	
	50	---	318	59.5
		355-470	414	

Regarding changes in the chemical composition observed by Fourier transform infrared spectroscopy, the initial sample of Tappi pine lignin showed the characteristic bands for guaiacyl ring (1266 cm^{-1}), syringil system (1325 cm^{-1}), OH and OCH_3. The authors reported that the Tappi lignin after 30 % and 50 % of mass loss presented bands in the FTIR spectra related to carbonyl group (1735-1720 cm^{-1}) and aromatic (1602 cm^{-1}) structures. In the case of the sulfate lignin after 30 % and 60 % of mass loss, the FTIR spectra revealed the formation of hydroxide and existence of carbonyl groups, aromatic rings and sulfur.

In another study, Domburg et al. (1970) used model compounds with typical structures and functional groups of lignin fragments to simulate the behavior of lignin macromolecule during thermal degradation. This approach allowed the authors to estimate the kinetic parameters and thermal stability of lignin. The four phenylpropane employed as model compounds in this study were 1-(4-hydroxyphenyl)propanone-1 (I), 1-(4-hydroxy-3-methoxyphenyl)propanol-1 (I1), l-(4-hydroxy-3-methoxy-phenyl)propanol-3 (III) and 1-(4-hydroxy-3-methoxy-phenyl)propen-1--ol-3 (IV). They were compared against the two units found in lignin: dehydrodivanillin (V) and dehydrodiisoeugenol (VI).

Table 4: Kinetic parameters obtained after Freeman-Carrol method (Domburg et al., 1970).

Compound	Temperature at the start of mass change (°C)	Temperature of the maximum rate of mass loss (°C)	Complete destruction	
			Temperature (°C)	Residue (Wt-%)
I	210	325	370	10
II	160	250; 275	425	16.5
III	220	330	370	8
IV	160	240; 420	600	34
V	280	325; 500	600	22.5
VI	350	405; 540	600	12

According to Table 4, compounds I and III have a similar thermal decomposition behavior. Both start to degrade at 210 °C, have maximum rate of weight loss around 330 °C and reach complete degradation at 370 °C. Compound I has two steps of decomposition in the temperature range of 260 to 325 °C and 325 to 370 °C. In contrast, compound III has only one step of degradation which happens between 250 and 370 °C. Also, the reports in the literature indicated that there was a rupture of C-C bonds in the propyl side chain during initial step of degradation of compound I and III, although concurrent C_{aryl}-C_{alky} bond breaking was possible.

Compounds II and IV present three step decomposition. While dehydration reactions of benzyl alcoholic groups and C-C bond breaking in the side chain (α- and β-carbons) are respectively accounted for the first and second step of decomposition of compound II, intermolecular condensation-polymerization reactions and C-C bond breaking in the side chain (α-carbons) are respectively responsible for the first degradation step of compound IV. In addition, it is noticed that activation energy in the case of compound IV is much lower than in the case of compound II.

Compounds V and VI undergo two and three step decomposition, respectively. According to the authors, compound V starts to degrade at 300 °C with a total mass loss of 12 % in the first step that would correspond to vanillin. The only way to obtain vanillin from compound V is the rupture of C-C bonds between guaiacyl groups. It was further stated that given the elementary composition and methoxy group content, the intermediate solid formed in the first step was similar to the initial compound with differences in the structural arrangement of the chemical groups. In the third degradation step, the intermediate compound formed degrades into carbonaceous material.

After the first step of thermal treatment of the compound VI, several chemical groups were absent in the FTIR spectra, suggesting that phenylcoumarane structures were decomposed via C-C bond breaking in the chains of the phenylpropane groups. In the second step, unstable intermediates were degraded at 450 °C. The authors argued that the increased initial thermal stability of compound VI was due to the presence of phenylcoumarane unit and the absence of reactive functional groups in its structure. Compounds with OH groups in the side chain (α-position) or double bonds attached to OH groups have low initial thermal stability, while its intermediates structures have high thermal stability. The presence of active groups in the side chain decreases the initial thermal stability.

2.2 Use of Agro-based Material in Thermoplastics

Fiber reinforced plastics have been studied since 1908, when cellulose fibers were used to reinforce phenolic resins. Initially, thermosetting resins were chosen as matrix systems for plant fibers because of the low processing temperatures required for these types of resins. Thermosetting resins have mechanical properties attributed to crosslinking reactions during the cure (polymerization), thus they do not require high temperature for melting like thermoplastics.

More recently thermoplastics are being explored as a matrix material for plant fibers reinforced polymer composites. Low cost of processing and recyclability are the main advantages of thermoplastic over thermosetting resins (John and Thomas, 2008; Kruger, 2007). Agricultural fibers such as wheat, soybean, corn and banana straw fibers and pineapple leaf fibers are being considered as reinforcement for thermoplastic resins including polyethylene (PE) (George et al., 1995), high density polyethylene (HDPE), and polypropylene (PP) (Avella et al., 1995; Bledzki et al., 2007; Hornsby[2] et al., 1997). Some of the limitations associated with the use of thermoplastics is the temperature required for melting. Polyethylene and polypropylene are often processed in the range of 180-210 ^{o}C, thus making it possible to incorporate plant fibers in the composition. Other thermoplastics of interest (polyamide, polyester, polycarbonate etc) have processing temperatures above 220 ^{o}C; in such cases the plant fibers decompose during compounding and processing. Thus, mineral fillers (calcium carbonate) and inorganic fibers (glass fibers) are generally used in the formulation of thermoplastics with processing temperatures above 220 ^{o}C.

2.3 Thermochemical Modification of Agro-based Fibers

Most of the research on modification of plant fibers reported in the literature is not related to improving thermal stability, but rather to enhance adhesion between the fiber and the matrix, mechanical properties and moisture absorption. For example, Hornsby et al. (Hornsby et al.[2], 1997) employed a silane treatment in order to enhance the adhesion between a matrix of polypropylene and wheat and flax fibers. It was found that these silane treatments had little or no effect on the

mechanical properties. However, the utilization of maleic anhydride was beneficial for fiber-matrix interaction resulting in a significant increase in the tensile yield strength.

2.3.1 Thermal Treatment

Different treatments aiming to increase the fiber-matrix adhesion or reduce the plant fibers water absorption have also produce improvements in thermal stability of the fibers as an indirect effect of these treatments. For example, Prasad et al. (Prasad, 2004) have proposed a thermomechanical treatment for hemp bast and stem fibers where the fibers were heated from 160 to 260 °C under air and inert atmosphere for 30 minutes inside a digester. It was found that in comparison with an inert atmosphere, the presence of oxygen did not cause a prominent difference in the loss of weight up to 220 °C. However, at higher temperatures there was a significant increase in the weight loss for the samples heated in air. This behaviour was attributed to the possible degradation of hemicellulose and cellulose under air atmosphere at 200 °C and above. Based on microscopic examination, the authors speculated that there was lignin migration to the outer surface of the hemp fibers; samples treated in the inert atmosphere did not present kink bands which may be the explanation for the migration of lignin to the surface. Another important observation is that all treatments investigated led to a certain level of separation of the fibers bundles, reflecting physical microstructure changes in the fibers.

Another method that relies on thermal modification of the components of plant fibers is the fabrication of carbon fibers using cellulose as precursor. The cellulose extracted from wood pulp can be initially converted chemically to fiber (rayon) and subsequently converted into carbon fiber following several steps. First, the cellulose fibers (rayon) are submitted to a process called stabilization. Typically this step happens in the range of temperature between 300 and 400 °C, under oxidative atmosphere and in the presence of an aqueous ammonium chloride solution or a dilute solution of phosphoric acid. The structure of the fiber is modified to form a structure that is more stable at higher temperatures. This modification happens through partial decomposition and formation of crosslinks. Decomposition products such as H_2O, CO and CO_2 may represent 50 to 60 wt-% of the original mass. Eventually, chain fragmentation or depolymerization may occur during this stage. The second step is the carbonization which involves heating to between 1000 and 1500 °C in order to remove the non carbon elements remaining on the sample. Further weight loss occurs and the yield after carbonization is around 25 % of the initial mass. The third and last step is responsible for

improving the properties of carbon fibers. The stretching of the fibers under high temperatures (around 2800 °C) aligns the graphene layers, thus increasing strength and modulus (Chawla, 1998; Savage, 1992). Carbon fibers are the prime material in the composites industry and are relatively very expensive.

The approach used for carbon fibers was applied by Bengisu and Yilmaz-(2002) in the oxidation and pyrolysis of chitosan as an alternative route for carbon fiber fabrication. The effect of temperature, time and pre-treatment of the fiber precursor with ammonium chloride were considered in the conversion of chitosan into carbon fibers. The authors used design of experiments to evaluate the effect of oxidation and pyrolysis. For the oxidation experiments, the temperature and time selected were 300 and 400 °C, and 60 and 360 minutes respectively; whereas, for the pyrolysis experiments the temperature and time used were 500 and 700 °C, and 6 and 60 minutes respectively. Both methods considered the treatment with ammonium chloride. The structure of the fibers were investigated with FTIR spectroscopy; it was demonstrated that the decomposition of pyranose ring with partial dehydration and the deamination were the main chemical reactions responsible for degradation of chitosan during the oxidation treatment. Also, there was the formation of aromatic rings. Oxidation was inhibited at the beginning of heat treatment when pre-treatment with ammonium chloride was used. However, in the absence of pre-treatment with ammonium chloride, oxidation readily took place. For example, 6 minutes at 400 °C were enough to achieve complete oxidation when no pre-treatment was applied. The authors speculate that NH_4Cl acts like a coating, creating a temporary physical barrier to oxidation. Whereas the powder with no pre-treatment was all black in color after 10 min at 300 °C; the comparable pretreated powders had cream to dark brown color. Unlike the rayon fibers, the chitosan fibers seem more suitable for thermal rearrangement reactions rather than degradation when in the presence of NH_4Cl. Therefore, the interaction between chitosan fibers and NH_4Cl affects the oxidation rate, making it smaller than in the case of rayon fibers.

2.3.2 Biochemical Treatment

There are many studies on extraction of fibers from plant stems using different methods such as mechanical, physical or chemical techniques. Zhang et al. (2008) studied the effect of the combination of steam explosion and biodegradation on the removal of lignin from wheat straw fibers. The authors reported that 19.94 % of the lignin was removed under 0.8 MPa pressure and at the ratio

of 1:20 (wheat straw/water) during the first step of steam explosion. After this initial step the material was submitted to biodegradation by utilizing an optimum medium with the white-rot fungi Trametes versicolors. Different times of biodegradation lead to different lignin content removal and consequently different thermal properties. The maximum removal of lignin was 55.4 %. The authors reported that steam-exploded wheat straw presented the highest peak in degradation temperature and onset of decomposition among all the different treatments used.

2.3.3 Alkali Treatment

Some studies have reported alkalinization of plant fibers. Feng et al. (2008) have found that high temperature alkali cooking has great effect on removing pectin, hemicellulose, and lignin from hemp fibers. The alkalization of hemp fiber at 150 °C leads to the removal of up to 79.1 % of hemicellulose and 83.5 % of lignin. These treated fibers appear to have better thermal stability. In contrast, Mwaikambo and Ansell (2002) reported that the alkalinization increased the amount of amorphous cellulose in the hemp fibers reducing the cellulose crystallite length and consequently reducing the thermal resistance. Furthermore, the alkali treatment did not remove all the hemicellulose and lignin from the fibers. This was attributed to the high crystallinity of hemp fiber due to fewer hydroxyl groups available to react with external chemicals during the treatment. In addition, the surface obtained after alkali treatment seems rougher in comparison with untreated hemp fibers (Figure 13).

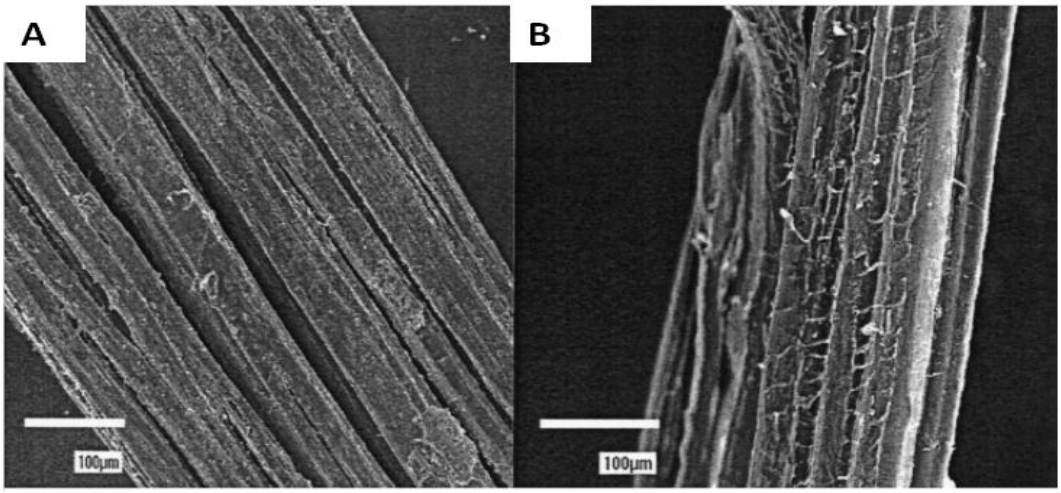

Figure 13: SEM image of untreated (a) and alkali treated (b) hemp fibers (Mwaikambo and Ansell, 2002).

In another study Ray et al. (2001) found that the alkali treatment of jute fibers resulted in loss of mass because of removal of hemicellulose. This loss of weight was responsible for a steep decrease in the density of these fibers and for the creation of voids. The removal of hemicellulose also caused the separation of the fiber bundle into finer and smaller filaments of cellulose and lignin due to a process termed fibrillation (Figure 14).

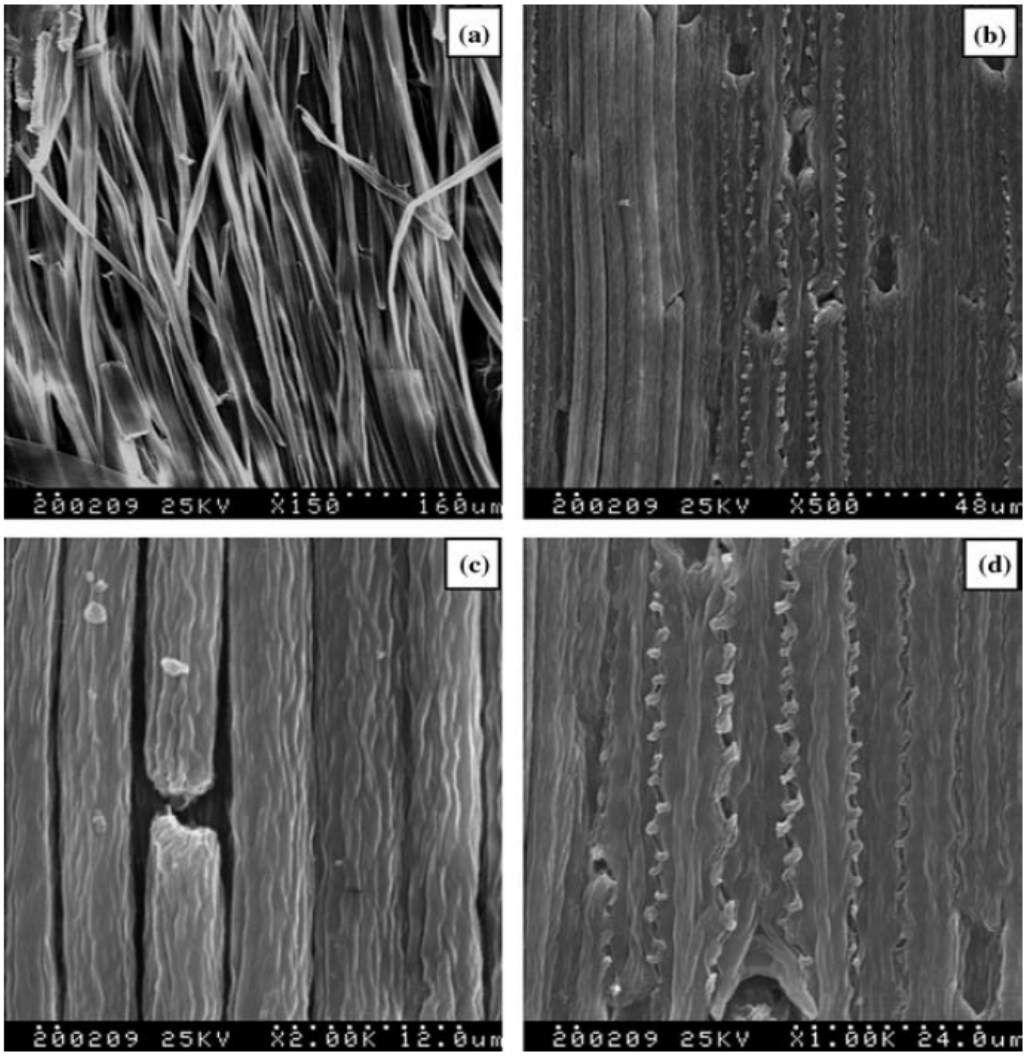

Figure 14: SEM images illustrate the effect of lignin and hemicellulose removal from wheat straw. Cellulose fibers in the outer surface (a, b, c) are exposed including (d) the fibers serrations (Liu et al., 2004).

This process allowed the cellulose fibers to rearrange in a compact manner leading to higher crystallinity and therefore improving the stiffness of the fiber. However, the increase in the treatment time leads to a fiber with brittle characteristics which diminished the stress transfer between the matrix and the fiber, reducing the mechanical properties of the composite.

2.3.4 Acetylation Treatment

Another widely used method to modify the characteristics of plant fiber is acetylation. It consists of the introduction of acetyl functional groups (CH_3COO^-) into an organic compound replacing the hydrogen atom of a hydroxyl group (OH) present in the chemical structure of cellulose, hemicellulose or lignin. During this esterification there is the formation of an ester by reaction of acetic anhydride as follows (Li et al., 2007):

$$\text{Fiber-OH} + CH_3\text{–C(=O)–O–C(=O)–}CH_3 \rightarrow \text{Fiber–O}COCH_3 + CH_3COOH$$

The acetylation of plant fibers involves several steps. The first one typically consists of a pre-treatment with sodium hydroxide (NaOH) solution which removes impurities on the surface of the fiber and activates the OH groups on the cellulose and lignin. Then the fibers are usually submitted to acetic acid solution and acetic anhydride solution with 2 drops of concentrated H_2SO_4. Whereas acetic acid is a good swelling agent, acetic anhydride does not have a good swelling property. On the other hand, the reaction of acetic acid with cellulose is not extensive, while acetic anhydride presents good interaction with cellulose. Therefore it is necessary to use both acetic acid and acetic anhydride in conjunction to achieve good degree of acetylation (Li et al., 2007; Mishra et al., 2003; Mwaikambo and Ansell, 2002; Sreekala and Thomas, 2003; Xiao-feng et al., 2006).

The main reasons for employing acetylation are to diminish the hydrophilicity of plant fibers, to improve adhesion between fiber and matrix, and to increase dimensional stability of composites. Since the moisture content has a deteriorating effect on the properties of a biocomposite, the potential benefits of acetylation are of great importance. For example, Nair et al. (2001) reported that acetylation of sisal fiber creates voids in the surface of the fiber leading to better mechanical interconnection with the matrix of polystyrene (PS). According to the authors another reason for this

increase in adhesion was the decrease in hydrophilicity nature of acetylated fiber. The thermal stability of the acetylated sisal fiber was improved by 50 % in comparison with untreated fiber at 300 °C. The thermal stability is associated with the capacity of a structure to dissipate energy. In the case of cellulose, the main mechanism for dissipation of thermal energy relies on the hydrogen bonding. While cellulose starts to become more amorphous, the ability of cellulose to dissipate thermal energy is reduced because of fewer hydrogen bonds. It is important to note that the thermal stability of the polystyrene composite reinforced with acetylated fiber was also improved. This occurred probably because of the greater intermolecular bonding between the hydrophobic PS matrix and the treated fiber.

In agreement with that, Sreekala and Thomas (2003) found that acetylated oil palm fibers have reduced hydrophilicity, thus contributing to decrease the water sorption behavior. The authors suggest that the waxy layer on the surface of the fibers responsible for bonding the water molecules to the fiber surface was removed by the acetylation treatment. In addition, the free hydroxyl groups on the surface of the fibers suffered important chemical modification with the introduction of an acetyl group which helped to change the diffusion coefficient. It is important to note that the sorption and permeability coefficient decrease as a result of the physical and chemical modifications of the fibers; whereas, the mechanical strength of the fibers were diminished upon treatment.

In order to overcome this decrease in mechanical properties Mishra et al. (2003) suggest the addition of small amounts of fiber glass to acetylated sisal and pineapple leaf fibers reinforced polyester composites. In the case of sisal/glass hybrid polyester composite submitted to acetylation, it was reported an improvement of 6 % in the flexural strength and of 15 % in the impact strength. The moisture absorption of both sisal polyester composite and sisal/glass hybrid polyester were significantly reduced by the addition of glass fiber and acetylated sisal fibers. The better interfacial bonding between acetylated sisal fibers and matrix as well the addition of glass fibers are accounted for the reduction in the moisture absorption.

2.3.5 Silane Treatment

Among the various chemical modifications proposed for enhancing compatibility and physical properties of plant fibers one of the most versatile and promising methods is the silane treatment. Silane compounds have been mainly used to create an interfacial bonding between glass fiber and

polymer matrix (Li, 2007; Plueddemann, 1991). More recently silane treatment was shown to effectively increase adhesion between plant fibers and polymeric matrices (Xanthos, 2010; Xie et al., 2010). Indeed silane based compounds are very common coupling agents. They have multifunctional molecules which might be represented by the general chemical formula $R\text{-}(CH_2)_n\text{-}Si\text{-}X_3$. While the R may represent functional or non- hydrolyzable groups such as vinyl, γ-aminopropyl or γ-methacreloxypropyne; the X typically corresponds to hydrolyzable groups such as chloro, methoxy or ethoxy.

The silane modifiers commercially available typically have R groups with non-polar structures. In this case, they will facilitate bonding with non-polar polymers. In the other hand, the X groups can react with the hydroxyl (OH) groups present in the surface of the fiber. This reaction occurs in the presence of water, where these X groups are hydrolyzed forming silanol groups (Si-OH). Through condensation reaction the silanol groups replace the OH groups and forms stable covalent bonds to the fiber surface. It is important to note that there is a formation of a crosslinked network between the matrix and the fiber. These reactions are illustrated in Figure 15.

Recently, researchers have observed improvement not only adhesion but also the thermal stability of plant fiber by using silane modification. For example, Rachini et al. (2009) compared the effect of two different chemical treatments on the thermal degradation behavior of hemp fibers. The authors used alkali and silane treatment. In the case of silane treatment γ-aminopropyltriethoxysilane (APS) was applied using a solution of water and ethanol at 120 °C for 2 hours under nitrogen atmosphere. The authors evaluated the effect of the solution of water/ethanol alone (without adding the silane compound, APS) during fiber treatment. This "blank" allowed the authors to subtract any improvements achieved due to extraction of the components of plant fibers such as pectin, hemicellulose and lignin. Table 5 summarizes the results of weight loss under different atmospheres. The study found that in comparison with untreated hemp fibers, ethanol/water treated hemp fibers have a lower weight loss when heated under argon atmosphere. While the first had lost 10 % of the initial mass, the second lost 6 % of the initial mass within the 200-280 °C temperature range. According to the authors, this difference can be explained by the removal of pectins and hemicellulose during the treatment process with water/ethanol solution (without silane). It was shown that pectins and hemicelluloses decomposed at low temperatures and therefore to use water/ethanol solution alone improved the thermal stability of the hemp fibers. This conclusion is corroborated by

the fact that the temperature of decomposition is higher for ethanol/water treated hemp fiber than for untreated hemp fiber (air and argon atmospheres and within the interval of 280-380 °C).

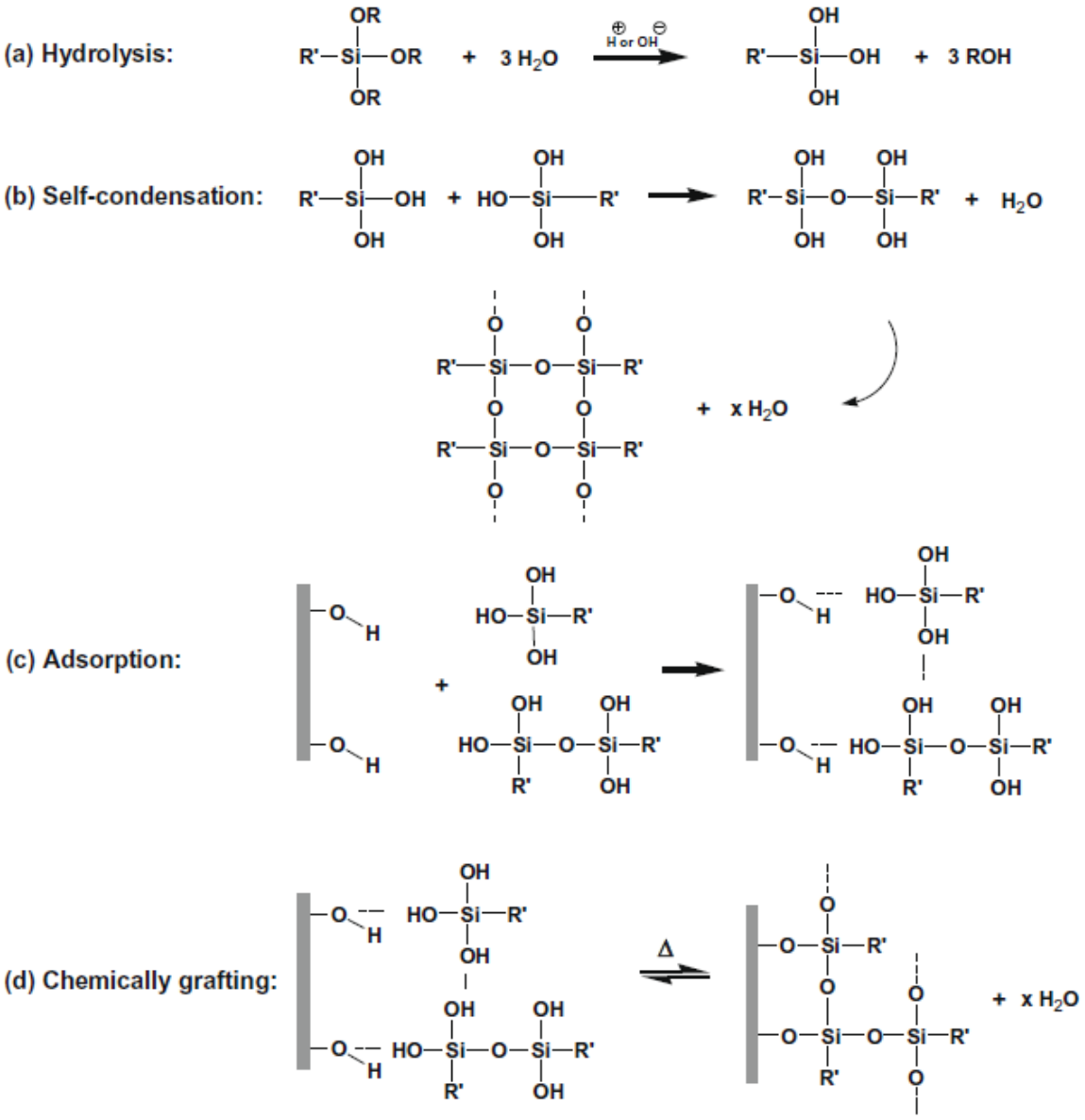

Figure 15: Possible chemical reactions during silane modification of plant fibers: (a) hydrolysis, (b) self-condensation, (c) adsorption and (d) chemical grafting (Xie et al., 2010).

In the same fashion, the silane treated hemp fibers have lower weight loss than natural hemp fibers under argon atmosphere. While 63 % of the mass of the untreated hemp fiber is lost in the temperature range of 150 to 380 °C, silane treated hemp fiber presented a weight loss of 53.3 %. When temperature is increased to 600 °C, this difference becomes smaller. While the addition of silane reduced the weight lost (about 10 %) in comparison with water/ethanol treatment under argon atmosphere; silane does not alter the temperature of thermal decomposition of hemp fiber under air atmosphere.

Table 5: Weight loss (%) under argon and air atmospheres (adapted from Rachini et al., 2009).

Atmosphere	Treatment	Temperature Range (°C)		
		40-150	150-380	380-600
Air	Untreated Hemp	7.2	61	27.3
	Ethanol/water	5	62.1	28.8
	Silane	5.3	61.8	27.5
Argon	Untreated Hemp	7.4	63	9
	Ethanol/water	6.4	62	10
	Silane	5.4	53.3	12

Another interesting study involving application of silane compounds was developed by Love et al. (2008). The authors functionalized the surface of wood pulp fiber with silica by means of azeotropic distillation. The azeotropic distillation was applied in an attempt to prevent the collapsing and distortion of the fiber structure during drying process. The objective was to confer glass properties to the wood pulp fiber. Therefore, properties such as stiffness, hydrophilicity and fire resistance would be enhanced as well as the possibility of use of these fibers as reinforcement for polymer composites. Different alkoxysilanes, solvents and methods for modification were tested. The two steps used during chemical modification were impregnation and hydrolysis. The first one consists of the application of azeotropic distillation where water present in the pores of the fiber was replaced by a

mixture of solvent and silane (tetraethoxysilane - TEOS). However, during silica modification using TEOS only physically absorbed silica was observed. In order to overcome this problem, the authors applied a second step, where the physically absorbed silanol groups were submitted to base-catalysed hydrolysis. This step would form polymeric silica and chemically bond the silica into the fiber surface. However, silica deposition was mostly located on the inner lumen wall rather than on the surface of the outer fiber walls (Figure 16). This happened due to the lack of chemical reaction during the first step which would anchor the silane reagent on the surface of the fiber. Without this anchoring the silane was leached or dislocated to the lumen and fiber surface during the washing procedure. In order to increase the control over the destination of the silica the authors tested a different silane compound which has higher reactivity than TEOS. It was intended to have silicon chemically bond to the fiber walls during the azeotropic distillation. This implies that the silica would be tightly bonded to the fiber walls prior to hydrolysis. According to the study, an even dispersion of silicon was achieved with application of triethoxychlorosilane (TECS). The small variance in the results of ash content after different washing times suggest that Si-O-Si bonds were formed prior hydrolysis. Actually, the authors speculate that TECS not only reacted with the hydroxyl groups of the cellulose surface, but could have also reacted with the phenolic groups of the lignin. This observation is particularly important in the case of plant fibers such as wheat straw and soy stem, because these two contain higher lignin content than the wood pulp fiber (2.4-6 %). Moreover, a mixture of TEOS and TECS could be used to cover the fiber walls, surfaces and internal void spaces rather than just the fibers walls.

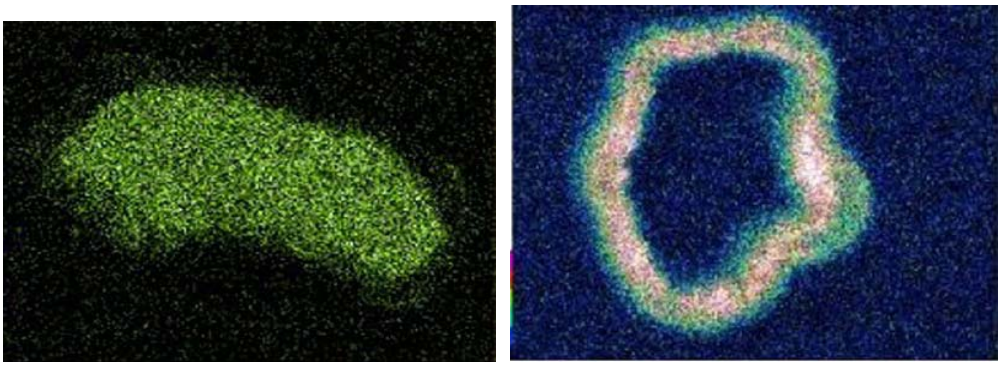

Figure 16: EDX micrograph of the cross section of kraft wood fiber modified using TEOS and TECS. Whereas picture (a-left) shows the lumen filled with silica, picture (b-right) presents the fibers walls filled with silica (adapted from Love et al., 2008).

2.3.6 Ultraviolet (UV) Light Treatment

To the best of our knowledge, ultraviolet light has not been employed in any attempt to enhance thermal stability of agro-based fibers but rather to simulate weathering (Klysov, A. A., 2007; Stark et al., 2004; Stark and Matuana, 2004; Stark and Matuana, 2006), induce polymerization of few types of polymers (Bashar et al., 1997; Dean et al., 2007; Khan et al., 2004) and functionalize the surface of non-polar polymers (Gassan and Gutowski, 2000; Hozumi et al., 2004, Onyiriuka, 1993; Mukhopadhyay, S. and Fangueiro, R., 2009; Zhang et al., 2000;).

Regarding wood weathering, it has been reported in the literature that UV irradiation can selectively degrade the lignin present in wood (Deka et al., 2008; Feist and Hon, 1984; Fengel and Wegener, 1989; Hon and Chang, 1984; Muller et al., 2003). In fact, lignin absorbs 80 to 95 % of the total irradiated UV light (Feist and Hon, 1984; Norrstrom, 1969), especially in the region between 280 and 300 nm. Because of that, it has been reported that just 72 hours of exposure to UV light with wavelength (λ) >300 nm is able to decrease the lignin content of spruce wood down to 20 % of the initial value (Muller et al., 2003). Similar to lignin, hemicellulose can also absorb UV light (5 to 20 %) and be removed (Deka et al., 2008; Norrstrom, 1969).

The lignin decay can be confirmed by observing the steep decrease on the characteristic aromatic band of lignin at 1510 cm^{-1} and the formation of carbonyl groups. New carbonyl bands in the region below 1700 cm^{-1} and region between 1700 and 1750 cm^{-1} indicates that there was oxidation of the plant fiber components (Deka et al., 2008; Muller et al., 2003; Hong and Chang, 1984). In addition, the ratio between the intensities of the lignin peak and a reference peak is also utilized to confirm the decrease of lignin content.

The removal of lignin and hemicellulose is reached through complex photochemical reactions. Initially, UV light is absorbed by the plant fiber components generating free radical species. Then, these species react with oxygen causing oxidation and ultimately photo-degradation of lignin and hemicellulose. The different reaction pathways which might lead to the photo-oxidation of lignin are represented in Figure 17.

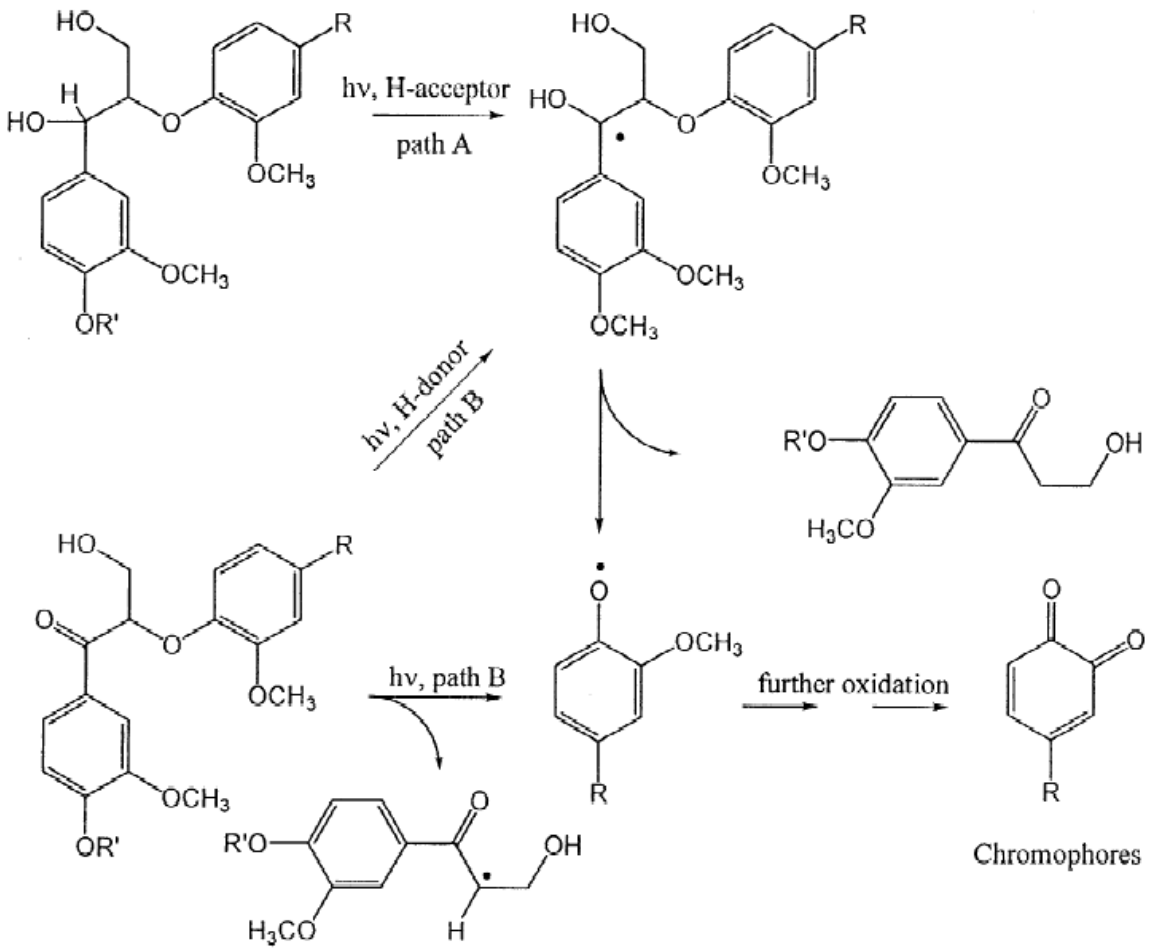

Figure 17: Formation of quinone structures due to the cleavage of the b-O-4 bond. Adapted from Muller et al., 2003

Chapter 3 - Understanding the Thermal Degradation and Chemical Kinetics of Wheat Straw Fiber

3.1 Introduction

The utilization of plant fibers in the production of thermoplastic composites has increasingly attracted different industries. The main reasons for this interest are the good mechanical properties, low density, non-abrasive nature, and low cost that plant fibers present, especially the ones obtained from agricultural residues which are also referred to as agro-based fibers (Woodhams et al., 1984; Pervaiz and Sain, 2004; Rouison et al., 2004).

Among the agricultural residues, there is interest especially in wheat straw fiber because of its low cost and availability in Canada (Avella et al., 1995) and worldwide. However, during the fabrication of thermoplastic composites, these plant fibers, including wheat straw, can suffer severe thermal degradation. Therefore, it is important to determine the maximum temperature that wheat straw fiber can be submitted to without depreciating the physico-chemical properties through thermal degradation.

For this reason, the thermal stability of six wheat straw samples was evaluated. The thermal degradation is evaluated here as the weight loss percentage as a function of temperature or time. This evaluation was carried out with the assistance of thermogravimetry analysis (TGA) under non-isothermal and isothermal conditions in different atmospheres (air or nitrogen). Thermal gravimetric analysis was chosen because of its widespread acceptance in academia and its use by industrial laboratories.

The chemical kinetics study was performed in an attempt to obtain a better understanding of the reaction mechanism responsible for the thermal degradation of wheat straw fiber. An isoconversional method was utilized to estimate the kinetic parameters (e.g., activation energy) of wheat straw degradation. Since the thermal degradation of natural fiber is a very complex process, the objective of this study was not to elucidate the elementary steps of the reaction mechanism but rather to establish a method for identification and selection of plant fiber with superior thermal stability necessary for compounding and manufacturing with thermoplastics.

In this way, it may be possible to develop methods to prevent or minimize the thermal degradation of natural fiber and expand the use of wheat straw fiber toward engineering thermoplastics (those with processing temperatures above 220 ^{o}C).

3.2 Materials and Methods

3.2.1 Materials

The wheat straw samples used throughout this chapter were provided by our industrial partners Omtec Inc and A. Schulman Inc. Table 6 summarizes the information available for the six wheat straw samples whereas Figure 18 shows the visual appearance of the wheat straw samples as received. It can be seen from the figure that the samples Pellet 1 and Pellet 2 were submitted to a process that compressed the wheat straw into pellets. Therefore, before utilization, these two samples were manually separated into small particles. On the other hand, the other four wheat straw samples have somewhat similar particle size upon visual inspection.

The wheat straw samples named Fine, Mid and Large consist of a soft white winter variety named AC Mountain and harvested at maturity as whole from commercial fields (Woodrill Farms) near Guelph, Ontario. Wheat straw was initially cut to approximately 3-5 cm, using a flywheel, and then fed directly to a rotary hammer mill. This ground wheat straw was screened through different sieves. For example, in the case of wheat straw sample named Mid, two sieves with mesh sizes of 16 and 35 were utilized to collect the fibers with size between mesh size of 16 (1.19 mm opening size) and mesh size of 35 (0.5 mm opening size).

The Large wheat straw consists of fibers that did not pass through the sieve with mesh size of 16 and therefore these fibers are bigger than the 1.19 mm opening size (mesh 16). In the same way, the wheat straw fibers with particle size below the mesh size of 35 (0.5 mm opening size) were named as Fine wheat straw. It should be clarified that these grinding and sieving steps were performed by our industrial supplier Omtec Inc.

The sample AWF was produced by American Wood Fiber. In contrast, no information was provided regarding the wheat straw samples named Pellet 1 and Pellet 2. These wheat straw samples were cultivated in the United States of America.

Table 6: Different characteristics of the wheat straw samples such as type, region of cultivation and fiber size.

Sample Name	Type	Cultivation Region	Fiber Size
Fine	soft white winter	Guelph,ON	WS < Mesh 35 (0.5 mm)
Mid	soft white winter	Guelph,ON	Mesh 16 (1.19 mm) >WS>Mesh 35 (0.5 mm)
Large	soft white winter	Guelph,ON	WS > Mesh 16 (1.19 mm)
AWF	N/A	USA	N/A
Pellet 1	N/A	USA	N/A
Pellet 2	N/A	USA	N/A

N/A: Not available, WS: wheat straw.

Figure 18: Wheat straw samples utilized in this chapter: (a) Pellet 01; (b) Mid WS; (c) Large WS; (d) Fine WS; (e) AWF 01; (f) Pellet 2.

3.2.2 Thermogravimetry Analysis (TGA)

The thermogravimetry analysis (TGA) of the wheat straw samples was performed under non-isothermal and isothermal conditions.

In the case of non-isothermal analysis, the temperature is increased from 35 to 800 °C using a heating rate of 10 °C/min. The test was performed under either air or nitrogen atmosphere (50 ml flow) and the sample weight is monitored as a function of the temperature. The heating rate of 10 °C/min is typically used for plastics and plant fibers because it allows proper heat transfer to the sample. The initial weight of the samples was approximately 10 mg. Among other information, the TGA data can be utilized to determine the beginning of the thermal degradation of the wheat straw samples. Similarly, differential thermogravimetry (DTGA) curves can be used to distinguish overlapping reactions and compare relative weight losses.

In addition, isothermal analysis was carried out to simulate the thermal degradation which wheat straw samples would suffer during a compounding process with thermoplastics. In order to minimize the weight loss during the heating step and achieve the targeted temperature as fast as possible, the heating rate of 50 °C/min was chosen to heat the samples from 35 to either 200 °C or 250 °C. After achieving the target temperature, the samples were kept at these constant temperatures (200 or 250 °C) for 30 minutes under either air or nitrogen atmosphere (50 ml flow).

It is important to notice that there are two different regions in the isothermal plot as illustrated by Figure 19. The first region is non-isothermal and goes from zero to five minutes. During these initial 5 minutes the temperature is increasing at a rate of 50 °C/minute (this is the equipment limitation, rates above 50 ^{o}C/min are not possible). The second region is the isothermal part of the graph where the temperature is constant at 250 °C. The isothermal region of the graph goes from five (5) minutes up to thirty (30) minutes. In order to avoid confusion, the non-isothermal region was omitted and only the isothermal region is shown in the isothermal graphs presented throughout this chapter. Figure 19 also demonstrates the procedure used to obtain the weight percentage after 10 minutes of exposure to 200 °C or 250 °C which are referred to as Wt200 and Wt250, respectively. It can be seen in Figure 19 that the weight percentage after 10 minutes of exposure to 250 °C (Wt250) is obtained at 15 minutes in the plot because the first five initial minutes are under non-isothermal conditions.

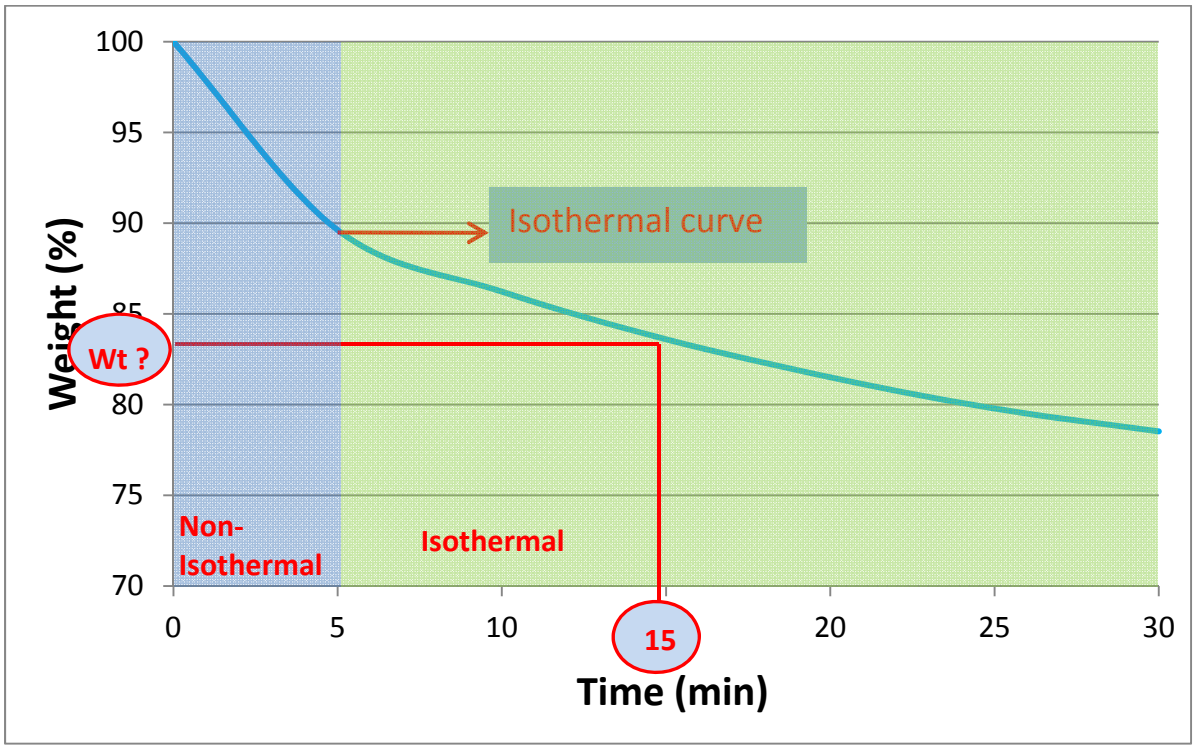

Figure 19: Non-isothermal and isothermal regions obtain during isothermal analysis. It is also illustrated the method used to obtain the weight percentage after 10 minutes under isothermal temperatures of 200 or 250 °C. (Note: the total 15 minutes in this graph corresponds to 10 minutes of isothermal conditions).

3.2.3 Kinetics of Isothermal Degradation of Wheat Straw Fiber

The kinetics of isothermal degradation behavior of wheat straw was examined under air atmosphere. The Mid WS sample was submitted to temperatures of 160, 180, 200, 220, 240 and 250 ºC under air flow. The initial size of the samples was about 3 grams and they were weighed using an analytical balance before and after being submitted to the thermal experiments. The samples were kept inside a convection oven for a period of time that varied from 2 minutes to up to 4000 minutes (2, 20, 200, 300, 400, 800, 1000, 1200, 2000, 3000, 3600 and 4000 min) at each one of the temperatures mentioned before.

The difference between the weight of the sample before and after the isothermal experiments represents the weight loss which was used to evaluate the kinetics of isothermal degradation of wheat straw fiber.

3.2.4 Chemical Composition Analysis

Chemical composition analysis of the wheat straw samples was carried out by AgriFood Laboratories located in Guelph, Ontario. A well-known method developed by Van Soest (Van Soest, 1963; Van Soest, 1968) was utilized to estimate the cellulose, hemicellulose and lignin content of the samples. The test uses two main indicators: Neutral Detergent Fiber (NDF) and Acid Detergent Fiber (ADF).

Neutral Detergent Fiber (NDF) indicates the total amount of cellulose, hemicellulose and lignin present in the natural fiber, that is, 100 % of cellulose, hemicellulose and lignin are recovered after NDF method; whereas during the second measurement (ADF) only cellulose and lignin are recovered, excluding hemicellulose. The subtraction of NDF and ADF indicators provides a good estimation of the hemicellulose content in the fiber.

Both Neutral Detergent Fiber (NDF) and Acid Detergent Fiber (ADF) are based on single extraction of components soluble in either neutral or acid detergents in a sequential order. First, the wheat straw is boiled in a neutral detergent solution, filtered, washed, dried and weighed. The solid fraction obtained is designated as Neutral Detergent Fiber (NDF). After that, the NDF solid fraction is submitted to the same procedure but using an acid detergent solution. This time, the solid fraction recovered after the procedure is called Acid Detergent Fiber (ADF). Then, the ADF solid fraction is treated with potassium permanganate. Lignin content is equal to the solid removed during the permanganate step (Garcia et al. 1997; Schmidt et al., 2002).

3.2.5 Chemical Kinetics Analysis: Isoconversional Method

Chemical kinetics studies the chemical reaction rates, that is, how fast the amounts of reactant and product change during a chemical reaction. Chemical kinetics also investigates how different experimental conditions (e.g., concentration of reactants, temperature, pressure etc) can affect the rate (i.e., speed) of a chemical reaction. For example, the speed of a chemical reaction usually increases when the temperature is increased.

Understanding and finding the reaction mechanism (i.e., the complete set of reactions taking place during the whole chemical reaction) responsible for a chemical reaction is one of the major practical application chemical kinetics. However, due to the complex nature of the natural fibers and even

more complex mechanism of thermal degradation, it is beyond the scope of this research to elucidate the reaction mechanism during the thermal degradation of natural fibers.

Nevertheless, knowledge about chemical kinetics can be useful in preventing or minimizing the thermal degradation of wheat straw fiber during the preparation of thermoplastic composites. More importantly, several kinetic models have been reported to be useful tools in quantifying the thermal degradation and were used to study the kinetics of plant fibers (Cai and Bi, 2009; Simon, 2004; Vyazovkin and Lesnikovich, 1990; Vyazovkin and Wight, 1997). These methods can be divided into model-fitting and isoconversional methods.

- *The model-fitting method* requires that a mathematical model be selected to describe the rate of the chemical reaction. However, many chemical reactions are indirect and take place through a complex mechanism. Even apparently simple chemical reactions may consist of complex or multi-step reactions which make it very difficult to find the correct mathematical model. For example, unimolecular reactions (i.e., only one molecule reacts) are likely to occur in a single step as in the decomposition of A into B ($A \rightarrow B$). However, sometimes a reaction appears to be unimolecular but this chemical reaction actually happens through a number of intermediate reactions which lead to the net result of decomposition A into B ($A \rightarrow B$).

- *The isoconversional method* has been extensively used in this task of revealing the reaction mechanism especially in the case of complex chemical reactions. Contrary to model-fitting methods, the isoconversional method is simple and does not require previous assumptions about a mathematical model for the reaction mechanism. These assumptions can lead to errors in the estimation of the kinetic parameters (i.e., apparent activation energy and pre-exponential factor, A) and therefore reaction mechanism. The isoconversional method utilizes the reaction rate of the chemical reaction at constant degrees of conversion to estimate the apparent activation energy. The variation of the activation energy with the extent of the reaction is then used to detect multi-step reactions.

The degree of conversion (denoted as α) is the extent of the thermal degradation reaction of wheat straw fiber and it is defined as the change in the amount of reactant (weight of wheat straw fiber) as a function of time according to Equation 1 below.

$$\alpha = \frac{(x_0 - x)}{(x_0 - x_f)} \qquad \textit{Equation 1}$$

Where x_0, x and x_f represent the initial, actual and final values of weight obtained from TGA analysis or other methods. This approximation is in agreement with other reports in the literature. Typically, the reaction rate ($d\alpha/dt$) is expressed as a function of two variables (temperature and conversion) according to Equation 2 (Simon, 2004; Vyazovkin and Lesnikovich, 1990; Vyazovkin and Wight, 1997).

$$\frac{d\alpha}{dt} = K(T) f(\alpha) \qquad \textit{Equation 2}$$

Where $K(T)$ denotes the reaction rate constant and f(α) is a conversion function. For many chemical reactions $K(T)$ shows Arrhenius type dependence:

$$K(T) = A \exp(-Ea / RT) \qquad \textit{Equation 3}$$

Where A is the pre-exponential factor, E_a is the apparent activation energy and R is the gas constant. Equation 4 is obtained from combination of the Equations 2 and 3:

$$\frac{d\alpha}{dt} = f(\alpha) A \exp(-Ea / RT) \quad \textit{Equation 4}$$

By integration of Equation 4, an integral type of kinetic function is obtained:

$$g(\alpha) = k(T)t \qquad \textit{Equation 5}$$

Assuming that the $g(\alpha)$ function has an Arrhenius type dependence and replacing the term $K(T)$ of the Equation 5 for the Arrhenius equation, the isoconversional equation (6) is obtained:

$$\ln t = \frac{E_a}{RT} - \ln\left[\frac{g(\alpha)}{A}\right] \qquad \textit{Equation 6}$$

If the conversion (i.e., the extent of the thermal degradation reaction, α) is constant, the second term of the Equation 6 is constant and apparent activation energy (Ea) can be obtained from the slope of the curve logarithm of time (ln t) versus temperature (1/T). The pre-exponential factor (A) can be obtained from the intercept of a straight line.

Figure 20 exemplifies the first part of the application of the isoconversional method. First, the isothermal curves of weight versus time are used to obtain the time needed to reach the degree of conversion ranging from 2 to 30 %. Then, these values are utilized to plot the curve of time (ln t) versus temperature (1/T) following Equation (6). One straight line curve is obtained for each degree of conversion (α) and the inclination of this straight line curve provides the apparent activation energy for this degree of conversion.

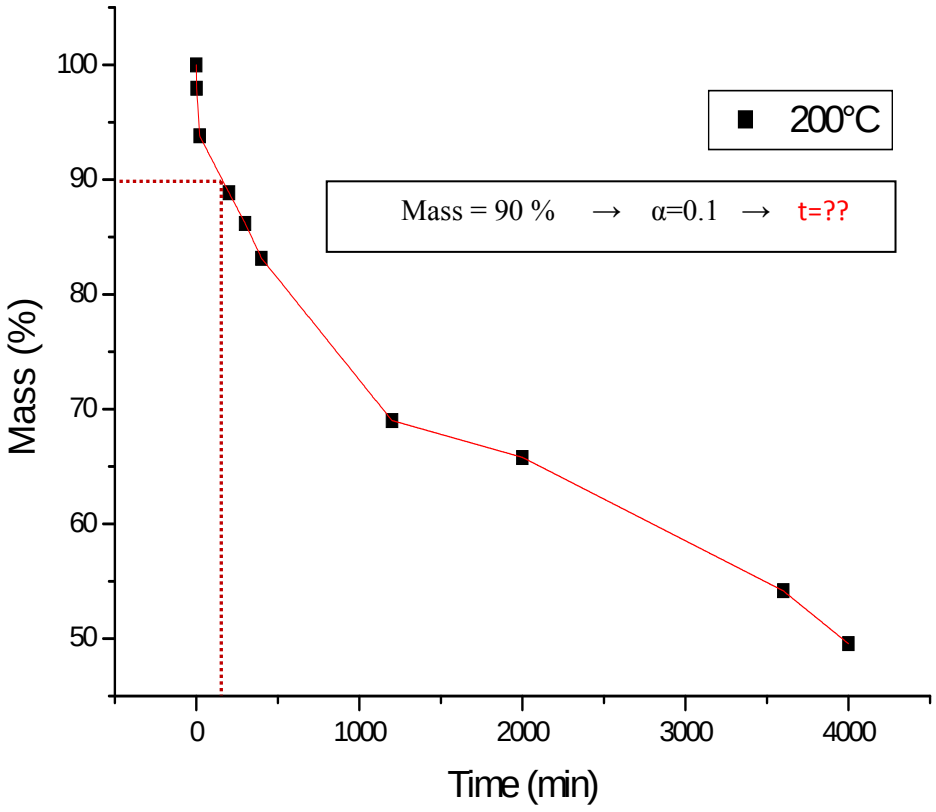

Figure 20: Example of application of isoconversional method to the thermo-oxidative degradation of wheat straw. The graphic is used to read the time at which a certain mass loss (or conversion) is reached.

3.3 Results and Discussion

The term “thermal stability” used throughout this thesis is defined as the variation in the weight (or mass) of a sample as a function of temperature or time or both. According to this definition, a sample that presents a lower weight loss at certain temperature has higher thermal stability. Mass changes can occur because of sublimation, evaporation, decomposition or chemical reaction transformations (Ehrenstein et al., 2004). It is important also to highlight that the word “degradation” is used here as a synonym of weight loss.

It is equally important to note that at the typical temperature of processing engineering thermoplastics (250 ^{o}C for example) plant fibers may undergo chemical reactions where the products are solids (instead of gases); in this case the products will not be accounted for when using thermal gravimetric analysis and those reactions will not be considered as thermal degradation. The understanding of those reactions is beyond the scope of this research, since the most detrimental thermal degradation of the plant fiber is when gases are formed (leaving bubbles or voids inside the composites).

The thermal stability of six different wheat straw samples was investigated here under oxidative (air) and inert (nitrogen) atmospheres using Thermogravimetry Analysis (TGA) under isothermal and non-isothermal conditions.

3.3.1 Thermal Stability of Wheat Straw Fiber under Non-Isothermal Conditions

Initially, the results regarding the non-isothermal TGA analysis are discussed. Figure 21 and Figure 22 present the curves of weight percentage as a function of temperature (i.e., non-isothermal conditions) obtained at a heating rate of 10 °C/min in air and nitrogen environments, respectively, for all six samples tested.

It is possible to observe in Figure 21 (A and B) that the curves representing Large and Mid WS samples (red solid and dark brown long dash, respectively) are shifted to the right compared to the other curves, especially Pellet 2 and AWF WS curves (brown square dot and dark green solid, respectively). This implies that the Large and Mid WS samples have their starting point of thermal degradation at higher temperatures than other wheat straw samples. It is easier to observe these differences in Figure 21 B which offers a close up view of the Figure 21 A.

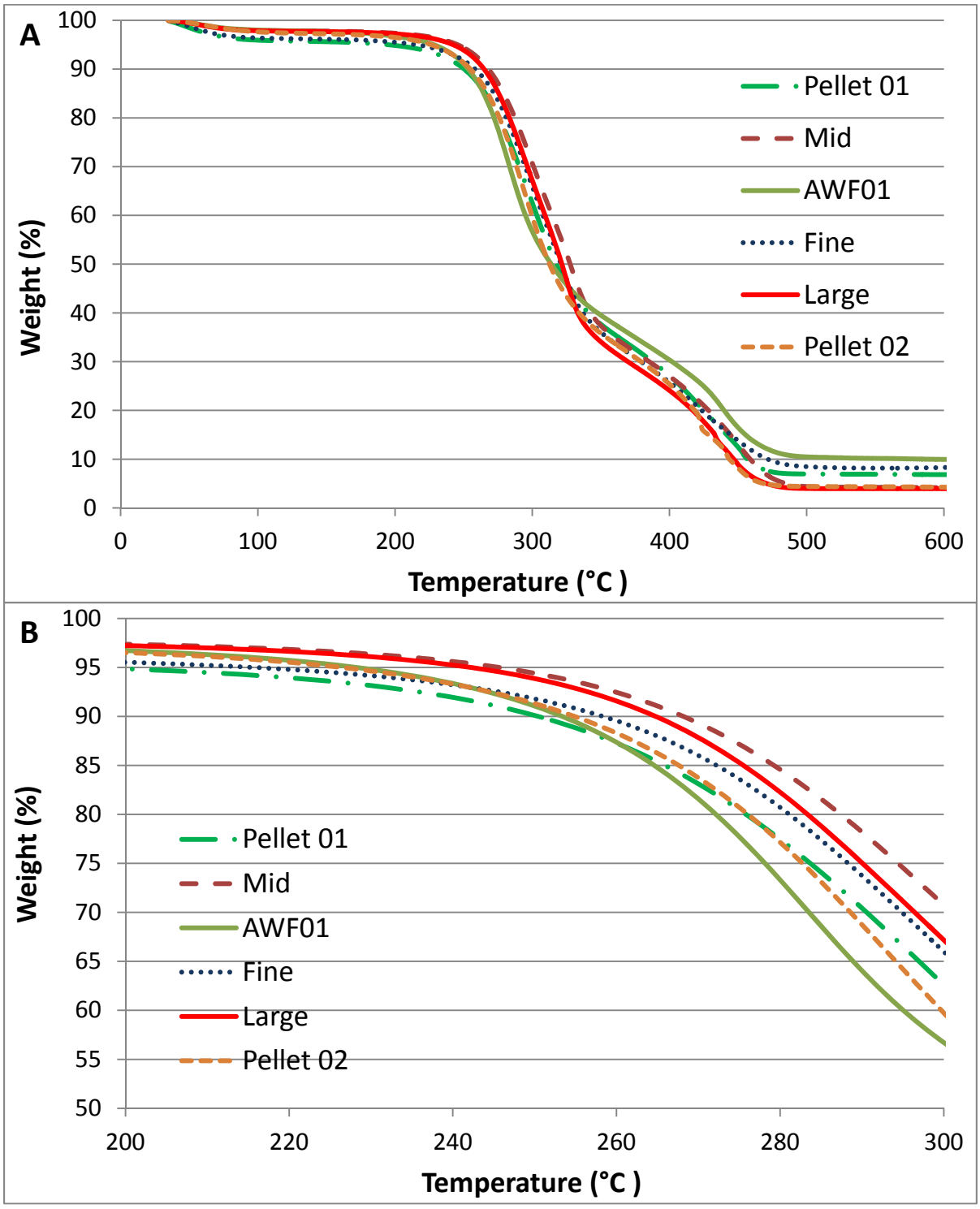

Figure 21: Thermogravimetry analysis (TGA) of the wheat straw samples using 10 °C/min heating rate and air atmosphere. Close up of the 200-300 °C region of the plot (A) is presented in the plot (B).

The possible reasons for these differences in the thermal stability of the wheat straw samples are discussed later in this chapter when the chemical composition of all six wheat straw samples is presented.

Similar to air, it can be seen from Figure 22 (A and B) that, under nitrogen atmosphere, the Large WS curve (red solid) is depicted at the right of the other TGA curves whereas the AWF WS curve (dark green solid) is located at the far left in the graph. However, this time, it appears that the differences between these curves are smaller than in the case of air atmosphere. As a consequence of that, thermal degradation of Large WS sample starts at only slightly higher temperatures than the degradation of other wheat straw samples in nitrogen atmosphere.

Based on these observations, it seems that Large and Mid WS samples have higher thermal stability than the other wheat straw samples, especially under air atmosphere.

However, it is difficult to determine the starting point of the degradation of the wheat straw samples by visually comparing the TGA curves. Even the onset temperature determined by software (e.g., Universal Analysis is the default software from TA Instruments installed in the TGA) can lead to higher variations on the starting temperature of degradation obtained because the onset temperature depends on the limits of each TGA curve set by the user.

Therefore, in order to reduce the variability when determining the beginning of the wheat straw thermal degradation, a specific value for weight loss (e.g., 1, 2, 5 or 10 %) can be selected as a reference. The temperature at this specific weight loss can be used to compare the differences in the thermal decomposition behavior of different samples (Ehrenstein et al., 2004). The temperature at 2 % of weight loss (denote as $T_{2\%}$) is commonly used as an indicator of how much degradation is acceptable for polymers. From this point on, the mechanical and thermal properties that are characteristic of a material start to be lost. The $T_{2\%}$ can be obtained from the TGA curves (Figure 21 and Figure 22), as illustrated by Figure 23.

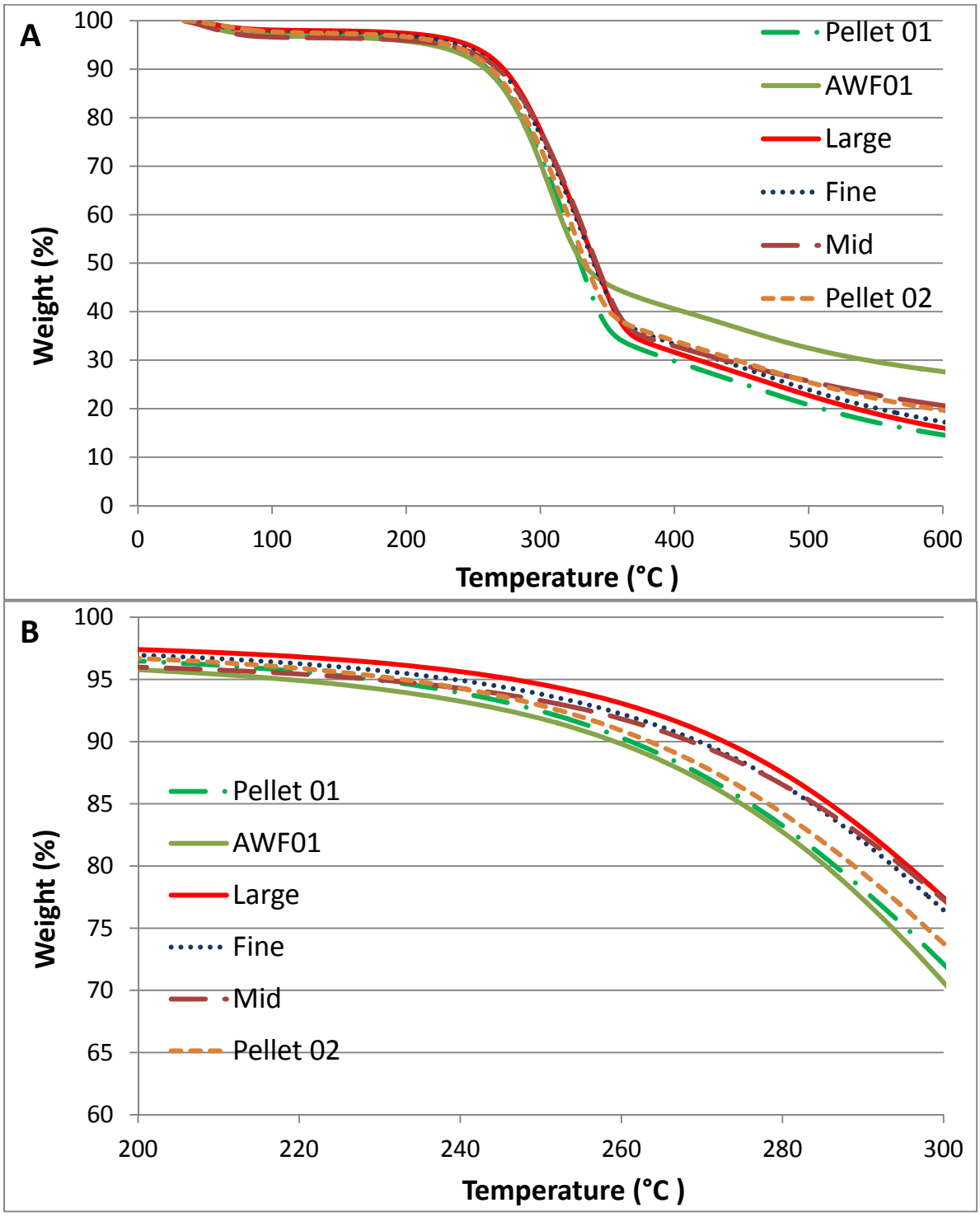

Figure 22: Thermogravimetry analysis (TGA) of the samples using 10 °C/min heating rate and nitrogen atmosphere. Close up of the 200-300 °C region of the plot (A) is presented in the plot (B).

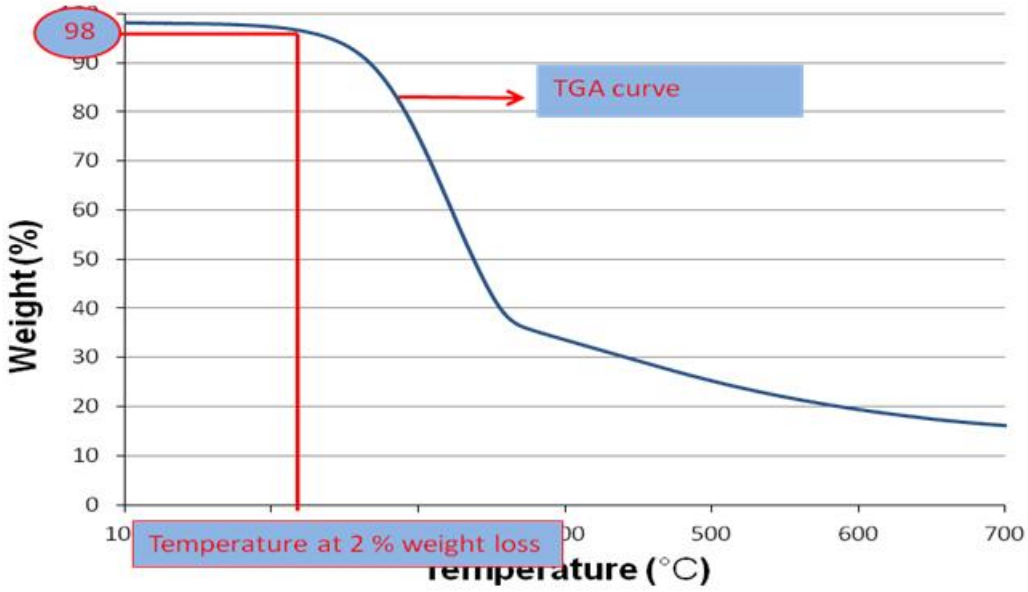

Figure 23: Procedure applied to obtain the temperature at 2 % weight loss from TGA curves.

The amount of moisture can vary from sample to sample. Therefore, the curves are normalized at 100 % at 150 ^{o}C. The 2 % of degradation ($T_{2\%}$) are obtained considering the 100 % at 150 ^{o}C. The moisture is all removed at 150 ^{o}C and all samples present a flat line around this temperature, making it very convenient for normalizing the weight loss. This procedure makes it easy to evaluate samples with different amounts of moisture and therefore it is not necessary to dry the samples before analysis.

Figure 24 displays the temperature where 2 % of degradation ($T_{2\%}$) happens for all six wheat straw samples. It can be seen that the Large and Mid WS samples have the 2% weight loss at higher temperatures than all the other samples in both air and nitrogen atmospheres. For example, the Mid WS sample under air and nitrogen had the $T_{2\%}$ at 237.8 and 238.1 °C, respectively; whereas, the AWF WS sample showed the 2 % weight loss at the lowest temperatures, 220.8 and 224.8 °C, under air and nitrogen, respectively.

The difference between the thermal stability ($T_{2\%}$) of these two wheat straw samples (Mid and AWF WS) is 17 and 13.3 °C in air and nitrogen, respectively. These differences do not represent a significant variation on the starting temperature of degradation. Natural fibers with different origin

(type and/or variety) tend to present considerably different chemical compositions and therefore higher variations in the samples' thermal properties.

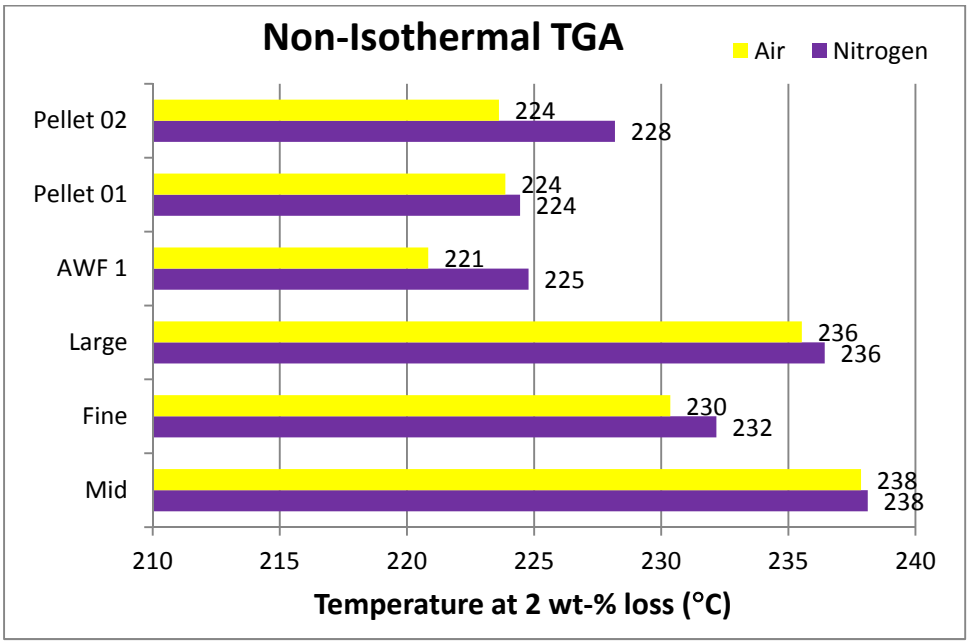

Figure 24: Effect of air and nitrogen atmospheres in the temperature at 2 % weight loss ($T_{2\%}$) of wheat straw samples during non-isothermal TGA analysis (10 °C/min heating rate).

In addition, the thermal degradation of wheat straw samples occurs generally faster in air than nitrogen atmosphere. For example, Figure 24 shows that the thermal degradation of Pellet 2 WS sample starts at 223.6 °C under air compared to 228.2 °C in nitrogen atmosphere.

It is easier to observe this difference by looking at the overlapping TGA and DTGA curves of Pellet 2 WS sample in air and nitrogen (Figure 25 A and B). It can be seen in Figure 25 that the curve representing Pellet 2 WS under nitrogen (brown dash) is displayed to the right of the curve for the test performed in air (blue solid). As a consequence, the thermal degradation of Pellet 2 WS sample starts at lower temperature in air than nitrogen atmosphere. In fact, the thermal degradation of all six wheat straw samples starts earlier in air atmosphere compared to nitrogen atmosphere even though Figure 25 shows only the TGA curves for one wheat straw sample (Pellet 2 WS) in order to facilitate the comparison.

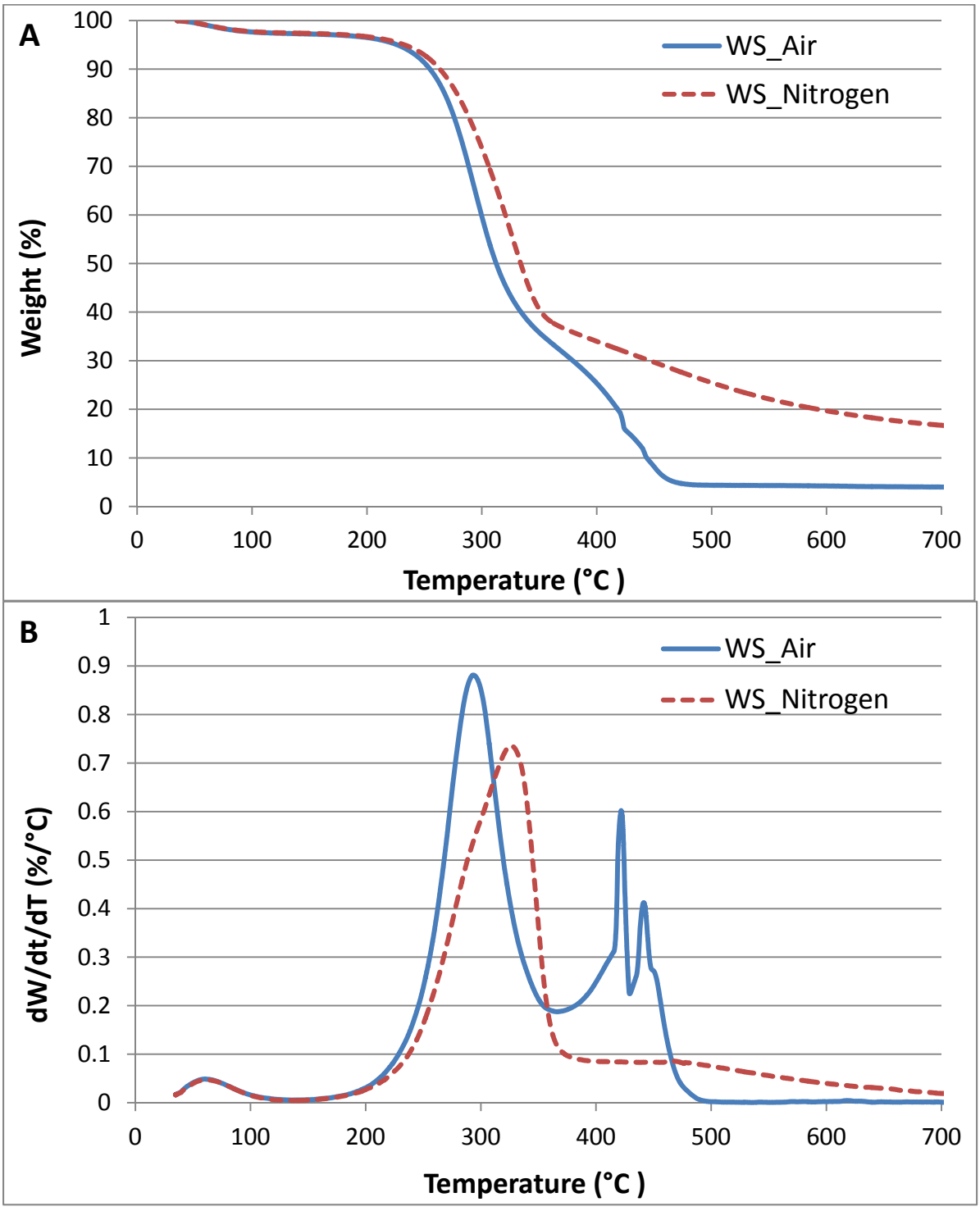

Figure 25: Comparison between TGA curves (A) and DTGA curves (B) obtained under air and nitrogen atmospheres for Pellet 2 sample.

It can also be seen in Figure 25 (A and B) that wheat straw fiber has four main weight loss steps under air atmosphere whereas, the thermal degradation of wheat straw under nitrogen atmosphere happens in three main weight loss steps. A weight loss step is a decrease on the weight of a sample with increasing temperature (and/or time) and can be identified by a drop in the TGA (thermogravimetry) curve (Figure 25 A). It should be clarified that similar thermal degradation behavior was observed for the other wheat straw samples even though just the case of Pellet 2 is graphically shown here. The data for the other samples are presented in the Appendix.

However, when there are several steps of weight loss, it may be difficult to determine the boundary between two weight loss steps utilizing only TGA curves (Figure 25 A). This happens because the multistep TGA curves generally do not have an interval with constant weight between two steps of weight loss, but rather a close succession of overlapping losses of weight.

In this case, the boundary between these two steps can be determined utilizing the time derivative signal dm/dt (Figure 25 B). The end of one weight loss step and the beginning of the next step is indicated by the smallest value on the differential thermogravimetry (DTGA) curve between the two steps and each weight loss step is represented by a peak in the DTGA curve (Ehrenstein et al., 2004).

In this way, it is possible to observe that the initial weight loss step is identical for both atmospheres (air and nitrogen). These steps are represented by the small drop in the weight of TGA curve (Figure 25 A) and by the small peak in the DTGA curves (Figure 25 B) both in the 35-130 °C temperature interval. These weight losses (5.3 and 5.1 wt-% in air and nitrogen, respectively) are consistent with the typical moisture content reported for WS fiber (between 4 and 7 wt-%, according to Hornsby et al., 1997; Sardashti, 2009) and therefore due to the evaporation of water from wheat straw samples.

After the first weight loss step caused by water removal, three peaks representing three different steps of weight loss can be observed in the DTGA curve of wheat straw under air atmosphere (Figure 25 B, blue solid). The first peak is located between the temperature range of 130 and 363.5 ºC with a weight loss of 62.6 wt-% (Figure 25 A and B, blue solid). The second peak happens between 363.5 and 430 ºC and the weight loss is approximately 17.8 wt-% whereas, the third peak is located between 430 and 500 ºC with a weight loss of 10.1 wt-%. Due to the oxidation of organic material that occurs up to 500 ºC, above this temperature there is no weight loss and only inorganic material (e.g., silica) is left in the residue (approximately 4.1 wt-% at 600 ºC).

Compared to air atmosphere, wheat straw fiber (Pellet 2 WS and the other wheat straw samples) is more thermally stable and has two steps of weight loss under nitrogen atmosphere after the initial removal of water. The first and main thermal degradation step occurs in the 130 to 375.80 ºC temperature range with a weight loss of 59.7 wt-% (Figure 25 A and B, red dash). The second peak happens between 375.8 and 600 ºC and the weight loss is approximately 16.1 wt-%.

Due to the inert atmosphere (nitrogen), there is a larger amount of residue left at 600 ºC (19.2 wt-%) compared to the residue left in oxidative atmosphere (4.1 wt-%). Similar values have been reported in the literature for wheat straw pyrolysis, that is, thermal degradation under nitrogen atmosphere (Alemdar and Sain, 2008; Sardashti, 2009; Yang[1] et al., 2007). Most of this residue (around 45 wt-%) is generated by the thermal degradation under nitrogen atmosphere of lignin which generally produces high amount of solid residue (Yang[1] et al., 2007). Above 600 ºC, there is only marginal weight loss because the residue left is mostly inorganic material.

The first weight loss step between 130 to 375.8 C ºC has been attributed to the pyrolysis of the three main wheat straw components, i.e., lignin, hemicellulose and cellulose (Hornsby[1] et al., 1997; Yang[1] et al., 2007). First lignin starts to thermally degrade at 190 ºC followed by hemicellulose at 210 ºC and finally cellulose at 315 ºC (Yang[1] et al., 2007). However, the rate of degradation of these three wheat straw components is significantly different. Lignin has the lowest degradation rate while hemicellulose has the highest one. Because of that, even though lignin starts to degrade first (at 190 ºC), hemicellulose is completely degraded before lignin and cellulose are completely degraded.

The main products generated during the pyrolysis of lignin, hemicellulose and cellulose are CO, CO_2, H_2, CH_4 and organic compounds. Hemicellulose releases primarily CO and CO_2 while lignin is the main component responsible for the CH_4 production. Organic compounds (e.g., C=O, C-O-C etc) are mostly generated from hemicellulose and cellulose at low temperatures, i.e., 200-400 ºC and 300-450 ºC, respectively (Yang[1] et al., 2007).

Similar thermal degradation behavior is observed under air atmosphere, even though the starting temperature of degradation of the wheat straw components (lignin, hemicellulose and cellulose) is lower compared to values found in nitrogen atmosphere. In addition, similar decomposition products are produced during the complex chemical reactions responsible for the thermal degradation of lignin, hemicellulose and cellulose in air atmosphere.

It can be concluded that Large and Mid WS samples are more thermally stable than other WS samples, especially Pellet 2 and AWF WS samples. However, these differences are small and the main thermal degradation of WS samples starts in a narrow window of temperature which goes from 220.8 to 237.8 °C and from 224.8 to 238.1 °C in the case of air and nitrogen atmospheres, respectively.

3.3.2 Thermal Stability of Wheat Straw Fiber under Isothermal Conditions

Understanding the thermal stability of wheat straw fiber under isothermal conditions (i.e., constant temperature) is especially important in the case of utilization of this fiber in thermoplastic composites. In this case, processing the fiber with thermoplastics requires exposure to isothermal temperatures between 200 and 250 ^{o}C depending on the polymer utilized.

Therefore, an attempt to simulate and estimate the thermal degradation that wheat straw samples would suffer during preparation of thermoplastic composites is made by studying the thermal stability of the wheat straw fiber samples using isothermal gravimetric analysis.

During this analysis, the wheat straw samples were heated (using 50 ^{o}C/min heating rate) from room temperature to the selected temperature (either 200 or 250 ^{o}C). Then this temperature was kept constant for 30 minutes under either air or nitrogen atmosphere. These two temperatures (200 and 250 ^{o}C) were chosen because they are typical temperatures for processing polypropylene (PP) and polyamide-6 (PA-6). These two thermoplastics are widely utilized and very relevant thermoplastics in the automotive industry.

Figure 26 presents the isothermal curves of weight percentage as a function of time at 200 °C for all the six wheat straw samples under air (A) and nitrogen (B) atmosphere. The figure does not show a significant difference between the thermal stability of the wheat straw samples regardless of the atmosphere utilized (air or nitrogen).

Along the entire interval of time (from 5 to 30 minutes) the weight difference between the most (Large WS) and least (AWF WS) thermal stable wheat straw samples was not greater than 3 % under nitrogen atmosphere and 4 % air atmosphere.

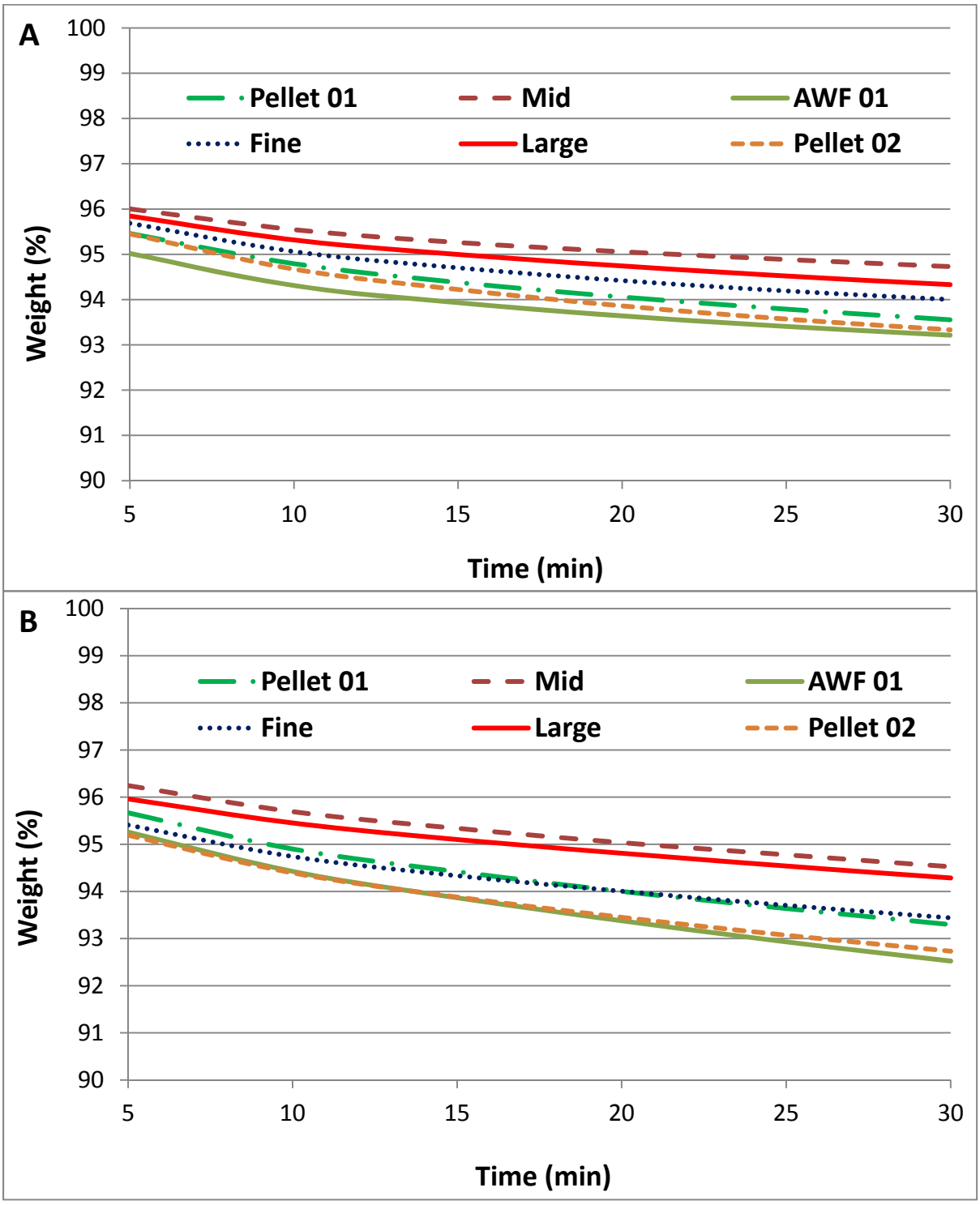

Figure 26: Isothermal curves obtained at 200 °C under nitrogen (A) and air (B) atmospheres for the wheat straw samples.

On the other hand, a different thermal behavior is observed when wheat straw is exposed to higher temperature (250 °C). This behavior depends on the wheat straw sample and atmosphere utilized.

In the case of nitrogen atmosphere, all the wheat straw samples curves are close to each other (Figure 27 A) whereas under air atmosphere there is a gap between the isothermal curves (Figure 27 B), especially the curves representing the most and least thermal stable wheat straw samples.

For example, under nitrogen atmosphere (Figure 27 A), even though the Large and Mid wheat straw curves (red solid and brown dash, respectively) are displayed at the top of the graph (region of smaller weight loss) and the curves representing Pellet 1 and AWF samples (green long dash dot and green solid, respectively) are located at the bottom of the graph; the separation between these curves (the most and least thermal stable samples) is small (between 0.4 and 1.5 %) and constant throughout the time of the isothermal test (5 to 30 minutes).

On the other hand, under 250 °C and air atmosphere (Figure 27 B), there is a larger gap between the most (Mid WS) and least (AWF WS) thermally stable wheat straw samples. The curve representing Mid WS sample (brown dash) is displayed at the top of the graph and even after 30 minutes of exposure to 250 °C, the Mid WS curve is above 80 % of weight. In contrast, the AWF WS curve (green solid) exhibits much sharper decline and is below the 80 % after approximately 15 minutes of heating at 250 °C. The AWF WS sample achieves the highest thermal degradation after 30 minutes when the AWF curve reaches the region of 60-65 %.

In order to quantify and compare the difference between the thermal stability of these wheat straw samples, the weight percentage for each wheat straw sample after 10 minutes of exposure to 200 and 250 °C (Wt200 and Wt250, respectively) was determined according to Figure 19 and presented from Figure 28 to Figure 31.

Ten minutes was chosen to represent the time that the wheat straw fiber would remain at high temperature inside of an extruder or injection moulding machines during the production of medium or large automotive components (with more than 3 lbs) such as interior trimming or dashboard, under the hood, or door trim panels for example. The residence time of each component varies from part to part or even from company to company. The goal here was to evaluate a time that is relevant in commercial applications.

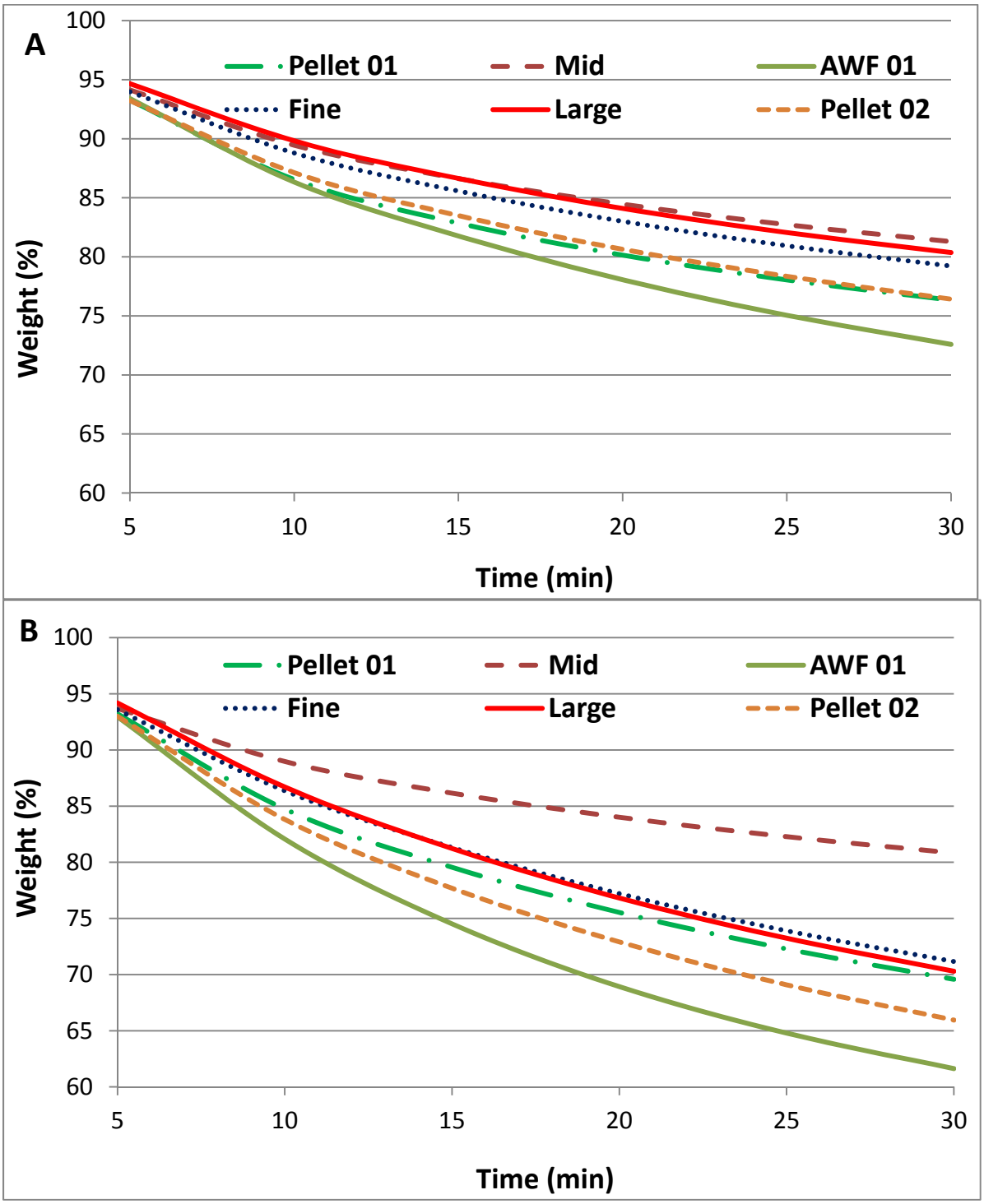

Figure 27: Isothermal curves obtained at 250 °C under nitrogen (A) and air (B) atmospheres for the wheat straw *samples.*

It can be seen from Figure 28 that all wheat straw samples suffered small thermal degradation (i.e., decrease on the initial weight) after 10 minutes of exposure to 200 °C. In addition, the thermal stability of wheat straw samples at 200 °C in nitrogen is similar to air atmosphere. For example, after 10 minutes of exposure at 200 °C the initial weight of the most (Mid WS) and least (AWF WS) thermal stable wheat straw samples have decreased to 95.3 and 93.9 %, respectively.

Therefore, these results indicate that wheat straw samples have low thermal degradation when exposed to 200 °C for 10 minutes independently of the atmosphere employed, either air or nitrogen.

This finding is in agreement with other research in our group that has demonstrated that it is possible to produce polypropylene filled with straw fiber manufactured by injection molding.

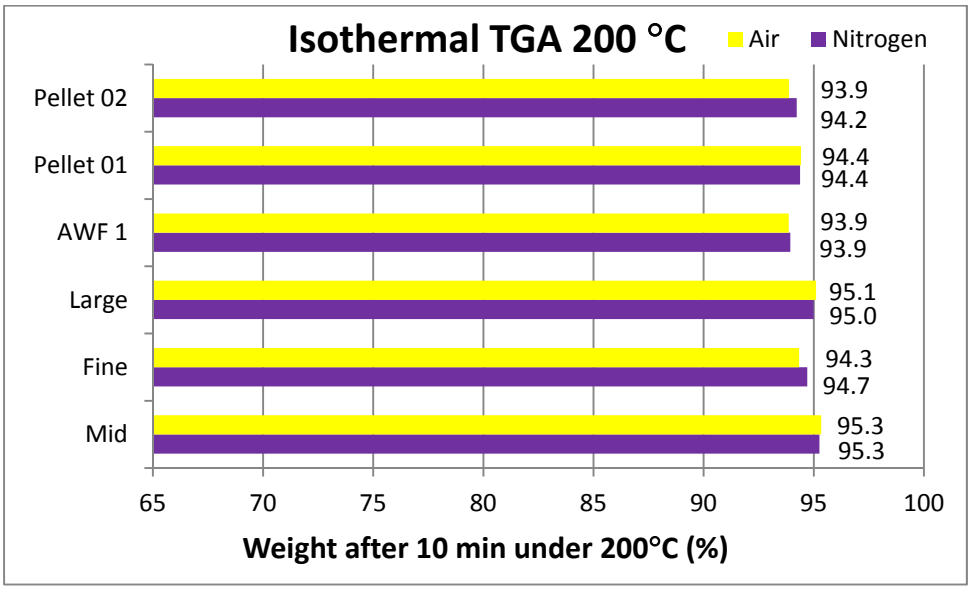

Figure 28: Effect of air and nitrogen atmospheres on the thermal stability (Wt200) of wheat straw samples during isothermal analysis at 200°C.

On the contrary, the thermal degradation of wheat straw samples at 250 °C is more pronounced in air than in nitrogen atmosphere. For example, it can be seen from Figure 29 that the initial weight of Pellet 2 WS sample is significantly reduced to 83.5 and 77.7 % under nitrogen and air atmospheres, respectively, after 10 minutes of exposure to 250 °C (Wt250). This way, the thermal degradation of

Pellet 2 WS sample is 5.8 % larger in air than in nitrogen atmosphere. Similar results were obtained for the other wheat straw samples, except for the Mid WS.

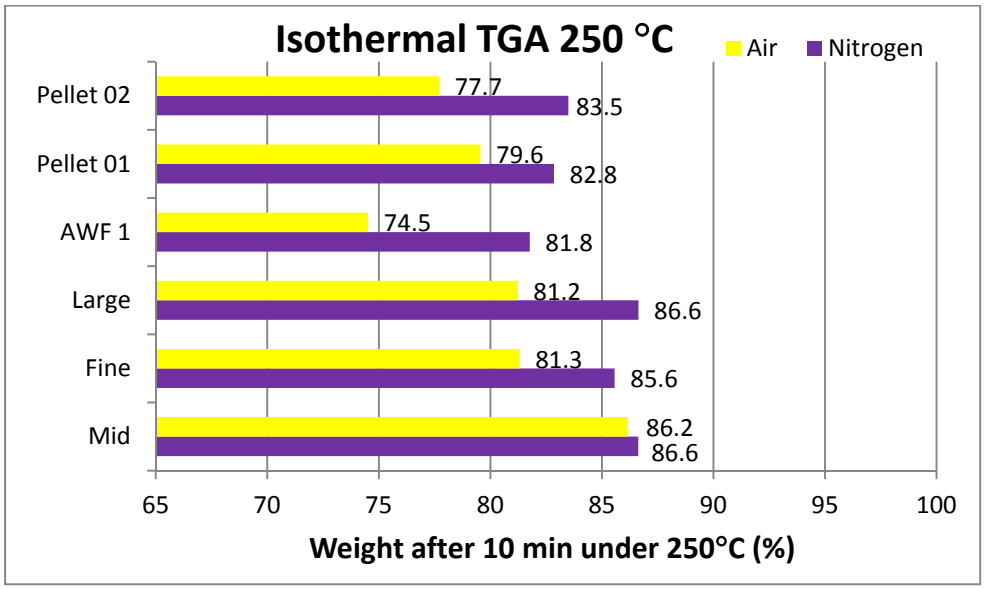

Figure 29: Effect of air and nitrogen atmospheres in the thermal stability (Wt250) of wheat straw samples under isothermal analysis at 250°C.

The average decrease on the initial weight (after 10 minutes, Figure 29) for the six wheat straw samples under nitrogen is 84.49 % (ranging from 86.6 to 81.8 %) whereas; this value is 80.08 % under air atmosphere (ranging from 86.2 to 74.5 %).

Since the thermal degradation of wheat straw fibers at 250 °C is bigger in air than in nitrogen atmosphere, the production of thermoplastics composites with straw fiber should be performed using nitrogen atmosphere if the processing temperature (compounding and molding) is in the vicinity of 250 ^{o}C.

Additionally, it is important to highlight the significant increase in the degradation of wheat straw samples when the temperature of exposure is raised from 200 to 250 °C as illustrated by Figure 30 and Figure 31. For example, increasing the temperature from 200 to 250 °C (under nitrogen

atmosphere) decreases the initial weight of Pellet 2 WS sample by 10.7 %, from 94.2 to 83.5 %, respectively (Figure 30).

The drop on the weight of Pellet 2 WS sample is even bigger (16.2 %, from 93.9 to 77.7 %) when the same temperature increase (from 200 to 250 °C) is performed under air atmosphere (Figure 31).

These results show that the thermal stability of wheat straw fiber is sufficient to produce composites with polypropylene because this polymer requires exposure to processing temperatures approaching only 200 °C rather than 250 °C.

On the other hand, there is a necessity of improving the thermal stability of wheat straw fiber in order to fabricate composites with engineering thermoplastics (like polyamide-6) with minimal or reduced thermal degradation. Also, wheat straw fibers degraded faster under air than nitrogen atmosphere at 250 °C. Because of that, it would be better to utilize nitrogen atmosphere when processing wheat straw fiber with polyamide-6 or other thermoplastics that have higher melting temperatures. Processing composites under nitrogen blanket is a procedure that can be implemented at industrial scale, however it requires modification of common equipment.

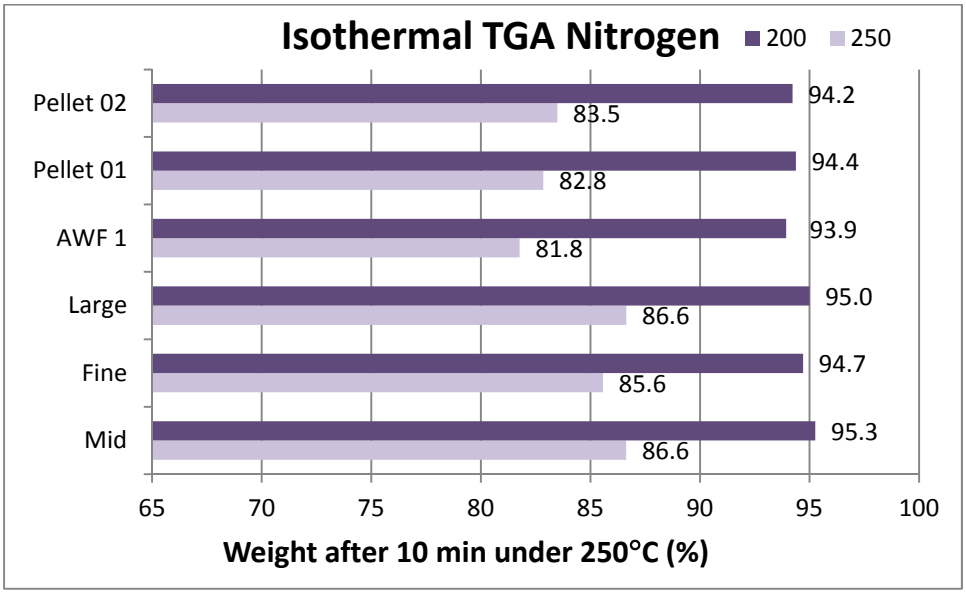

Figure 30: Effect of temperature increment (from 200 to 250 °C) on the thermal stability (Wt200 and Wt250) of wheat straw samples during isothermal analysis under nitrogen atmosphere.

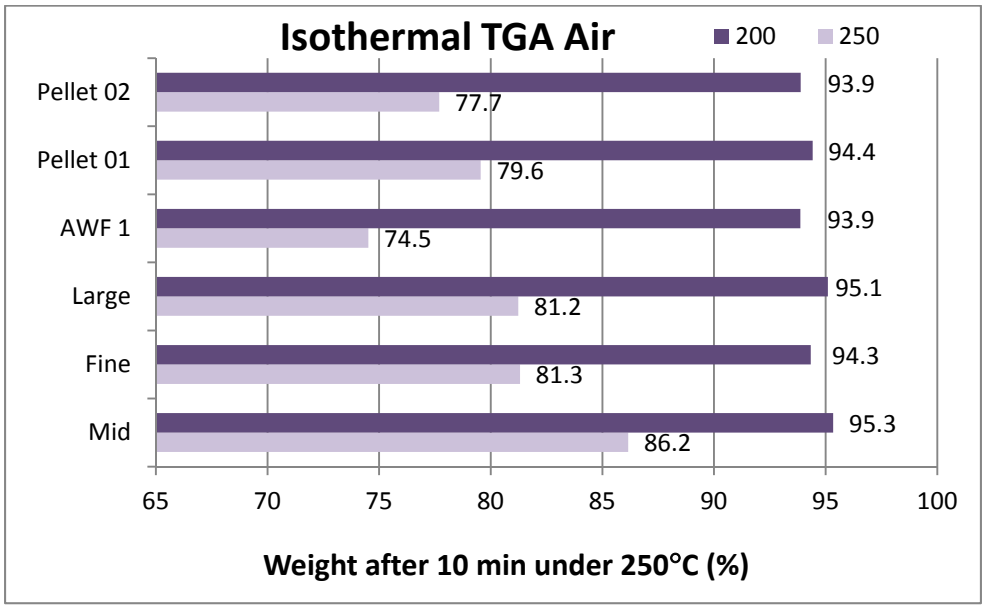

Figure 31: Effect of temperature increment (from 200 to 250 °C) on the thermal stability (Wt200 and Wt250) of wheat straw samples during isothermal analysis under air atmosphere.

3.3.3 Chemical Composition of Wheat Straw Samples

In an attempt to understand the different thermal behavior of the wheat straw samples observed in the previous section, the chemical composition analysis was performed. The samples were analyzed by an external laboratory (AgriFood Laboratories, in Guelph) because of the low cost of analysis and the fact that this test is not implemented in our research laboratory in Waterloo. The method was described previously in this document (Material and Methods section).

Plant fibers are mostly made of cellulose, hemicellulose, lignin and other low molecular weight compounds such as pectin and sugars. Low amounts of inorganic materials (e.g., silica) may also be present in the fibers (Feng et al., 2008; Hornsby[1] et al., 1997; Mohanty et al., 2005; Mwaikambo and Ansell, 2002; Lawther et al., 1996; Sun et al., 1998; White and Ansell, 1983; Kiran, 1986).

It has been widely reported in the literature that the chemical composition of plant fibers can affect their thermal stability (Alemdar and Sain, 2008; Feng et al., 2008; Hornsby[1] et al., 1997; Ouajai and

Shanks, 2005; Zhang et al., 2008). For example, the higher cellulose content of hemp fiber has been suggested as the reason for the higher thermal stability of hemp fiber compared to other plant fibers containing lower cellulose content (Feng et al., 2008; Ouajai and Shanks, 2005).

The amount of cellulose, hemicellulose, lignin, ash and others components for each wheat straw sample is presented in Figure 32. Table 7 shows the average amount as well as the highest and lowest values of these wheat straw components (i.e., cellulose, hemicellulose, lignin etc).

It can be seen from Figure 32 that cellulose along with hemicellulose are the most abundant components of wheat straw samples. The average amount of cellulose and hemicellulose were 43.6 and 25.6 wt-%, respectively (Table 7).

On the other hand, the least abundant wheat straw components are lignin and inorganic material (ash content) which correspond in average to 8.1 and 5.8 wt-%, respectively.

Interestingly, on average 16.8 wt-% of wheat straw samples are made of different materials which are not individually identified by the chemical composition test. However, it is believed that these materials are mostly moisture and low molecular weight compounds (e.g., pectin, waxes, water soluble sugars etc); therefore they are all included in the same group which is named here Soluble Materials or Others (Sardashti, 2009, Guettler, 2009). Therefore, wheat straw samples have higher amount of these soluble materials (Others) than either lignin or inorganic material. This observation is important because these soluble materials start to evaporate at very low temperatures (40-60 °C).

In addition, Table 7 shows also the variation in the amount of each wheat straw component, that is, the difference between the wheat straw sample with the highest and the lowest amount of each one of the wheat straw components (i.e., cellulose, hemicellulose, lignin, ash and soluble) according to the equation shown below.

$$Variation\ (\%) = \frac{(WS_H - WS_L)}{WS_H} \qquad \textit{Equation 7}$$

It is possible to observe that among all the wheat straw components, cellulose is the one that suffers the lowest content variation which was only 9.3 %. The highest and lowest cellulose contents were 45.5 and 41.3 wt-% belonging to Mid and Pellet 2 WS samples, respectively.

Table 7: Average, and, the highest and lowest values of wheat straw components.

Composition	WS_H (Highest)	WS_L (Lowest)	Range[A] (wt-%)	Variation[B] (%)	Average (wt-%)	Standard Deviation
Hemicellulose	27.9	20.7	7.2	25.7	25.6	2.5
Lignin	9.9	6.3	3.5	35.8	8.1	1.3
Cellulose	45.5	41.3	4.2	9.3	43.6	1.8
Ash	10.2	3.5	6.8	66.2	5.8	2.5
Others	19.6	13.5	6.1	31.7	16.8	2.3

A: Range=WS_H - WS_L; B: Variation (%) = (WS_H- WS_L/ WS_H)*100 (Equation 1)

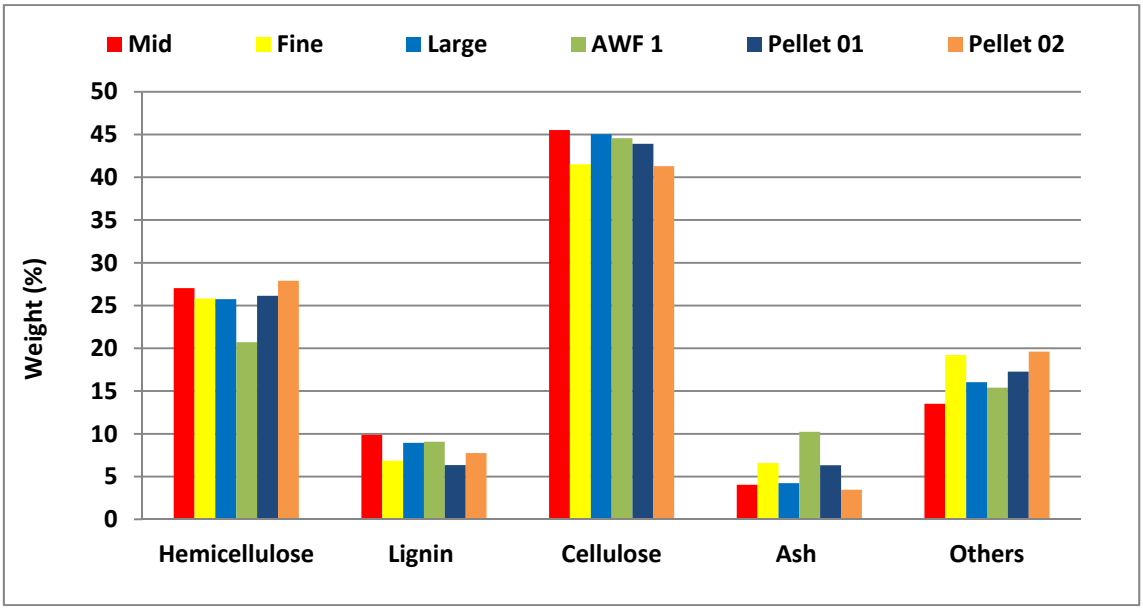

Figure 32: Chemical composition of the wheat straw samples.

Compared to cellulose, the hemicellulose content suffered a bigger variation going from 20.71 wt-% in AWF sample to 27.9 wt-% in Pellet 2 sample. The difference between these two wheat straw samples corresponds to a variation of 25.7 % on the hemicellulose content.

Lignin and inorganic material (ash) presented the highest variation on its amount. The ash content went from 3.5 wt-% in Pellet 2 WS sample to 10.2 wt-% in AWF WS sample which represents a

variation of 66.2 % between these two samples. Similarly, lignin content ranged from 6.4 wt-% in Pellet 1 WS sample to 9.9 wt-% in Mid WS sample. The difference between these two wheat straw samples (3.5 wt-%) correspond to a 35.8 % variation on the lignin content.

These variations in the chemical composition of wheat straw samples can be caused by different factors such as wheat straw type (variety), maturity and cultivation conditions (place, season, temperature, amount of rain, type of soil etc).

It has been widely suggested that different chemical composition can lead to plant fibers with significantly different thermal stability behavior (Feng et al., 2008; Hornsby[1] et al., 1997; Mohanty et al., 2005; Mwaikambo and Ansell, 2002). For example, hemp fiber has higher cellulose content than wheat straw, around 67-78 % and 34-40 %, respectively and it is believed that the higher cellulose content is one of the reasons for the higher thermal stability of hemp fiber which starts to thermally decompose at a temperature 50 °C higher than wheat straw (Feng et al., 2008; Hornsby[1] et al., 1997; Ouajai and Shanks, 2005; Mohanty et al., 2005).

In the same way, the variations in the chemical composition of wheat straw samples may explain the different thermal stability behaviors of the six wheat straw samples.

For example, Mid WS sample has the lowest amount of soluble materials (Others) and the highest cellulose content among all the six wheat straw samples. The higher cellulose content combined with lower content of soluble materials may be the reason for the high thermal stability presented by the Mid WS sample.

It is well-known that cellulose has the highest thermal stability among the wheat straw components. On the other hand, hemicellulose and especially soluble materials start to evaporate (or thermally degrade) at lower temperatures (230 °C and 40-60 °C, respectively).

Therefore, samples with higher content of hemicellulose and soluble materials are expected to start degradation at lower temperatures. This corresponds well with the case of Pellet 2 WS sample which presents the lowest cellulose content (41.3 wt-%) along with the highest hemicellulose and soluble materials contents (27.9 and 19.6 wt-%, respectively). As a consequence, Pellet 2 WS sample has one of the lowest thermal stability among all six wheat straw samples.

In an attempt to verify if there is a simple connection between the chemical composition and thermal stability of the wheat straw samples which could be easily visualized, the content of each

wheat straw component (i.e., cellulose, hemicellulose etc) was plotted against the thermal stability values (i.e., $T_{2\%}$, Wt200, Wt250) for all the six wheat straw samples.

These plots are presented from Figure 33 to Figure 36 and it appears that altering the amount of the wheat straw components affects the thermal stability (i.e., $T_{2\%}$, Wt200, Wt250) of the wheat straw samples. For example, it can be seen in Figure 33 that wheat straw samples with higher cellulose content seem to have better thermal stability.

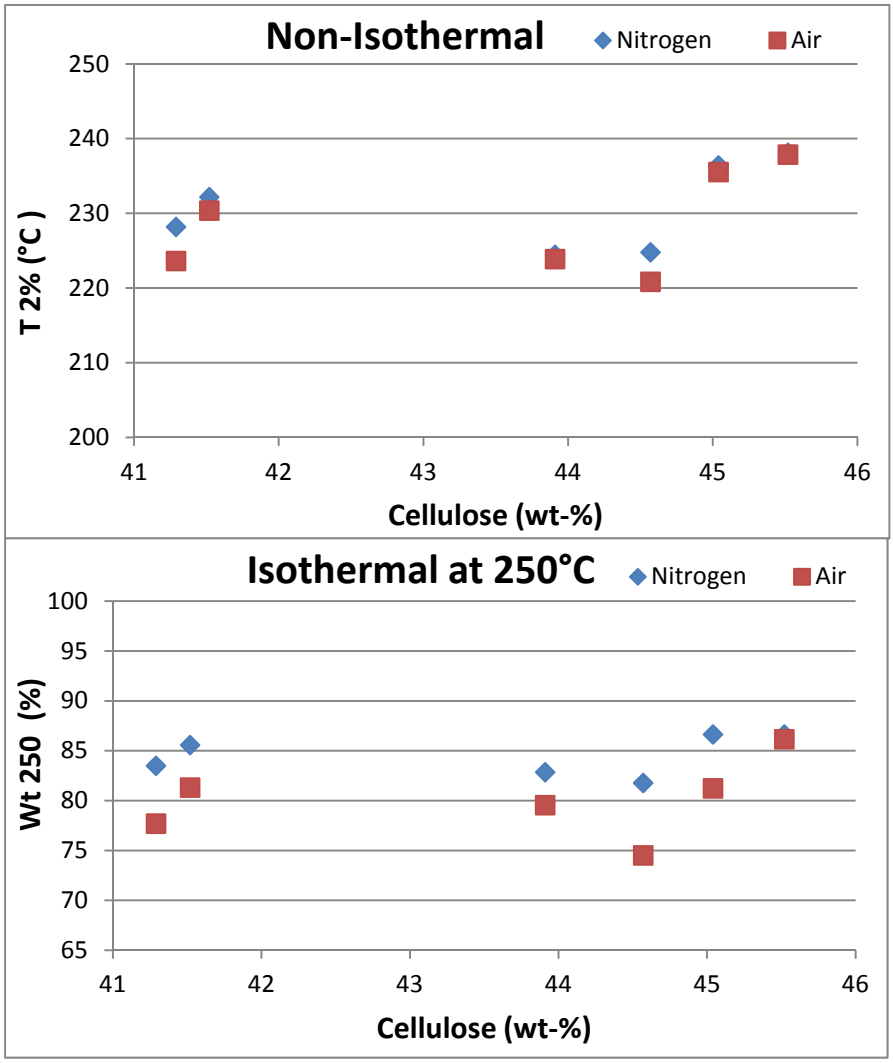

Figure 33: Thermal stability ($T_{2\%}$ and Wt250) versus the cellulose content of the six wheat straw samples.

However, this behavior was not observed for all wheat straw samples (two samples in the case of cellulose content) and thereby it was not possible to determine a clear trend such as a linear relationship between amount of cellulose or any other wheat straw components and thermal stability.

For example, AWF WS sample has low amounts of hemicellulose (and soluble materials - Others) and therefore AWF WS sample should have a good thermal stability. However, this wheat straw sample has one of the lowest values of thermal stability.

Therefore, it seems that there is a more complex relationship between chemical composition and thermal stability of wheat straw samples. This could happen because of the complex structure interconnecting the individual components of the wheat straw fiber and the interaction between the chemical reactions responsible for the thermal degradation of these wheat straw components. In this way, it is very likely that a more complex model it is necessary to accurately describe the relationship between chemical composition and thermal stability of the wheat straw samples.

First the wheat straw components are tightly interconnected in the cell wall, which makes it difficult to isolate the effect of each one of these wheat straw components in the thermal stability of the whole straw fiber. In fact, it is very difficult to extract each one of the wheat straw components (cellulose, hemicellulose or lignin) without modifying them. Because of that, the actual cellulose present in the wheat straw sample is different from the cellulose extracted and commercially available for example.

Second, there is interaction between the individual wheat straw components during thermal degradation which makes it very complex to measure the effect of individual components in the thermal stability of the whole wheat straw fiber. For example, lignin starts its thermal degradation at the lowest temperature, but at elevated temperatures it works as an antioxidant (preventing thermal degradation) for other components. Therefore, the products of degradation of one wheat straw component (lignin) may affect the rate of thermal degradation of other wheat straw components (such as cellulose).

Because of these reasons, it was not possible to observe a simple relationship between chemical composition and thermal stability of wheat straw samples. This relationship is likely to be very complex and it may not be possible to describe it in detail with the experiments carried out in this research.

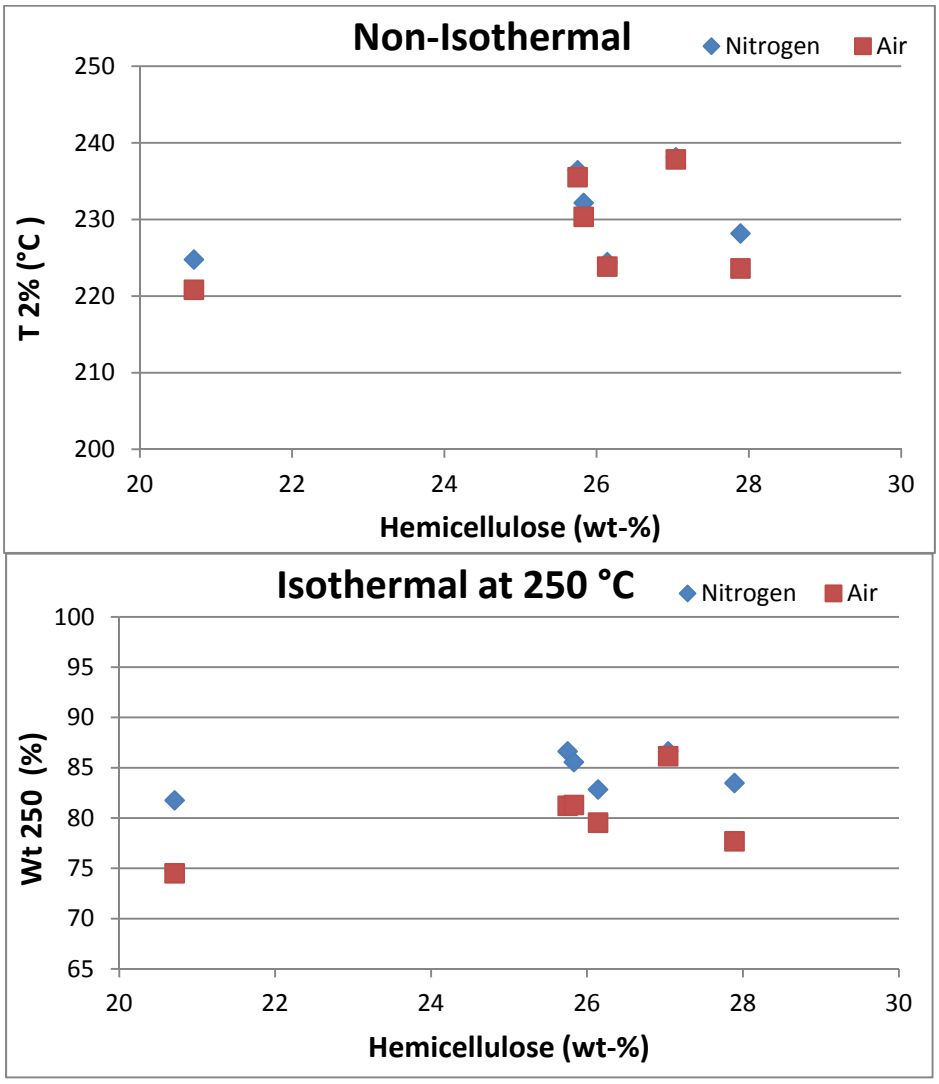

Figure 34: Thermal stability ($T_{2\%}$ and Wt250) versus the hemicellulose content of the six wheat straw samples.

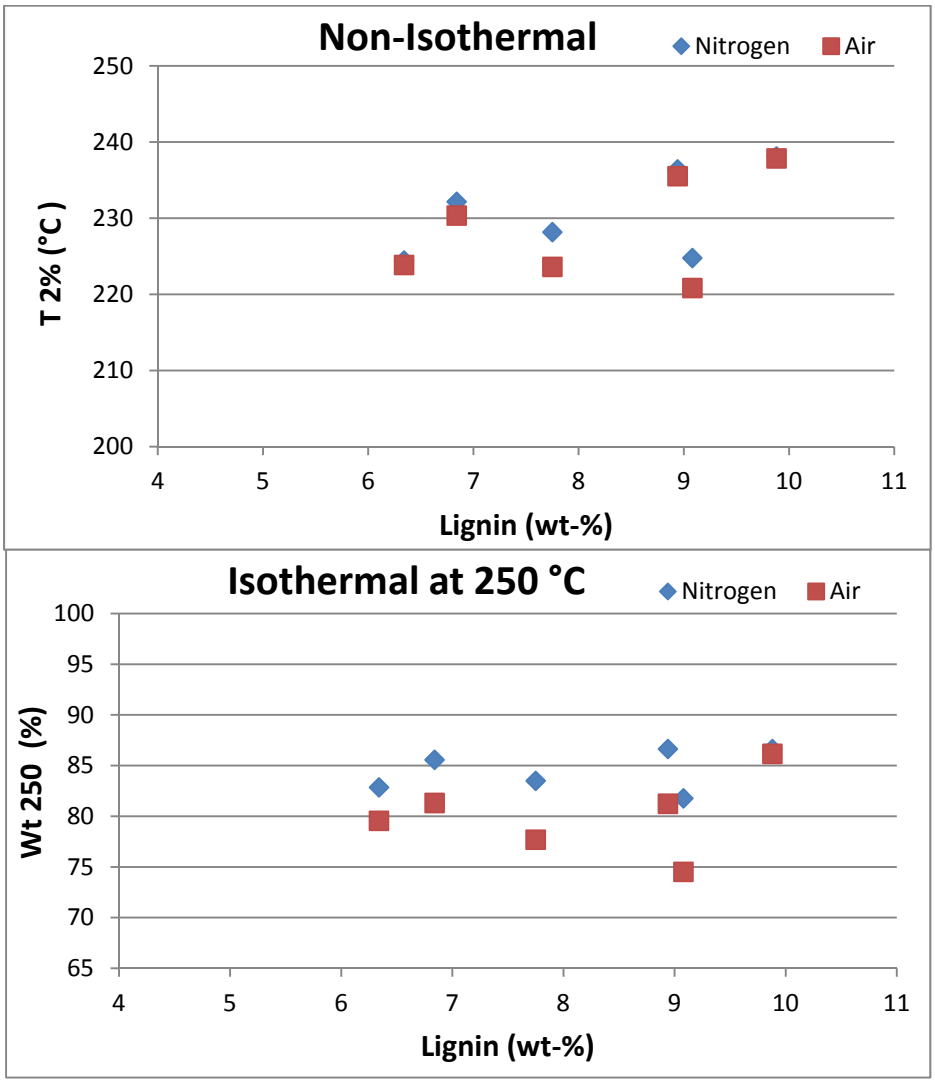

Figure 35: Thermal stability ($T_{2\%}$ and Wt250) versus the lignin content of the six wheat straw samples.

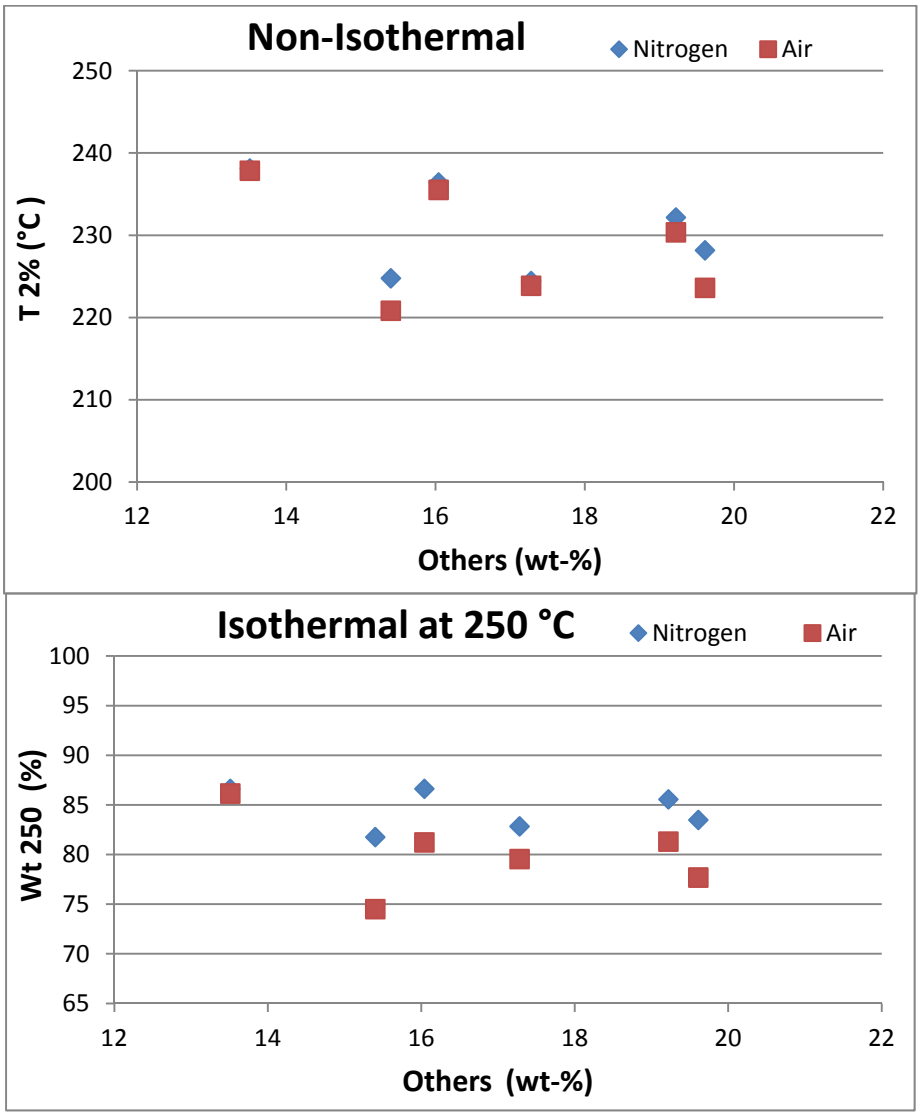

Figure 36: Thermal stability ($T_{2\%}$ and Wt250) versus the Others (soluble material) content of the six wheat straw samples.

3.3.4 Chemical Kinetics of Thermal Degradation of Wheat Straw Fiber

A chemical kinetics study of the thermal degradation was performed with the assistance of an isoconversional method as an attempt to quantify the thermal stability of the straw fibers. It is expected that this knowledge can be utilized to identify and select fibers with superior thermal stability and consequently to prevent or minimize the thermal degradation of straw fiber during the preparation of thermoplastic composites.

Initially, the isothermal curves of weight versus time (Figure 37) for the Mid wheat straw sample at different temperatures and air atmosphere are discussed. After that, the chemical kinetic study of the thermal degradation process is presented.

It can be observed in Figure 37 that the curves representing 160 and 180 °C isothermal (red dot and dark square curves, respectively) have a different shape compared to the isothermal curves of 240 and 250 °C (red dot and dark square curves, respectively).

The difference in the shape of the curves demonstrates the influence of temperature on the rate of thermal degradation (i.e., speed of weight loss) and is more pronounced in the time interval of 0-400 minutes (highlighted in Figure 37).

Therefore, at lower temperatures (i.e., 160 and 180 °C) the thermal degradation is minimal and progresses slowly. For example, even after 400 minutes of exposure at temperatures of 160 and 180 °C, wheat straw has suffered a weight loss of 9.5 % and 11.1 %, respectively. These values are not very significant considering that from 4 to 7 % of these weight losses can be attributed to the evaporation of water.

On the other hand, thermal degradation becomes faster and more severe as the temperature is continuously increased especially above 240 °C. For example, wheat straw fibers suffer a weight loss of 38 % and 62.5 % after 400 minutes at 220 and 240 °C, respectively.

In the same fashion, the time needed to reach a certain weight loss is dramatically reduced as temperature increases. For example, 10 % of degradation (which is equivalent to 90 % of the initial weight) happens after 468 minutes (7hs48min) at 180 °C whereas the same degree of degradation is reached after only 12 minutes at 240 °C.

The information presented in Figure 37 can be utilized to study the chemical kinetics of the thermal degradation of wheat straw fibers.

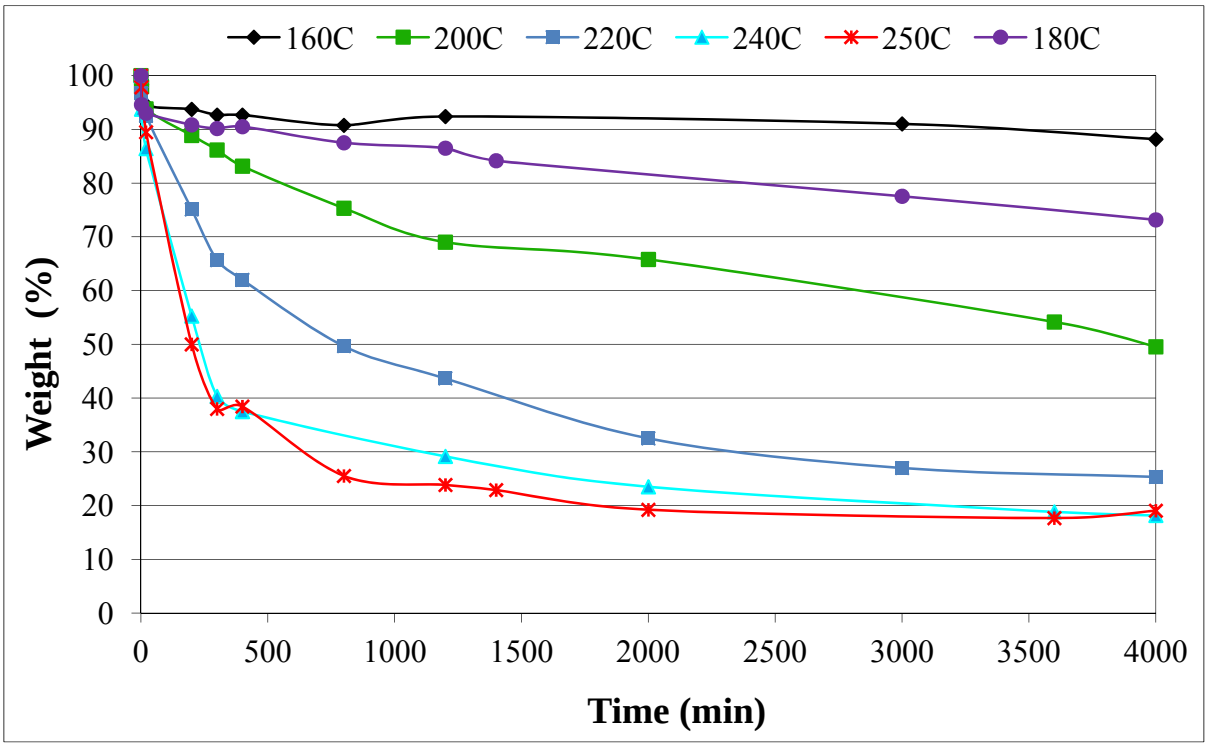

Figure 37: Weight versus time curves for thermooxidative degradation of wheat straw.

An isoconversional method (described in the Materials and Methods section) was used to estimate kinetic parameters (e.g., apparent activation energy) and model the degradation process. In general, isoconversional methods allow studying the reaction mechanism of complex reactions (such as thermal degradation of wheat straw) without the necessity of previous assumptions on the reaction mechanism model. This way, errors, such as the determination of kinetics parameters and reaction mechanism, caused by the selection of a kinetic model are avoided.

Note that the isoconversional method was carried out only under air; it was not carried out under nitrogen atmosphere due to experimental limitations (at the time of this research the laboratory was not equipped with an oven where the samples could be kept under a nitrogen atmosphere).

During the application of the isoconversional method, the isothermal curves (Figure 37) were utilized to determine the time needed to reach a weight loss (also referred to as degree of conversion) ranging from 2 to 30 % (2, 2.5, 5, 7.5, 10, 12.5, 15, 17.5, 20, 22.5, 25, 27.5 and 30 %). Figure 20 (in the Materials and Methods section) illustrates the procedure used to obtain the time.

Then, these data were utilized to plot the curves presented in Figure 38 which represents the relationship between the time needed to reach different weight losses (ranging from 2 to 30 %) under each isothermal temperature (varying from 200 to 250 °C). These curves are also referred to as dependence (i.e., relationship) of time (ln time) on temperature (1/T).

It can be seen (Figure 38) that the inclination of the straight lines is increasing as the thermal degradation (degree of conversion) increases from 2 to 30 % (dark blue diamond curve at the bottom and light blue axis curve at the top, respectively). Figure 39 offers a close up of the region where this change is more pronounced, i.e., between 2 and 10 % of conversion.

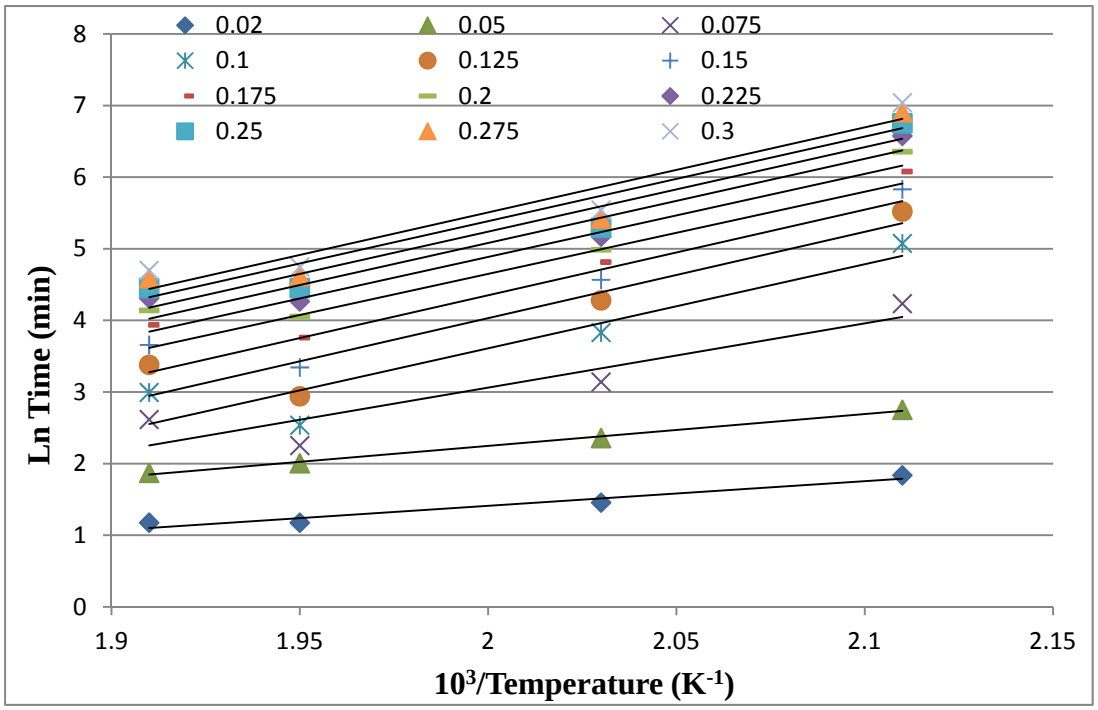

Figure 38: Application of Isoconversional method for the thermooxidative degradation of wheat straw. The degree of conversion ranges from 2 to 30 % (bottom to top, respectively).

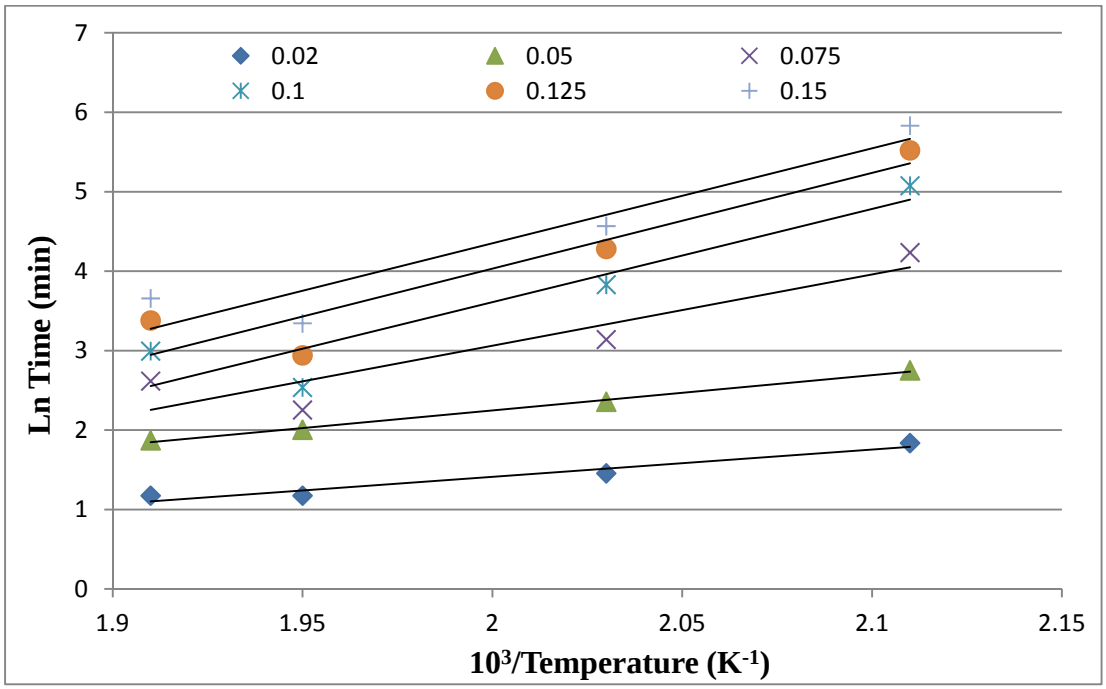

Figure 39: Dependence of time (logarithm) on temperature (1/T) in the 0.02-0.15 conversion range.

The inclination of these straight lines was utilized to calculate the apparent activation energy which is summarized in Table 8 and Figure 40. Because a complex multi-step process is treated as a single-step reaction when applying the isoconversional method, the activation energy obtained with this method is called apparent and does not represent the true activation energy of elementary steps.

It can be observed in Figure 40 that the activation energy increases when thermal degradation (conversion) goes from 2 to 10 %. Above 10 % of conversion, the activation energy is constant and therefore there is no change in the degradation reaction.

This behavior (i.e., the increasing activation energy with the degree of conversion, Figure 40) is characteristic of a multi-step competing and consecutive reaction process and it has been observed especially at the beginning of the thermal degradation of polymers (Vyazovkin and Lesnikovich, 1990; Vyazovkin and Wight, 1997). For example, the thermal decomposition of polypropylene exhibits similar increase in the activation energy with conversion. It is believed that the competing reactions involved in the thermal decomposition of polypropylene are pyrolysis and oxidation.

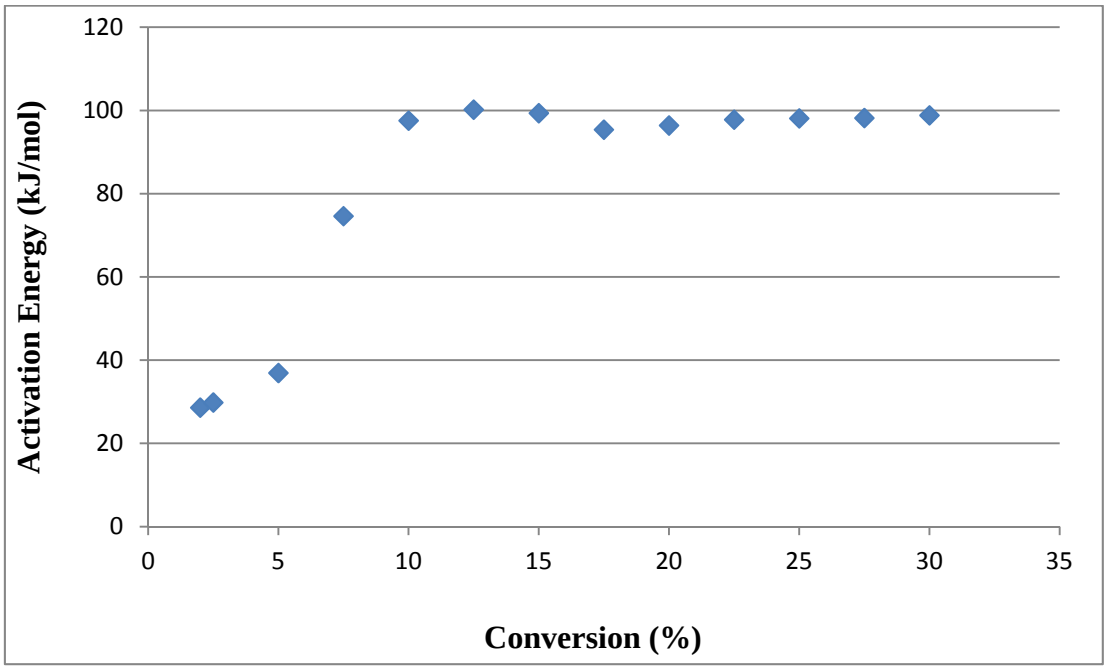

Figure 40: Dependence of activation energy on conversion indicating that thermal degradation of wheat straw is a multi-step process with competing reaction.

Competition between these two chemical reactions is responsible for the shape of the curve of activation energy and conversion (Vyazovkin and Lesnikovich, 1990; Vyazovkin and Wight, 1997).

The thermal decomposition of other polymers (such as polystyrene, polyethylene and poly (imide-siloxane)) can also be explained by competing reactions even in the absence of oxygen. In this case, the degradation of individual macromolecules is competing with the intermolecular degradation reaction (Vyazovkin and Wight, 1997).

Therefore, these observations suggest that the thermal degradation of wheat straw (in the temperature interval of 200 to 250 °C) is a multi-step process where competing and consecutive reactions are occurring at the same time, especially at the beginning of the thermal degradation, i.e., between 2 and 10 % of weight loss. After that (above 10 % of conversion), the activation energy is constant which indicates that there is no change in the degradation mechanism reaction.

In accordance with these observations, it has been suggested that the thermal degradation of plant fibers occurs in only one step for temperatures below 240 °C whereas, a two-step reaction is observed

when the temperature is increased above this value, that is 240 °C (Di Blasi and Lanzetta, 1997; Lanzetta and Di Blasi, 1998).

For example, according to Lanzetta and Di Blasi, 1998, the thermal degradation of xylan (main component of hemicellulose), wheat straw and corn stalk under nitrogen atmosphere is a one-step reaction at temperature below 240 °C and becomes a two-step reaction above this temperature. In the latter case, the first step produces a solid reaction intermediate with lower degree of polymerization along with volatiles. The next degradation step completely degrades this solid (the product from the first reaction step) producing char and more volatiles.

A similar change in the reaction mechanism (from one to two-step reaction) is a plausible explanation for the thermal degradation behavior under air atmosphere observed here for the wheat straw fibers.

However, the isoconversional method does account for the elementary steps and therefore can only be used without mechanistic interpretation.

Because of that, in order to verify the validity of this assumption, it is suggested that future work be carried out to perform a new chemical kinetics study utilizing a two-step reaction mathematical model. Additionally, further investigation would also be necessary in order to determine whether or not this assumption is valid for thermal degradation of wheat straw fibers under air atmosphere. It is possible that more than two reactions (and physical transformations) are occurring during the thermal degradation of wheat straw in air atmosphere. The detailed elucidation of the elementary steps of the thermal degradation of the wheat straw fiber is beyond the scope of the research presented in this document.

Table 8: Kinetic parameters of the thermal degradation of wheat straw fiber under air determined after isoconversional method.

Conversion (%)	R^2	Ea ($kJ.mol^{-1}$)
2	0.95	28.61
2.5	0.73	29.84
5	0.99	36.93
7.5	0.85	74.61
10	0.87	97.56
12.5	0.88	100.21
15	0.9	99.36
17.5	0.92	95.39
20	0.93	96.40
22.5	0.93	97.80
25	0.93	98.10
27.5	0.93	98.20
30	0.93	98.83

3.4 Conclusions

In this chapter, the thermal stability and chemical composition of several wheat straw samples from different regions of North America were evaluated with the assistance of thermogravimetry and chemical composition analyses.

TGA results indicate that the starting point of the wheat straw samples thermal degradation does not significantly vary with wheat straw type and cultivation region. For example, the main thermal degradation of wheat straw samples starts in a narrow window of temperature which goes from 220.8 to 237.8 °C and from 224.8 to 238.1 °C in the case of air and nitrogen atmospheres, respectively. The more thermally stable samples are Large and Mid.

This way, utilization of wheat straw in large scale is possible because different wheat straw samples (from different types and regions) can be used together without significantly affecting the thermal stability of the entire straw sample.

Additionally, chemical composition results for all the samples showed that the average content of cellulose, hemicellulose, lignin, and inorganic material are 43.6, 25.6, 8.1 and 5.8 wt%, respectively. More important, there is a relatively small variation in the wheat straw components. For example, among all these components, lignin and inorganic material were the ones with the highest relative variation (around 35.8 % and 66.2 %, respectively) followed by hemicellulose and cellulose.

Therefore, treatment methods targeted to alter different chemical components of wheat straw will be effective regardless of the wheat straw type or cultivation region. At the same time, the most effective treatments could be applied to other plant fibers because similar chemical components are found throughout plant fibers including wheat straw.

Furthermore, the thermal degradation of wheat straw depends on the atmosphere (air or nitrogen) and temperature when under isothermal conditions. More precisely, wheat straw fibers degrade faster under air than nitrogen atmosphere at 250 °C. Because of that, it would be advisable to utilize a nitrogen atmosphere when processing wheat straw fiber with polyamide-6 or other thermoplastics that have higher melting temperatures.

In this thesis, three different alternatives have been developed to improve the thermal stability of wheat straw and make possible to compound it with engineering thermoplastics (those with

processing temperatures above 220 ^{o}C). These alternatives treatments are discussed in the next chapters.

Chapter 4 - Thermochemical Modification of the Wheat Straw Fiber

4.1 Introduction

The main goal of this chapter is to evaluate the effect of different thermochemical treatments on the thermal stability of the wheat straw samples. The yield and thermal stability were utilized to evaluate the performance of the thermochemical treatments.

Two sets of experiments using full factorial design were conducted in order to study different variables. This experiment design allows evaluating the effect of each variable (also referred to as factor) as well as the interactions between these variables on the response variables, i.e., thermal stability and yield.

The initial screening of variables included temperature, time and pre-treatment using ammonium chloride (NH_4Cl). The second screening studied the effect of ammonium chloride concentration and mixing method besides temperature and time.

The rationale of using a chemical treatment is based on practices from other areas. For example, ammonium chloride is utilized in the first step of carbon fiber fabrication (called stabilization) using rayon or cellulose fibers as precursors. This stabilization step allows converting the fibers chemical structure into a more thermally stable form (Bengisu and Yilmaz, 2002; Chawla, 1998; Savage, 1993). According to those reports (Bengisu and Yilmaz, 2002), the mechanism for improving the thermal stability is based on the fact that ammonium chloride can interact with the fiber affecting its oxidation rate and making the fiber more susceptible to thermal rearrangement.

Regarding these thermal rearrangement reactions, Domburg et al. (1970) suggested that the mechanism of thermal degradation of lignin models depends on the chemical structure. Those authors further state that lignin can be converted into more thermally stable structures through removal of the reactive functional groups in the side chain. Since rayon and cellulose fibers are natural polymers mainly formed by cellulose, lignin and hemicellulose, this approach could be successfully applied in the case of others plant fibers such as wheat straw fiber.

It is expected that the ammonium chloride pre-treatment can produce similar results when applied to straw fiber, making the wheat straw fiber more suitable for thermal rearrangement reactions rather than degradation.Therefore, in this chapter, the potential to enhance the thermal stability of wheat

straw samples via application of different thermochemical treatments is investigated. Initially, the samples are chemically pre-treated using ammonium chloride. After that, the ammonium chloride pre-treated fibers are submitted to different thermal treatments under oxidative atmosphere. The extent of thermal stability improvement is evaluated with the assistance of thermogravimetry analysis (TGA).

4.2 Materials and Methods

4.2.1 Materials

The Mid wheat straw fiber used in this chapter was provided by our industrial partner (Omtec Inc, Table 9). The details regarding the harvesting and grinding steps as well as the samples labeling were presented before in Chapter 3 (in the Materials section).

Table 9: Materials used during the thermochemical treatment of wheat straw samples.

Materials	Type/Grade	Supplier/Manufacturer
Ammonium chloride	GR ACS	EMD
Wheat Straw Mid	Soft white winter variety	Omtec Inc.

4.2.2 Experimental Setup

A custom built apparatus was utilized to thermally treat the wheat straw samples. This apparatus consists basically of a gas manifold, a quartz tube and a furnace with heating capacity up to 1,100 ºC. The schematic diagram of the apparatus is shown in Figure 41.

The manifold allows the use of different atmospheres (e.g., nitrogen, argon vacuum) during the thermal treatment. The valves are needed to control the flow of gases into the manifold. The quartz tube is required because common glass cannot resist high temperatures without compromising its dimensional stability. Ceramic crucibles were used to hold the samples inside the furnace during thermal treatment. This apparatus was built specifically for this research project; it was not available in the laboratory before this project started.

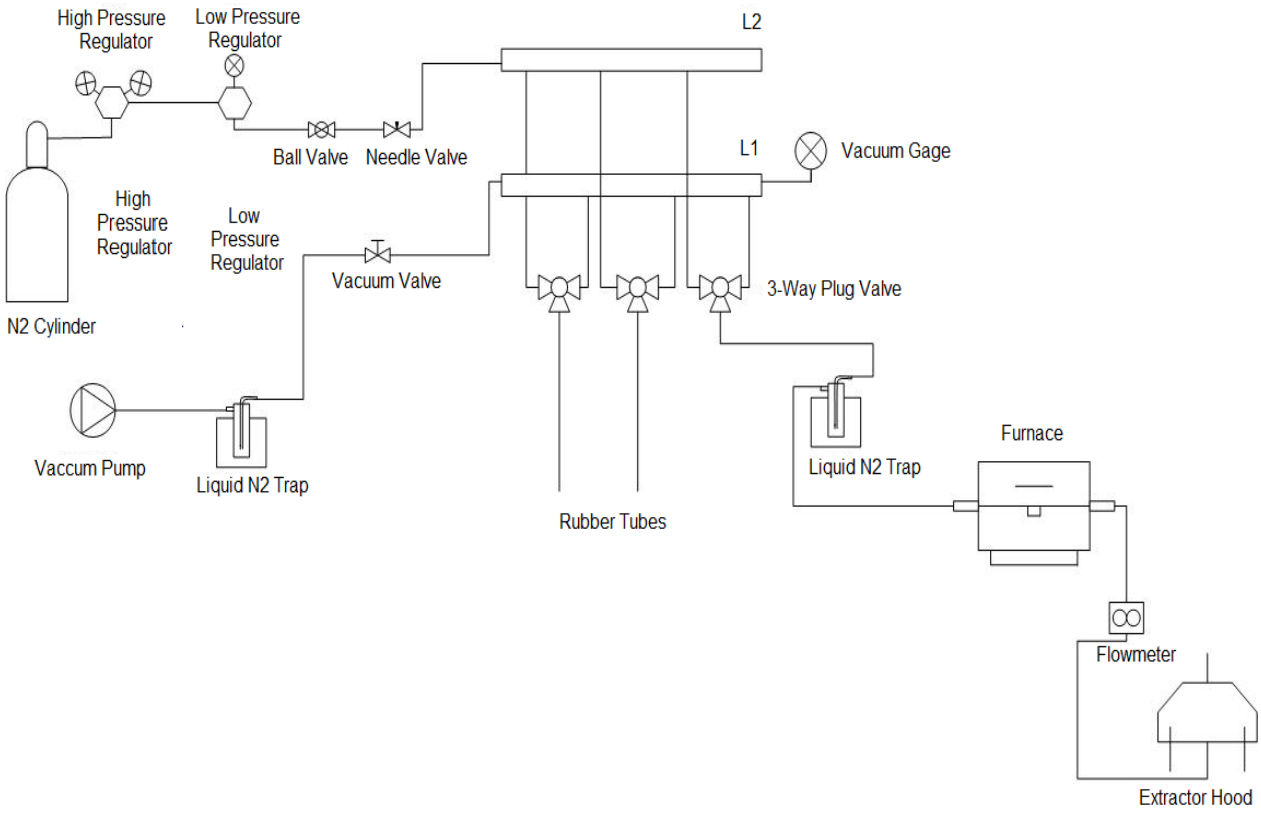

Figure 41: Schematic representation of the apparatus utilized during the thermochemical treatments of wheat straw samples.

4.2.3 The Thermochemical Treatment of the Wheat Straw Fiber

A full factorial design of experiments was utilized to evaluate the effect of different variables on two responses: the thermal stability and the yield of the samples obtained after the treatment. Two sets of experiments were performed and are summarized in Figure 42.

In the first one (Experiment #01), temperature, time and the use or not of ammonium chloride pre-treatment were considered. Each one of these variables was studied at two different levels (e.g., temperature at 250 and 350 ºC) according to Figure 42 and Table 10.

In the second experiment (Experiment #02), four variables were studied using two levels for each variable according to Figure 42 and Table 11. Based on the results of the first experiment, the values of temperature and time were reduced. Two new variables were included, concentration of

ammonium chloride and method of mixing the ammonium chloride and wheat straw. It should be noted that the experiments were performed at random order during both Experiment #01 and Experiment #02 sets in order to avoid the influence of any experimental bias in the results.

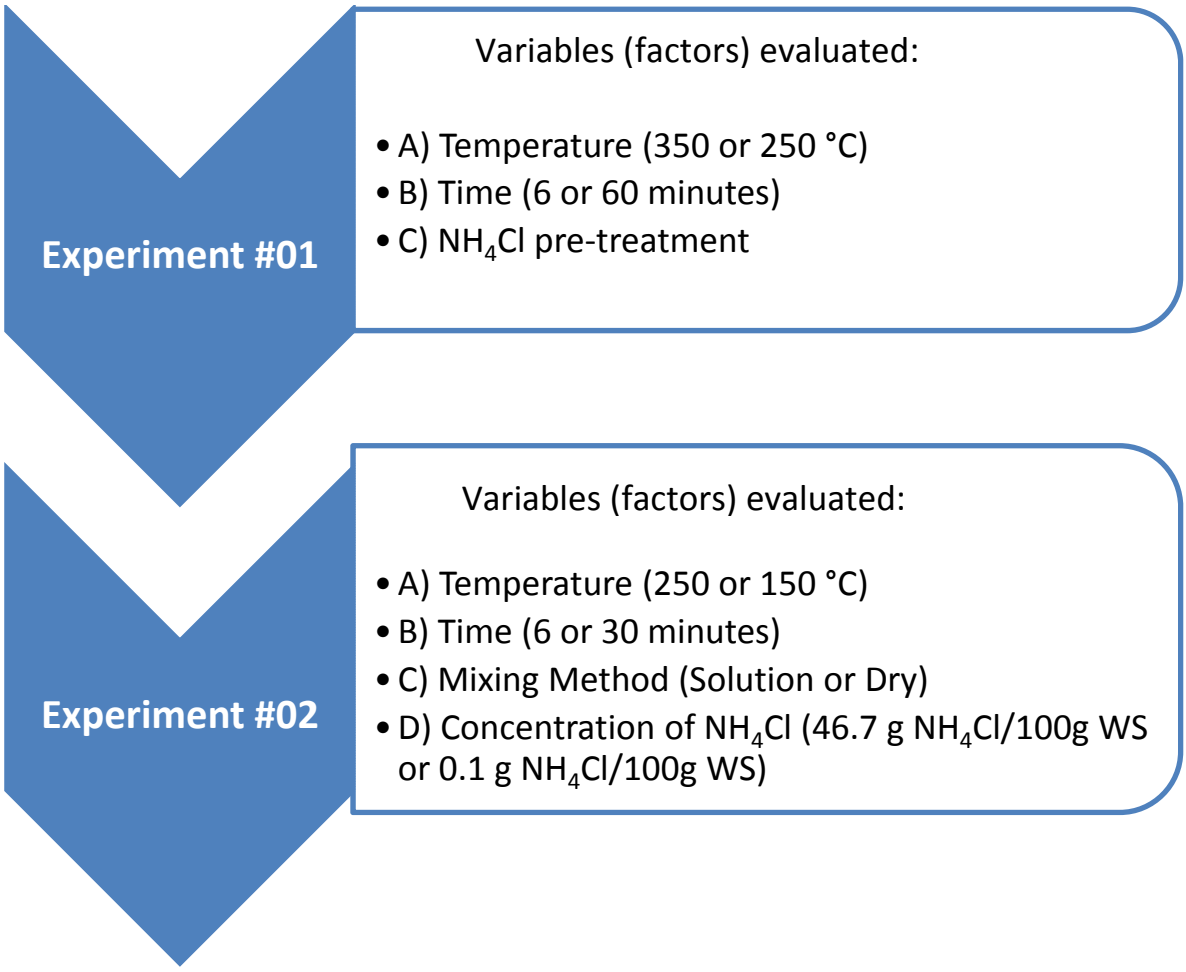

Figure 42: Diagram shows the two sets of experiments and its variables.

4.2.3.1 Experiment #01

Chemical Pre-treatment

A saturated solution of ammonium chloride in water (5.6 mol/L) was used to impregnate the wheat straw samples before the thermal treatment. The mixture containing the ammonium chloride solution

and wheat straw was placed inside a beaker and stirred for 1 hour at 60 ºC. After this time, the mixture was filtered and dried for 24 hours at 90 ºC. It should be noted that the uptake of ammonium chloride by wheat straw was not calculated.

Thermal Treatment

After the chemical pre-treatment, the thermal treatment was carried out at 250 ºC and 350 ºC inside a tubular furnace (Lindberg furnace model 55030) under air atmosphere for 6 and 60 minutes. These upper and lower levels of time applied to the thermal treatment were selected based on preliminary experiments and similar processes reported in the literature (Bengisu and Yilmaz, 2002; Chawla 1998; Dobele et al., 1999; Rosas et al., 2009; Savage, 1993).

Table 10 shows all combinations of the three factors (temperature, time and NH_4Cl pre-treatment) investigated during the Experiment #01. Samples were weighed before and after the thermal treatment in order to calculate the yield of material obtained.

Table 10: Samples labels and the treatment conditions applied during the Experiment #01.

Samples Label	Thermal Treatment		Chemical Treatment
	Temperature (°C)	Time (minutes)	Pretreatment with NH_4Cl
350C_6min_NH_4Cl	350	6	Yes
250C_6min_NH_4Cl	250	6	Yes
350C_60min_NH_4Cl	350	60	Yes
250C_60min_NH_4Cl	250	60	Yes
350C_6min	350	6	No
250C_6min	250	6	No
350C_60min	350	60	No
250C_60min	250	60	No

4.2.3.2 Experiment #02

Chemical Pre-treatment

In the second set of experiments, two different methodologies to impregnate the wheat straw samples with ammonium chloride were applied. The first one (referred to as Solution) utilized an aqueous solution and followed the exactly same procedure described for the Experiment #01. The only difference was that two concentrations of ammonium chloride (High, 46.7 g NH_4Cl/100g wheat straw, and Low, 0.1 g NH_4Cl/100g wheat straw) were employed.

The second methodology (called Dry mixing) consisted of mixing the wheat straw and the ammonium chloride with the assistance of a mortar and a pestle (dry, no assistance of solvent). The mixture was stirred for 15 minutes. It should be noted that the uptake of ammonium chloride by wheat straw was not calculated.

Thermal Treatment

After the chemical pre-treatment has been done, the thermal treatment was performed at 150 ºC and 250 ºC for 6 and 30 minutes under air atmosphere. The upper and lower levels of process parameters were selected based on the previous experiment (Experiment #01) and similar processes reported in the literature (Bengisu and Yilmaz, 2002; Chawla 1998; Dobele et al., 1999; Rosas et al., 2009; Savage, 1993). Table 11 shows all combinations of the four factors (temperature, time, mixing method and NH_4Cl concentration) studied during the Experiment #02.

Table 11: Samples labels and the treatment conditions applied during the Experiment #02.

Samples Label	Thermal Treatment		Chemical Treatment	
	Time (minutes)	Temperature (°C)	Mixing Method	NH_4Cl Concentration
250C_30min_Sol_High	30	250	Solution	High[A]
250C_6min_Dry	6	250	Dry mixing	Low[B]
150C_6min_Sol	6	150	Solution	Low
250C_30min_Sol	30	250	Solution	Low
150C_6min_Dry_High	6	150	Dry mixing	High
250C_6min_Sol_High	6	250	Solution	High
150C_30min_Dry	30	150	Dry mixing	Low
150C_6min_Dry	6	150	Dry mixing	Low
150C_30min_Sol_High	30	150	Solution	High
250C_6min,_Dry_High	6	250	Dry mixing	High
250C_6min_Sol	6	250	Solution	Low
250C_30min_Dry_High	30	250	Dry mixing	High
250C_30min_Dry	30	250	Dry mixing	Low
150C_30min_Sol	30	150	Solution	Low
150C_30min_Dry_High	30	150	Dry mixing	High
150C_6min_Sol_High	6	150	Solution	High

High[A]: 46.7 g NH_4Cl/100g wheat straw; Low[B]: 0.1 g NH_4Cl/100g wheat straw

4.2.4 Thermogravimetry Analysis (TGA)

The thermogravimetry analysis (TGA) of the wheat straw samples was performed under non-isothermal conditions. During the analysis, the temperature is increased from 35 to 800 °C using a

heating rate of 10 °C/min. The test was performed under nitrogen atmosphere (50 ml flow) and the sample weight is monitored as a function of the temperature. The initial weight of the samples was approximately 10 mg. The TGA data was utilized to determine the temperature at 2 % of degradation ($T_{2\%}$) and the weight loss at 250 and 275 °C (Wt Loss250 and Wt Loss275) for the straw samples.

4.3 Results and Discussion

The thermal degradation of wheat straw samples is treated here as complex reaction. For the sake of simplicity the degree of the thermal degradation is measured using two parameters: temperature at 2 % of degradation ($T_{2\%}$) and weight loss at 250 and 275 °C (Wt Loss250 and Wt Loss275). Both parameters were obtained from the TGA curves.

The $T_{2\%}$ is the temperature where 2 % of degradation is reached. The procedure applied to obtain the $T_{2\%}$ from TGA curves is explained in detail in the previous chapter, Results and Discussion section. The weight loss at 250 and 275 °C is defined as the mass loss at a temperature of either 250 or 275 °C. The Wt Loss250 and Wt Loss275 can be obtained from the TGA curves as illustrated in Figure 43.

It should be noted that the values of weight loss (Wt Loss250 and Wt Loss275) were normalized using the weight loss at 150 °C as a reference (done for all samples). Therefore, the weight at 150 °C was computed as zero and the weight loss at 250 °C is the difference between the weight at 150 and 250 °C before normalization. It is believed that such procedure allows computing only the weight loss changes due to thermal degradation rather than evaporation of water or other volatile components. For example, the weight loss percentage (wt-%) for sample 350C_6min at 150 and 250 °C was 94.06 % and 93 %, respectively. The subtraction of both values gives 1.06 % which is computed as the weight loss at 250 °C for this sample after normalization.

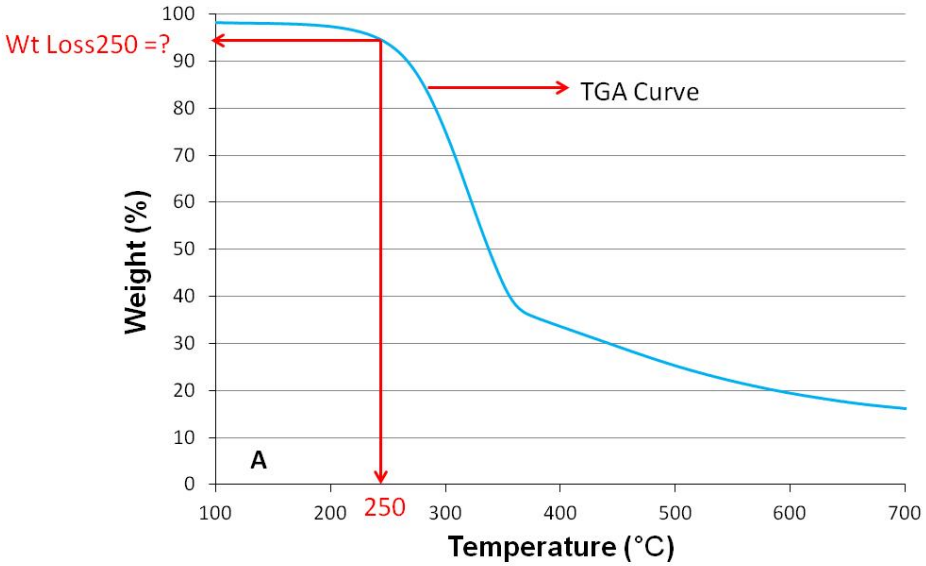

Figure 43: Procedure applied to obtain the weight loss at 250 and 275°C from TGA curves.

4.3.1 The Yield after Experiment #01

Initially, the influence of the three factors (Temperature, Time and NH_4Cl pre-treatment) in the yield was investigated using statistical analysis. The yield is the mass of the sample after the treatment. The mass of the sample decreases with the thermal treatment because of removal of volatiles and chemical reactions producing gases.

The analysis of variance (Anova) results indicates that the main factors Temperature and Time are significant, whereas the factor NH_4Cl pre-treatment is not affecting the yield. In addition, the interactions between the factors Temperature and Time as well as Time and NH_4Cl pre-treatment are also significant for the yield.

It is important to notice that in statistical analysis, the main effects of factors (e.g., Temperature and Time) have limited meaning when there are also significant interactions (Temperature and Time interaction) between these main factors. In other words, it is necessary to evaluate together the effect of temperature and time in the yield. Because of that, only the interactions between Temperature and Time as well as Time and NH_4Cl pre-treatment are further evaluated here.

Figure 44 and Figure 45 present the Temperature and Time interaction as well as the Time and NH_4Cl pre-treatment interaction, respectively. It can be seen from Figure 44 that that the temperature does not significantly affect the yield when the longer treatment time (60 minutes) is utilized. On the other hand, in the case of the shorter treatment time (6 minutes), increasing the treatment temperature significantly reduces the yield. Figure 44 also shows that the highest yield is reached when the treatment is performed using the shorter time and the lower temperature (6 minutes and 250 °C, respectively).

In addition, Figure 45 suggests that the time has small impact on the yield when the thermal treatment is conducted in the absence of ammonium chloride; whereas increasing the time of the thermal treatment largely decreases the yield if ammonium chloride is being utilized. It can be seen from Table 12 that the highest yield (74.3 %) is reached utilizing the shorter treatment time and ammonium chloride pre-treatment.

According to Experiment #01, temperature does not considerably affect the yield when the longer treatment time (60 minutes) is used. For example, compared to sample 250C_60min_NH_4Cl, increasing treatment temperature from 250 to 350 °C reduces the yield of the sample 350C_60min_NH_4Cl only 5.1 %, from 21.4 to 16.3 % (Table 12). It seems that the yield is already very low in this case (60 minutes) and perhaps, because of that, increasing the treatment temperature does not significantly reduce the yield. In agreement with this observation, the yield is very sensitive to temperature if the shorter treatment time is chosen (6 minutes). For example, increasing treatment temperature from 250 to 350 °C when the time is 6 minutes (samples 250C_6min and 350C_6min) decreases the yield by 34.2 %, from 62.1 to 27.9 % (Table 12).

In addition, the yield is drastically influenced by the use or not of NH_4Cl pre-treatment, regardless of the thermal treatment time. For example, the sample 250C_60min_NH_4Cl has 52.9 % drop (from 21.4 to 74.3 %, Table 12) in the yield compared to the sample 250C_6min_NH_4Cl.

Therefore, in order to maximize the yield, lower temperature (250 °C), shorter time (6 minutes) and ammonium chloride should be employed during the thermochemical treatment of wheat straw samples.

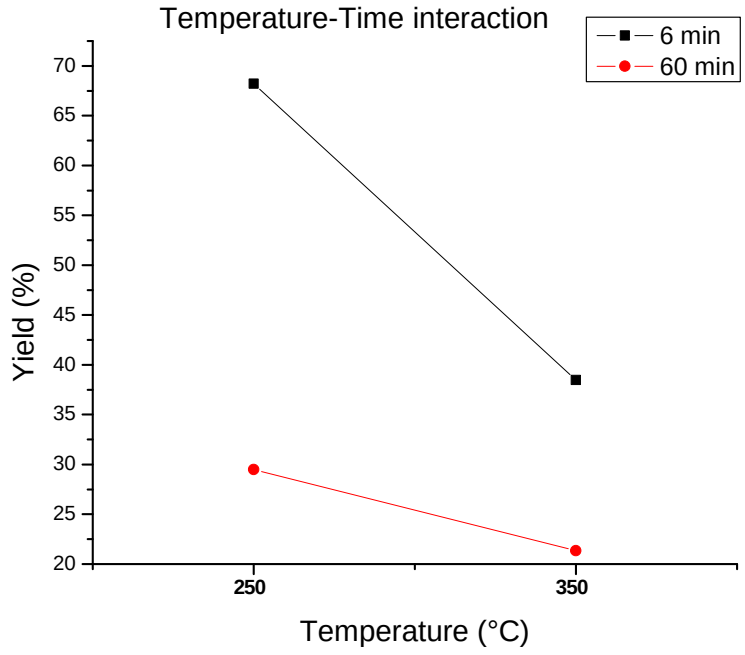

Figure 44: Effect of Temperature-Time interaction in the yield obtained after thermal treatment

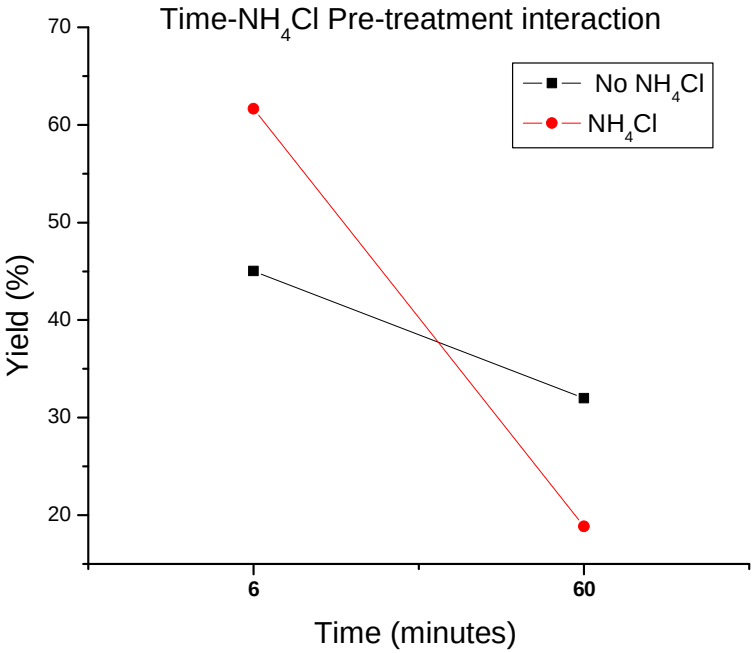

Figure 45: Effect of Time-NH_4Cl pre-treatment interaction in the yield obtained after thermal treatment.

Table 12: Weight loss, $T_{2\%}$ and yield obtained for each sample after the application of the treatment described in the table (Experiment #01).

Sample Label	Treatment	Weight loss 250°C (%)	$T_{2\%}$ (°C)	Yield (%)
350C_60min_NH_4Cl	350 °C, 60min, NH_4Cl	0.93	331.7	16.3
250C_60min	250 °C, 60min, No NH_4Cl	0.55	321.8	37.6
350C_60min	350 °C, 60min, No NH_4Cl	0.92	321.3	26.4
350C_6min	350 °C, 6min, No NH_4Cl	1.06	319.0	27.9
250C_6min	250 °C, 6min, No NH_4Cl	1.23	265.3	62.1
250C_6min_NH_4Cl	250 °C, 6min, NH_4Cl	32.0	189.2	74.3
250C_60min_NH_4Cl	250 °C, 60min, NH_4Cl	14.9	174.2	21.4
350C_6min_NH_4Cl	350 °C, 6min, NH_4Cl	51.8	173.7	49.0
Untreated wheat straw	No treatment	3.90	231.4	N/A

N/A: Not applicable, $T_{2\%}$: Temperature at 2 wt-% of weight loss.

4.3.2 The Thermal Stability of the Samples after Experiment #01

In order to evaluate the effect of the thermochemical treatments on the thermal stability of the samples, the weight losses (wt-%) at 250 and 275 °C (Table 12) were obtained directly from the TGA curves and utilized to perform the statistical analysis. It should be noted that a normalization procedure (described in the Results and Discussion section of this chapter) was applied in order to remove the weight loss due to water evaporation.

Since there is just one reading for each experimental condition, normal probability plot, rather than analysis of variance (Anova), was applied in order to evaluate the significance of each factor (i.e., Temperature, Time and NH_4Cl pre-treatment). Figure 46 and Figure 47 depict the normal probability plot using the weight losses (wt-%) at 250 and 275 °C, respectively.

It can be seen from Figure 46 and Figure 47 that only the factor NH_4Cl pre-treatment deviates from the straight line which indicates that the factor NH_4Cl pre-treatment may be significant.

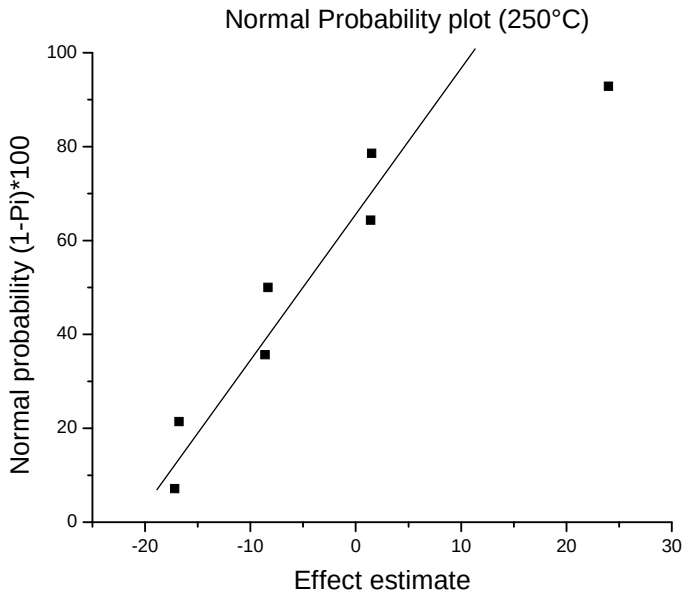

Figure 46: Normal probability plot for estimated effects at 250 ºC.

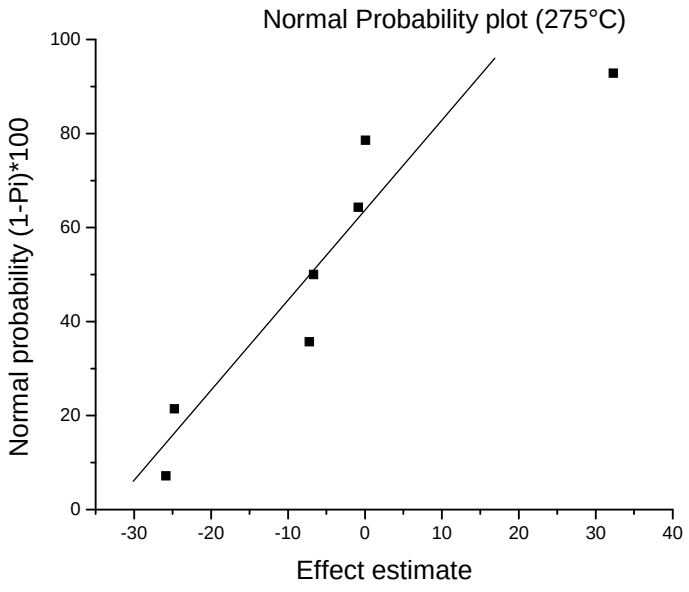

Figure 47: Normal probability plot for estimated effects at 275 ºC.

Further analysis of variance (Anova) was performed in order to determine the importance of the factor NH_4Cl pre-treatment. The error needed in the analysis of variance was obtained by combining together the effect of all the other factors and factors interactions that were considered not significant.

However, the Anova analysis indicates that the factor NH_4Cl pre-treatment is not significant for the thermal stability of the samples (i.e., weight loss at 250 and 275 °C obtained from non-isothermal TGA curves).

Therefore, according to the statistical analysis results (normal probability plot and Anova), none of the factors (i.e., Temperature, Time and NH_4Cl pre-treatment) studied during Experiment #01 are affecting the thermal stability of the treated wheat straw samples.

A different way to evaluate the thermal stability results is simply comparing the thermochemical treated samples against the untreated wheat straw sample.

Table 12 depicts the weight loss (%) at 250 and 275 °C as well as the $T_{2\%}$ for all different thermochemical treatments performed in Experiment #01 and the untreated wheat straw; whereas Figure 48 graphically presents the temperature at 2 % of weight loss ($T_{2\%}$). It can be seen from the figure that the sample treated at 250 °C, for 60 minutes without ammonium chloride (250C_60min) presented the best overall thermal stability with 0.55 % weight loss at 250 °C and $T_{2\%}$ at 321.8 °C.

However, the sample mass obtained after the treatment (i.e., yield) was very low, around 38 %. In addition, this sample was very dark (showing an aspect of burned) after the treatment (Figure 49); therefore it is very likely that the mechanical properties of the fiber were severely compromised.

When combining good thermal stability with high yield, the wheat straw sample treated at 250 °C, for 6 minutes and without ammonium chloride (sample 250C_6min) showed the best results, with a yield of 62 %, only 1.23 % weight loss at 250 °C and $T_{2\%}$ at 265.3 °C. The $T_{2\%}$ result represents a 14.6 % improvement (from 231.4 to 265.3 °C) in the thermal stability compared to the untreated wheat straw sample.

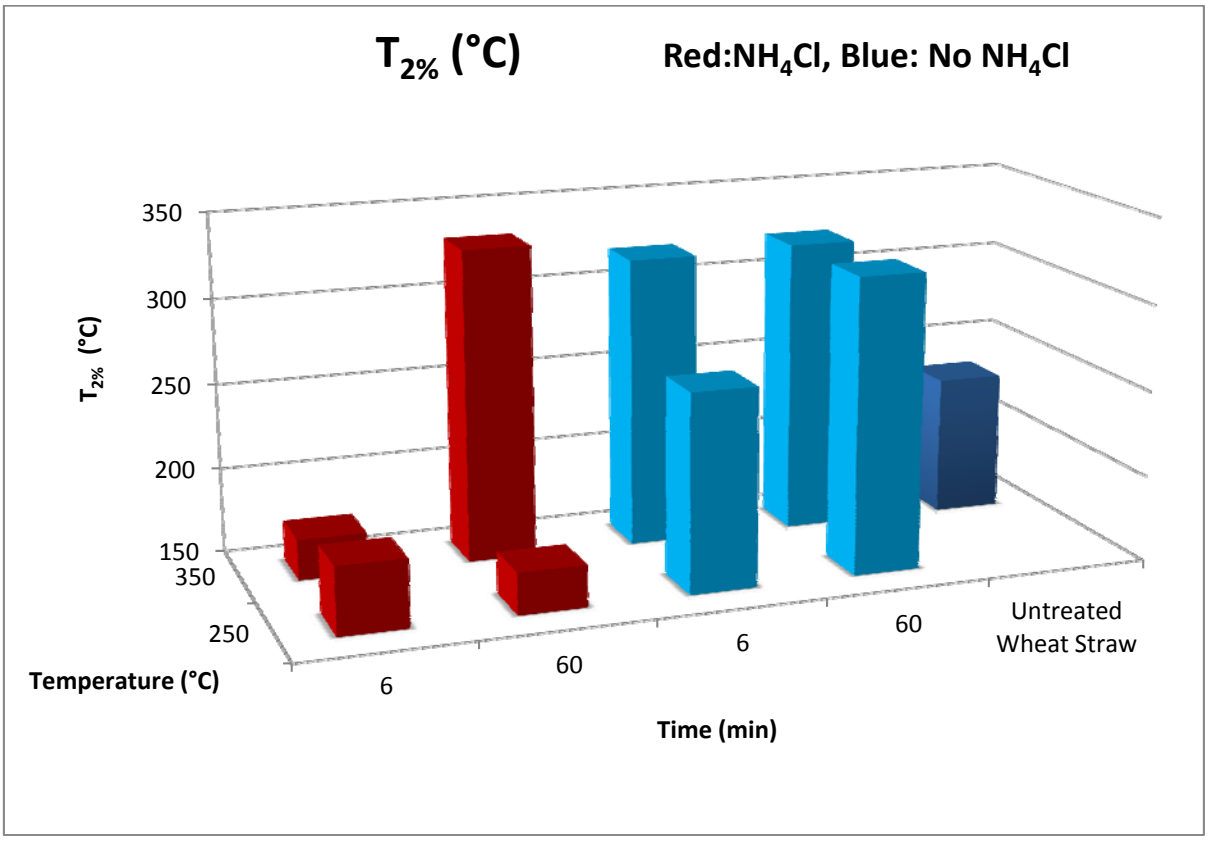

Figure 48: Temperature at 2% of weight loss obtained from TGA curves (see labels in Table 12).

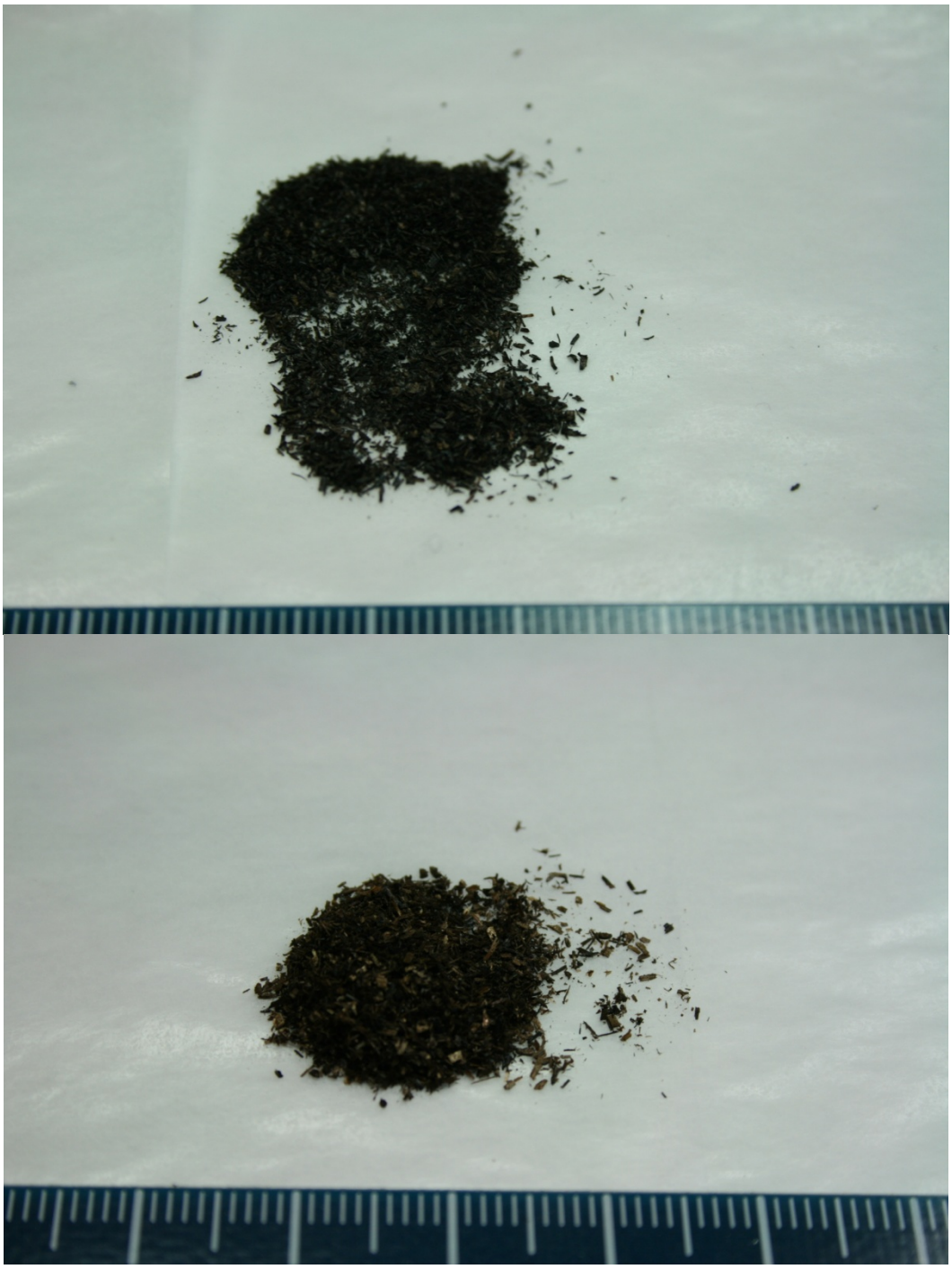

Figure 49: Appearance of the samples 250C_60min (top) and 250C_6min (bottom) after thermochemical treatment.

4.3.3 The Yield of Experiment #02

Experiment #01 suggested that a combination of high yield and good thermal stability could be achieved by using factors Temperature and Time at low levels: 250 °C and 6 minutes, respectively. Consequently it was decided to explore the range of temperature from 150 to 250 °C and time from 6 to 30 minutes for the thermal treatment.

Two new factors were added to the variables to further study the effect of ammonium chloride: a) Mixing method and b) NH_4Cl concentration. It is believed that those factors may play an important role in the yield and thermal stability of the thermochemical treated samples.

According to the results of analysis of variance, the yield is affected by the factors Temperature and Time as well as the interaction between these two factors (Temperature and Time interaction). The other two factors, Mixing method and NH_4Cl concentration, did not seem to influence the yield. Because there is a significant interaction between the factors Temperature and Time, only this interaction (Temperature and Time interaction) is further evaluated here.

The effect of the interaction between Temperature and Time in the yield of material obtained after the thermochemical treatments is plotted in Figure 50. It is possible to observe that the temperature slightly affects the yield when the shorter thermal treatment time (6 min) is used. On the contrary, when the thermal treatment is performed using the longer time (30 minutes), increasing the temperature drastically reduces the yield.

Therefore, in order to maximize the yield, lower temperature and shorter time (150 °C and 6 minutes) should be employed during the thermal treatment of the wheat straw samples, consistent with observations noted in Experiment #01.

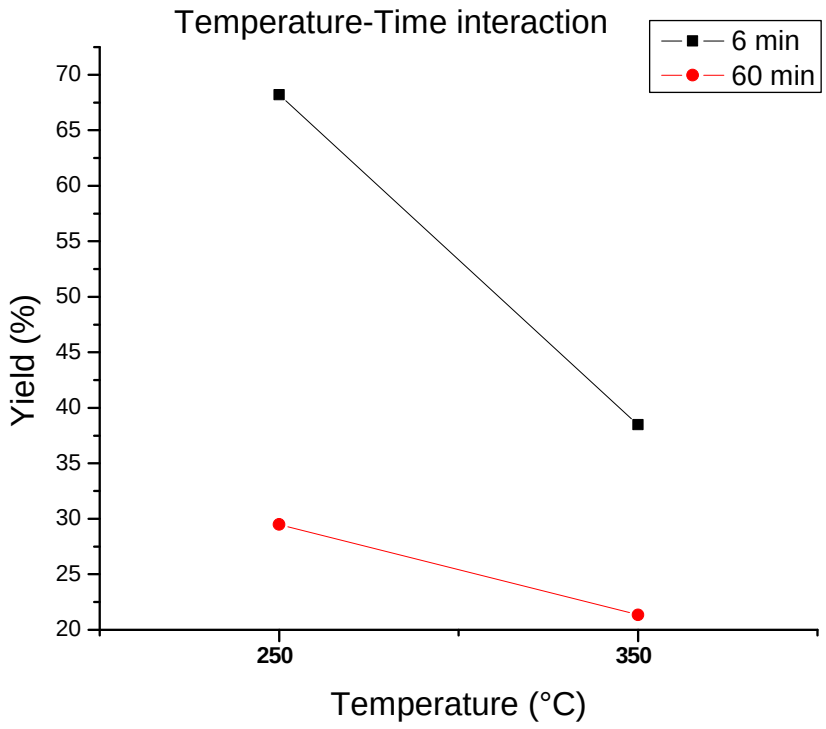

Figure 50: Effect of Temperature-Time interaction in the yield obtained after thermal treatment.

4.3.4 The Thermal Stability of the Samples after Experiment #02

In order to measure the effect of the thermochemical treatment on the thermal stability of the samples, the weight loss at 250 and 275 °C (Wt Loss250 and Wt Loss275) for each samples were obtained from the non-isothermal TGA curves and summarized in Table 13. It should be noted that the values were obtained after the application of the same normalization procedure previously described.

Because there is only one reading for each experimental condition, normal probability plot was employed to decide the importance of each factor (i.e., Time, Temperature, Mixing method and NH_4Cl concentration) during the statistical analysis. Figure 51 shows the normal probability plot for all treatments at 250 °C, while Figure 52 contains the same analysis at 275 °C.

Table 13: Weight loss, $T_{2\%}$ and yield obtained for each sample after the application of the treatment described in the table (Experiment #02).

Sample Label	Treatment	Weight loss 250 °C (%)[4]	$T_{2\%}$ (°C)	Yield (%)
250C_30min_Dry	250 °C, 30min, Dry, Low	1.06	268.0	46.41
250C_30min_Sol	250 °C, 30min, Sol, Low	1.57	254.6	61.04
250C_6min_Sol	250 °C, 6min, Sol, Low	2.80	242.0	92.40
150C_30min_Sol	150 °C, 30min, Sol, Low	2.90	240.5	89.68
150C_6min_Sol	150 °C, 6min, Sol, Low	3.40	235.7	89.92
250C_30min_Sol_High	250 °C, 30min, Sol[1], High	2.89	230.7	34.23
250C_6min_Dry	250 °C, 6min, Dry[2], Low	4.50	227.9	94.36
150C_30min_Dry	150 °C, 30min, Dry, Low	4.62	227.0	93.93
150C_6min_Dry	150 °C, 6min, Dry, Low	4.66	225.0	95.05
250C_6min,_Dry_High	250 °C, 6min, Dry, High	36.90	187.2	93.13
150C_6min_Dry_ High	150 °C, 6min, Dry, High	40.69	186.2	96.30
150C_30min_Dry_ High	150 °C, 30min, Dry, High	46.50	184.8	95.04
250C_30min_Dry_ High	250 °C, 30min, Dry, High	17.87	181.1	50.74
250C_6min_Sol_ High	250 °C, 6min, Sol, High	35.00	179.3	67.44
150C_6min_Sol_ High	150 °C, 6min, Sol, High	32.50	173.7	75.02
150C_30min_Sol_ High	150 °C, 30min, Sol, High	34.42	172.3	68.18
Untreated wheat straw	No treatment	3.90	231.4	N/A[3]

Sol[1].: Solution; Dry[2]: Dry mixing; N/A[3]: Not applicable; 4: from non-isothermal TGA

It can be seen that most of the points are falling along the straight line except for the factor NH_4Cl concentration. Therefore, this factor was further analyzed utilizing analysis of variance. The error mean square was obtained by pooling all these effects considered negligible.

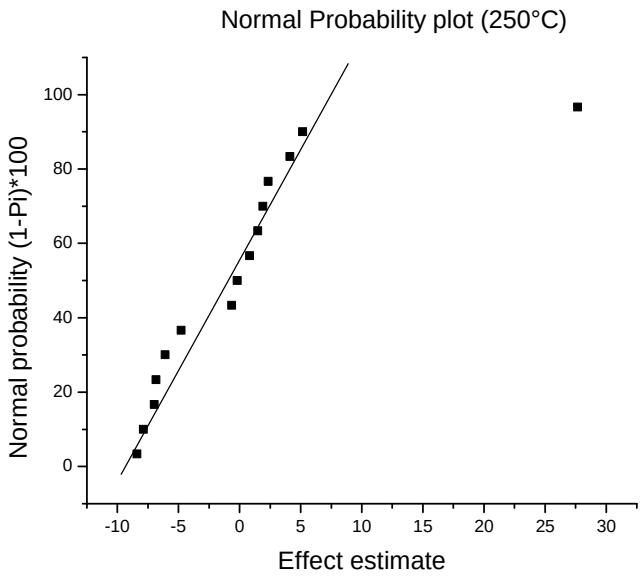

Figure 51: Normal probability plot for estimated effects using weight losses at 250 ºC.

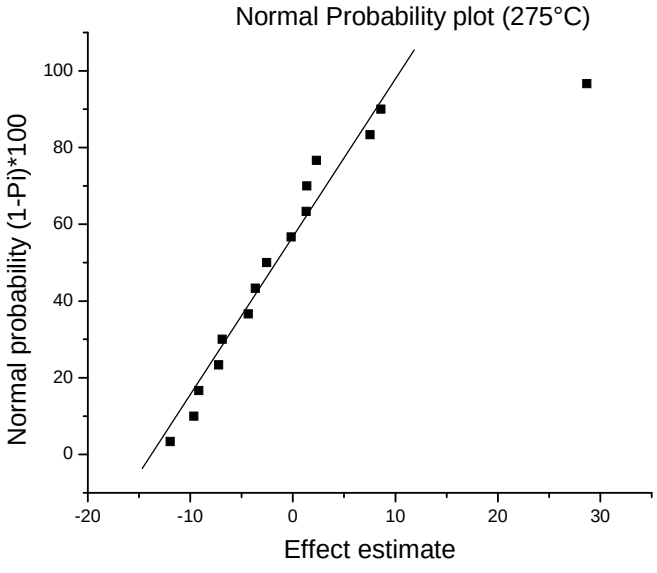

Figure 52: Normal probability plot for estimated effects using weight losses at 275 ºC.

The Anova results indicate that the factor NH_4Cl concentration is significantly influencing the thermal stability of the treated samples. Since there are not other main factors or interactions that appear to be important, only the main effect of the factor NH_4Cl concentration is plotted in Figure 53 and Figure 54 for analysis.

As it can be observed from the figures, the factor NH_4Cl concentration shows a positive effect on the response which means the weight loss (at 250 and 275 °C) increases as the concentration of ammonium chloride increases. Therefore, lower ammonium chloride concentration should be utilized to maximize the thermal stability of the wheat straw samples.

After the statistical analysis, the effect of each factor (i.e., time, temperature, mixing method and NH_4Cl concentration) in the thermal stability and yield is shown in Figure 55 and Table 13.

Figure 55 (top graph) and Table 13 shows that the sample 250C_30min_Dry (treated at 250 °C for 30 minutes using dry mixing method with Low concentration of ammonium chloride) has the best overall thermal stability with $T_{2\%}$ at 268.0 °C and only 1.06 % weight loss at 250 °C. The $T_{2\%}$ result represents a 15.8 % improvement (from 231.4 to 268.0 °C) in the thermal stability compared to the untreated wheat straw sample. However, the yield obtained after this treatment was low, 46.4 %.

The best combination of yield and thermal stability was achieved by treating the sample at 250 °C for 30 minutes using solution mixing method with Low concentration of ammonium chloride (sample 250C_30min_Sol). This sample had a yield of 61 %, only 1.57 % weight loss at 250 °C and $T_{2\%}$ at 254.6 °C. In comparison with the untreated wheat straw sample, the improvement on the thermal stability ($T_{2\%}$) of this sample is approximately 10 %.

Figure 56 shows the appearance of these two samples after the thermochemical treatment. It seems that the sample 250C_30min_Dry (top) suffered slightly more thermal degradation than the sample 250C_30min_Sol (bottom) during the thermochemical treatment. However, both samples had significant thermal degradation and therefore, it is expected that the mechanical properties of these samples were considerably compromised. This way, the potential reinforcement effect of these samples would be very small.

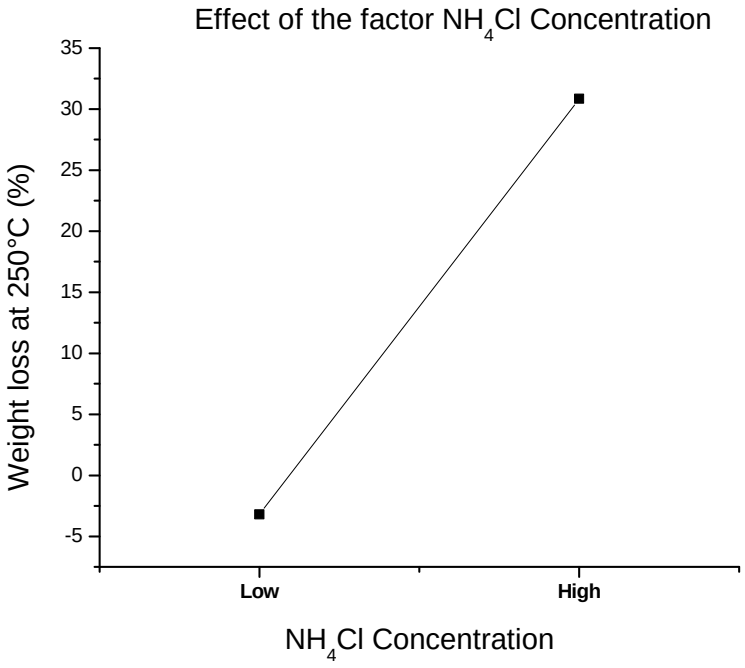

Figure 53: Effect of the NH_4Cl concentration on the average weight loss at 250 ºC (from TGA).

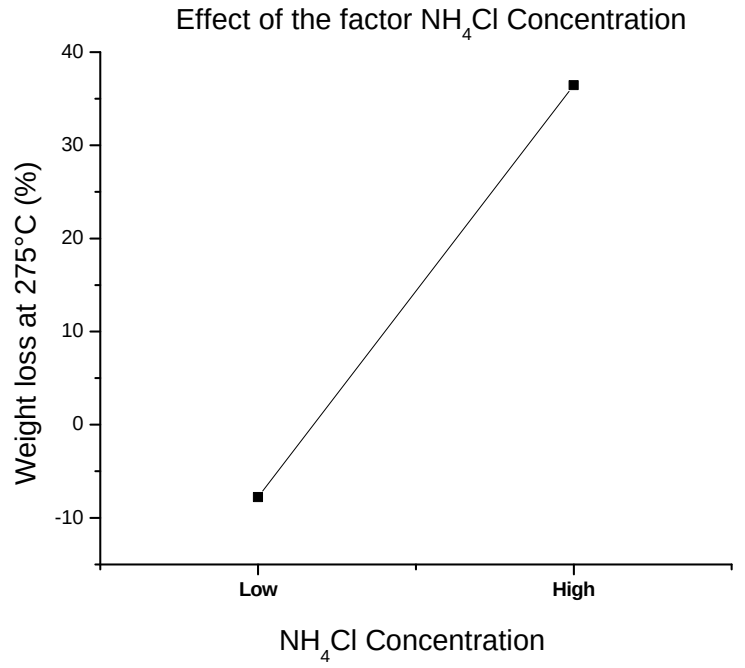

Figure 54: Effect of the NH_4Cl concentration on the average weight loss at 275 ºC (from TGA).

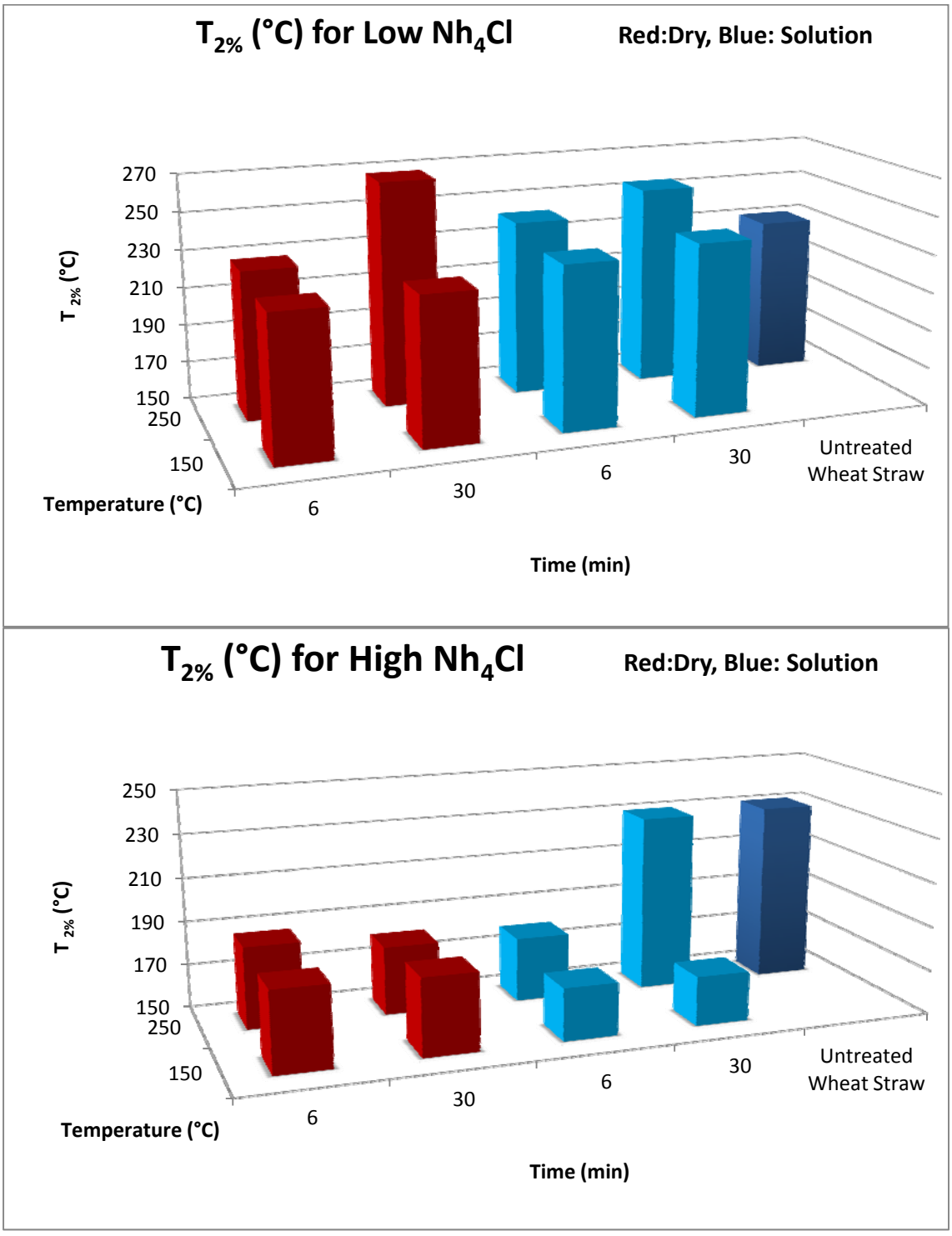

Figure 55: The $T_{2\%}$ values for the thermochemical treated samples using Low (top) and High (bottom) concentration of NH_4Cl.

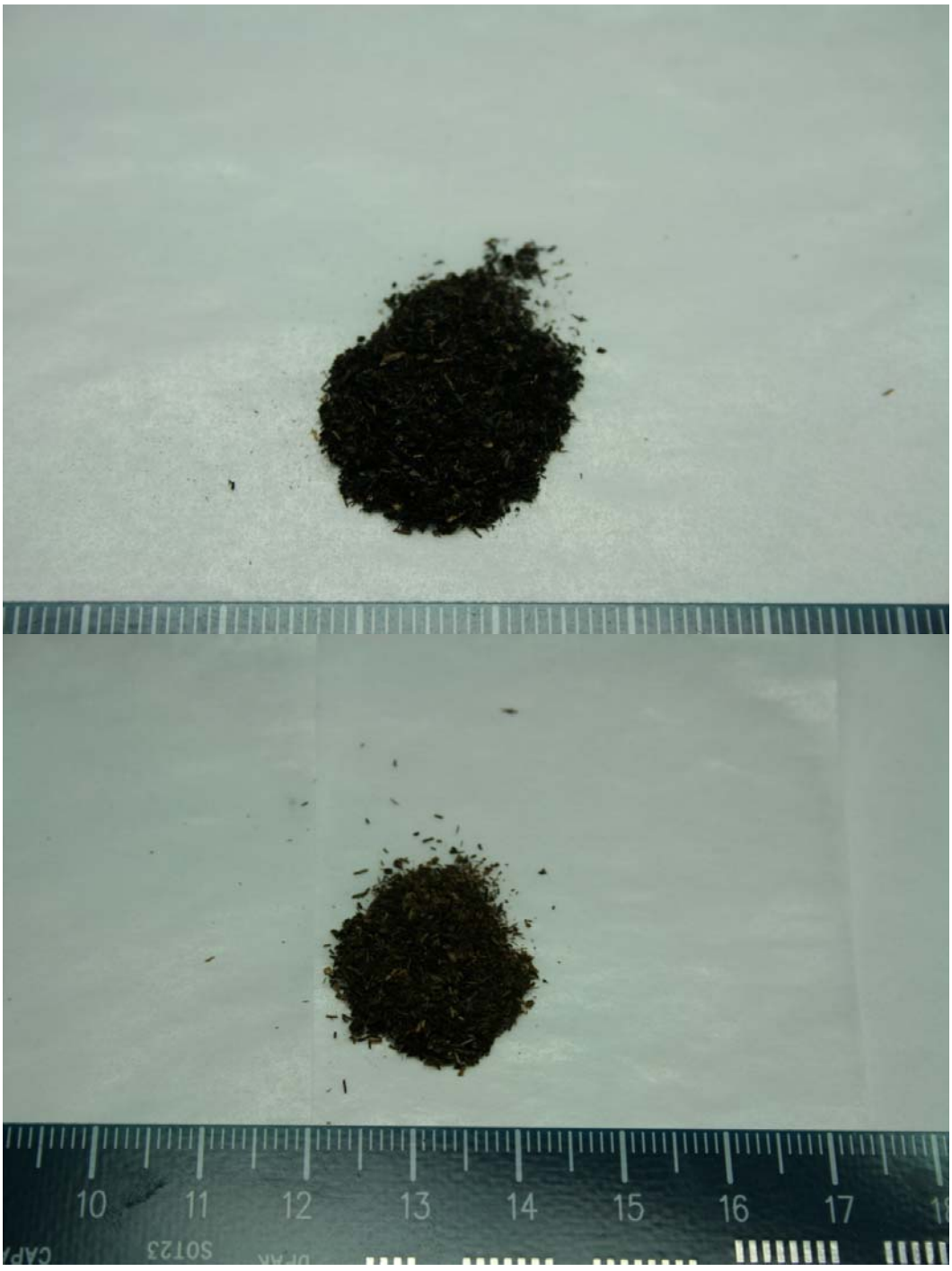

Figure 56: Appearance of the samples 250C_30min_Dry (top) and 250C_30min_Sol (bottom) after thermochemical treatment.

4.4 Conclusions

According to statistical analysis performed in this chapter, the yield depends on the temperature and time utilized during the thermal treatment. Increasing the temperature and especially the time of the thermal treatment drastically reduces the yield. Therefore, in order to maximize the yield, the thermal treatment should be performed utilizing shorter time and lower temperature (6 minutes and 250 °C, respectively).

On the other hand, in the first experiment (Experiment #01) none of the factors (temperature, time and ammonium chloride pre-treatment) studied appear to affect the thermal stability of the wheat straw samples; whereas in the second experiment (Experiment #02), the concentration of ammonium chloride influences the thermal stability of the samples. However, the samples with higher thermal stability were treated either without (Experiment #01) or with very low concentration (Experiment #02) of ammonium chloride. This indicates that ammonium chloride plays a very small (if any) role in improving the thermal stability of the wheat straw samples

The comparison between untreated and thermochemical treated samples suggests that the thermal treatments using lower temperature and shorter time are an interesting option to increase the thermal stability of the samples without compromising the yield. For example, a good combination of thermal stability enhancement and yield was achieved in the case of samples 250_6min (with 62 % yield and $T_{2\%}$ at 265.3 °C) and 250_30min (with 61 % yield and $T_{2\%}$ at 254.6 °C).

Thus, thermal treatments utilizing these regions of temperature and time should be explored in more detail in the future work as an attempt to achieve a combination of higher yield and thermal stability.

Chapter 5 - Development of Methodology for Silane Modification

5.1 Introduction

This chapter presents the second method utilized to improve the thermal stability of wheat straw fiber, i.e., silane modification. Achieving wheat straw fiber with better thermal stability would allow the fabrication of wheat straw fiber composites with high processing temperature polymers such as polyamides. Polyethylene and polypropylene can be processed using temperatures below 220 ^{o}C whereas; polyamides require a processing temperature of 240 ^{o}C or higher.

The efficiency of the silane modification depends on choosing the appropriate silane modifier and set of reaction conditions for each silane modifier. In this work, two types of silane modifiers are used: chlorosilane and alkoxysilane. The silane modification is a reaction between a silane compound (the modifier) and the surface of wheat straw.

Finding the best set of reaction conditions for silane modifications presents different challenges. First, the set of reaction conditions that is suitable for alkoxysilane modifiers most likely will not be appropriate for chlorosilane. In fact, a set of reaction conditions that is suitable for one specific alkoxysilane modifier may not be appropriate for another alkoxysilane modifier. Also, the chemical structures of these silane modifiers (e.g., organofunctional group R in the $R\text{-}(CH_2)_n\text{-}Si\text{-}X_3$ silane structure) affect the modification.

The majority of the literature regarding the utilization of silane modifiers refers to alkoxysilane modification of glass fiber and other inorganic fillers (Blum et al., 1991; Giessler and Mack, 2003; Pantano et al., 1992; Plueddemann, 1991; Li, 2007; Wesson et al., 1992). Very limited information is available regarding modification of agro-based fibers with alkoxysilane modifiers and virtually none with chlorosilane modifiers. In most of the cases, the reasons for using silane modifiers were either improving mechanical bond between agro-based fiber and a composite matrix or reducing the hydrophilic character of these fibers (Hornsby et al., 1997; Nair et al., 2001; Sreekala and Thomas, 2003).

Therefore, it is important to conduct an experimental study to determine both the best set of reaction conditions for silane modification with alkoxysilane and chlorosilane modifiers and the best silane modifiers that will provide the highest enhancement on the wheat straw thermal stability.

In order to achieve these objectives, this chapter is divided in four set of experiments. The first two sets were designed to investigate how the reaction conditions affect the hydrolysis and deposition of silane modifiers into wheat straw (Figure 57). The last two sets were intended to examine how different silane modifiers chemical structures such as the type of organofunctional group (R in the R-$(CH_2)_n$-Si-X_3 silane structure), the length of the linker between the organofunctional group and silicon atom (number of carbons in -$(CH_2)_n$-) and type of hydrolysable group (X) influence the silane deposition and the overall thermal stability of the silane treated wheat straw.

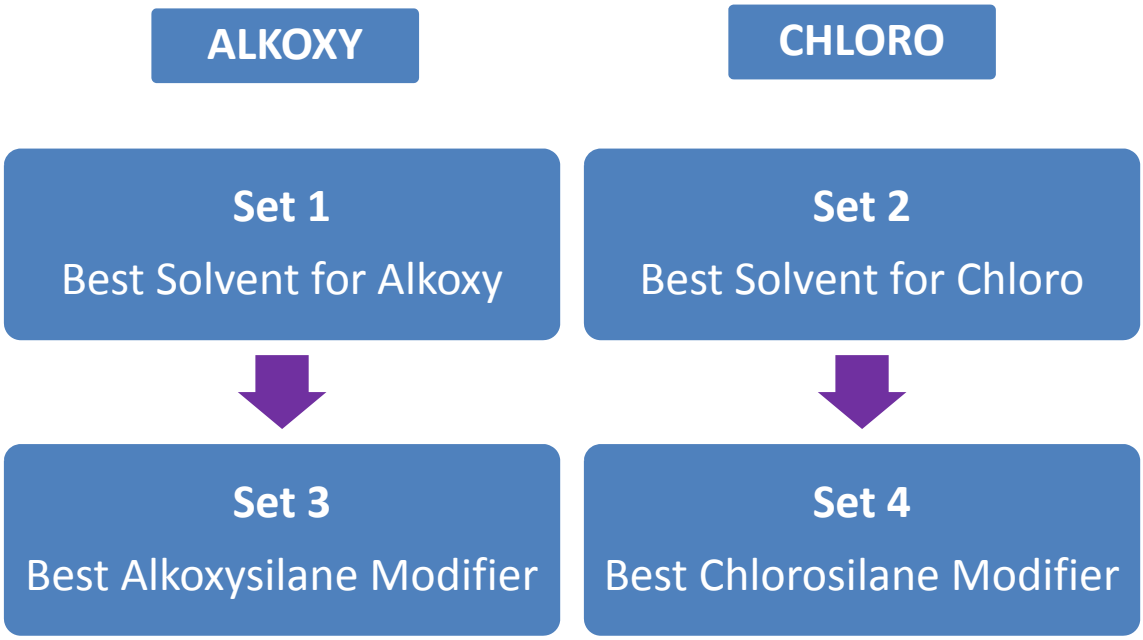

Figure 57: Diagram showing the main outputs expected from each set of experiments.

5.2 Materials

The wheat straw fiber was supplied by Omtec Inc. located in Mississauga, Canada. The wheat straw consists of soft white winter variety with particles size between mesh size of 35 (1.19 mm opening) and 16 (0.5 mm opening). Wheat straw fractionated with these sieves sizes is called here Mid wheat straw.

The list with the different solvents and silane modifiers used throughout this chapter is presented in the Table 14 below.

Table 14: List of equipments used in the Chapter 5.

Equipment/Materials	Manufacturer
Analytical balance AB304-S	Mettler Toledo
DSC Q2000	TA Instruments
Oven 5890A GC	Hewlett Packard
Hot Plate	VWR
TGA Q500	TA Instruments
Methanol	Sigma-Aldrich
Ethanol	Sigma-Aldrich
Toluene	Sigma-Aldrich
Ethyl acetate	Sigma-Aldrich
Tetrahydrofuran	Sigma-Aldrich
Acetone	Sigma-Aldrich
2-Propanol	Sigma-Aldrich
(3-Glycidoxy) propyltrimethoxysilane	Gelest Inc.
7-Octenyltrichlorosilane	Gelest Inc.
3-Aminopropyltrimethoxysilane	Gelest Inc.
Ureiodopropyltriethoxysilane	Gelest Inc.
Ethyltrichlorosilane	Gelest Inc.
n-Octadecyltrichlorosilane	Gelest Inc.
n-Octyltrichlorosilane	Gelest Inc.
3-Acryloxytrichlorosilane	Gelest Inc.
Tetrachlorosilane	Gelest Inc.

5.3 Methods

5.3.1 Alkali Pre-treatment of Wheat Straw Fiber

A two step process, as represented in Figure 58, was used to modify wheat straw fiber. First the fiber was submitted to an alkali treatment in order to remove waxy coatings and facilitate access to

hydroxyl groups present in the surface of the wheat straw. Then silane modification was performed using the alkali treated wheat straw which is described in the next section.

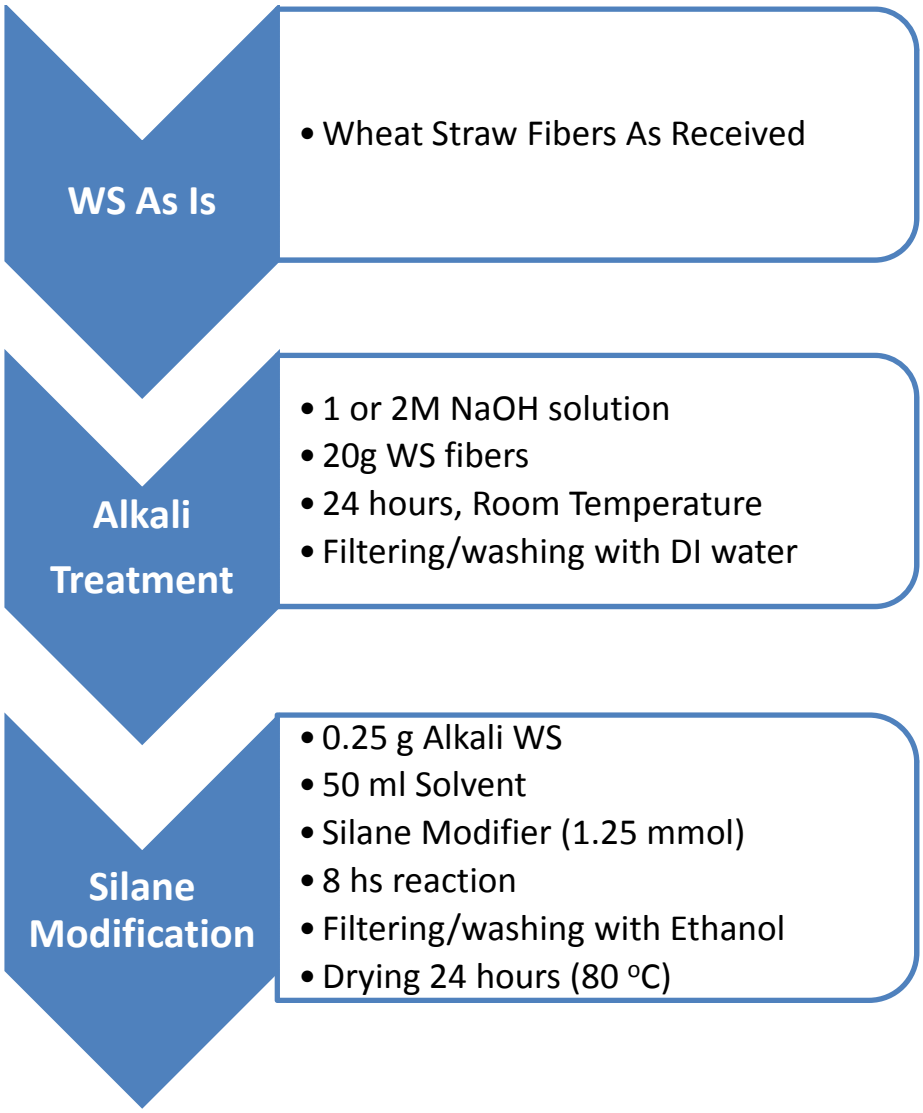

Figure 58: Flowchart representing the wheat straw treatments steps: alkali and silane.

In the case of the alkali treatment, both 1 and 2 molar alkali solution of sodium hydroxide (NaOH) was prepared using 0.5 L of deionized water. Wheat straw fiber as received was placed inside a glass beaker together with the alkali solution and stirred for 24 hours at room temperature. Then the alkali

treated wheat straw was washed with deionized water and filtered several times. The pH of the solution containing the alkali treated wheat straw was adjusted to 7 using a diluted solution of acetic acid. Once again the alkali treated wheat straw was washed with deionized water and filtered two times in order to remove any residual of acetic acid. Finally, the alkali treated fiber was oven dried at 80 ^{o}C for 24 hours.

5.3.2 Silane Modification of Wheat Straw Fiber with Alkoxy and Chlorosilane Modifiers

Four sets of experiments were conducted to study the modification of wheat straw fiber with organosilanes modifiers. Throughout these four sets, the silane modification of wheat straw fiber was carried out using the following procedure. Prior to any silane modification, the wheat straw fiber was submitted to a 24 hours pre-treatment using either a 1 or 2 molar alkali solution as described previously section (Alkali Pre-treatment of Wheat Straw Fiber).

The silane modification reactions were performed using 0.25 grams of wheat straw fiber, 50 ml of solvent and 5mmole g^{-1} of silane modifier (as described by Figure 58). The system was refluxed under gentle stirring for 8 hours under the boiling temperature of the solvent or combination of solvents. After this period of time, the reaction was stopped and cooled to room temperature. The mixture was filtered using filter paper and washed twice with ethanol to remove any non-reacted silane modifier. Finally, the silane modified fiber was dried in an oven for 12 hours at 80 ^{o}C.

Table 15 summarizes all the sets of silane modification experiments performed in this chapter. The column label in this table presents the nomenclature utilized for each one of the experiments. The different types of solvents or combination of solvents, types of silane modifiers and other reaction conditions are presented in the next three columns, respectively.

The aim of the first and second sets of experiments was to obtain the most suitable reaction conditions (e.g., type of solvent and, acidification and pre-hydrolysis of silane solution) to perform the alkoxy and chlorosilane modifications which maximize the deposition of silane and the thermal stability of the silane treated wheat straw. In order to achieve this maximization, hydrolysis has to be accelerated and condensation minimized. It is believed that hydrolyzed species are more reactive and prone to deposit in the surface of wheat straw fiber. On the contrary, condensation of these

hydrolyzed species produces oligomers which are less reactive and more likely to precipitate in the solvent (Plueddemann, 1991).

It is important to emphasize that different reaction conditions (e.g., different solvents) will lead to different hydrolysis and condensation rates. Also, the most suitable set of reaction conditions for alkoxysilane modifiers are most likely not appropriate for chlorosilane modifiers. Therefore, it is necessary to conduct an independent investigation for each one of these classes of silane modifiers.

In the case of the first set of experiments, named Alkoxy Solvent, the reaction condition variables included type of solvent, pH level and pre-hydrolysis of the silane modifier solution. The goal was to obtain the best combination of these reaction conditions for alkoxysilane deposition in the wheat straw fiber. The alkoxysilane (3-glycidoxy) propyltrimethoxysilane (referred to as Glycidoxy) was chosen along with different solvents (ethanol, methanol and water) and combination of solvents for testing (see Table 15). When a combination of solvents was used, different proportions of water and ethanol were tested. In the case of methanol, no other solvent was added. These solvents covered different range of boiling temperature and polarity. All the samples were submitted to acidification and pre-hydrolysis steps.

The objective of the second set of experiments, which was labeled Chloro Solvent, was to determine the best reaction conditions for the deposition of chlorosilane modifiers into wheat straw. The reaction conditions studied were limited to the type of solvent. For this set, acidification and pre-hydrolysis of the silane modifier solution were not considered. Seven different solvents and 7-Octenyltrichlorosilane (named as 7-Octenyl) were selected for testing based on literature review and manufacturer recommendations (Silanes & Silicones Gelest Catalog). The chosen solvents have different properties such as boiling temperature and polarity. For example, polar protic and aprotic solvents (methanol and THF, respectively) as well as non-polar solvents (toluene) were explored. These differences are likely to produce different hydrolysis and condensation rates. More details are given in Table 15.

The best set of reaction conditions established in the previous sets of experiments (Alkoxy Solvent and Chloro Solvent) were utilized to test different types of alkoxysilane and chlorosilane modifiers during the third and fourth sets of experiments. The goal was to determine, among different potential candidates, the alkoxysilane and chlorosilane modifiers which can produce the highest increase on the thermal stability of wheat straw.

Under the same reaction conditions, the nature and size of the non-hydrolyzable group (i.e., R group in the $R-(CH_2)_n-Si-X_3$ silane chemical structure) attached to the silicon atom of the silane modifier will affect the rates of hydrolysis and condensation. Thus, silane modifiers bearing different types of organofunctional groups (i.e., non-hydrolyzable groups such as amine, vinyl, epoxy etc) as well as chemical structure (e.g., the length of the linker group CH_2) were explored.

Table 15: Summary of the variables studied during silane modification experiments and its labels.

Set of Experiments	Label	Solvent (v%)	Silane Modifier	Reaction Conditions
Set 1 ALKOXY SOVENT	Methanol_WS	Methanol	Glycidoxy	Acidified + Pre-Hydrolysis (1h)
	E80+W20_WS	80Ethanol + 20Water		
	E95+W5_WS	95 Ethanol + 5Water		
	W100_WS	100Water		
Set 2 CHLORO SOLVENT	Acetone_WS	Acetone	7-Octenyl	None
	Ethanol_WS	Ethanol		
	Ethyl_WS	Ethyl Acetate		
	Propanol_WS	2-Propanol		
	Methanol_WS	Methanol		
	Toluene_WS	Toluene		
	THF_WS	Tetrahydrofuran		
Set 3 ALKOXY TYPE	Amino_WS	80Ethanol + 20Water	Amino	Acidified + Pre-Hydrolysis (1h)
	Ureiodo_WS		Ureiodo	
Set 4 CHLORO TYPE	Ethyl_WS	Methanol	Ethyl	None
	Octadecyl_WS		Octadecyl	
	7-Octenyl_WS		7-Octenyl	
	Octyl_WS		Octyl	
	Acryloxy_WS		Acryloxy	
	Tetra_WS		Tetra	

CONSTANTS: Reaction time: 8 hours; Reaction Temperature: BP Solvent; Pre-treatment: 2M Alkali solution

The aim of the third set of experiments, labeled Alkoxy Type, was to determine the alkoxysilane modifiers which provoke the biggest increase in the thermal stability of wheat straw fiber. The reaction conditions used during this set of experiments were obtained in the Alkoxy Solvent set of experiments (first) and kept constant throughout the Alkoxy Type set.

Wheat straw fiber was modified utilizing two different alkoxysilane modifiers (Table 15). The molecule of these alkoxysilane modifiers has different organofunctional (i.e., non-hydrolyzable) groups but similar hydrolyzable groups (R and X in the $R\text{-}(CH_2)_n\text{-}Si\text{-}X_3$ molecule, respectively). It is believed that different functional groups will lead to different amounts of grafted silane during silane modification of wheat straw fiber.

It is important to highlight that during this set of experiments, the wheat straw fiber was treated with an alkali solution of 1 molar instead of 2 molar prior to the silane modification. This reduction of the alkali solution concentration was an attempt to determine whether or not the thermal stability of wheat straw fiber would significantly change when the concentration of the alkali solution used to treat wheat straw fiber is decreased. Using lower concentration of alkali solution can bring two benefits. First, there is a reduction in the cost of the alkali treatment by using less sodium hydroxide. Second, the amount of wheat straw fiber obtained after the alkali treatment will increase because of the lesser removal of the wheat straw components.

After alkali treatment, part of the initial wheat straw mass is lost due to removal of different components of wheat straw (e.g., waxy, low molecular components, hemicellulose and lignin). Therefore, it is reasonable to expect that reducing the concentration of alkali solution will increase the mass obtained after alkali treatment.

Seven different chlorosilane modifiers were evaluated during the fourth set of experiments which was named Chloro Type. Methanol, one of the best solvents obtained from the Chloro Solvent set of experiments (second set), was used as the solvent. The main differences between the studied silane modifiers were the type of organofunctional group (R) as well as the length of the linker ($\text{-}(CH_2)_n\text{-}$) between the organofunctional group and the silicon atom (R and $\text{-}(CH_2)_n\text{-}$ in the $R\text{-}(CH_2)_n\text{-}Si\text{-}X_3$ silane structure, respectively). It is expected that these differences will influence the amount of grafted silane and therefore the thermal stability of wheat straw should be affected. The chlorosilane modifiers which promote the highest improvement on thermal stability of wheat straw will be selected for further studies.

For all four sets of experiments, two different wheat straw samples were utilized as reference in order to determine the improvements achieved due only to the silane modification.

The first reference is the wheat straw as received (without any treatment) and named As Is_WS. The second one is the wheat straw sample submitted to alkali treatment (described in the previous section, Alkali Pre-treatment of Wheat Straw Fiber). This sample is referred to as Alkali_WS.

In the case of the Alkoxy Type and Chloro Type (third and fourth sets, respectively) sets of experiments, a third reference sample was added in order to investigate whether or not the reaction conditions used to perform the silane modification could affect the thermal stability of wheat straw. Alkali treated wheat straw was submitted to the same reaction conditions employed for silane modification but without any silane modifiers. The sample was refluxed for 8 hours using either a combination of 80 % ethanol and 20 % water or methanol as solvent (third and fourth sets of experiments, respectively). The sample obtained after this procedure was named Alk_Reflux_WS.

5.3.3 Thermogravimetry analysis (TGA)

Thermogravimetry analysis experiments under isothermal conditions and non-isothermal conditions were used in order to rank the efficacy of the different set of silane modification experiments in terms of improving the thermal stability. The TGA analysis was performed with the assistance of Q500 series equipment from TA instruments. About 10 mg of sample was placed into a Pt crucible and subjected to isothermal and non-isothermal analysis. The first was conducted at 250 ^{o}C under 50ml flow of nitrogen during 30 minutes. During non-isothermal analysis, the temperature was increased from room temperature to 800 ^{o}C applying a heating rate of 10 ^{o}C/min under air atmosphere.

5.3.4 Grafted Silane

The main objective of the silane modification is to deposit different types of silane modifiers into the surface of wheat straw fiber. It is possible to determine whether the modification was successful or not by calculating the actual amount of silane modifier grafted to wheat straw. Equations 8 and 9 allow us to calculate the grafted amount and the grafting yield of silane modifier, respectively (Herrera et al., 2004; Reddy and Simon, 2010).

$$\text{Grafted amount (mequiv/g)} = \frac{(W_{200} - W_{600})\ x\ 10^3}{[100 - (W_{200} - W_{600})]\ x\ M} \qquad \textit{Equation 8}$$

$$\text{Grafted yield (\%)} = \left(\frac{\text{Grafted amount}}{[\text{Silane}]}\right)\ x\ 100 \qquad \textit{Equation 9}$$

where, M is the molecular mass of the silane modifier and [Silane] is the initial concentration of silane employed for modification. The (W_{200} - W_{600}) was calculated according to Equation 10. W_{200} and W_{600} are the weight at 200 and 600 ^{o}C, respectively, obtained from TGA analysis (under air atmosphere and heating rate of 10 ^{o}C/min). For each sample, the difference between the weight at 200 and 600 ^{o}C (W_{200} and W_{600}, respectively) was determined. Then, in order to distinguish between the weight loss due to thermal degradation of wheat straw fiber and silane modifier, the weight difference (W_{200}-W_{600}) of silane treated wheat straw samples was subtracted from the weight difference (W_{200}-W_{600}) of a reference wheat straw sample (e.g., Alk_Reflux), as described by Equation 10. The reference sample was submitted to alkali and reflux with methanol treatments, mimicking the treatments applied to silane samples.

$$(W_{200} - W_{600}) = (W_{200} - W_{600})_{\substack{Silane\\ Modified\\ Sample}} - (W_{200} - W_{600})_{\substack{Reference\\ Sample}} \qquad \textit{Equation 10}$$

5.4 Investigation of Reaction Conditions for Silane Modification

The efficacy of the silane modification depends on the formation of reactive Si-OH species called silanols (Castellano et al., 2004; Plueddemann, 1991; Salon et al., 2007). The formation of these groups occurs through the hydrolysis of the hydrolysable groups such as methoxy, ethoxy and chloro present in the silane molecule. The hydrolysis rate of silane forming silanols groups and these silanols condensation rate are governed mostly by both the reaction conditions (e.g., pH, type of solvent, temperature, concentration and use of catalyst) as well as the nature and size of silane modifier (i.e., organofunctional, non-hydrolyzable and hydrolyzable groups present in the silane molecule). The

self-condensation between silanols groups leads to the formation of less reactive structures such as dimer, linear siloxane and ultimately three-dimensional polysiloxane (Salon et al., 2007). Because of that, it is desirable that the rate of hydrolysis be maximized and the rate of condensation minimized. Therefore, the goal was to determine the set of reaction conditions where the hydrolysis reaction is accelerated and the self-condensation reaction inhibited. Thus, the highest silane grafting and thermal stability enhancement of wheat straw will be achieved. The experimental study was divided into two parts. The first one (Alkoxy Solvent) dealt with alkoxysilane modifiers and the second (Chloro Solvent) included only chlorosilane modifiers.

Both set of experiments were carried out following the silane modification procedure described previously with a constant time of reaction of 8 hours.

5.4.1 The Best Set of Reaction Conditions for Alkoxysilane Modifiers

The goal of the Alkoxy Solvent set of experiments was to obtain the most favorable set of reaction conditions for alkoxysilane modification where the deposition of silane and the thermal stability of wheat straw are maximized.

Prior to the Alkoxy Solvent set of experiments, a preliminary study was conducted using a mixture of 80 % ethanol and 20 % water (volume) as solvent. Its objective was to compare the effect of three different reaction conditions. First, the pure solvent mixture (80 % ethanol and 20 % water) was tested. The second reaction condition included acidification of the solvent mixture. The third one studied a combination of acidification and pre-hydrolysis of the solvent mixture. The silane modifier was included in all these three reaction systems.

The acidification step consisted of adding small amounts of acetic acid in order to catalyze the hydrolysis reaction of the methoxy groups present in the molecule of the alkoxysilane modifier. The pre-hydrolysis step allowed the solution containing solvent, silane modifier and acetic acid to be stirred for 1 hour prior to addition of wheat straw fiber.

It was observed that utilizing acidification along with pre-hydrolysis produced the best results in terms of enhancement of thermal stability of wheat straw fiber. Because of that, acidification and pre-hydrolysis were adopted throughout the Alkoxy Solvent set of experiments. These results are not presented here in an effort to make this section more clear and concise.

Table 16 presents the four reaction conditions tested during Alkoxy Solvent set of experiments. The main differences between these four reaction conditions were the solvent which included either one or a mixture of two different solvents. In the case of methanol, neither another solvent nor water was added to the reaction system. When a mixture of ethanol and water was employed as solvent, their concentration were either (95/5 v/v) or (80/20 v/v). Also a solution of a 100% of water as solvent was tested. All four solvent or combination of solvents were submitted to both, acidification and pre-hydrolysis steps.

Table 16: Summary of experimental conditions used during alkoxysilane modification in the Alkoxy Solvent (first) set of experiments.

Label	Solvent	Boiling Point (^{o}C)[A]	Reaction Conditions	Silane Modifiers
Methanol_WS	Methanol	64.7		
E95+W5_WS	95v%Ethanol + 5v%Water	78.2	Acidified +	
E80+W20_WS	80v%Ethanol + 20v%Water	78.8	Pre-	Glycidoxy
W100_WS	100v%Water	100	Hydrolysis (1h)	
As Is_WS	None	---	---	None
Alkali_WS	Water	---	2M alkali	None

A: Adapted from Handbook of Chemistry and Physics (Haynes, W.M. 2012); CONSTANTS: Reaction time: 8 hours; Reaction Temperature: Solvent boiling point; Pre-treatment: 2M alkali solution; Silane modifier: 1.25 mmol of (3-glycidoxypropyl) trimethoxysilane.

The alkoxysilane chosen for testing was (3-glycidoxy) propyltrimethoxysilane (Glycidoxy). This silane modifier represents a class of alkoxysilane with a neutral organofunctional group. This class of silane modifier is called neutral because it does not readily undergo hydrolysis in contact with water. Actually, hydrolysis of these alkoxysilane modifiers is a very slow process and special conditions such as acid pH are required. Once the best set of reaction conditions is determined for Glycidoxy modifier, this information can be used for other silane modifiers of the same class which have similar hydrolysis mechanism.

Table 16 summarizes the different combination of solvents and other experimental conditions employed for each one of the experiments.

The thermal stability of the wheat straw samples, i.e., the changes on the weight of a sample as a function of temperature, was investigated with the assistance of thermal gravimetric analysis. The results of this analysis under air atmosphere are depicted in Figure 59.

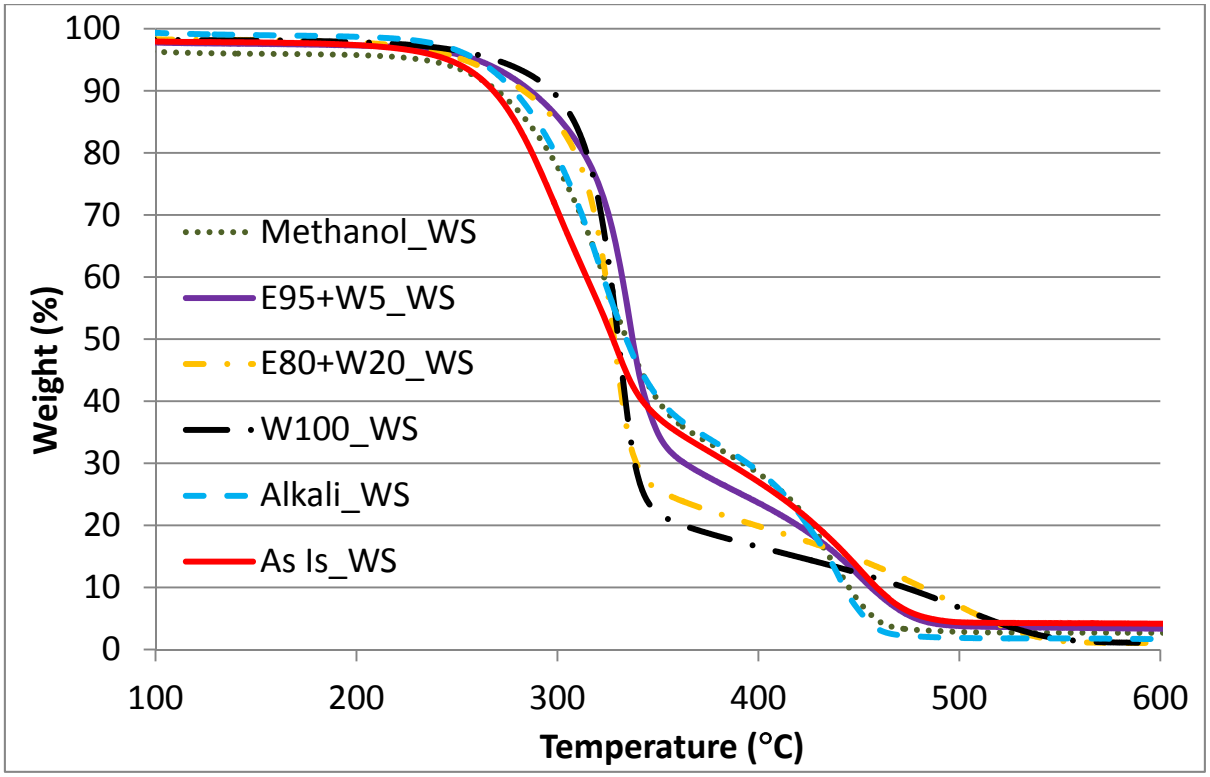

Figure 59: Weight (%) as a function of temperature obtained from TGA analysis performed using 10°C/min heating rate and air atmosphere for Alkoxy Solvent set of experiments samples.

It can be seen from this figure that increasing the amount of water present during silane modification increases the thermal stability of the wheat straw samples. The curves representing W100_WS (black long dash dot), E80+W20_WS (yellow dash dot) and E95+W5_WS (purple solid) samples are located at the right of the curves of As Is_WS (red solid) and Alkali_WS (blue dash). This implies that these silane treated samples (W100_WS, E80+W20_WS and E95+W5_WS) have

their starting point of thermal degradation at higher temperatures than the untreated and alkali treated samples (As Is_WS and Alkali_WS). Moreover, when no water is added during silane modification (Methanol_WS sample), no improvement on thermal stability is observed. In fact, the curve for Methanol_WS sample is displayed in the same region of the curve for alkali treated sample.

The starting point of thermal degradation of the samples was estimated using the temperature at 2 % of weight loss ($T_{2\%}$) which is the temperature where 2 % of the weight is lost. The procedure to obtain the $T_{2\%}$ is described in detail in Chapter 3 (Result and Discuss section).

Figure 60 depicts the $T_{2\%}$ results for all treated and untreated samples. It is possible to confirm that the starting point of thermal degradation of W100_WS, E80+W20_WS and E95+W5_WS samples is shifted to higher temperatures. For example, the beginning of thermal degradation of W100_WS sample was increased by 7.48 % (from 238 to 255.8 ^{o}C) and 3.94 % (from 246.1 to 255.8 ^{o}C) in comparison with the untreated (As Is_WS) and alkali treated (Alkali_WS) samples, respectively. As the amount of water during silane modification decreases, the $T_{2\%}$ also decreases. The E95+W5_WS sample exhibits either modest (3.32 % - from 238 to 245.9 ^{o}C) or none (from 246.1 down to 245.9 ^{o}C) improvement on the $T_{2\%}$ with respect to As Is_WS and Alkali_WS samples, respectively.

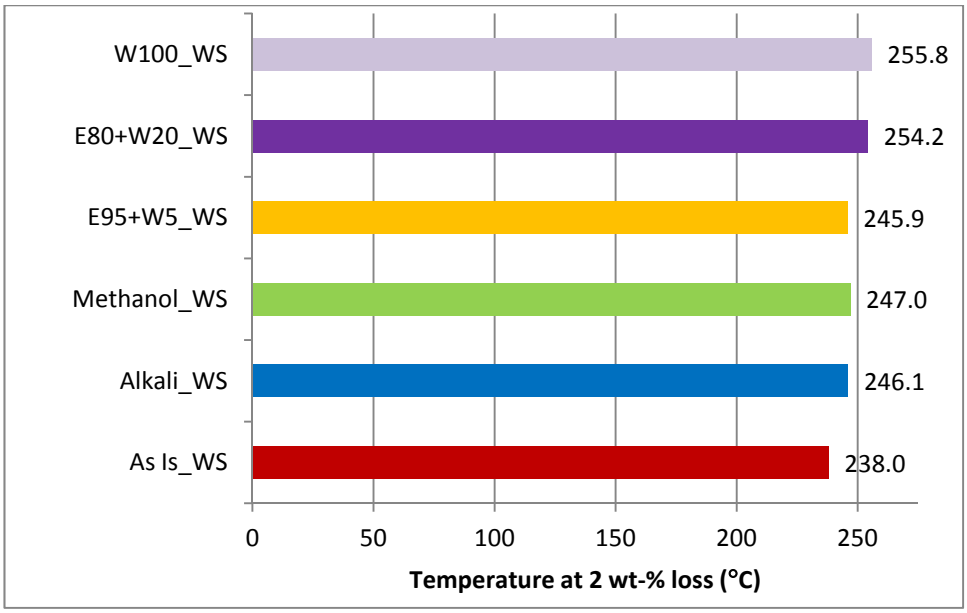

Figure 60: Temperature at 2 % weight loss obtained from TGA analysis using 10 ^{o}C/min heating rate and air atmosphere for the Alkoxy Solvent set of experiments samples.

Furthermore, similar behavior on the thermal stability of the samples is observed when they are submitted to isothermal heating at 250 ^{o}C under nitrogen atmosphere. This condition was chosen because it is similar to the processing conditions utilized during the compounding and processing of polyamides composites. The objective of this test is to measure the thermal degradation of wheat straw fiber that would occur in conditions somewhat similar to those encountered during compounding with polyamides. Figure 61 shows that W100_WS (light pink solid), E80+W20_WS (dark blue round dot) curves are displayed at the top of the graph. Even after 30 minutes of exposure to 250 ^{o}C, the W100_WS and E80+W20_WS curves remain above the 90 % mark which represents less than 10 % of weight loss. In the contrary, As Is_WS (red lozenge curve), Alkali_WS (blue square curve) and E95+W5_WS (yellow square curve) samples exhibit a poor thermal stability. Even after short periods of time (between 10 and 15 minutes), the As Is_WS, Alkali_WS and E95+W5_WS curves exhibit a steeper decrease and are placed below the 90 weight percentage region (Figure 61). All these three samples ended with less than 85 % of their initial weight after 30 minutes of exposure to 250 ^{o}C.

The weight percentage of each sample after 10 minutes of exposure to 250 ^{o}C (Wt250) was obtained from Figure 61 and plotted in Figure 62. Ten minutes is the typical residence time for processing of thermoplastics composites (considering compounding, molding and cooling times). This plot clearly demonstrates that the thermal stability (i.e., the Wt250 value) is higher when silane modification was performed using higher amounts of water. For example, the Wt250 values for the W100_WS and E80+W20_WS samples were 2.49 % (from 89.4 to 91.6 %) and 4.84 % (from 89.4 to 93.7 %) higher than the one for Alkali_WS sample, respectively. Actually, if no water is added during silane modification (Methanol_WS sample), the Wt250 value for Methanol_WS sample is 3 % (from 89.4 down to 86.7 %) smaller than the value for Alkali_WS sample and similar to the value for As Is_WS sample (86.6 %).

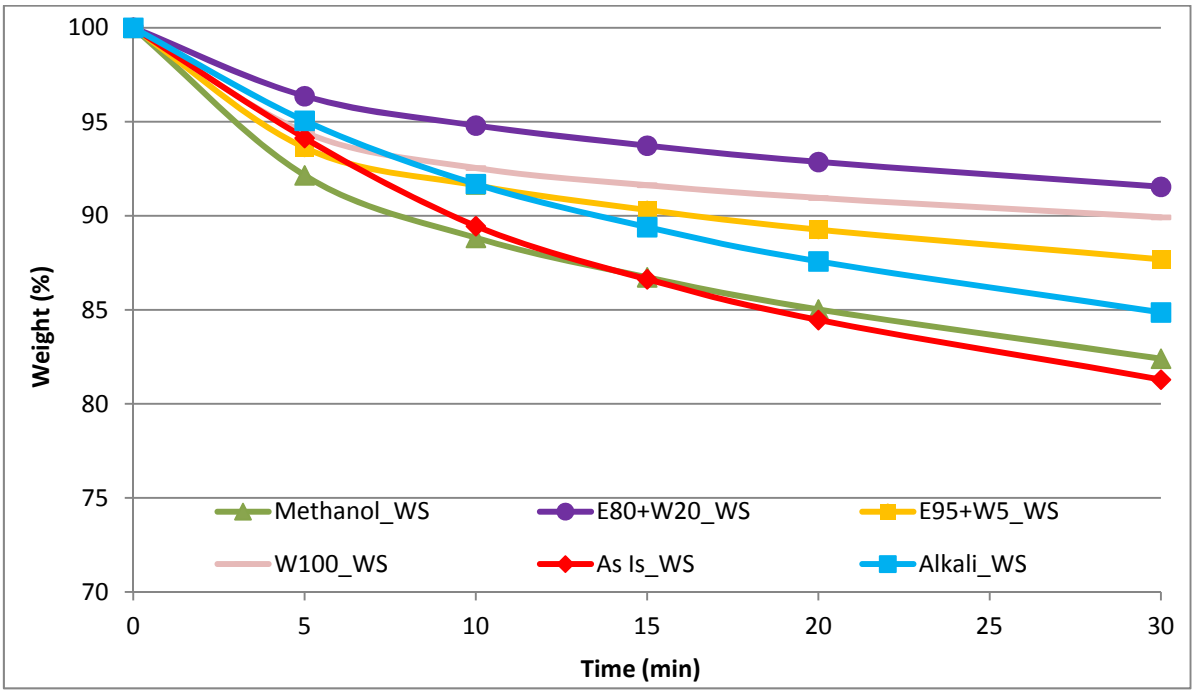

Figure 61: Isothermal curves obtained at 250 °C under nitrogen atmosphere for the Alkoxy Solvent set of experiments samples.

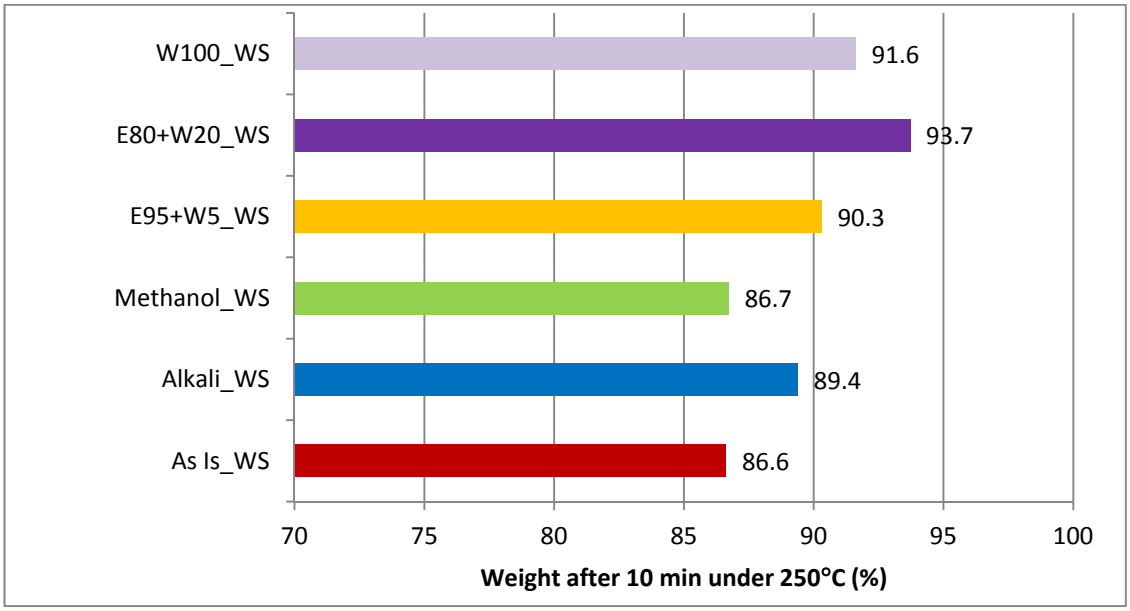

Figure 62: Weight percentage left after 10 minutes (Wt250) under isothermal heating at 250 °C for the Alkoxy Solvent set of experiments samples.

Similar findings were reported by Castellano et al. (2004). In the absence of water, extremely small amounts of cyanoethyltrimethoxysilane (CES) modifier were grafted to cellulose fiber. The authors explain that the methoxy groups of CES were not hydrolyzed and therefore could not react with the hydroxyl (OH) groups of cellulose. However, when increasing amounts of moisture were added to the reaction system, progressively higher amounts of the silane modifier were grafted to the cellulose fiber. Interestingly, when dried lignin was utilized, CES was chemically grafted even in the absence of water.

According to those authors the higher acidity of phenolic OH groups (lignin) in comparison with aliphatic OH groups (cellulose) justifies the higher reactivity of phenolic OH groups towards the methoxy groups of CES. Similar results were obtained with other silane modifiers such as aminopropyltrimethoxysilane and glycidylpropyltrimethoxysilane.

Figure 63 depicts the grafted silane percentage for the silane treated samples. The amount of water utilized during silane modification directly affects the amount of silane grafted to wheat straw fiber. Higher amounts of silane were found grafted to wheat straw fiber when increased levels of water were utilized. For example, silane modification performed with 100 and 20 % of water as solvent (W100_WS and E80+W20_WS samples, respectively) produced the highest amount of grafted silane (2.92 and 2.82 %, respectively). Reducing the amount of water to 5 % (E95+W5_WS sample) drastically decreases the grafted silane to 0.62 %. This value represents a reduction of approximately 4.5 times on the grafted silane percentage with respect to W100_WS and E80+W20_WS samples. In the same way, if no water is added to the system during silane modification, case of the Methanol_WS sample, virtually no silane is grafted to wheat straw fiber (0.07 %). These findings are in agreement with the thermal stability ($T_{2\%}$ and Wt250) of the silane treated fiber.

In fact, Figure 64 and Figure 65 show that increasing the amount of grafted silane increases the thermal stability of the silane treated fiber. Thus, the enhancement of the thermal stability may be credited to the amount of silane modifier grafted to wheat straw fiber.

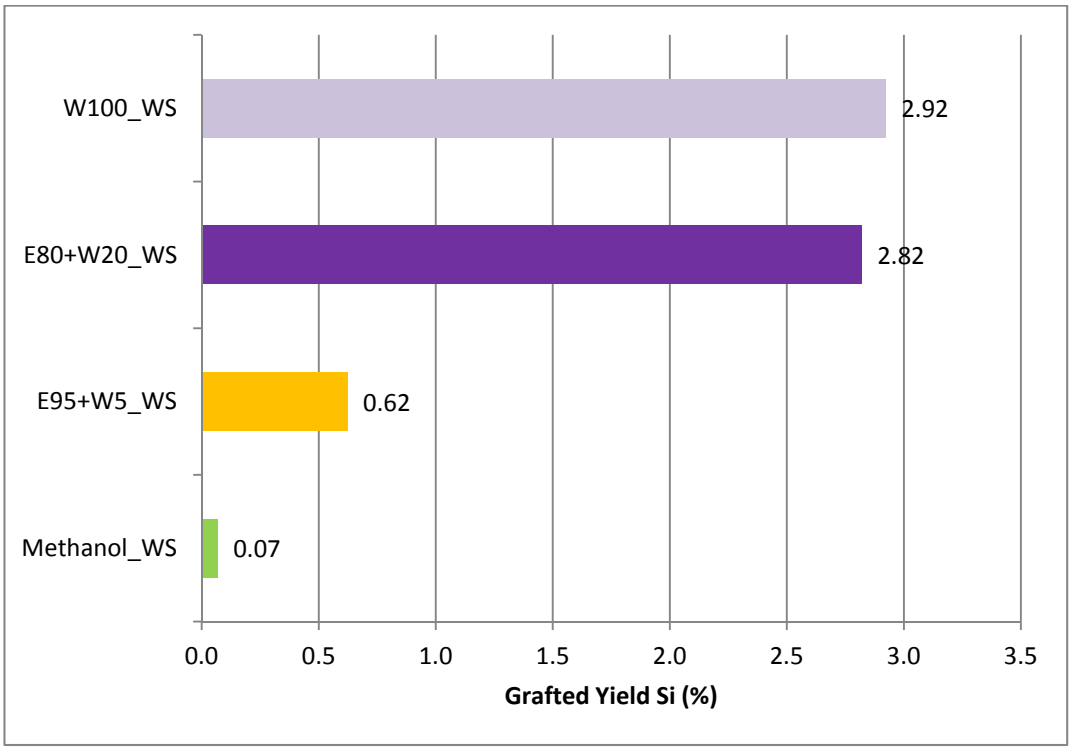

Figure 63: Silane (%) grafted into wheat straw as a function of solvent used during the Alkoxy Solvent set of experiments.

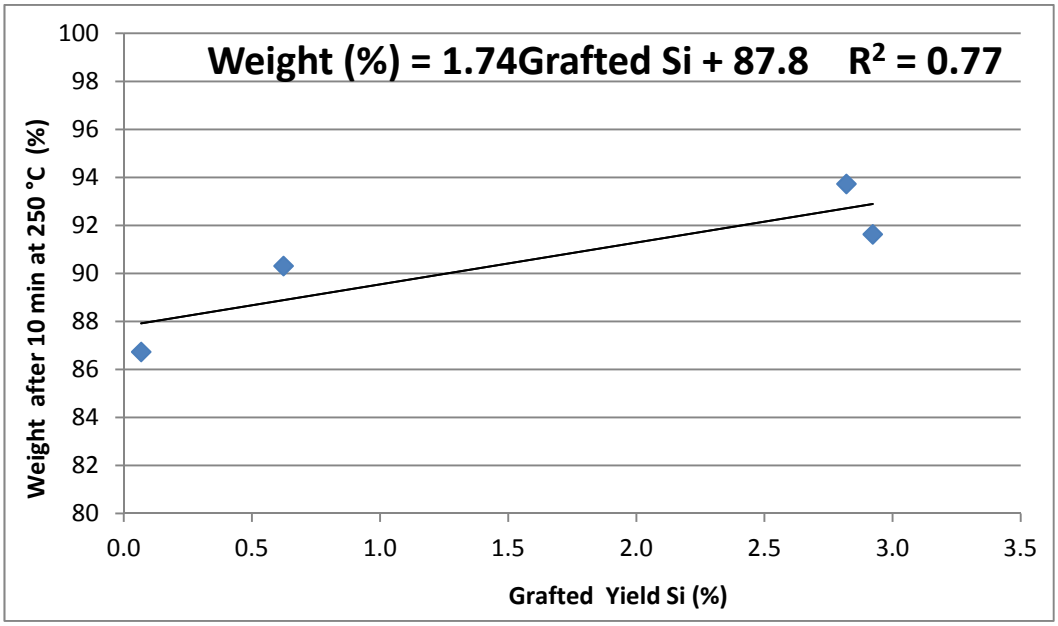

Figure 64: Weight (%) left after 10 minutes (Wt250) under isothermal heating at 250 °C as a function of silane (%) grafted into wheat straw for the Alkoxy Solvent set of experiments samples.

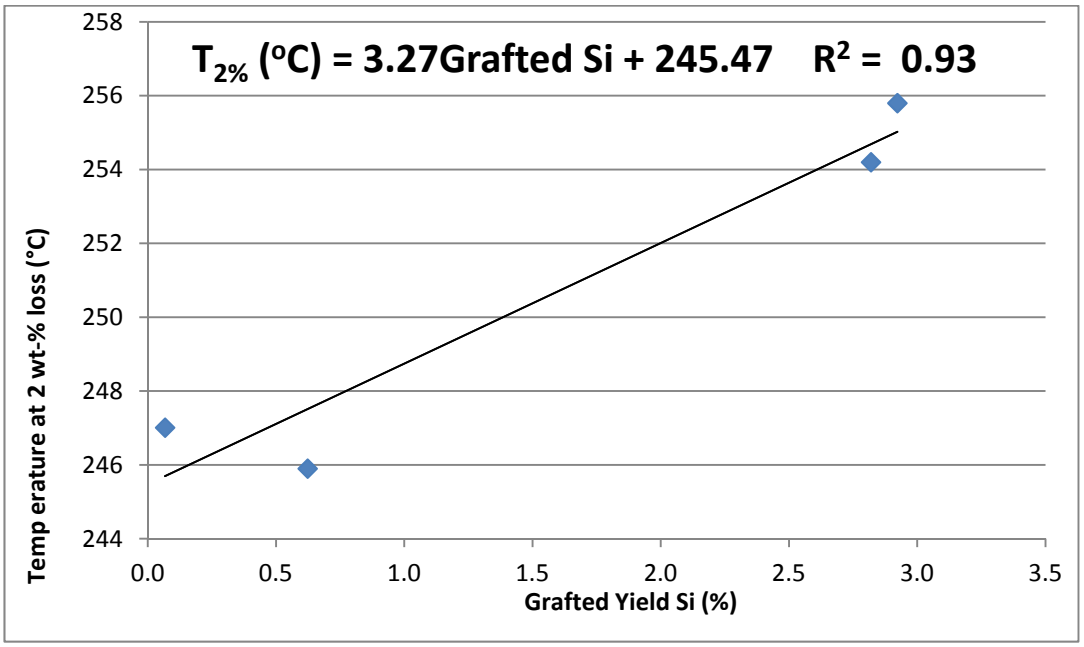

Figure 65: Temperature at 2 % weight loss (obtained from TGA analysis using 10 °C/min heating rate under air atmosphere) as a function of silane (%) grafted into wheat straw for the Alkoxy Solvent set of experiments samples.

Further proof of the silane modification is provided by the ash content measurements. Figure 66 shows the ash content results for all samples. It can be seen that a lower content of inorganic material is present in the case of silane treated samples, especially in the ones with higher amount of grafted silane (e.g., W100_WS sample: 1.09 % and E80+W20_WS sample: 1.05 %). The percentage of inorganic material increases as we move to samples displaying lower grafted silane percentage (e.g., E95+W5_WS sample: 2.41 % and Methanol_WS sample: 2.68 %) or without silane treatment (e.g., Alkali_WS sample: 2.69 % and As Is_WS sample: 4.14 %).

Achieving wheat straw fiber with better thermal stability is the main goal of this work. That would allow the fabrication of composites with this wheat straw fiber and high processing temperature polymers such as polyamides. Therefore, the Wt250 value was used as the main parameter to decide whether a silane treatment is good or poor. This parameter gives the extent of the thermal degradation of wheat straw fiber after 10 minutes of exposure to 250 °C. The wheat straw samples with the lowest thermal degradation under these conditions will have a higher chance to be successful compound with polyamides.

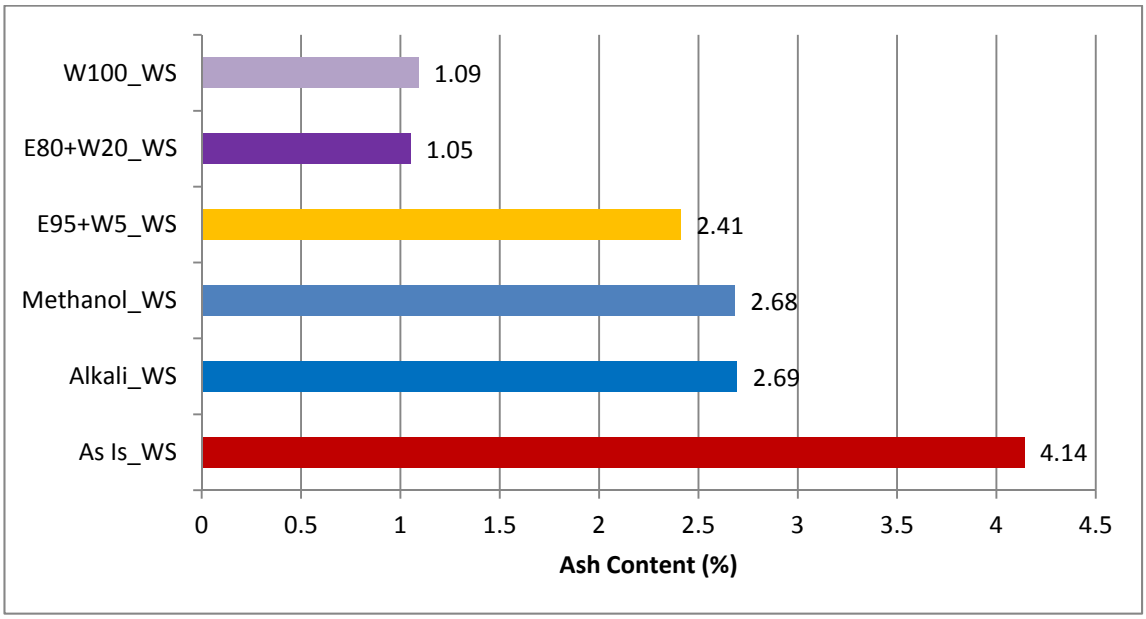

Figure 66: Ash content (mass left at 600 °C under air atmosphere) for the Alkoxy Solvent set of experiments samples.

Based on the results obtained from the Alkoxy Solvent set of experiments, summarized in Table 17, the best set of reaction conditions is a combination of two solvents (80 % ethanol + 20 % water) as well as the application of acidification and pre-hydrolysis steps. The use of 100 % water as a solvent (W100_WS) also provides good results. When these reaction conditions are employed to perform silane modification of wheat straw fiber, the highest amount of grafted silane and thermal stability improvement are achieved. Furthermore, when a lower amount of water is utilized (E95+W5_WS), the silane treated sample presents significantly smaller values of grafted silane and thermal stability.

The amount of water can affect the rate of hydrolysis and condensation of silanols groups (Blum et al., 1991; Plueddemann, 1991). One can speculate that in the case of E95+W5_WS sample, sufficient amount of water is not available for the hydrolysis to take place as fast as in the case of W100_WS and E80+W20_WS samples. If the hydrolysis rate is too slow, few silanols groups are formed and the interaction between the silane modifier and hydroxyl groups of the fiber is compromised. With lower amount of water present (E95+W5_WS sample), probably a longer period of time would be necessary to achieve the same degree of hydrolysis as in the case of W100_WS and E80+W20_WS samples. It

is reported in the literature that using a 10:1 acetone-water mixture at pH 3.9, the complete hydrolysis of Glycidocy modifier was not achieved even after several hours. In contrast, when the ratio acetone-water was increased from 10:1 to 1:1, the complete hydrolysis of aminopropyltrimethoxysilane (Amino) was reached after 5 minutes instead of the initial 200 minutes (Blum et al., 1991).

Thus, the reaction conditions employed for E80+W20_WS sample will be utilized to evaluate different types of alkoxysilane modifiers in the Alkoxy Type set of experiments (third set).

Table 17: Summary of thermal stability and grafted silane results for alkoxysilane modification of wheat straw fiber using different solvents.

Sample	$T_{2\%}$ (^{o}C)	Wt250 (%)	Grafted Si (%)	Overall Performance
Methanol_WS	247.0	86.7	0.07	Poor
E95+W5_WS	245.9	90.3	0.62	Poor
E80+W20_WS	254.2	93.7	2.82	Good
W100_WS	255.8	91.6	2.92	Good
Alkali_WS	246.1	89.4	---	Reference
As Is_WS	238.0	86.6	---	Reference

5.4.2 The Best Set of Reaction Conditions for Chlorosilane Modifiers

The objective of Chloro Solvent set of experiments was to obtain the best set of reaction conditions for silane modification of wheat straw which provides the highest deposition of silane and increase on thermal stability.

Based on preliminary screening of different chlorosilane modifiers, 7-octenyltrichlorosilane (7-Octenyl) was selected to study how different reaction conditions, namely different organic solvents, affect the deposition of this chlorosilane modifier (7-Octenyl) on the wheat straw fiber.

Seven different solvents with different boiling temperatures and polarities were tested. It is expected that these differences will cause different hydrolysis and condensation rates. All these

solvents are recommended by different manufactures of silane modifiers. These reaction conditions and test labels are summarized in Table 18.

Table 18: Summary of experimental conditions utilized during the Chloro Solvent set of experiments.

Label	Solvent	Chemical Formula	Polarity		
			Class	Polar bond ($MPa^{1/2}$)	Hydrogen bond ($MPa^{1/2}$)
Toluene_WS	Toluene	C_6H_5-CH_3	Non-polar	1.4	2.0
Ethyl_WS	Ethyl Acetate	CH_3-C(=O)-CH_2-CH_3	Non-polar	5.3	7.2
THF_WS	Tetrahydrofuran	/-CH_2-CH_2-O-CH_2-CH_2-/	Polar aprotic	5.7	8.0
Acetone_WS	Acetone	CH_3-C(=O)-CH_3	Polar aprotic	10.4	7.0
Propanol_WS	2-Propanol	CH_3-CH-(OH)-CH_3	Polar protic	6.1	16.4
Ethanol_WS	Ethanol	CH_3-CH_2-OH	Polar protic	8.8	19.4
Methanol_WS	Methanol	CH_3-OH	Polar protic	12.3	22.3
As Is_WS	None	---	---	---	---
Alkali_WS	Water	---	---	---	---

CONSTANTS: Reaction time: 8 hours; Reaction Temperature: Solvent boiling point; Pre-treatment: 2M alkali solution; Silane modifier: 1.25 mmol of 7-octenyltrichlorosilane.

Looking at Table 18 it is possible to see that toluene has the lowest values of polar bond (δP) and hydrogen bond (δH) and therefore is considered non-polar solvent. In comparison with toluene,

tetrahydrofuran (THF) has higher polar bond (δP) but lower hydrogen bond (δH) values and because of that these solvents are classified as polar aprotic. Both methanol and ethanol have the highest values of polar bond (δP) and hydrogen bond (δH) and therefore, they are classified as polar protic solvents.

Figure 67 displays the curves of weight as a function of temperature (from TGA) for wheat straw samples modified with chlorosilane modifier (7-Octenyl) as well as the reference samples (As Is_WS and Alkali_WS). For clarity purpose, the curves representing silane modified samples using propanol, ethyl acetate and acetone as solvent are omitted. Figure 67 demonstrates that changing the polarity of the solvents utilized for silane modification affects the thermal stability of the silane treated samples. For example, the curves representing silane treated samples using polar protic solvents (Ethanol_WS and Methanol_WS – yellow long dash dot and purple dash, respectively) were shifted to the right (i.e., they have the onset of weigh loss at higher temperatures than the other samples) in comparison with the curves of polar aprotic solvent (THF_WS – dark green dash dot), non-polar solvent (Toluene_WS – light blue long dash) and non-silane treated samples (As Is_WS and Alkali_WS – red solid and dark blue round dot, respectively). Unlike Ethanol_WS and Methanol_WS samples, the curves representing Toluene_WS and THF_WS samples are placed between the As Is_WS and Alkali_WS samples curves. As a consequence of that, thermal degradation of Ethanol_WS and Methanol_WS samples starts at significantly higher temperatures than in the case of Toluene_WS and THF_WS samples.

In order to compare quantitatively the differences of the beginning of the thermal degradation of the samples, the temperature at 2 % of weight loss ($T_{2\%}$) was determined following the procedure described previously in Chapter 3 (Result and Discuss section).

Figure 68 displays the temperature at 2% weight loss for all the treated and untreated samples. It can be seen that the $T_{2\%}$ has significantly increased when the silane treatment is applied using polar protic solvents. For example, the Ethanol_WS and Methanol_WS samples have the 2 % of weight lost at 270.9 and 261.9 °C, respectively; whereas, the untreated (As Is_WS) and alkali treated (Alkali_WS) samples show the 2 % of degradation at significantly lower temperatures, 238.0 and 246.1 °C, respectively. The enhancement on the thermal stability of Ethanol_WS and Methanol_WS samples was 13.81 and 10.02 % in comparison with the untreated sample (As Is_WS) and 10.08 and 6.42 % when comparing with the alkali treated sample (Alkali_WS), respectively.

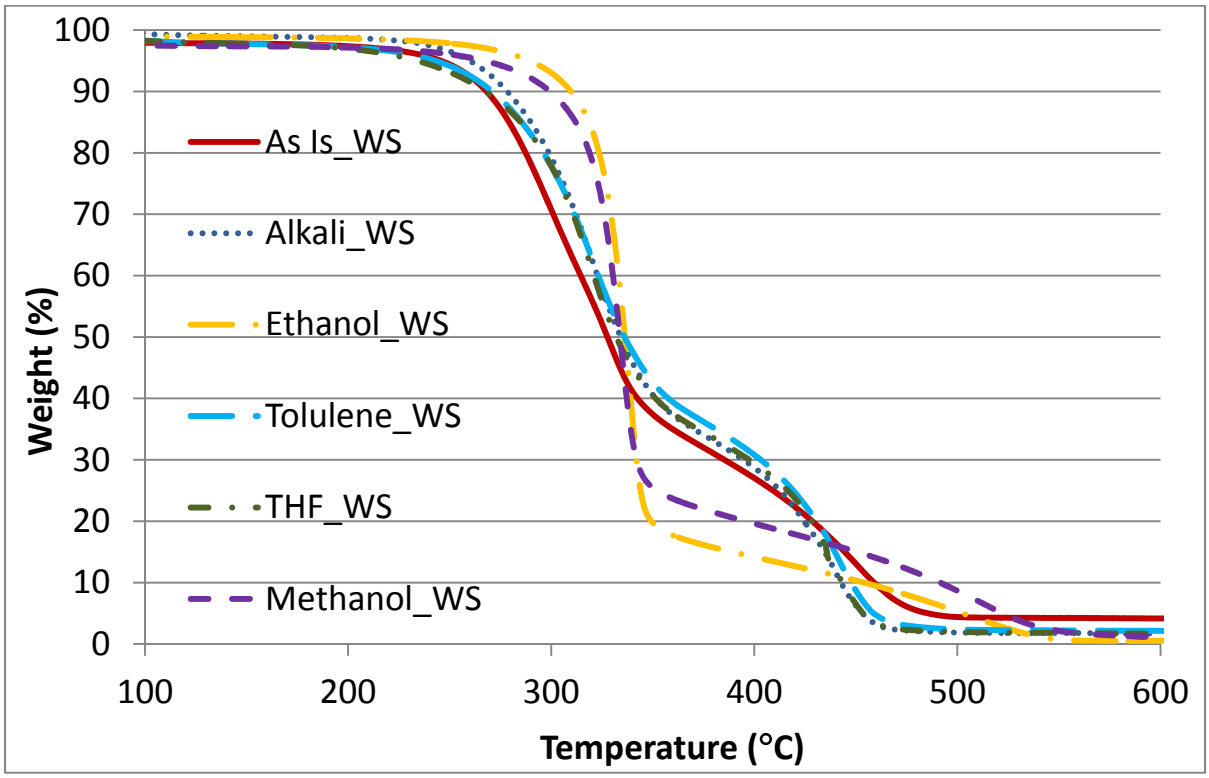

Figure 67: Weight (%) as a function of temperature obtained from TGA analysis performed using 10 °C/min heating rate under air atmosphere for the Chloro Solvent set of experiments samples.

In contrast, when the silane modification of wheat straw fiber was performed using non-polar (e.g., toluene) or polar aprotic (e.g., THF) solvents, there was no improvement in the thermal stability ($T_{2\%}$) of the silane treated samples in comparison with the untreated sample (As Is_WS) and alkali treated sample (Alkali_WS). For example, the Toluene_WS and THF_WS samples have the 2 % of weight lost at 235.1 and 224.1 °C, respectively. These values are lower than the $T_{2\%}$ values presented by the untreated sample (238.0 °C) and alkali treated sample (246.1 °C).

Likewise, the same trend was observed during isothermal gravimetric analysis performed under the constant temperature of 250 °C. It can be seen from Figure 69 that the Ethanol_WS and Methanol_WS curves (yellow square dot and purple square dot, respectively) are portrayed in the region of smaller weight loss in the graph (at the top); whereas the curves representing non-silane treated samples (As Is_WS and Alkali_WS, red triangular dot and blue round dot lines, respectively) and silane treated samples utilizing non-polar and polar aprotic solvents (Toluene_WS and THF_WS

dark green solid and light green lozenge lines, respectively) are displayed in the region of the graph where the weight loss is bigger (bottom part of the graph).

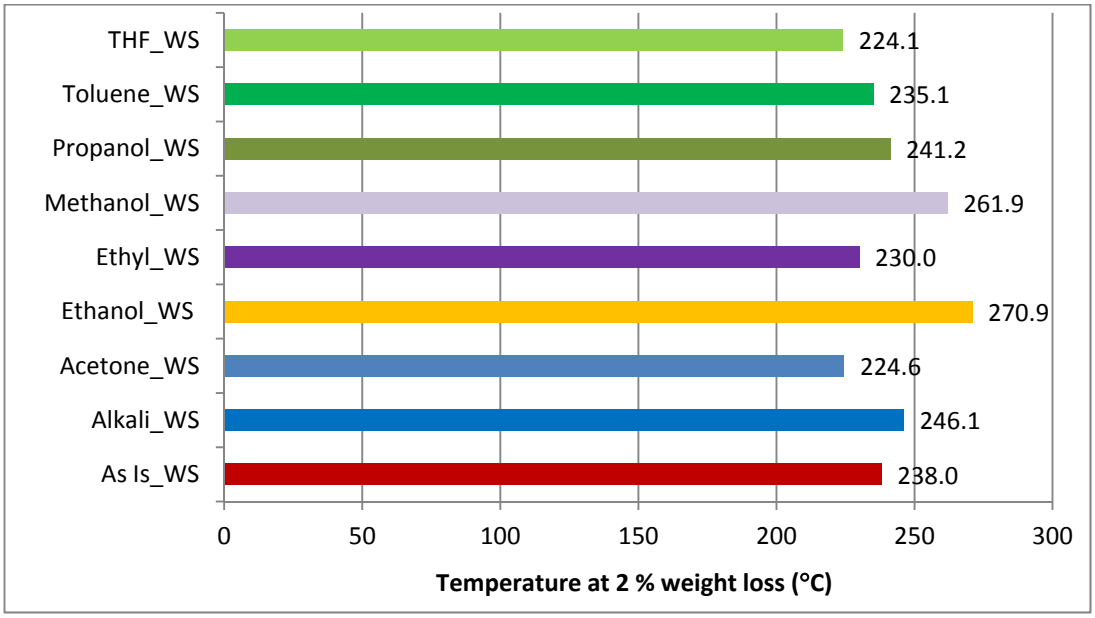

Figure 68: Temperature at 2 % weight loss obtained from TGA analysis using 10 °C/min heating rate under air atmosphere for the Chloro Solvent set of experiments samples.

Figure 70 shows that after 10 minutes of exposure to 250 °C, Alkali_WS and especially As Is_WS samples have their initial weight significantly reduced to 89.4 and 86.6 %, respectively. If these samples are processed for 30 minutes at 250 °C, even more severe thermal degradation takes place decreasing the initial weight to 84.9 and 81.3 % in the case of alkali treated and untreated samples, respectively (Figure 69).

On the other hand, after 10 minutes at 250 °C, the initial weight of Methanol_WS and Ethanol_WS samples has decreased to 95.2 and 93.1 %, respectively (Figure 70). These values are 6.5 and 4.1 % higher than the one for Alkali_WS sample, respectively. The higher thermal stability of Methanol_WS and Ethanol_WS samples permits these samples to be exposed to 250 °C for long periods of time with minimal thermal degradation. For example, even after 30 minutes at 250 °C, 93.9 and 91.8 % of the initial weight of the Methanol_WS and Ethanol_WS samples remains (Figure 69).

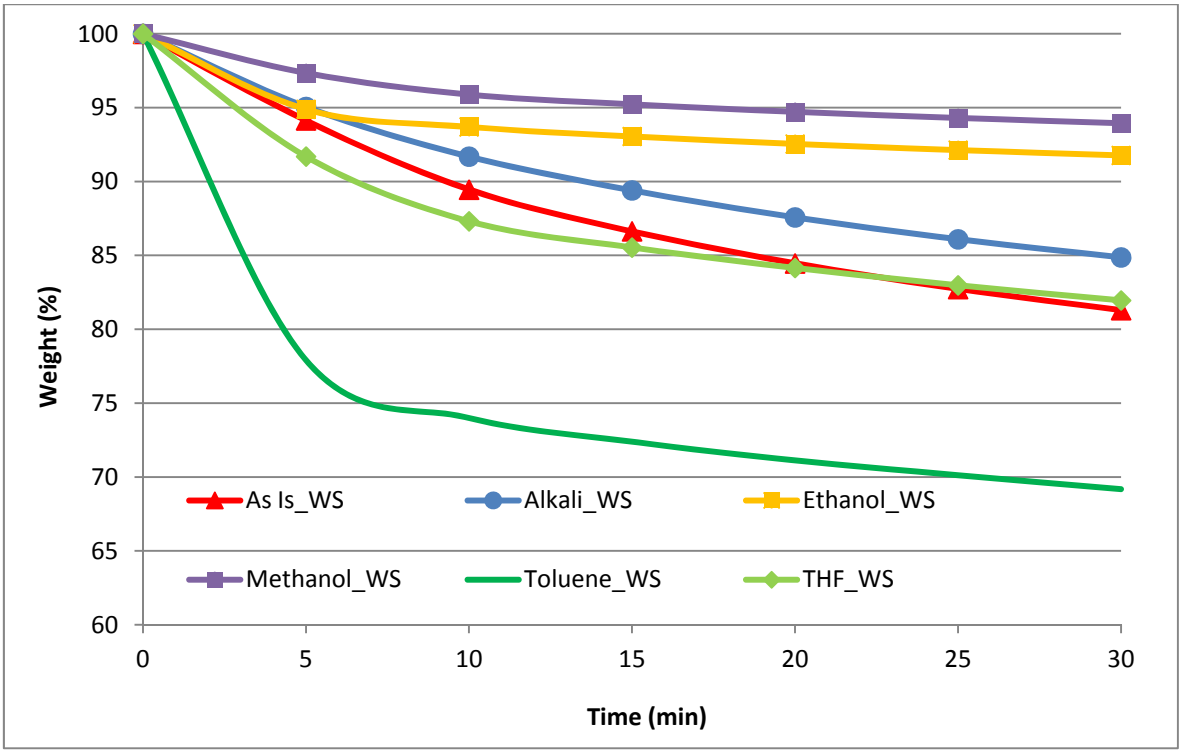

Figure 69: Isothermal curves obtained at 250 °C under nitrogen atmosphere for the Chloro Solvent set of experiments samples.

Surprisingly, there was one silane treated sample (Toluene_WS) that presented lower thermal stability than either Alkali_WS or As Is_WS samples (Figure 69). The initial weight of Toluene_WS sample sharply decreases to 72.4 % after 10 minutes of exposure to 250 °C (Figure 70). This value is 16.4 and 19.0 % lower than in the case of As Is_WS and Alkali_WS samples.

Figure 71 shows the grafted silane percentage for the different solvents used to perform the silane modification of wheat straw. The highest amount of grafted silane was obtained when methanol and ethanol were used as solvents (2.4 and 3.9 %, respectively), while the lowest amount was obtained by Toluene_WS and THF_WSsamples (1.4 and 2.2 %, respectively). In the same way, the highest improvement in thermal stability ($T_{2\%}$ and Wt250 values) were displayed by Methanol_WS and Ethanol_WS samples, whereas the lowest values of $T_{2\%}$ and Wt250 were shown by Toluene_WS and THF_WSsamples.

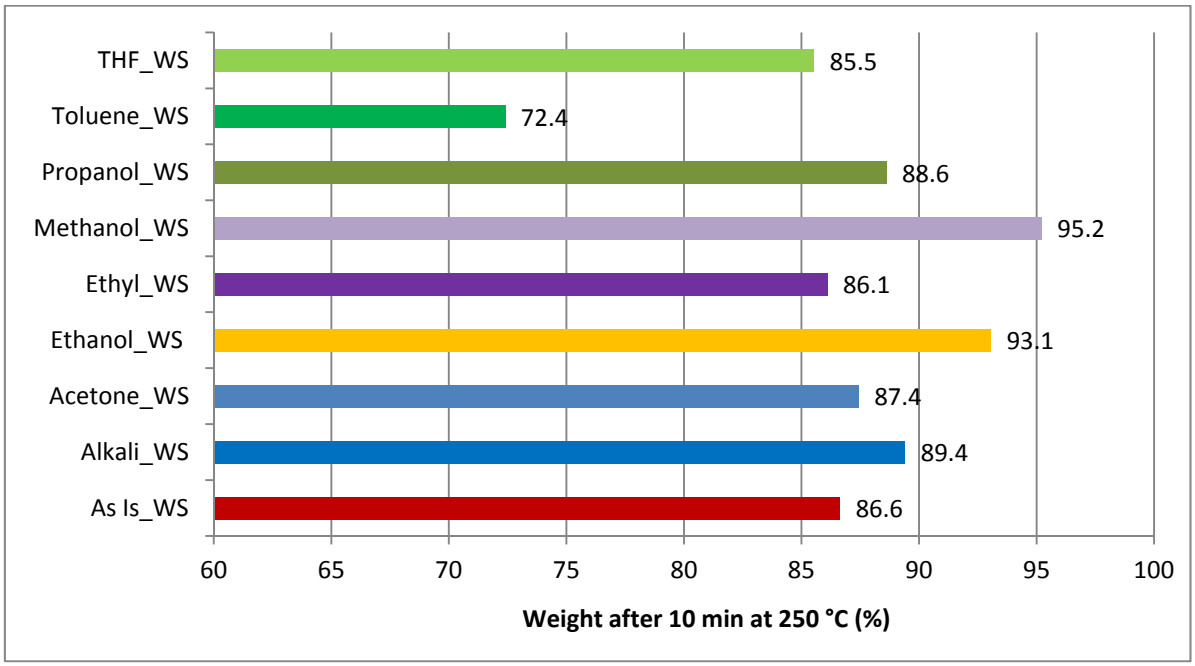

Figure 70: Weight (%) left after 10 minutes (Wt250) under isothermal heating at 250 °C and nitrogen atmosphere for Chloro Solvent set of experiments samples.

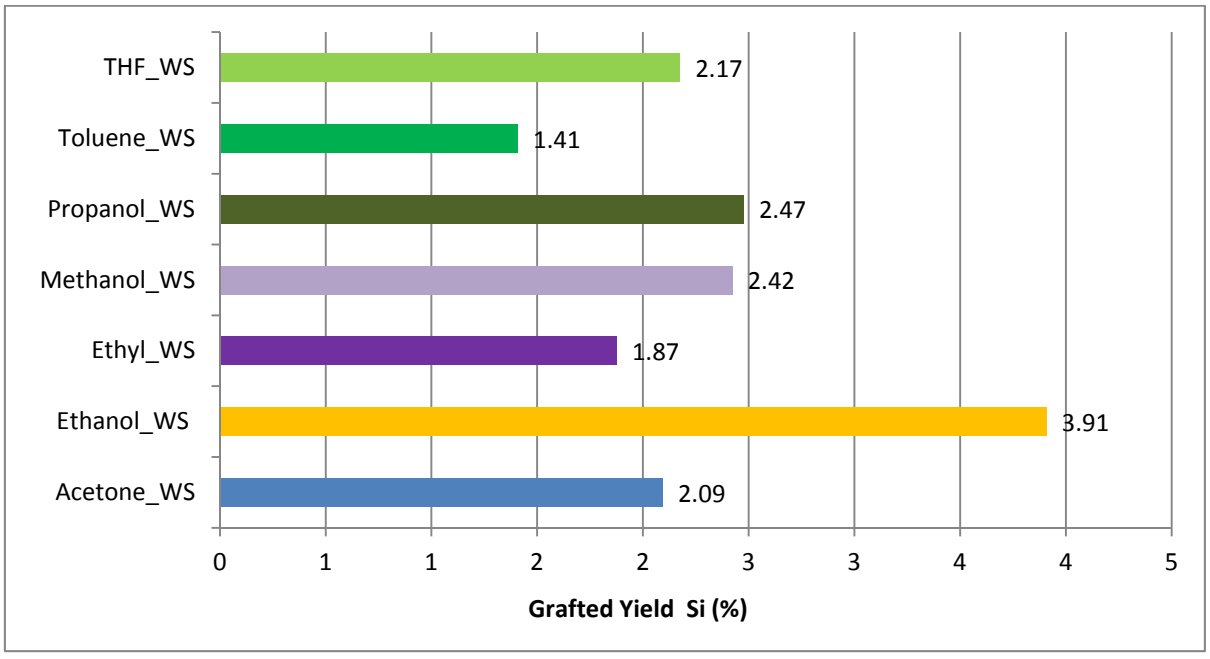

Figure 71: Silane (%) grafted into wheat straw according to the solvent used during Chloro Solvent set of experiments.

It seems that the amount of silane grafted to wheat straw fiber is the main factor responsible for the differences in thermal stability of silane treated samples. Figure 72 and Figure 73 suggest that increasing the amount of silane grafted to the wheat straw fiber increases the values of the $T_{2\%}$ and Wt250 of silane treated samples. However, these observations do not represent a correlation between amount of silane modifier grafted to wheat straw fiber and its thermal stability.

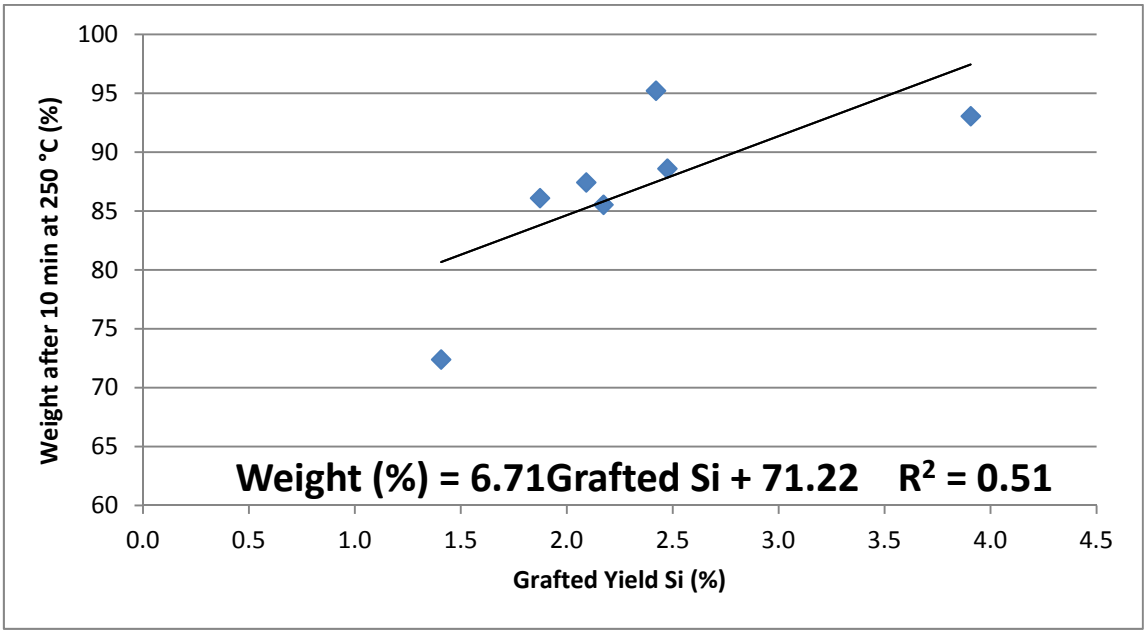

Figure 72: Weight (%) left after 10 minutes under isothermal heating at 250 °C and nitrogen atmosphere as a function of silane (%) grafted into wheat straw during Chloro Solvent set of experiments.

Additional proof of the silane modification can be obtained from the ash content measurements. A higher content of organic material should be observed in the silane treated sample if the silane modification is successful. Therefore, the percentage of inorganic material is expected to decrease as the amount of silane modifier increases. This supposition is confirmed by the ash content data presented in the Figure 74. It can be seen that the samples having higher amount of grafted silane have lower ash content percentage (e.g., Ethanol_WS – 0.54 %). On the other hand, samples

displaying lower grafted silane percentage show higher ash content percentage (e.g., Toluene_WS – 2.15 %).

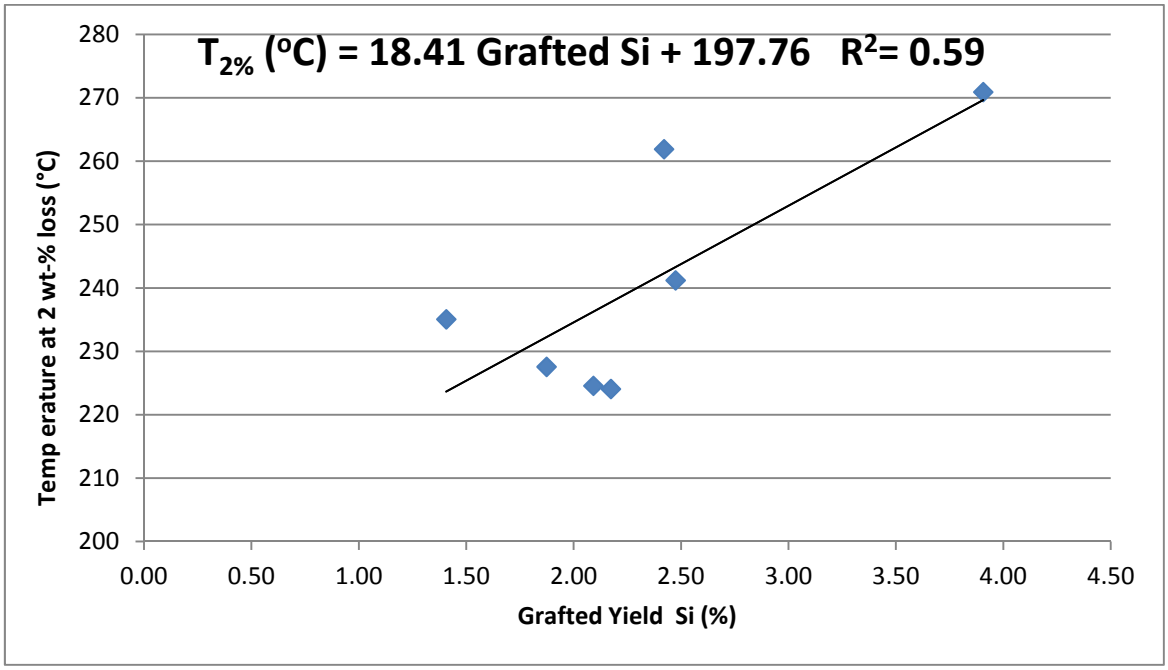

Figure 73: Temperature at 2 % weight loss (obtained from TGA analysis using 10 °C/min heating rate under air atmosphere) as a function of silane percentage grafted into wheat straw during Chloro Solvent set of experiments.

The different polarity of these solvents as well as the possible presence of water during silane modification may be accounted for the different silane amounts grafted to wheat straw fiber and ultimately, different levels of thermal stability of the samples.

It is possible to influence the amount and even the chemical structure of the polymeric silane formed during silane modification by controlling the hydrolysis and condensation rates. One way of achieving this is by selecting organic solvents with different levels of miscibility with water (i.e., polarity) and reactivity towards the chlorosilane modifiers.

The hydrolysis and condensation of chlorosilane modifiers can occur through three different routes. First, if water is present, the chlorosilane modifier can undergo hydrolysis by reacting with the water and producing alkoxysilane which will have their alkoxy groups (Si-OR) replaced by silanols (Si-

OH). These silanols groups can condensate with hydroxyl groups of wheat straw producing chemically stable bonds or staying physically adsorbed in the surface of the fiber via hydrogen bonds.

Water may be present, even though wheat straw was dried prior silane modification and no water was added to the system. Some atmospheric water may be absorbed by the silane solution during the preparation steps which included weighing and placing inside a glass flask the solvent, silane modifier and wheat straw.

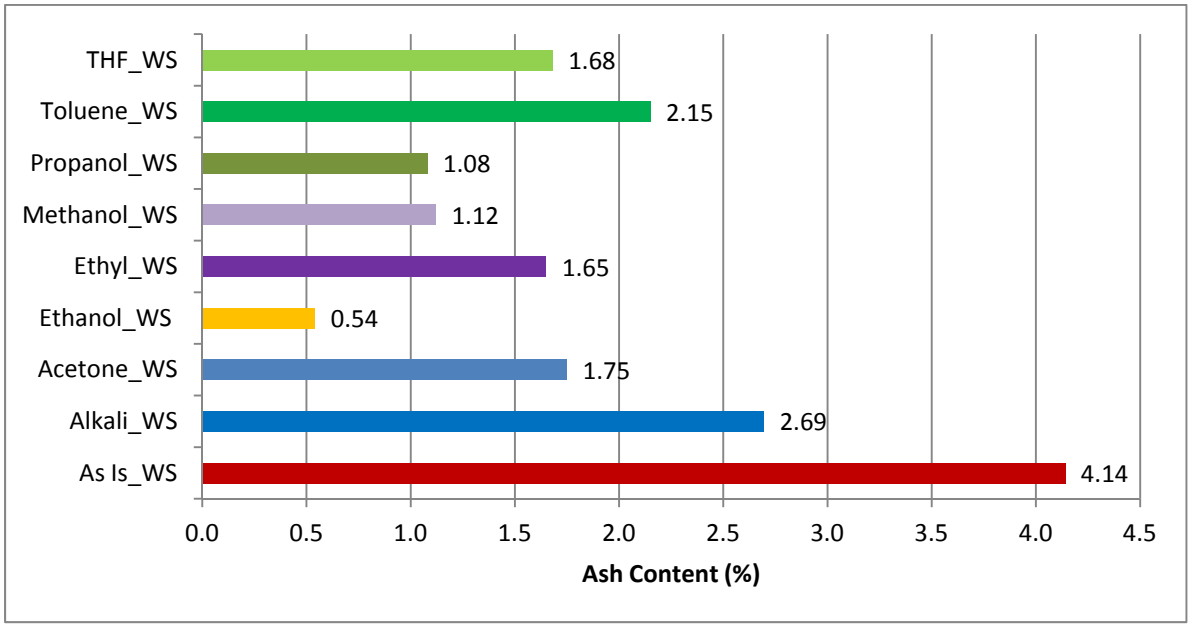

Figure 74: Ash content (mass left at 600 °C under air atmosphere) for Chloro Solvent set of experiment samples.

However, if no water is present, there are other two optional routes which can lead to hydrolysis and deposition of the chlorosilane modifier. The second option is the use of alcohol solvents (e.g., methanol and ethanol) which can react with the chlorosilane modifier producing an alkoxysilane and hydrochloric acid (HCl). The hydrochloric acid also reacts with the solvent yielding small amounts of water and alkyl halide. This water provokes the hydrolysis of the alkoxysilane which condenses with the hydroxyl group on the surface of the wheat straw fiber. Non polar or polar aprotic solvents (e.g.,

toluene and THF) cannot react with chlorosilane modifier and therefore, hydrolysis of chlorosilane modifier is not possible through this route when toluene or THF are employed as solvent.

The third route for grafting silane to wheat straw is the direct displacement of the silane chlorines (i.e., Cl in the Si-Cl) by the silanols (i.e., OH groups present in the surface of wheat straw fiber) through nucleophilic substitution (Silanes & Silicones Gelest Catalog 4000-A, 2008). This option is available for polar aprotic (THF), polar protic (methanol, ethanol) and non-polar (toluene) solvents. The use of polar aprotic solvents favors the nucleophilic substitution through S_N2 reaction (bimolecular nucleophilic substitution), whereas the utilization of polar protic solvents benefits the S_N1 reaction (unimolecular nucleophilic substitution) because of the solvent ability to stabilize the ionic intermediates and solvate the leaving group (Lowry and Richardson, 1987).

The S_N2 reaction requires an unhindered primary center in order to allow the backside route attack to be performed by the nucleophile (i.e., OH groups). Even though 7-Octenyl modifier is a primary center, the bulky octenyl group attached to the silicon atom may cause steric hindered effects and not favor the S_N2 reaction. This may explain the lowest amount of silane grafted when THF and toluene were employed as a solvent.

Instead, the S_N1 reaction is more likely to happen which is in accordance with the higher amount of silane grafted when ethanol and methanol were utilized for silane modification.

Table 19 summarizes the results of the Chloro Solvent set of experiments. Polar protic solvents (e.g., methanol and ethanol) promoted the highest deposition of silane modifier into the wheat straw. As a consequence, Ethanol_WS and Methanol_WS samples had the highest enhancement on their thermal stability. On the other hand, polar aprotic or non polar solvents (e.g., THF and toluene) proved to be less effective for silane modification, providing samples with significantly lower amounts of grafted silane. Because of that, the Toluene_WS and THF_WS samples start to thermally degrade at similar or lower temperatures as As Is_WS and Alkali_WS samples.

Using the thermal stability of the silane treated samples under isothermal conditions (Wt250) as the main criterion; it is possible to conclude that methanol is the best solvent for chlorosilane modification of wheat straw fiber. Therefore, methanol will be employed as solvent during the Chloro Type set of experiments (fourth) which will investigate different types of chlorosilane modifiers.

Table 19: Summary of thermal stability and grafted silane results for Chloro Solvent set of experiments.

Sample	$T_{2\%}$ (°C)	Wt250 (%)	Grafted Si (%)	Overall Performance
THF_WS	224.1	85.5	2.17	Poor
Toluene_WS	235.1	72.4	1.41	Poor
Methanol_WS	261.9	95.2	2.42	Excellent
Ethanol_WS	270.9	93.1	3.91	Excellent
Alkali_WS	246.1	89.4	---	Reference
As Is_WS	238.0	86.6	---	Reference

5.5 Investigation of Different Types of Alkoxysilane and Chlorosilane Modifiers

The best set of reaction conditions established in the previous set of experiments (Alkoxy Solvent and Chloro Solvent) were utilized to test different types of alkoxysilane and chlorosilane modifiers during the third and fourth sets of experiments. Both sets of experiments were performed according to the silane modification procedure described previously (in the Methods section) with a constant time of reaction of 8 hours. The third set (Alkoxy Type) discusses alkoxysilane modifiers while the fourth set (Chloro Type) considered only chlorosilane modifiers. The goal was to determine, among different potential candidates, the alkoxysilane and chlorosilane modifiers which can produce the highest increase on the thermal stability of wheat straw fiber.

The differences in the structure of the alkoxysilane and chlorosilane modifiers molecules are likely to affect the degree of silane modification and thermal stability enhancement that can be achieved.

For example, if the same reaction conditions and hydrolysable group (X) are employed, the hydrolysis and condensation rates of silanols groups will be determined by the nature and size of the silane modifier molecule. Some organofunctional groups (R) have the ability to accelerate or inhibit the hydrolysis and condensation reactions. For example, silane modifiers bearing an amine groups suffer almost immediately hydrolysis under aqueous conditions. The subsequently self-condensation of the silanols formed is also a very fast process. These aminosilane modifiers have the unique ability to stay soluble in aqueous solution even after becoming oligomers whereas most of other silane

modifiers would form unreactive precipitates. On the other hand, silane modifiers containing epoxy groups (e.g., Glyxidoxy) are known to hydrolyze very slowly and under special conditions (Plueddemann, 1991).

In addition to the nature, the size of the silane molecule can influence its deposition into wheat straw. Small molecules (e.g., tetrachlorosilane modifier) are more prone to self-condensation. As the size of the molecule increases, the propensity to undergo hydrolysis and condensation decreases owing to steric hindrance effects (special and geometric constrains).

For these reasons, it is important to carry out an experimental study to determine the best alkoxysilane and chlorosilane modifiers which can produce the highest degree of silane modification and thermal stability enhancement for wheat straw.

5.5.1 Performance of Different Types of Alkoxysilane Modifiers

The aim of the third set of experiments was to select the alkoxysilane modifiers which can promote the most substantial increase on thermal stability of wheat straw.

The best reaction conditions to perform alkoxysilane modification determined in the first set of experiments (Alkoxy Solvent) were a mixture of 80 % ethanol with 20 % water used as a solvent along with acidification and pre-hydrolysis steps. These conditions were applied to investigate the potential of two alkoxysilane modifiers to increase thermal stability of WS fiber. The main difference between these silane modifiers was the nature of the organofunctional group (R of $R\text{-}(CH_2)_n\text{-}Si\text{-}X_3$ silane molecule). Ureiodosilane modifier has diamine and carbonyl groups, whereas aminosilane modifier bears an amine group (see Table 20 for a detailed description of the experiment performed in this section). It is believed that these differences will influence the amount of grafted silane and thermal stability of silane treated sample.

Since the ultimate reason for modifying the wheat straw is to combine them with polyamide (such as nylon-6) and produce a composite, it is important to highlight that this class of aminosilane modifiers may have the ability to react with polyamide polymers and work as a compatibilizing agent between the matrix (polyamide) and the dispersed phase (wheat straw fiber).

Table 20: Alkoxysilane modifiers, reference samples and its labels studied during the Alkoxy Type (third) set of experiments.

Label	Modifiers	Chemical Structure	Pre-treatment
Ureiodo_WS	Ureiodopropyltriethoxy silane	$H_2NCONH(CH_2)_3Si(OCH_2CH_3)_3$	1M Alkali WS
3-Amino_WS	3-Aminopropyltrimethoxy silane	$H_2N(CH_2)_3Si(OCH_3)_3$	
As Is_WS	None		Untreated WS
Alkali_WS	None		1M Alkali WS
Alk_Reflux_WS	None		1M Alkali WS + Reflux with methanol
CONSTANTS: Reaction time: 8 hours; Reaction Temperature: Solvent boiling point; Pre-treatment: 1M Alkali; Silane modifier concentration: 1.25 mmol.			

Figure 75 portrays the TGA results for the samples modified with two different types of alkoxysilane modifiers (Ureiodo and Amino) as well as the untreated samples. It is very clear in the plot that the Ureiodo_WS curve (yellow long dash) is displayed at the right of the other curves. This displacement indicates that Ureiodo_WS sample has had its thermal stability increased. This behavior was not observed for the other silane treated sample (Amino_WS – purple square dot) which had its TGA curve placed between the Alkali_WS (blue dash) and Alk_Reflux_WS (dark green round dot) curves.

Figure 76 quantifies the beginning of thermal degradation of treated and untreated samples by using Figure 75 to obtain the temperature at 2 % of weight loss ($T_{2\%}$). Figure 76 confirms that the starting temperature of degradation of Ureiodo_WS sample is moved to higher temperatures. The $T_{2\%}$ of Ureiodo_WS sample is increased by 4.94 % (from 238 to 249.8 ^{o}C), 0.96 % (from 247.4 to 249.8 ^{o}C) and 1.67 % (from 245.7 to 249.8 ^{o}C) in comparison with As Is_WS, Alkali_WS and Alk_Reflux_WS samples, respectively. Unlike Ureiodo_WS sample, Amino_WS sample did not show any enhancement on its thermal stability. In fact, the $T_{2\%}$ of Amino_WS sample (243 .9 ^{o}C) is 1.43 and 0.74 % smaller than Alkali_WS (247.4 ^{o}C) and Alk_Reflux_WS (245.7 ^{o}C) samples, respectively.

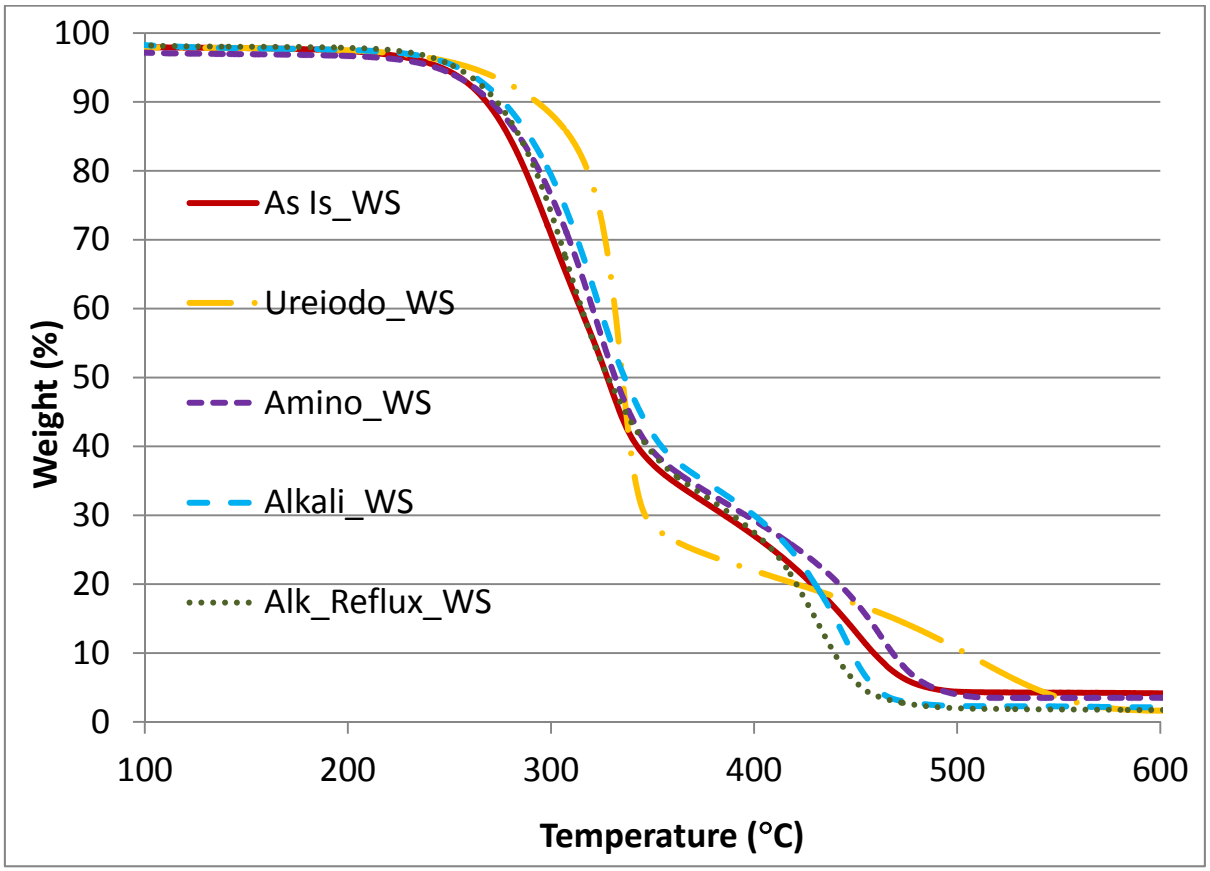

Figure 75: Weight (%) as a function of temperature obtained from TGA analysis performed using 10 °C/min heating rate under air atmosphere for the Alkoxy Modifier set of experiments samples.

Similar trend is noticed when the samples are submitted to isothermal heating at 250 °C under nitrogen atmosphere. For example, Ureiodo_WS curve (yellow square line) is displayed in the region of highest thermal stability of Figure 77. Even after 30 minutes of exposure to 250 °C, the Ureiodo_WS sample retains more than 90 % of its initial weight. On the other hand, Amino_WS sample (purple round curve) did not present the same performance. In fact, As Is_WS (red solid curve), Alkali_WS (blue dash curve), Alk_Reflux_WS (dark green round dot curve) and Amino_WS samples exhibit poor thermal stability. The curves for all these samples exhibited a sharp decrease on their weight even within few minutes of exposure to heating. Then, as time passed the thermal degradation of the samples became more severe. After 30 minutes of exposure to 250 °C, less than 85 % of the initial weight was left for most of the samples.

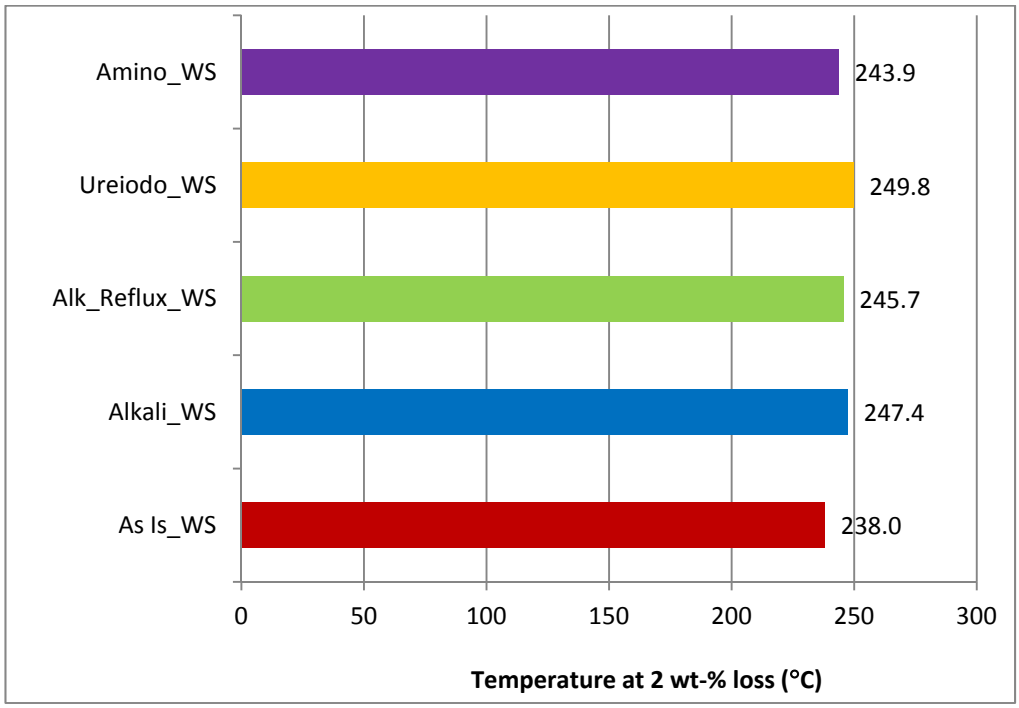

Figure 76: Temperature at 2 % weight loss obtained from TGA analysis using 10 °C/min heating rate under air atmosphere for the Alkoxy Type set of experiments samples.

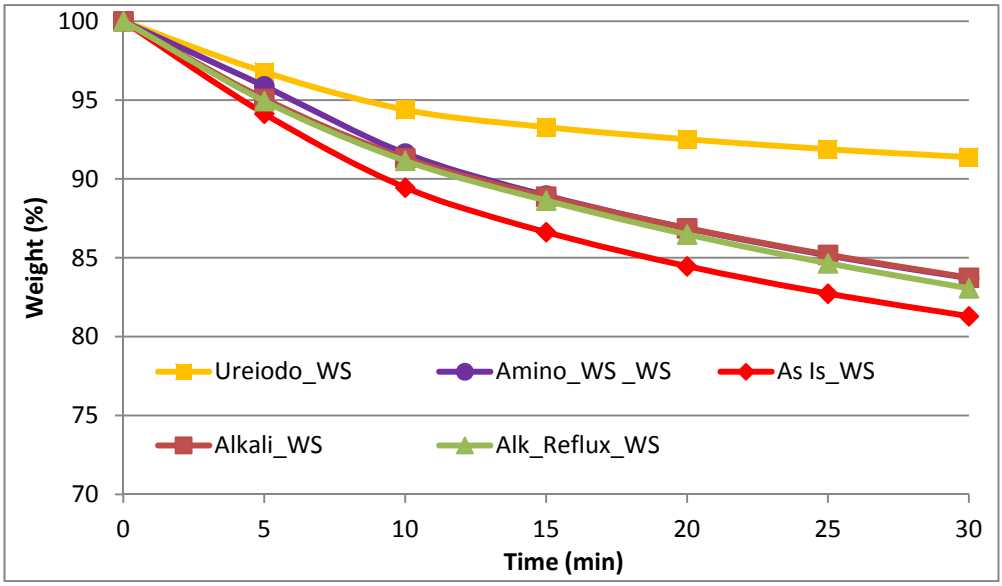

Figure 77: Isothermal curves obtained at 250 °C under nitrogen atmosphere for the Alkoxy Type set of experiments samples.

The weight percentage after 10 minutes of exposure at 250 ^{o}C (Wt250) is summarized in the Figure 78 for all the samples. The thermal stability (i.e., Wt250) is higher when silane modification was performed using Ureiodo modifier. The Ureiodo_WS sample Wt250 value (93.3 %) is 7.68 %, 4.96 % and 5.26 % higher than the As Is_WS (86.6 %), Alkali_WS (88.9 %) and Alk_Reflux_WS (88.6 %) samples values, respectively. In the contrary, if Amino modifier is utilized for silane modification of wheat straw, a lower Wt250 value is obtained (89.0 %) and virtually no improvement is observed with respect to Alkali_WS and Alk_Reflux_WS samples.

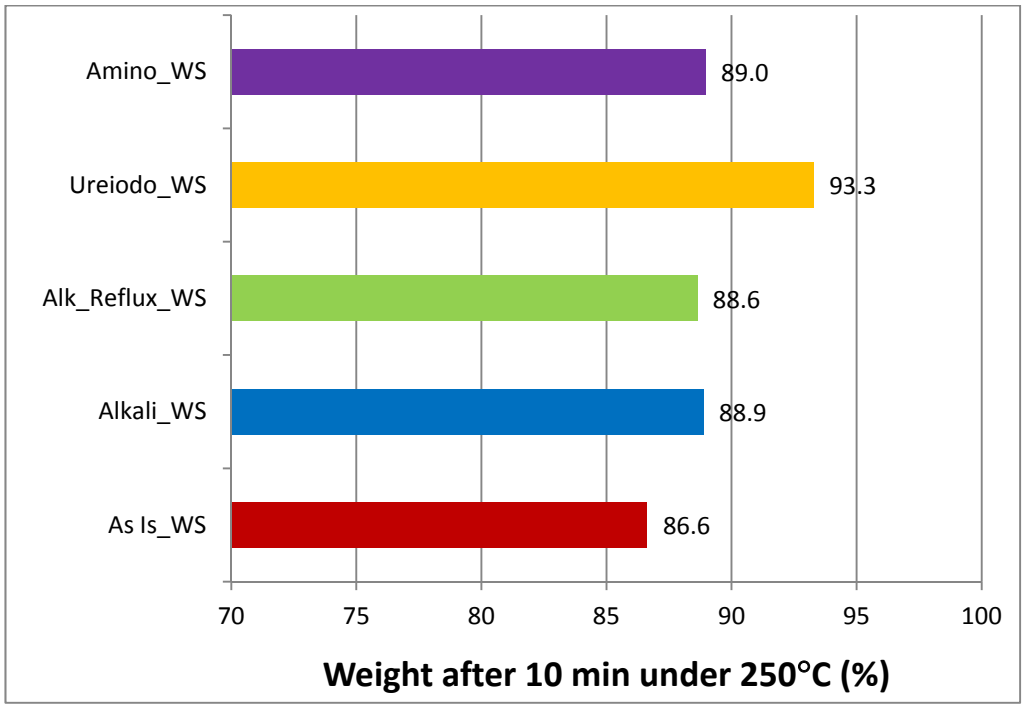

Figure 78: Weight (%) left after 10 minutes (Wt250) under isothermal heating at 250 ^{o}C and nitrogen atmosphere for the Alkoxy Type set of experiments samples.

In addition, the effect of different concentrations of alkali treatment on the thermal behavior of wheat straw was investigated. This was an attempt to reduce the amount of sodium hydroxide (NaOH) used during alkali pre-treatment and unnecessary cost. It can be seen from Table 21 that increasing the concentration of the alkali solution from 1 to 2 molar did not significantly altered the thermal stability of the alkali treated samples. For example, comparing with the 1 molar alkali treated

sample, the 2 molar alkali treated sample has 0.53 % decrease on the $T_{2\%}$ (from 247.4 to 246.1 ^{o}C) and 0.56 % increase on the Wt250 (from 88.9 to 89.4 %). This difference between the samples treated with 1 molar (Alkali_WS-1 M) and 2 molar (Alkali_WS-2 M) are almost nonexistent. Therefore, it is suggested that in future studies the reduction of the concentration of the alkali solution be investigated as a way to reduce the cost of the treatment.

Table 21: Thermal stability comparison between 1 and 2 molar alkali treated samples.

Sample	$T_{2\%}$ (^{o}C)	Wt250 (%)	Alkali Treatment
As Is_WS	238.0	86.6	Reference
Alkali_WS (1M)	247.4	88.9	1 molar
Alkali_WS (2M)	246.1	89.4	2 molar

Figure 79 clearly depicts that the amount of Ureiodo modifier grafted to wheat straw (1.61 %) was 2.7 times bigger than in the case of Amino modifier (0.60 %). This considerable difference in the silane grafted percentage may be responsible for the different thermal behavior of the silane treated samples. The higher improvement on thermal stability ($T_{2\%}$ and Wt250) was achieved by the sample with the highest amount of silane grafted (Ureiodo_WS), whereas much lower grafted silane percentage led to no enhancement on thermal stability of the silane treated sample (Amino_WS).

Figure 80 presents the ash content, the amount of inorganic material left at 600 °C under air atmosphere, for all samples. As expected a higher content of organic material is present in the case of silane treated samples. It is possible to observe in Figure 80 that increasing the silane modifier content decreases the percentage of the inorganic material. For example, the sample with the highest percentage of silane grafted (Ureiodo_WS) has the lowest ash content (1.62 %); while the sample with lower amount of grafted silane (Amino_WS) depicts higher amount of inorganic material (3.52 %) (ash content). Surprisingly, the ash content of Amino_WS sample is higher than the one of Alk_Reflux_WS sample.

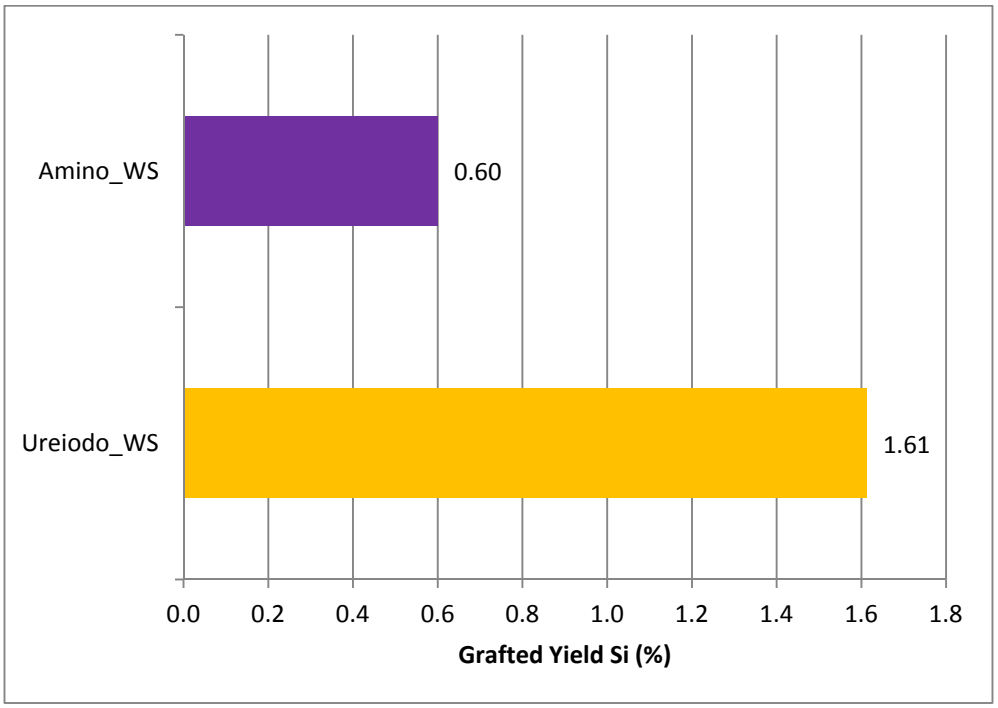

Figure 79: Silane (%) grafted into wheat straw as a function of alkoxysilane modifier used.

One possible explanation for this finding is that during silane modification with Amino modifier, more organic material has been extracted in comparison with Ureiodo_WS and Alk_Reflux_WS samples. Due to the large number of experiments, a duplicate of the experiment with Amino modifier has not been performed in order to test this hypothesis.

Table 22 summarizes the performance of the two alkoxysilane modifiers utilized to modify the wheat straw samples. It can be seen that alkoxysilane modification employing Ureiodo modifier produced higher deposition of silane modifier into the wheat straw fiber than Amino modifier. The higher deposition of Ureiodo modifier was translated only in a mild enhancement of the Wt250 of Ureiodo_WS sample, whereas the $T_{2\%}$ of this sample was not improved when compared to the three reference samples.

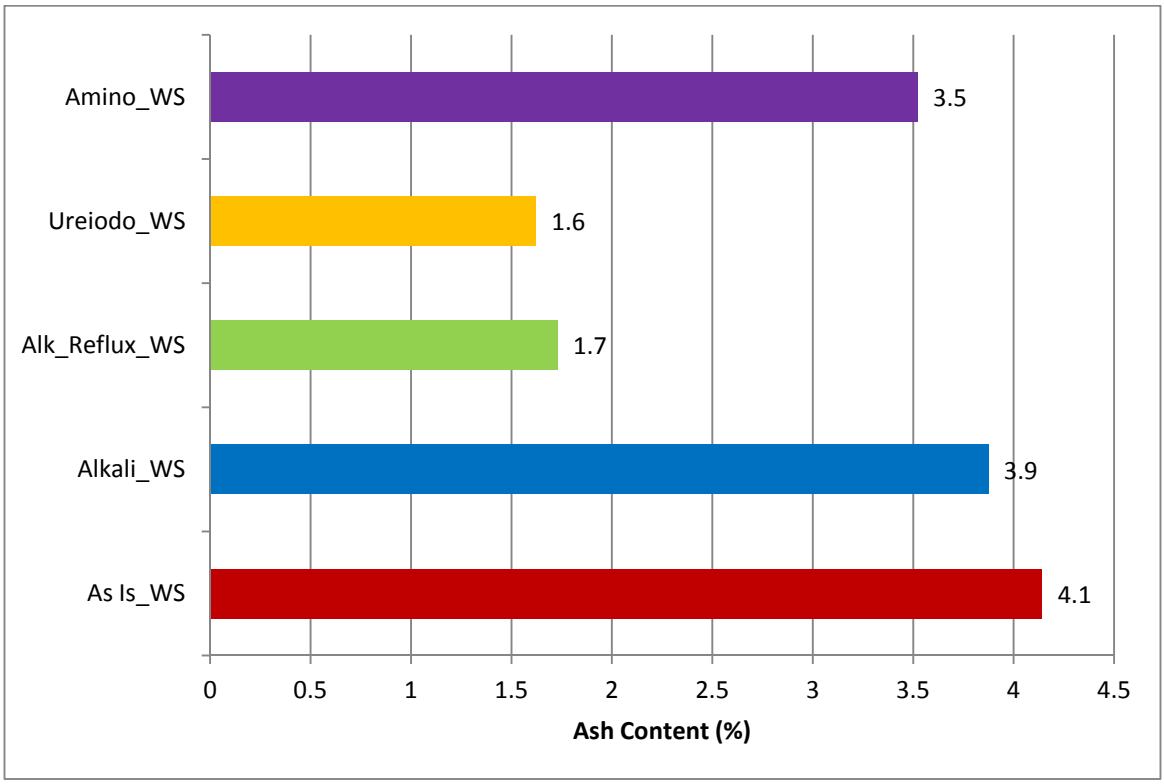

Figure 80: Ash content (mass left at 600 °C under air atmosphere) for the Alkoxy Type set of experiments samples.

Under the same hydrolytic condition, methoxy groups undergo hydrolysis faster than ethoxy groups, therefore it is expected that Amino modifier which has methoxy groups will likely form silanols groups faster than Ureiodo modifier. Another factor contributing to decrease the hydrolysis rate of Ureiodo modifier is the length of its non-hydrolyzable group. Increasing the size of the non-hydrolyzable group of an alkoxysilane modifier decreases the hydrolysis rate (Borup and Weissenbach, 2010). Since, the non-hydrolyzable group of Ureiodo modifier is bigger than the one of Amino modifier, the hydrolysis rate of Ureiodo modifier is smaller than for Amino modifier.

Consequently, one can speculate that the degree of condensation is higher for Amino modifier than Ureiodo modifier even though these aminosilanol groups are relatively stable against condensation and precipitation under acid-catalyzed conditions (Plueddemann, 1991). This higher degree of self-condensation of Amino modifier could lead to the formation of less reactive structures such as linear

siloxane and rigid three dimension polysiloxane which would justify the lower silane deposition into wheat straw. Supporting this idea, Plueddemann (1991) has reported that alkoxy groups of aminosilanes modifiers are almost instantly hydrolyzed and then converted into oligomers when prepared in aqueous solution without any pH (potential of hydrogen) adjustment (Beari et al., 2001; Plueddemann, 1991).

Despite the small improvement in thermal stability after alkoxysilane modification, the use of alkoxysilane modifiers will be studied further as there might be important gain on compatibility and ultimate mechanical properties of alkoxy-treated WS/polyamide composite. In addition, there is the possibility that the amine functional groups present in these silane modifiers react with hydroxyl groups of lignin and hemicellulose through hydrogen bonds.

Table 22: Summary of thermal stability and grafted silane results for wheat straw samples modified with two different alkoxysilane modifiers.

Sample	$T_{2\%}$ (^{o}C)	Wt250 (%)	Grafted Si (%)	Overall Performance
Amino_WS	243.9	89.0	0.60	Poor
Ureiodo_WS	249.8	93.3	1.61	Reasonable
Alk_Reflux_WS (1 M)	245.7	88.6	---	Reference
Alkali_WS (1 M)	247.4	88.9	---	Reference
As Is_WS	238.0	86.6	---	Reference

5.5.2 Performance of Different Types of Chlorosilanes Modifiers

The second set of experiments (Chloro Type) established that the best solvent to perform chlorosilane modification was methanol because the highest thermal enhancement of wheat straw was achieved using this solvent. Therefore, methanol was chosen to evaluate the efficacy of the silane modification using seven different types of chlorosilane modifiers (see Table 23 for complete description of the experiments performed in this section). These silane modifiers have different types of organofunctional groups and lengths of the linker between the organofunctional group (R) and the silicon atom (Si) (R and $-(CH_2)_n-$ in the $R-(CH_2)_n-Si-X_3$ silane structure, respectively). It is reasonable

to suppose that these differences will lead to different amounts of silane deposited into wheat straw and, consequently to different degrees of thermal stability enhancement of silane modified sample.

The chlorosilane modifiers which impart the highest improvement on thermal stability of wheat straw will be selected for further studies.

Table 23: Chlorosilane modifiers, reference samples and its labels investigated in the Chloro Type (fourth) set of experiments.

Label	Modifiers	Chemical Structure
Ethyl_WS	Ethyltrichlorosilane	CH_3-CH_2-Si-$(Cl)_3$
Octadecyl_WS	n-Octadecyltrichlorosilane	CH_3-$(CH_2)_{16}$-CH_2-Si-$(Cl)_3$
7-Octenyl_WS	7-Octenyltrichlorosilane	H_2C= CH_2-$(CH_2)_6$-CH_2-Si-$(Cl)_3$
Octyl_WS	n-Octyltrichlorosilane	CH_3-$(CH_2)_6$-CH_2-Si-$(Cl)_3$
Acryloxy_WS	3-Acryloxypropyltrichlorosilane	H_2C= CH-C=O-O-$(CH_2)_3$-Si-$(Cl)_3$
Tetra_WS	Tetrachlorosilane	Si-$(Cl)_4$
As Is_WS	None	Untreated WS
Alkali_WS	None	2M Alkali treated WS
Alk_Reflux_WS	None	2M Alkali treated WS + Reflux with methanol
CONSTANTS: Solvent: Methanol; Reaction time: 8 hours; Reaction Temperature: Solvent boiling point; Pre-treatment: 2M Alkali WS; Silane modifier concentration: 1.25 mmol.		

In order to facilitate visualization of the curves, Figure 81 shows the TGA curves for the samples modified with two of the six different types of chlorosilane modifiers (Acryloxy and Octadecyl) studied in this set of experiment as well as the reference samples (As Is_WS, Alkali_WS and Alk_Reflux_WS). Overall, it is difficult to merely quantify the starting point of the degradation of the WS samples by visual inspection (i.e., the temperature in the TGA curve where the weight starts to drop). However, it is very clear in the plots that all the chlorosilane treated samples (Acryloxy - dark green square dot curve and Octadecyl – yellow long dash dot curve) have the starting point of the degradation at higher temperatures than in the case of untreated samples (As Is_WS – dark red solid

curve, Alkali_WS – dark blue dash curve and Alk_Reflux_WS - light blue round dot curve). Although the TGA results for the samples treated with the other four chlorosilane modifiers (Ethyl, 7-Octenyl, Octyl and Tetra) are not shown, these samples displayed curves similar to the ones of Acryloxy_WS and Octadecyl_WS samples presented in Figure 81.

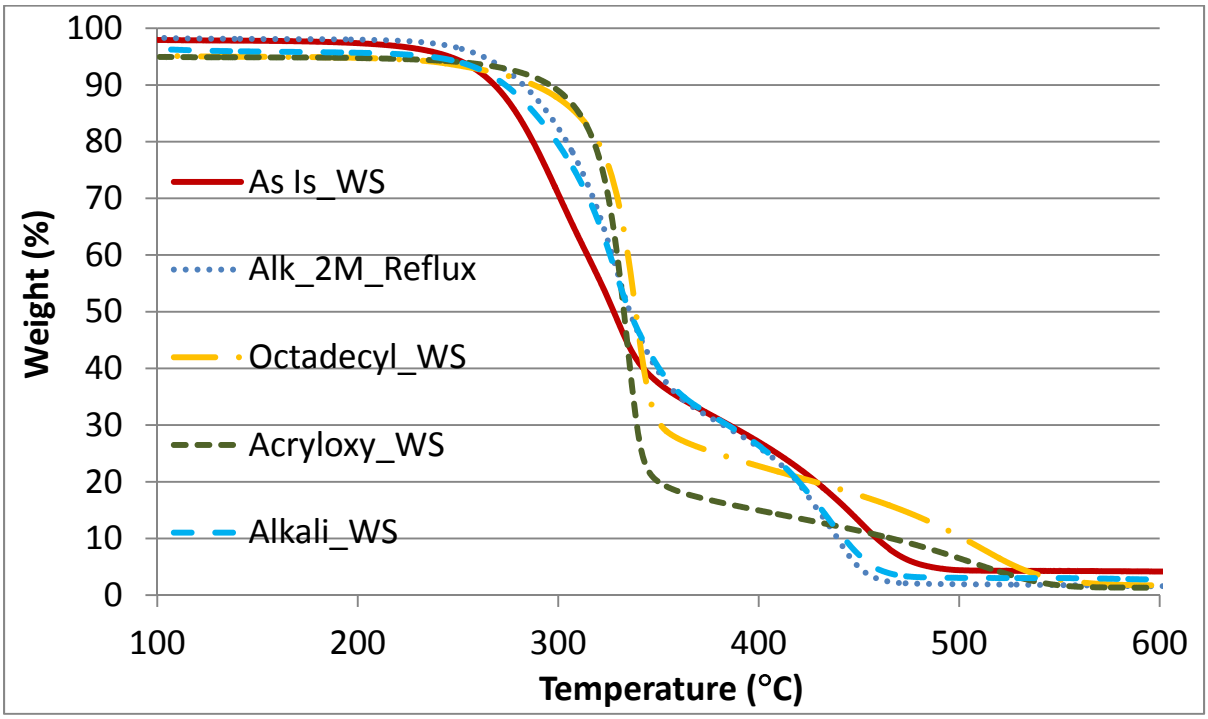

Figure 81: Weight (%) as a function of temperature obtained from TGA analysis performed using 10° C/min heating rate under air atmosphere for the Chloro Type set of experiments samples.

In order to quantify the increase on the onset of thermal degradation, the temperature at 2 % of weight loss ($T_{2\%}$) is summarized in Figure 82. This figure displays the temperature at 2% weight loss for all the treated and untreated samples. It can be seen that the $T_{2\%}$ has significantly increased when the chlorosilane treatment is applied to the wheat straw samples. This temperature increment is more evident in the case of Acryloxy_WS and Ethyl_WS samples.

For example, after the silane modification with Ethyl modifier, the thermal stability was enhanced by 13.8 % (from 238.0 to 270.9 °C), 10.1 % (from 246.1 to 270.9 °C) and 6.5 % (from 254.3 to 270.9

°C) in comparison with the WS samples without any treatment (As Is_WS), alkali treated (Alkali_WS) and alkali treated followed by reflux with methanol (Alk_Reflux_WS), respectively. However, the highest gain on thermal stability was achieved when Acryloxy silane modifier was applied to WS fiber. The increment on thermal stability was 15 % (from 238.0 to 273.7 °C), 11.2 % (from 246.1 to 273.7 °C) and 7.7 % (from 254.3 to 273.7 °C) in comparison with the reference samples As Is_WS, Alkali_WS and Alk_Reflux_WS, respectively.

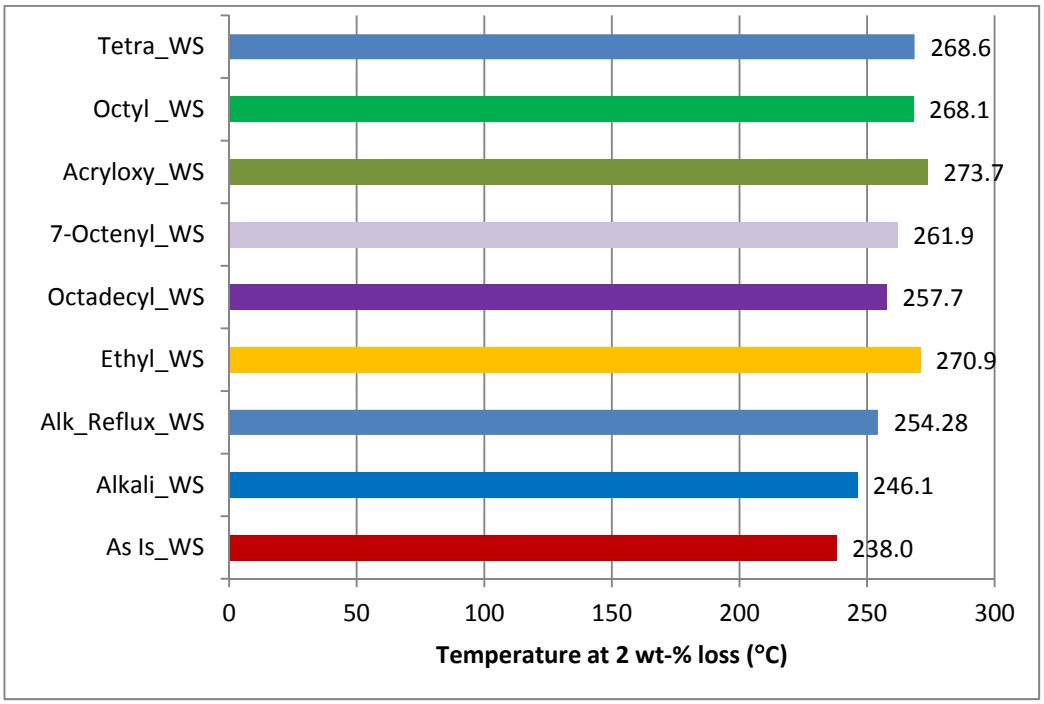

Figure 82: Temperature at 2 % weight loss obtained from TGA analysis using 10 °C/min heating rate under air atmosphere for the Chloro Type set of experiments samples.

Figure 83 shows the curves obtained from the isothermal gravimetric analysis performed under nitrogen atmosphere at constant temperature of 250 °C. It can be seen from Figure 83 that the curves of silane treated samples (purple star and overlapping curves) are depicted at the top of the graph, region where the weight loss is smaller; whereas the curves representing non-silane treated WS (red lozenge, dark blue round dot and light blue square) are in the lower part of the graph. In fact, the

weight loss due to thermal degradation is remarkably larger in the case of As Is_WS (without any treatment), followed by Alkali_WS and Alk_Reflux_WS samples.

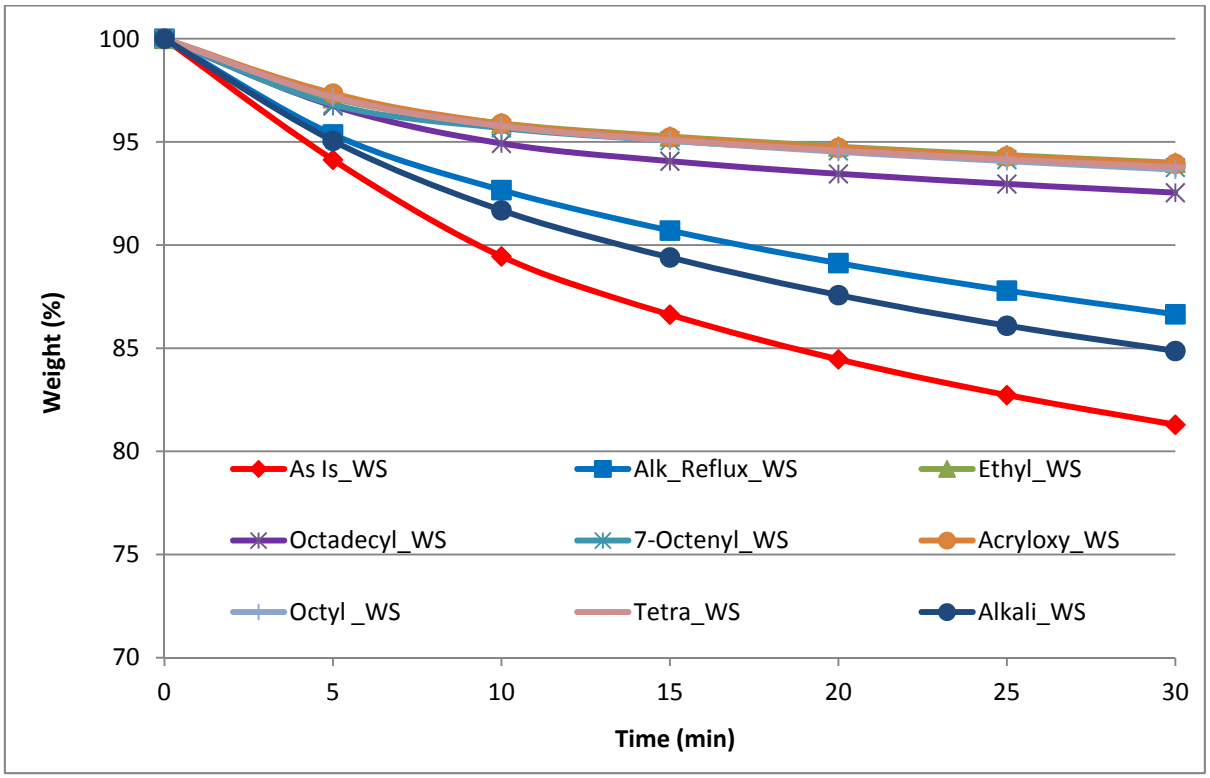

Figure 83: Isothermal curves obtained at 250 °C under nitrogen atmosphere for the Chloro Type set of experiments samples.

Figure 84 exhibits the weight percentage after 10 minutes under nitrogen atmosphere and 250 °C (Wt250) for all treated and untreated samples. After this period of 10 minutes at 250 °C, the initial weight of As Is_WS, Alkali_WS and Alk_Reflux_WS samples have decreased to 86.63 %, 89.4 and 90.71 %, respectively. In contrast, the higher degree of thermal stability of the Ethyl_WS sample is enough to allow this sample to be processed at 250 °C for 10 minutes with 95.27 % of the initial weight remaining which represents a weight loss of only 4.73 %. After the silane modification with Ethyl modifier, the enhancement on the thermal stability (Wt250) of Ethyl_WS sample with respect to As Is_WS, Alkali_WS and Alk_Reflux_WS samples have reached 9.97, 6.56 and 5.03 %, respectively. Other silane modifiers such as 7-Octenyl, Octyl, Acryloxy and Tetra have also provided

enhancement on thermal stability similar to Ethyl modifier. This increment on thermal stability would allow the silane treated samples to be processed with polyamides at 250 °C with minimal thermal degradation as compared to the untreated samples.

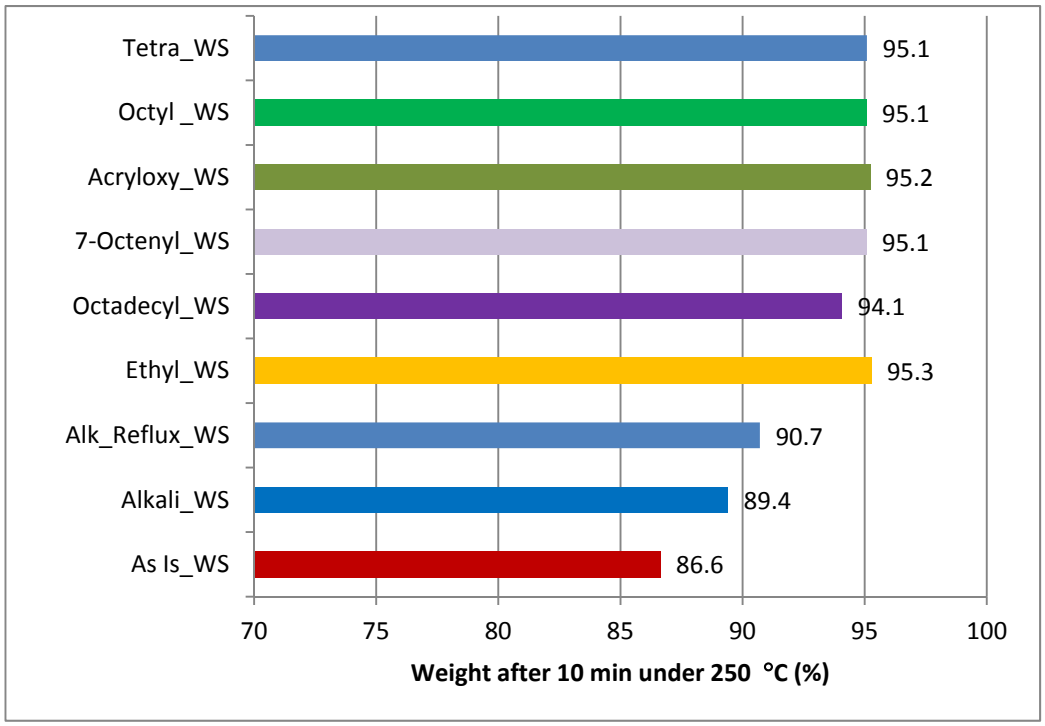

Figure 84*: Weight (%) left after 10 minutes (Wt250) under isothermal heating at 250 °C and nitrogen atmosphere for the Chloro Type set of experiments samples.*

It is important to highlight that a mild improvement on thermal stability is achieved after alkali treatment (Alkali_WS sample) and reflux with methanol (Alk_Reflux_WS sample). Furthermore, these improvements are smaller when measured under isothermal (Wt250) than non-isothermal ($T_{2\%}$) conditions.

For example, there is a gain on thermal stability of 3.39 % (from 238.0 to 246.1 °C) when the wheat straw fiber (As Is_WS sample) is submitted to an alkali treatment (Alkali_WS sample). Subsequently, there is a further increase on the $T_{2\%}$ of 3.32 % (from 246.1 to 254.3 °C) when the

alkali treated sample is submitted to reflux with methanol (simulating the silane reaction conditions, Alk_Reflux_WS sample).

In contrast, these enhancements are more modest under isothermal conditions. For example, there is an improvement of 3.20 % (from 86.6 to 89.4 %) on the Wt250 when As Is_WS sample is treated with an alkali solution. Then, the improvement on the Wt250 is even smaller, 1.46 % - from 89.4 to 90.7 %, when Alkali_WS sample is submitted to reflux with methanol (Alk_Reflux_WS sample).

In accordance with the findings reported here, Rachini et al. (2009) have also reported an increase on the thermal stability of hemp fiber submitted to alkali and solvent extraction treatments. Those authors suggest that these treatments partially removed hemicellulose and pectins from hemp fiber and consequently, increased the cellulose percentage. In the case of the alkali hemp, the removal of pectin and hemicellulose reached 7 % of the initial mass (from 10 to 3 %), whereas the solvent extracted hemp suffered a 4 % decrease on the pectin and hemicellulose percentages (from 10 to 6 %). This removal of hemicellulose and pectins shifted the thermal decomposition temperature of alkali and solvent extracted hemp fiber towards higher values.

The increase on thermal stability after silane modification may be credited to the amount and type of silane grafted to wheat straw fiber. Figure 85 shows the grafted silane percentage for each one of the silane modifiers utilized.

The highest amount of grafted silane was achieved when Ethyl Tetra and Acryloxy chlorosilane modifiers (3.49, 3.47 and 2.57 %, respectively) were applied, whereas the lowest amount was obtained by Octadecyl modifier (1.73 %). In the same fashion, while the Ethyl_WS, Tetra_WS and Acryloxy_WS samples shown the highest improvement on thermal stability ($T_{2\%}$ and Wt250 values), the Octadecyl_WS sample had the lowest values of $T_{2\%}$ and Wt250.

In fact, Figure 86 and Figure 87 show that increasing the amount of silane grafted to the WS fiber increases the values of the $T_{2\%}$ and Wt250 of silane treated samples. However, these observations do not indicate a correlation between amount of silane modifier grafted to WS fiber and its thermal stability. It should be noted that there are different types of silane modifiers being utilized and therefore, different grafting mechanisms could be affecting the relationship between amount of grafted silane and thermal stability improvement.

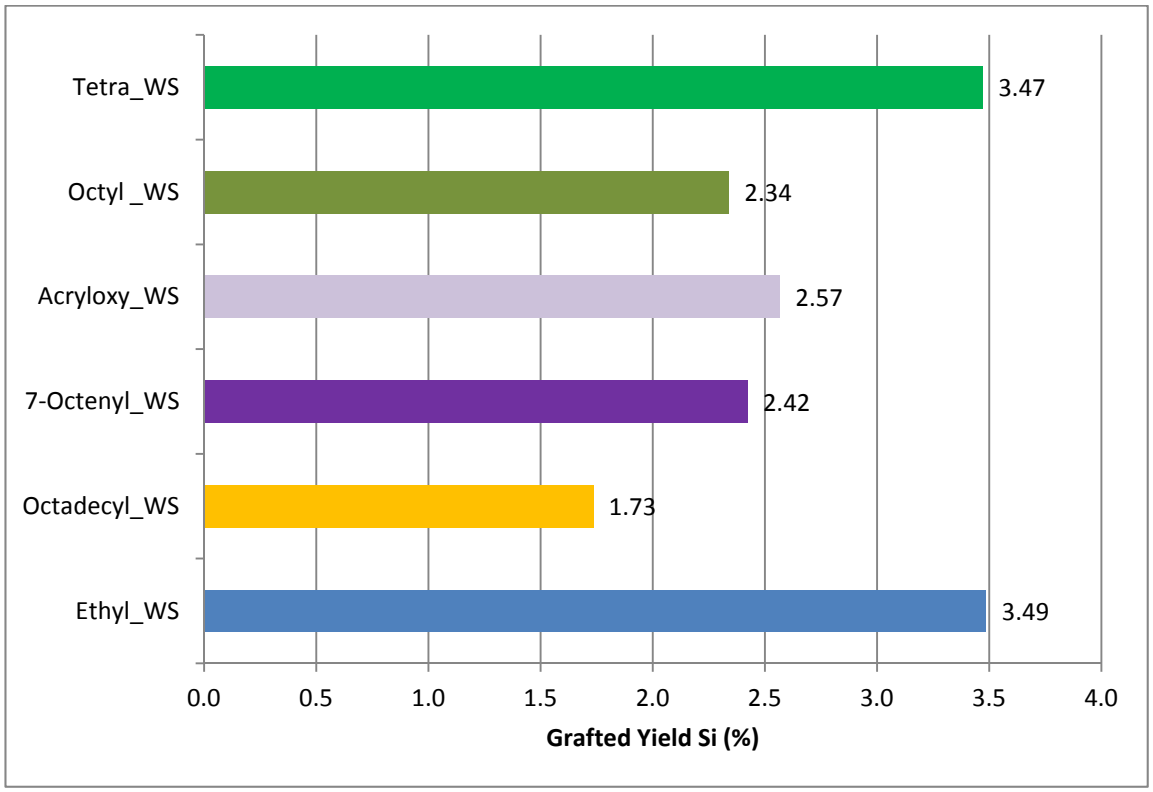

Figure 85: Silane (%) grafted into wheat straw fiber as a function of chlorosilane modifiers used.

Using X-ray photoelectron spectroscopy (XPS), Pickering et al. (2003) have observed that radiata pine fiber had its silicon concentration increased to 2.3 and 3.2 % after treatment with aminopropyltriethoxysilane and dichlorodiethylsilane. These numbers are consistent with the finds reported here in the two last set of experiments (Alkoxy Type and Chloro Type). Only in the case of dichlorodiethylsilane, those authors found evidence of ether linkages between the hydroxyl groups of the wood fiber and silane modifier. This may indicate that the more reactive nature of the hydrolyzable group present in the dichlorodiethylsilane (which has chlorine) favored the grafting of silane into wood fiber surface.

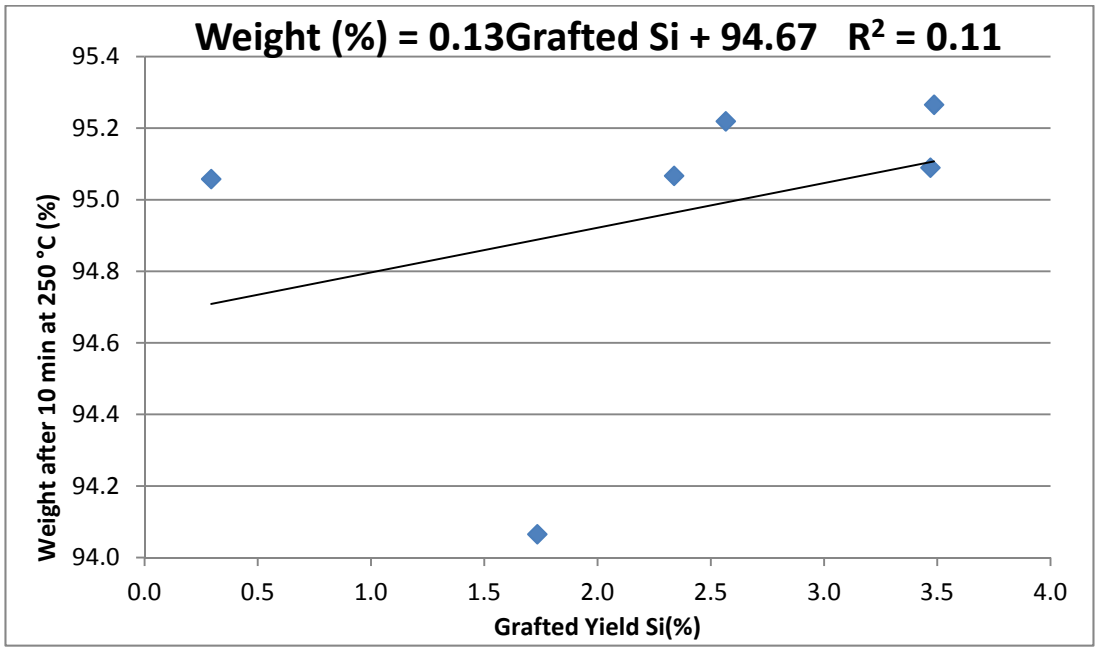

Figure 86: Weight (%) left after 10 minutes under isothermal heating at 250 °C as a function of silane (%) grafted into wheat straw fiber.

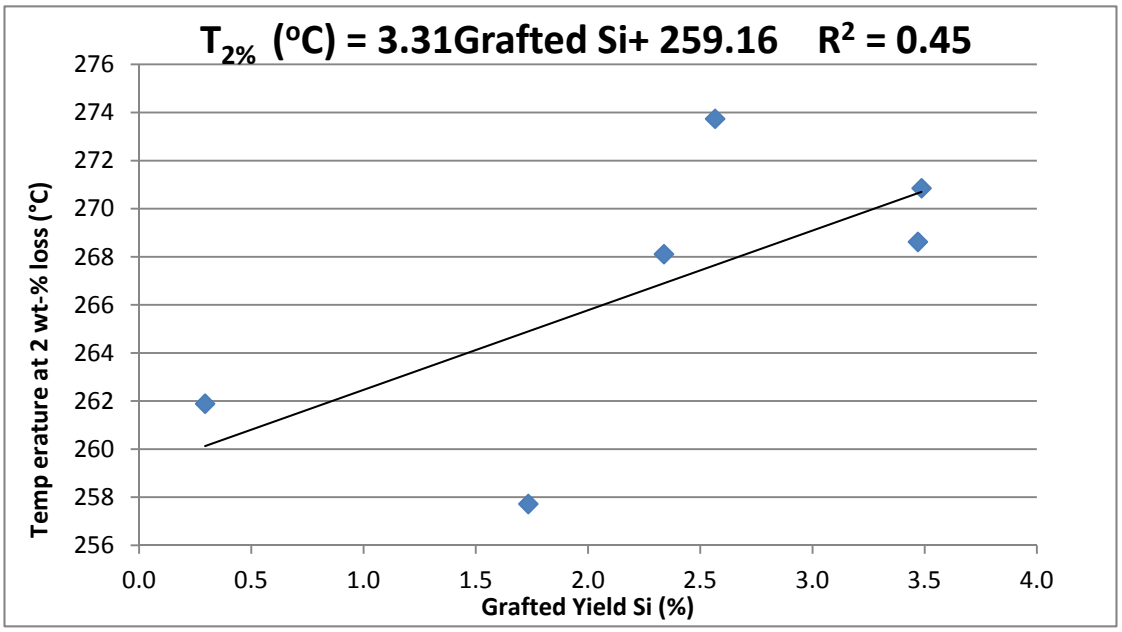

Figure 87: Temperature at 2 % weight loss (obtained from TGA analysis using 10 °C/min heating rate under air atmosphere) as a function of silane percentage grafted into wheat straw fiber.

Figure 88 depicts the ash content, the amount of inorganic material left at 600 °C under air atmosphere, for all silane treated samples. If the silane modification is successful, a higher content of organic material should be present in the silane treated samples. Therefore, it is expected that an increase in the silane modifier content will be reflected by a decrease of the percentage of the inorganic material. This supposition is supported by the results of Figure 88. It shows that the samples with highest percentage of silane grafted, Ethyl and Acryloxy, have the lowest ash content; while the samples with lower amount of grafted silane depict high amount of inorganic material (e.g., Octadecyl_WS).

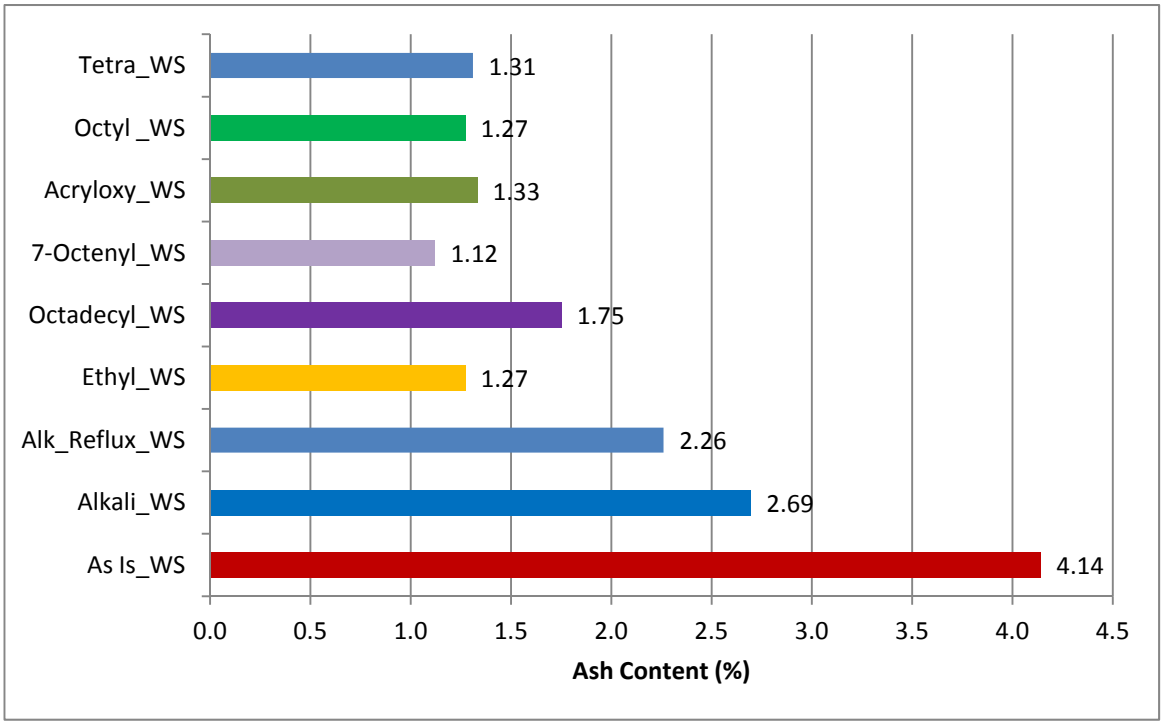

Figure 88: Ash content (mass left at 600 °C under air atmosphere) for the Chloro Type set of experiments samples.

The amount of silane modifier that will graft into wheat straw fiber depends on the levels of hydrolysis and condensation of the silane modifier in the solution. Reaction conditions (e.g., pH, temperature and stir rate of the solution, solvent, amount of water, concentration of silane modifier, use of catalyst etc) and the nature of the silane modifier (i.e., non-hydrolyzable and hydrolyzable

groups present in the silane molecule) are the factors that can influence these rates of hydrolysis and condensation. Since the reaction conditions and hydrolyzable group (which was chlorine) are the same for all the seven silane modifiers used during the Chloro Type set of experiments, the differences on the hydrolysis and condensation rates are due to the different non-hydrolyzable groups (i.e., R in the $R\text{-}(CH_2)_n\text{-}Si\text{-}(X)_3$ silane molecule) present in each one of the silane modifiers.

For example, owing to steric hindrance effect cause by the bulky R group of Octadecyl modifier ($R = CH_3\text{-}(CH_2)_{16}\text{-}CH_2\text{-}$), the reactive silanol monomers of Octadecyl will have more difficulties to access the hydroxyl groups on the surface of the wheat straw fiber. On the other hand, the reactive monomers of Ethyl and Tetra modifiers are smaller and can more easily diffuse into cell walls and/or physically adsorb into wheat straw fiber surface (Abdelmouleh et al, 2002; Donath et al., 2004; Hill et al., 2004; Xie et al., 2010).

At the same time, the self-condensation of free silanol groups promotes the formation of oligomers via formation of -Si-O-Si- bonds (crosslinking). Decreasing the size of the non-hydrolyzable groups (R) increases the tendency of silane molecules to undergo self-condensation (crosslinking). For example, the rate of condensation of trimethylsilanol ($R = CH_3$) is 10^3 and 10^6 faster than triethylsilanol ($R = CH_2\text{-}CH_3$) and triphenylsilanol ($R = C_6H_5$), respectively (Cella and Carpenter, 1994).

Based on this information, the self-condensation of Ethyl and Tetra reactive monomers is expected to be faster than the self-condensation of Octadecyl reactive monomers because the Octadecyl modifier R group contains eighteen carbon atoms, whereas Ethyl and Tetra modifiers R groups have two and zero carbon atoms, respectively.

Therefore, it is reasonable to assume that a larger amount of solid polysiloxane is formed in the case of Ethyl_WS and Tetra_WS samples than Octadecyl_WS sample. The bigger size of these polymeric layers is responsible for the higher thermal stability demonstrated by Ethyl_WS and Tetra_WS samples in comparison with Octadecyl_WS sample. Generally, this polymeric layer is located on the surface of the wheat straw fiber. Extra opportunities for hydrogen bonding with the hydroxyl groups of the fiber is provided by the -Si-O-Si- bond present in the polysiloxane layer which is stable against hydrolysis.

After silane modification, further heating can remove water and convert hydrogen bonds into the -Si-O-C- covalent bond which then can connect the reactive silane modifier forms (i.e., monomers and

oligomers) and hydroxyl (OH) groups of the wheat straw fiber (Abdelmouleh et al., 2002; Castellano et al., 2004; Valadez-Gonzalez et al., 1999). Even though the -Si-O-C- covalent bond may not be stable against hydrolysis, it has been shown that the silane modifiers grafted to the treated fibers are resistant against water leaching (Abdelmouleh et al, 2002; Donath et al., 2004; Hill et al., 2004). For example, Donath et al. (2004) claim that methyltriethoxysilane and vinyltrimethoxysilane can either graft or polymerize in the surface of Corsican pine sapwood. This way, according to the authors, only small amounts of silane were leached out even after five leaching cycles.

In the case of the Acryloxy, 7-Octenyl and Octyl modifiers, it seems that the non-hydrolyzable groups (R = H_2C=CH-C=O-O-$(CH_2)_3$-; R = H_2C=CH_2-$(CH_2)_6$-CH_2-; R = CH_3-$(CH_2)_6$-CH_2-, respectively) are not large enough to provoke steric hindrance effect since the amount of grafted silane and thermal stability of the samples treated with these silane modifiers are similar to the ones of Ethyl_WS and Tetra_WS samples.

Furthermore, the strong affinity of acryloxy groups towards the hydroxyl groups of wheat straw promotes an extra opportunity for hydrogen bonding between the Acryloxy modifier and the wheat straw besides the reactive silanols of Acryloxy modifier. The affinity between Acryloxy groups and hydroxyl groups increases the changes of adsorption to wheat straw fiber and justifies the good thermal stability shown by Acryloxy_WS sample.

Table 24 shows the performance of the samples treated with four different chlorosilane modifiers. It can be seen that chlorosilane modifiers bearing different types of organofunctional groups (R) proved to be efficient to enhance the thermal stability of wheat straw fiber. The highest amount of grafted silane and improvement on thermal stability was achieved when small size silane molecules (i.e., shorter linker (CH_2) or functional groups R) were utilized (e.g., Ethyl_WS and Octyl_WS samples). In contrast, when relatively large silane molecules (e.g., Octadecyl modifier) were employed, the grafting of silane, and therefore the increment on the thermal stability of wheat straw were smaller.

Based on these observations, the chlorosilane modifiers with the best performance under isothermal conditions (e.g., Ethyl, 7-Octenyl, Tetra and Octyl) will be utilized to produce composites of polyamide and silane treated samples.

Table 24: Summary of thermal stability and grafted silane results for Chloro Type set of experiments.

Sample	$T_{2\%}$ (°C)	Wt250 (%)	Grafted Si (%)	Overall Performance
Acryloxy_WS	273.7	95.2	2.57	Excellent
Ethyl_WS	270.9	95.3	3.49	Excellent
7-Octenyl_WS	261.9	95.1	2.42	Good
Octadecyl_WS	257.7	94.1	1.73	Reasonable
Alk_Reflux_WS	254.3	90.7	---	Reference
Alkali_WS	246.1	89.4	---	Reference
As Is_WS	238.0	86.6	---	Reference

5.6 Conclusions

In this chapter, two classes of silane modifiers, alkoxysilane and chlorosilane, along with different reaction conditions (such as pH, temperature of the solution, different solvents, amount of water, use of catalyst etc) were evaluated for silane modification of wheat straw. The goal was to obtain the silane modifiers along with the set of reaction conditions that could impart the highest thermal stability enhancement for wheat straw. Promising thermal stability improvement was achieved after silane modification of wheat straw.

The experimental work shows that the reaction conditions required to successfully graft alkoxysilane are different from the ones necessary for chlorosilane modifiers. In the case of alkoxysilane modifier, the amount of water seems to play an important role in the success of the silane modification. The best set of reaction conditions for silane modification is a combination of two solvents (80 % ethanol + 20 % water) as well as the application of acidification and pre-hydrolysis. The use of 100 % water as a solvent also provides positive results as well.

In the case of chlorosilane modifiers, it appears that the polarity of the solvents utilized during silane modification of wheat straw is critical. Polar protic solvents (e.g., methanol and ethanol) promoted the highest deposition of chlorosilane modifier (7-Octenyl) and thermal stability enhancement of the wheat straw fiber. Among the different polar protic solvents tested, methanol is

the best solvent for silane modification utilizing the 7-Octenyl modifier and therefore seems promising choice for other chlorosilane modifiers.

In addition, among the different types of alkoxysilane modifiers tested in this chapter, Ureiodo modifier provided the best results. However, the thermal stability enhancement achieved with the utilization of Ureiodo modifier was not significant. The 2 % of weight loss was reached at 249.8 ^{o}C which represents only 4.96 % increase in comparison with the untreated sample.

On the other hand, several chlorosilane modifiers significantly improved the thermal stability of wheat straw. The size of the chlorosilane modifiers molecules seems to be of crucial importance in the success of the silane modification. The best results were achieved using chlorosilane modifiers with small size molecules. These molecules have small non-hydrolyzable groups (R) and small linkers (-$(CH_2)_n$-) between the non-hydrolyzable group and the silicon atom (R and -$(CH_2)_n$- in the R-$(CH_2)_n$-Si-X_3 silane molecule, respectively).

The highest chlorosilane deposition and thermal stability enhancement was reached utilizing Acryloxy, Ethyl and 7-Octenyl chlorosilane modifiers. The beginning of the thermal degradation ($T_{2\%}$) of the sample treated with Acryloxy modifier is increased by 15 % (from 238 to 273.7 ^{o}C) in comparison with the untreated sample.

Overall, chlorosilane modifiers provided considerably higher thermal stability enhancement than alkoxysilane modifiers. However, the alkoxysilane modifiers contain organofunctional groups that act as coupling agents for polyamides, and therefore this advantage should be explored.

In order to increase the thermal stability obtained with the alkoxysilane modifiers, a combination of alkoxysilane and chlorosilane modifiers will be evaluated in the next chapter. The chlorosilane modifiers are extremely reactive and undergo hydrolysis very fast. The hydrolysis of these chlorosilane modifiers produces water and can stimulate and speed the hydrolysis reaction of the alkoxysilane.

Therefore, it is expected that the combination of alkoxysilane and chlorosilane modifiers can provide the higher thermal stability enhancement observed here for chlorosilane modifiers together with increased compatibility with polyamides.

Chapter 6 - Wheat Straw Fiber/Polyamide-6 Composites

6.1 Introduction

In the previous chapter, considerable enhancement on the thermal stability of the wheat straw fiber was achieved by using different silane treatments. In this chapter, that knowledge is applied to produce composites of engineering thermoplastics with wheat straw fiber. It is showed that the enhancement on the thermal stability of straw fiber is sufficient to allow the fabrication of wheat straw/polyamide-6 (WS/PA-6) composites with reduced thermal degradation of the wheat straw fiber. Additionally, the effect of the alkali and silane treatments on the straw fiber and mechanical properties (flexural, impact, etc) of the WS/PA-6 composites is investigated.

Thermal degradation can be very severe during the composite fabrication steps especially in the case of agro-based fibers exposed to high processing temperatures. The thermal degradation of the straw fiber may affect different composite properties, especially mechanical, optical (e.g., transparency or color) and other physical properties (e.g., odor or appearance).

It is expected that the improvement in thermal stability after the silane treatment can minimize the thermal degradation of the straw fiber during the fabrication of WS/PA-6 composites. In order to verify this hypothesis a set of experiment, called Thermal Set, was performed to establish a relationship between the thermal stability of the wheat straw samples and the thermal stability of the composites. For that, the thermal stability and the color of the wheat straw samples were evaluated before and after compounding with polyamide-6.

In the second part of the chapter, another set of experiments, called Mechanical Set, was carried out to evaluate the changes caused by the alkali and silane treatments on the wheat straw samples and mechanical properties of the WS/PA-6 composites.

The remainder of this chapter is organized as follows. Section 6.2 enlists the material used through this chapter. Section 6.3 presents the procedures utilized to perform the experiments of Thermal Set as well as the discussion of the results obtained.

The second part of this chapter, Mechanical Set, is presented in the Section 6.4 which describes the procedures utilized to perform the experiments and discuss the results obtained with these experiments.

6.2 Materials

The wheat straw used in this chapter was provided by Omtec Inc. The details regarding harvesting and grinding steps as well as samples labeling were presented before in the Chapter 3. Table 25 summarizes the differences between the sizes of Mid and Large wheat straw samples while Figure 89 compares the appearance of these wheat straw samples.

Table 25: Table presents the difference between the size of Mid and Large wheat straw samples.

WS Type	Fiber Size
Large	Fiber > 1.19 mm (Mesh 16)
Mid	1.19 mm (Mesh 16) > Fiber > 0.5 mm (Mesh 35)

Figure 89: The Mid (left) and Large (right) wheat straw samples employed in the Chapter 6.

It should be highlighted that the Mid wheat straw sample was utilized during both sets of experiments, Thermal Set and Mechanical Set. The Large wheat straw sample was employed only during the Mechanical Set of experiments. The detailed lists of the materials (solvents, organosilane modifiers and other chemicals) and equipment used throughout this chapter are presented in the tables below (Table 26 and Table 27).

Table 26: List of equipment used in Chapter 6.

Equipment	Manufacturer
Analytical balance AB304-S	Mettler Toledo
DSC Q2000	TA Instruments
Hot Plate	VWR
FTIR Tensor 27	Bruker Optik GmbH
FESEM gold coating unit Desk II with Argon (inert gas)	Denton Vacuum, USA
Field Emission Scanning Electron Microscope (FESEM) Leo 1530 with EDX/OIM PV9715/69 ME	Leo Gemini AMETEK Inc.
Injection Moulding Apparatus RR/TSMP	Ray-Ran
Mini-jector Injection Moulding Machine Model 55 – Wasp Series	
MiniLab Extruder Haake	Thermo Electron Corporation
Oven - Model 5890A GC	Hewlett Packard
Mechanical Test Machines – Model 120Q1000 Dual column systems	TestResources Inc.
Monitor/Impact Tester – Model 43-02-01	Testing Machines Inc. (TMI)
Specimen Notch Cutter – Type XQZ-I	Chengde JinJian Testing Instrument Co., Ltd.
Stereo Microscope MZ6	Leica Microsystems GmbH.
TGA Q500	TA Instruments
Tzero Hermetic low-mass pan and lid (DSC)	TA Instruments
XRD Instrument, 30 kV, 30 mA, with Cu Kα radiation	Bruker Instrument Inc.

Table 27: List of materials used in this chapter.

Materials	Type/Grade	Supplier/Manufacturer
Polyamide 6 (Nylon 6)	Aegis H8202NLB PA6	A. Schulman Inc.
Wheat Straw Mid	Soft white winter variety	Omtec Inc.
Wheat Straw Large	Soft white winter variety	A. Schulman Inc.
Ureiodopropyltriethoxysilane	Alkoxysilane	Gelest Inc.
n-Octyltrichlorosilane	Chlorosilane	Gelest Inc.
Tetrachlorosilane	Chlorosilane	Gelest Inc.
7-Octenyltrihlorosilane	Chlorosilane	Gelest Inc.
Methanol	Solvent/HPLC	Sigma-Aldrich
Ethanol	Solvent/HPLC	Sigma-Aldrich
Irganox 1010	Antioxidant	Ciba Inc.
Butylamine	Purum ≥ 98% (GC)	Sigma-Aldrich

6.3 Evaluating the Thermal Stability of Wheat Straw Samples during the Fabrication of Wheat Straw/Polyamide-6 Composites

The set of experiments performed in this section is called Thermal Set. It has two main objectives. The first one is to evaluate if the silane treatment conducted on larger amount of the wheat straw (i.e., several grams) than before (i.e., several milligrams) will provide similar thermal stability enhancement as was observed in Chapter 5. The second objective is to verify if the wheat straw samples with higher thermal stability will suffer less thermal degradation during the actual fabrication of WS/PA-6 composites by extrusion and injection molding. Figure 90 lists in detail the goals of this set of experiments.

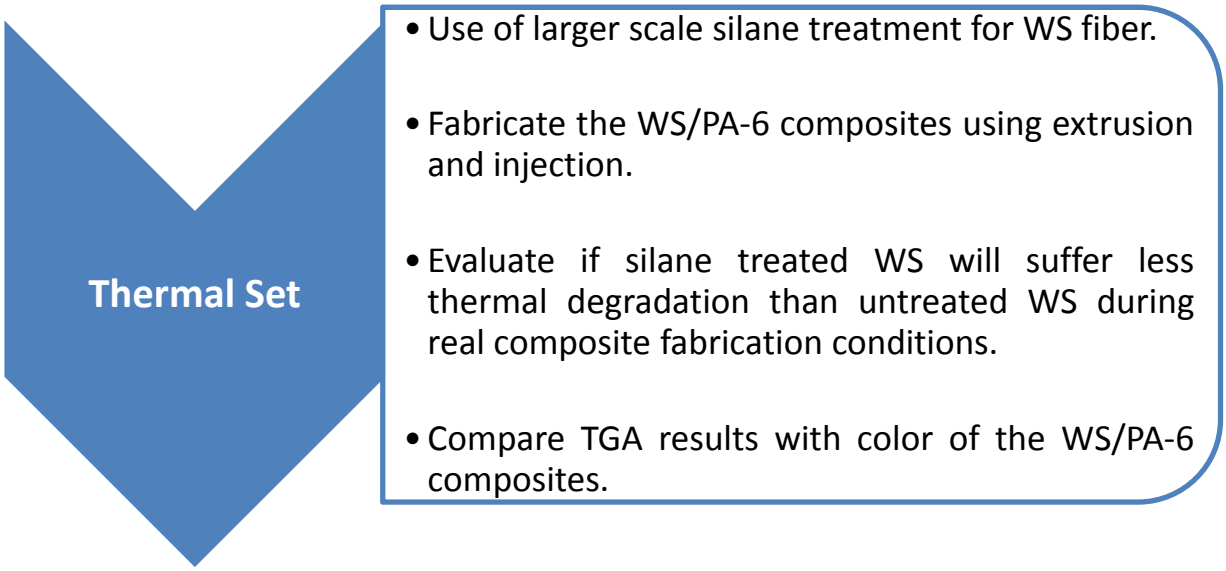

Figure 90: Diagram shows the objectives of the first part of this chapter, Thermal Set of experiments.

6.3.1 Silane Treatment

Similar to Chapter 5, the wheat straw fiber was pre-treated with alkali solution following the procedure described in Methods section. Compared to the previous chapter, the only difference here was the larger scale of the alkali pre-treatment performed. Therefore, a greater amount of straw fiber (150 grams), sodium hydroxide (120 grams) and deionized water (3 L) were utilized for alkali pre-treatment.

The same procedure presented in Chapter 5 (see Methods section) was utilized here to perform the silane treatment of alkali treated wheat straw samples. The differences between the silane treatment used here and the one in Chapter 5 are highlighted in Table 28. Larger amounts of wheat straw (20 grams) and methanol (450 ml) were utilized here compared to the ones in Chapter 5. The treatment time was also modified. The silane treatment time was 8 hours in Chapter 5 whereas in this section (Thermal Set), the treatment time was decreased to 6 hours. This treatment time reduction was

performed in order to potentially reduce the silane treatment cost and fiber breakage. In addition, different combinations of silane modifiers were tested in this section.

Table 29 shows the experimental parameters used for the silane treatment performed in this section. Two wheat straw samples (7-Octenyl and Octyl) were treated with a different type of chlorosilane modifier, whereas a combination of chlorosilane and alkoxysilane modifiers was utilized for treatment of the third wheat straw sample (Ureiodo+7-Octenyl). This alkoxysilane modifier (Ureiodopropyltriethoxysilane) is commonly used as coupling agent for polyamides because of the chemical group ureiodo present in its molecule. Therefore, it is expected that the alkoxysilane modifier can improve bonding between wheat straw and polyamide-6.

In the previous chapter, it was observed that alkoxysilane modifiers were less reactive towards the hydroxyl groups of the wheat straw fiber than chlorosilane modifiers. In an attempt to promote the bonding reaction between the alkoxysilane modifier and the wheat straw fiber, the ureiodo alkoxysilane modifier was mixed with another two chlorosilane modifiers. It is expected that the higher reactivity of these chlorosilane modifiers could speed the hydrolysis step of the alkoxysilane modifier and the overall reaction with the hydroxyl groups of the wheat straw fiber.

Table 28: Comparison between the parameters employed for silane treatment in the Thermal Set and Chapter 5.

Label	Wheat Straw (grams)	Wheat Straw Type	Methanol (ml)	Treatment Time (hours)	Silane ($mmole.g^{-1}$)
Chapter 5	0.25	Mid	50	8	1.25
Thermal Set	20	Mid	450	6	1.75 – 2.19 [a]

[a]: see Table 29 for details.

Table 29: List of labels, silane modifiers and its concentrations employed for Thermal Set of silane treatment.

Label	Silane Modifiers	Concentration (mmole.g^{-1})	Concentration (g)
7-Octenyl	7-Octenyl	1.97	7.25
Octyl	Octyl	2.19	8.15
Ureiodo+7-Octenyl	Ureiodo	1.02	4.05
	7-Octenyl	0.75	2.75

6.3.2 Fabrication of the Wheat Straw/Polyamide-6 Composites

The fabrication of the wheat straw/polyamide-6 (WS/PA-6) composites involves two main steps: extrusion and injection molding. During extrusion, the wheat straw fiber is mixed with polyamide-6 in order to obtain a homogenous mixture of these two materials. After that, the extruded material is fed into an injection mold machine and the final shape and size of the WS/PA-6 composite is obtained.

6.3.2.1 Extrusion of the Wheat Straw Samples with Polyamide-6

Wheat straw/polyamide-6 composites were prepared by the melt-mixing method using extrusion. The equipment used was the Haake Minilab Microcompounder with a co-rotating conical twin screws (Figure 91). Based on preliminary testing and literature review (Amintowlieh, 2010; Xu, 2008), the operating conditions of the extruder were set at the temperature of 235 ^{o}C and the screw speed of 60 rotation per minute (rpm).

Initially, a mixture of polymer and antioxidant, called here masterbatch, was prepared prior to the actual composite extrusion step. This step took place prior to the addition of the wheat straw fiber in order to avoid problems with the incorporation and dispersion of the antioxidant into the composite. Dispersion problems can occur during the extrusion because of the volume and weight differences between the antioxidant (very fine powder) and the other composite components (wheat straw and polyamide-6 which are fibers and bulky pellets, respectively). This initial step (masterbatch

preparation) allows achieving a homogenous mixture between the polymer and the antioxidant. This masterbatch was pelletized by cutting the extruded material with scissors in approximately 4 mm of length.

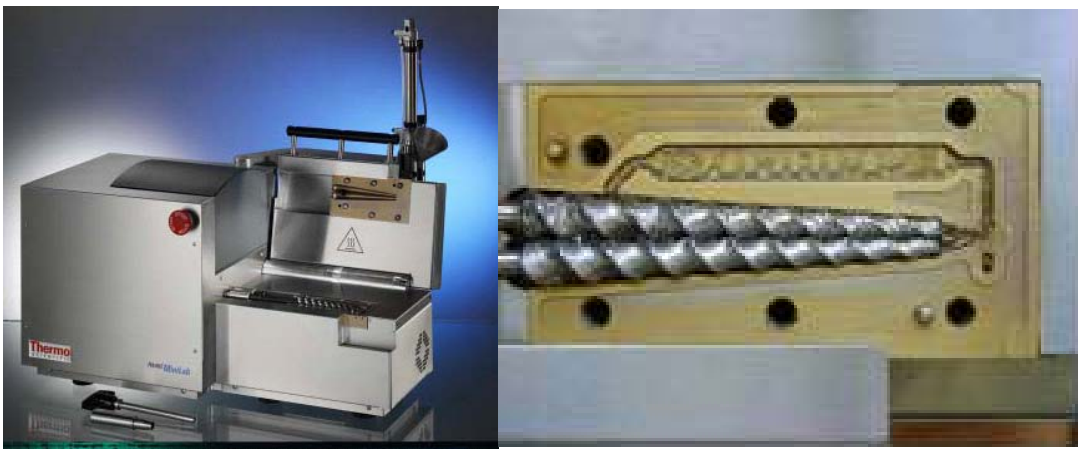

Figure 91: Haake Minilab Micro-Compounder (left) and its conical screws (right) used to prepare the WS/PA-6 composites.

After that, all the composite components (wheat straw fiber, polymide-6 and masterbatch) were hand mixed prior to feeding the extruder in order to get a uniform mixture. The obtained extruded composites (Figure 92) were cut into smaller pieces (called pellets) by scissors in order to use them in injection molding.

Figure 92: WS/PA-6 composites pellets obtained after extrusion with (a) untreated, (c) silane treated Mid wheat straw.

6.3.2.2 Injection Molding Using Mini-Jector Injection Molding Machine

A laboratory injection moulding machine (Ray-Ran RR/TSMP, Figure 93) was utilized to obtain injected composite bars for mechanical tests. The extruded pellets were fed inside the barrel of the injection machine and kept for approximately 10 minutes. The temperature of the barrel was set at 240 ^{o}C. Once the composite was completely melted which was indicated by polymer coming out of the injection nozzle, the melted composite was injected by a pneumatic piston into the metallic mold.

The pressure applied by the piston and the temperature of the mold were approximately 100 psi and 85 ^{o}C, respectively. This pressure was held for 10 seconds for each bar to guarantee that the mold was completely filled.

It is important to mention that previous injection attempts using lower mold temperatures (50-60 ^{o}C) failed because the polymer was cooled down before filling completely the mold. This problem

was avoided by increasing the temperature of the mold. Also, it is likely that increasing the piston pressure could solve this problem; however, this was not possible due to equipment limitations.

Seven different batches (or runs) were prepared according to Table 30. The column Label in the table presents the nomenclature utilized for all the runs. Different chemical treatments used are shown in the first part of the label, while the last part of the label represents the form of the WS/PA-6 composites which are either in the extruded (Ex) or injected (Inj) form. Therefore, the labels differing only by these suffixes (Ex or Inj) represent exactly the same composite sample and they contain exactly the same components. For example, As Is_Ex and As Is_Inj represent the extruded and injected forms, respectively, of the WS/PA-6 composite containing untreated wheat straw fiber (called As Is).

Table 30: Labels and amount of each component utilized for the extruded and injected WS/PA-6 composites.

Run #	Label		WS Treatment[1]	Fiber WS[2] (wt-%)[3]	Polymer PA-6 (wt-%)
	Extruded	Injected			
1	7-Octenyl_Ex	7-Octenyl_Inj	7-Octenyl		
2	Octyl_Ex	Octyl_Inj	Octyl	15	84.9
3	Ureiodo+7-Octenyl_Ex	Ureiodo+7-Octenyl_Inj	Ureiodo+7Octenyl		
4	As Is_Ex	As Is_Inj	None		
5	Alk_Ex	Alk_Inj	Alkali	15	84.9
7	PA-6_Ex	PA-6_Inj	None	0	99.9

[1]: see Table 29 for detail; [2]: Mid wheat straw; [3]: weight percentage.

Six of these composite samples (from run #1 to 6) had the same amount of wheat straw, polyamide-6 and antioxidant (Irganox), i.e., 15, 84.9 and 0.1 wt-%, respectively. The main difference among these composites was the chemical treatment applied to the wheat straw sample (i.e.,

untreated, alkali and silane treated) as shown in Table 30. The seventh batch consisted of pure polyamide-6 and antioxidant (0.1 wt-%).

As a preliminary observation, the relatively long residence time of the wheat straw inside the injection machine barrel caused the samples to have darker colors than the extruded composite samples. The color change can be observed by comparing Figure 92 and Figure 94. In the same way, the odor noticed during injection step was stronger than in the extrusion step.

Figure 93: Lab scale Ray Ran injection moulding machine used to inject the composite bars.

Figure 94: WS/PA-6 composites test bars obtained from injection molding process.

6.3.3 Thermogravimetry Analysis (TGA)

The thermal gravimetric analysis (TGA) of the samples was performed using a Q500 series from TA Instruments. The samples were submitted to a constant heating rate of 10 °C/min ranging from 35 to 800 °C under air atmosphere. The amount of organosilanes grafted and the grafting yield were calculated using the TGA data obtained for alkali wheat straw fibers.

Also, isothermal gravimetric analysis was carried out. The samples were heated from 35 to 200 °C and 35 to 250 °C using a heating rate of 50 °C/min. After achieving these temperatures, samples were kept at 200 or 250 °C for 30 minutes under nitrogen atmosphere.

6.3.4 Results and Discussion of the Thermal Set

As mentioned previously, the main goal of the Thermal Set of experiments are to evaluate the thermal stability of wheat straw samples, especially the samples obtained after the larger scale alkali and silane treatments, and to verify if the wheat straw samples with higher thermal stability will suffer less thermal degradation during the actual fabrication of composites of wheat straw and polyamide-6 (WS/PA-6).

In order to evaluate the thermal degradation during the fabrication of the WS/PA-6 composites, visual color examination and TGA analysis were performed before and after each step of the composite fabrication which are summarized by the diagram in Figure 95.

The fabrication of polymer composites generally involves two main steps. Initially, the wheat straw fiber is compound with the polymer (polyamide-6) and other additives using an extruder in a process called extrusion. The resulting material has the form of a long thread which has to be cut into small pellets. These pellets are then used to feed an injection moulding machine in a process referred to as injection. Objects with different shapes and sizes can be obtained depending on the injection machine and mold utilized. Figure 95 also shows the samples (at the right inside the rectangle) evaluated for each one of the three set of experiments. For example, the set Extruded Composites contains five samples (7-octenyl_Ex, Octyl_Ex, Ureiodo + 7-octenyl_Ex, Alkaly_Ex, As Is_Ex and PA-6_Ex). These composite samples were prepared according to Table 29 and 30; the labels used to describe these samples are also shown in Table 29 and 30.

First, the thermal stability and color of pure wheat straw samples (both silane treated and untreated) were examined. The results obtained in that phase are referred to as WS Samples set. Similarly, the Extruded Composites and Injected Composites sets contain the color and TGA analysis results for extruded and injected WS/PA-6 composites, respectively.

Initially, the thermal degradation of wheat straw samples without addition of polyamide-6 is discussed utilizing the results of WS Samples set.

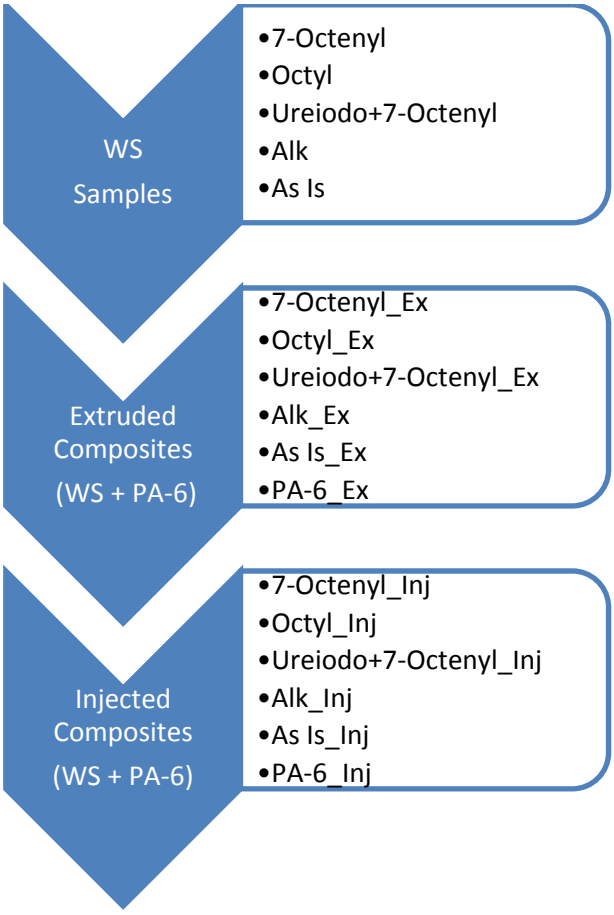

Figure 95: Thermal Set of experiments was divided in three sets: WS Samples, Extruded Composites and Injected Composites.

Throughout this section, samples containing untreated wheat straw are identified by letter A, alkali treated wheat straw by letter B and silane treated wheat straw by letters C, D and E (Octyl, Ureiodo+7-Octenyl and 7-Octenyl, respectively). Figure 96 shows the color of wheat straw samples (i.e., treated and untreated wheat straw samples) before (top picture) and after (bottom picture) exposure to heating at 250 °C under nitrogen atmosphere. There was a significant color change after exposure of these samples to high temperature. The amount of color change and darkening is used as a qualitative indication of thermal degradation. A color change towards black indicates thermal degradation, similar to the carbonization process.

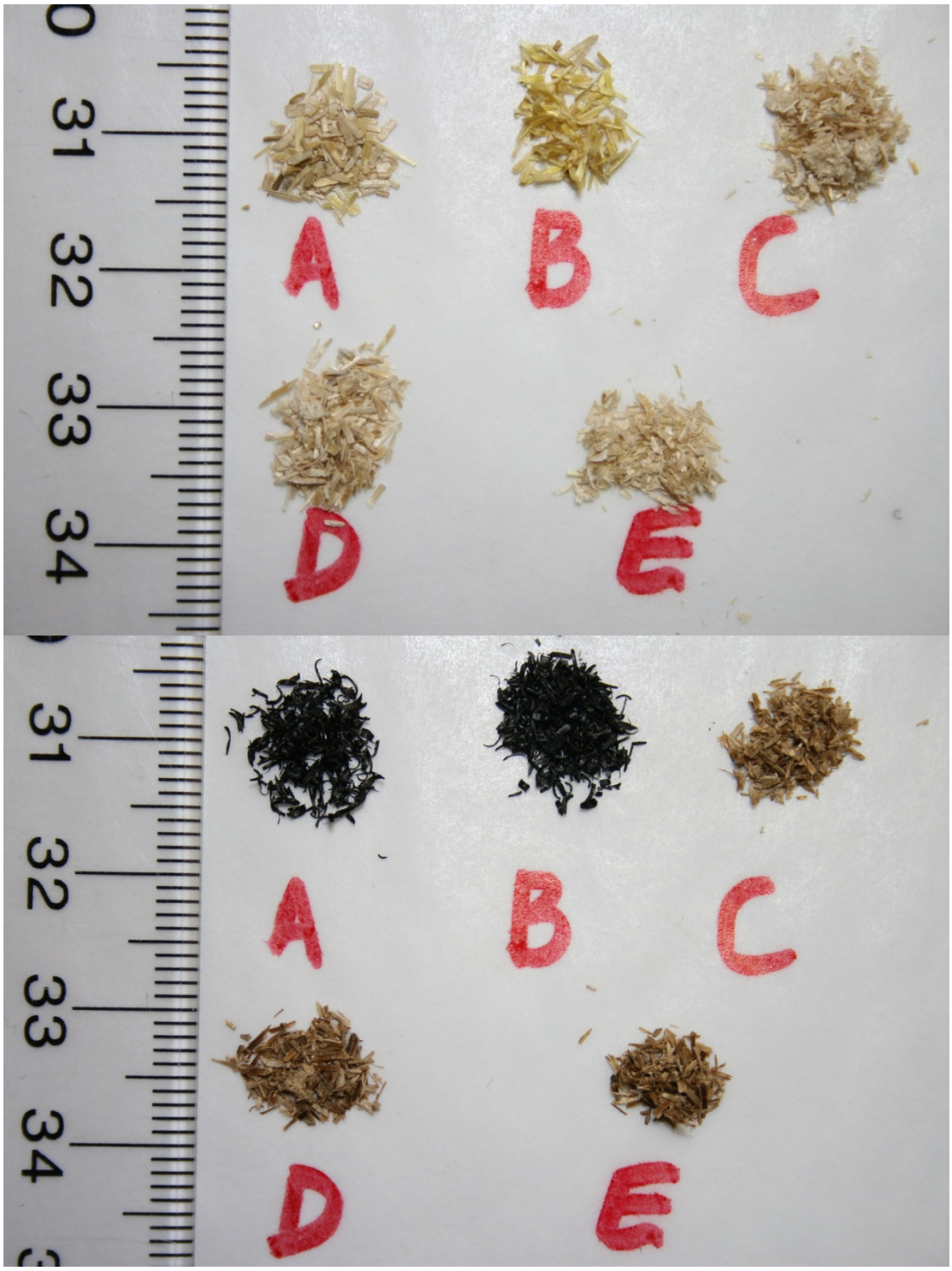

Figure 96: Wheat straw samples before (top picture) and after (bottom picture) isothermal analysis at 250 °C under nitrogen atmosphere. Samples A = As Is, B = Alk, C = Octyl, D = Ureiodo+7-Octenyl and E = 7-Octenyl.

It is possible to observe that before exposure to any heating (top picture in Figure 96), all the wheat straw samples have a similar yellow color. In contrast, after exposure to 250 °C during 30 minutes (bottom picture in Figure 96) all the silane treated wheat straw samples (C, D and E in Figure 96) have a significant lighter color than the alkali treated and untreated wheat straw samples (B and A in Figure 96, respectively). This observation indicates that the silane treated wheat straw samples suffered less thermal degradation than alkali treated and untreated wheat straw samples.

In order to verify if the samples with lighter color have suffered less thermal degradation, the color results were compared with the TGA results. The non-isothermal and isothermal TGA results are presented in Figure 97 and Figure 98, respectively. Overall, these results confirm that wheat straw samples with lighter color (silane treated samples C, D and E in Figure 96) after 30 minutes of exposure to heating (250 °C) have higher thermal stability.

The silane treated wheat straw samples present higher thermal stability than untreated and alkali treated samples under non-isothermal TGA analysis. For example, the $T_{2\%}$ (i.e., the temperature at 2 % of weight loss) of the silane treated wheat straw samples Octyl, Ureiodo+7-Octenyl and 7-Octenyl was increased by 27 °C (from 238.0 to 265.0 °C), 19.7 °C (from 238.0 to 257.7 °C) and 35.4 °C (from 238.0 to 273.4 °C) compared to untreated wheat straw sample.

In the same fashion, under isothermal conditions, the wheat straw samples with lighter color (i.e., silane treated samples) have also better thermal stability than the wheat straw samples with darker color (i.e., untreated and alkali treated samples). The changes on the weight percentage for 10 minutes at 250 °C (Wt250) are summarized in the Figure 98. It can be seen that the silane modified wheat straw samples have lower weight loss than untreated and alkali treated wheat straw samples. For example, the initial weight of the Octyl, Ureiodo+7-Octenyl and 7-Octenyl WS samples slightly decreases from 100 to 94.8, 93.9 and 94.4 %, respectively. This reduction was more severe in the case of alkali and untreated wheat straw samples (Alk and As Is) which had their initial weight decreasing from 100 to 88.9 % and from 100 to 86.6 %, respectively.

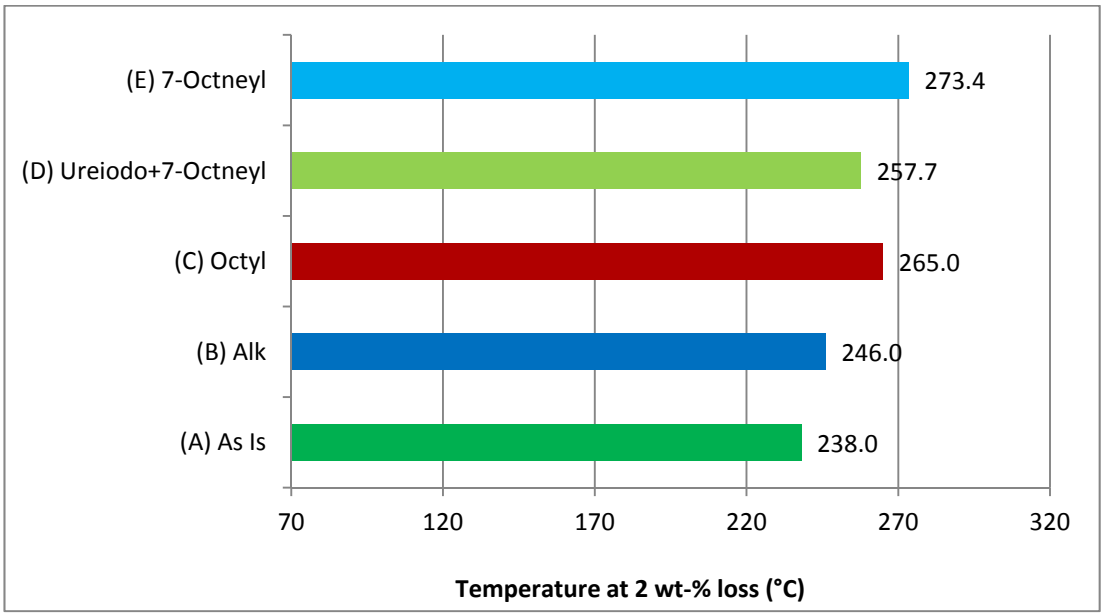

Figure 97: Temperature at 2 % weight loss for the WS Samples set of experiments obtained from non-isothermal TGA analysis (10 °C/min heating rate and air atmosphere).

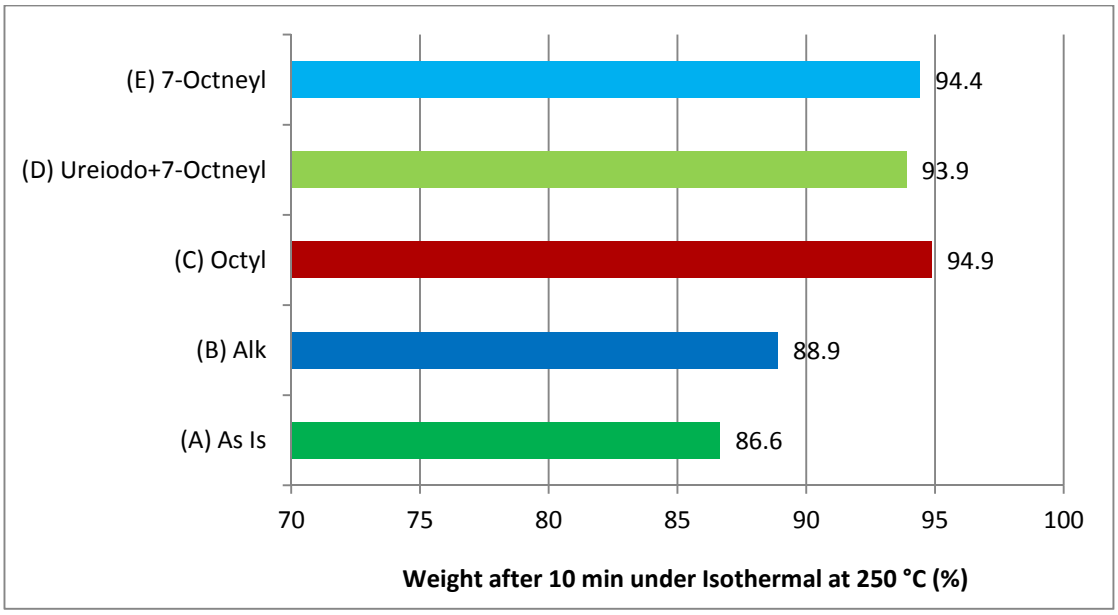

Figure 98: Percentage of the initial weight left after isothermal analysis (250 °C and nitrogen atmosphere) of the WS Samples set of experiments.

If both Octyl and untreated wheat straw samples are exposed to 250 °C during 10 minutes, the weight loss of Octyl WS sample (5.2 %) will be 8.2 % smaller than the weight loss of untreated WS sample (13.4 %). Consequently, these results indicate that composites utilizing wheat straw silane treated samples would suffer less thermal degradation during the composite fabrication process than composites using alkali and untreated wheat straw samples.

The TGA results also show that the silane treatment of larger amount of wheat straw (i.e., 5-10 grams) was successful and therefore the thermal stability enhancement obtained in the larger scale silane treatment of wheat straw was similar to the improvement observed for smaller scale silane treatment (i.e., 0.25 grams) in the previous chapter.

The thermal degradation and color change of wheat straw samples were investigated during the actual WS/Polyamide-6 composite fabrication steps: extrusion and injection molding. It is possible to observe that the color and thermal stability of the composite were influenced by the wheat straw sample employed. In general, composites utilizing silane treated wheat straw samples showed lighter colors and better thermal stability or resistance to thermal degradation.

By comparing the color of different extruded and injected WS/PA-6 composite samples (Figure 99 and Figure 100, respectively), it is clear that there is a higher shift to darker color in the case of composite samples containing untreated and alkali treated wheat straw fiber (samples A and B in Figure 99 and 12) than for the composites with silane treated wheat straw samples (samples C and D in Figure 99 and 12).

For example, when untreated wheat straw is extruded with polyamide-6, the resulting composite (sample A in Figure 99- As Is_Ex) has an intense black color indicating extensive thermal degradation of the untreated wheat straw. In contrast, extruded composites containing silane treated wheat straw samples (samples C and D in Figure 99 -Octyl_Ex and Ureiodo + 7-Octenyl_Ex, respectively) show a light golden color which denotes lower thermal degradation.

In fact, Figure 101 shows that the extruded material containing untreated wheat straw (As Is_Ex in Figure 101) displays the lowest thermal stability during non-isothermal TGA analysis (i.e., $T_{2\%}$ = 285.9 °C) and the darkest color (sample A in Figure 99). Whereas the extruded composite containing silane treated wheat straw (Octyl_Ex in Figure 101) has the highest thermal stability (i.e., $T_{2\%}$ = 310.5 °C) along with the lightest color (sample C in Figure 99).

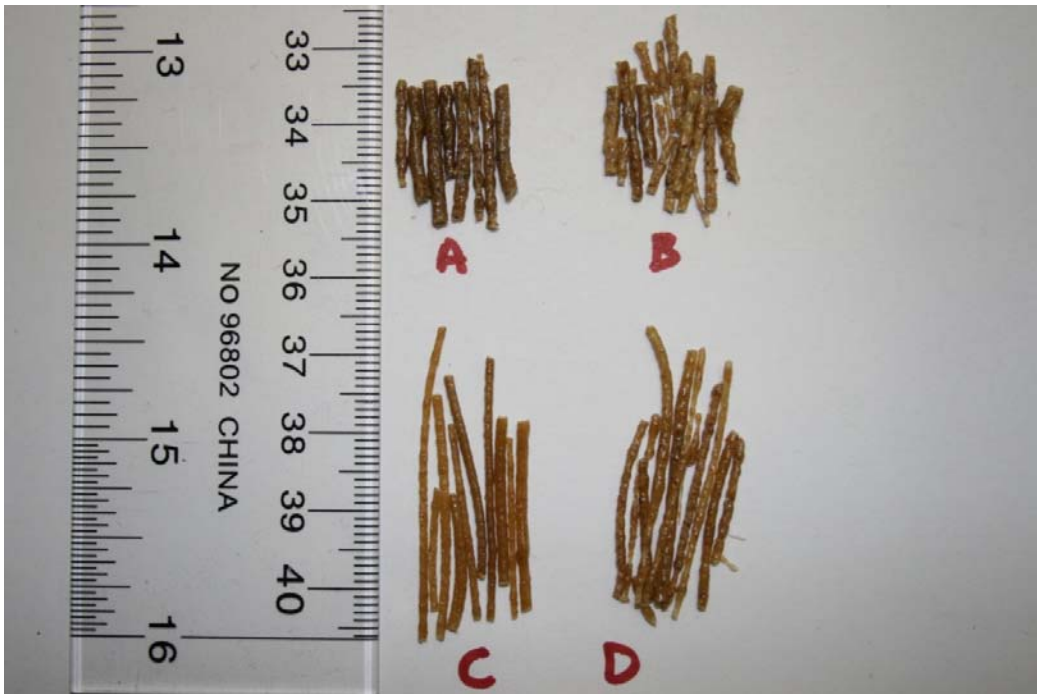

Figure 99: Extruded Composites samples A = As Is_Ex, B = Alk_ Ex, C = Octyl_Ex and D = Ureiodo+7-Octenyl_Ex.

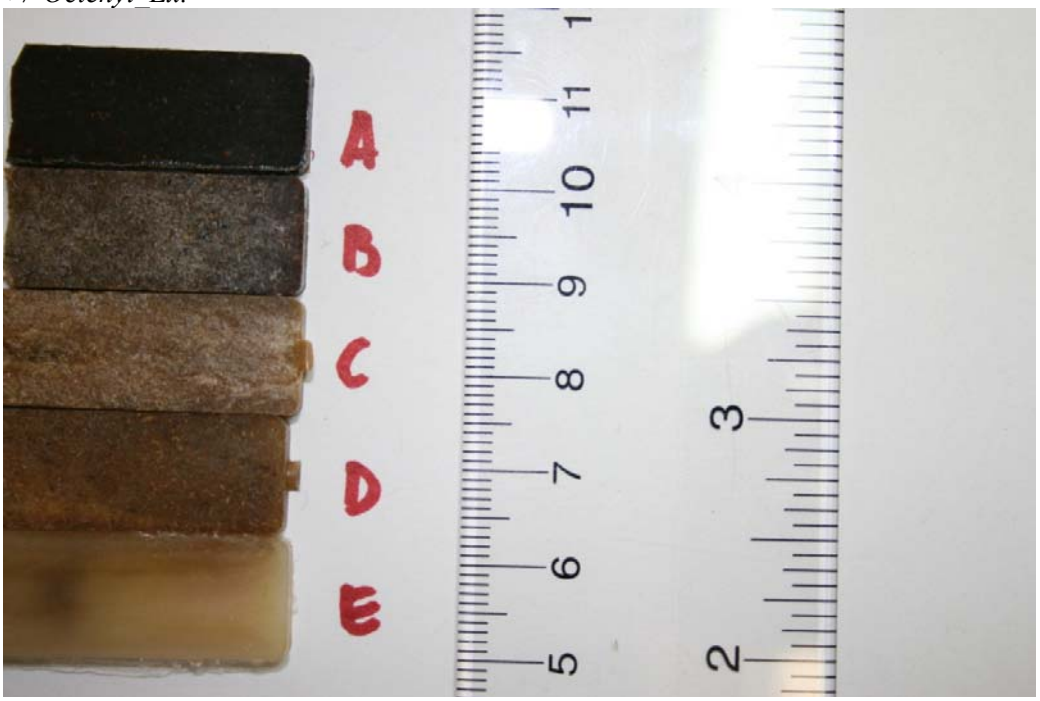

Figure 100: Injected Composites samples A = As Is_Inj, B = Alk_Inj, C = Octyl_Inj, D = Ureiodo+7-Octenyl_Inj and E = PA-6_Inj.

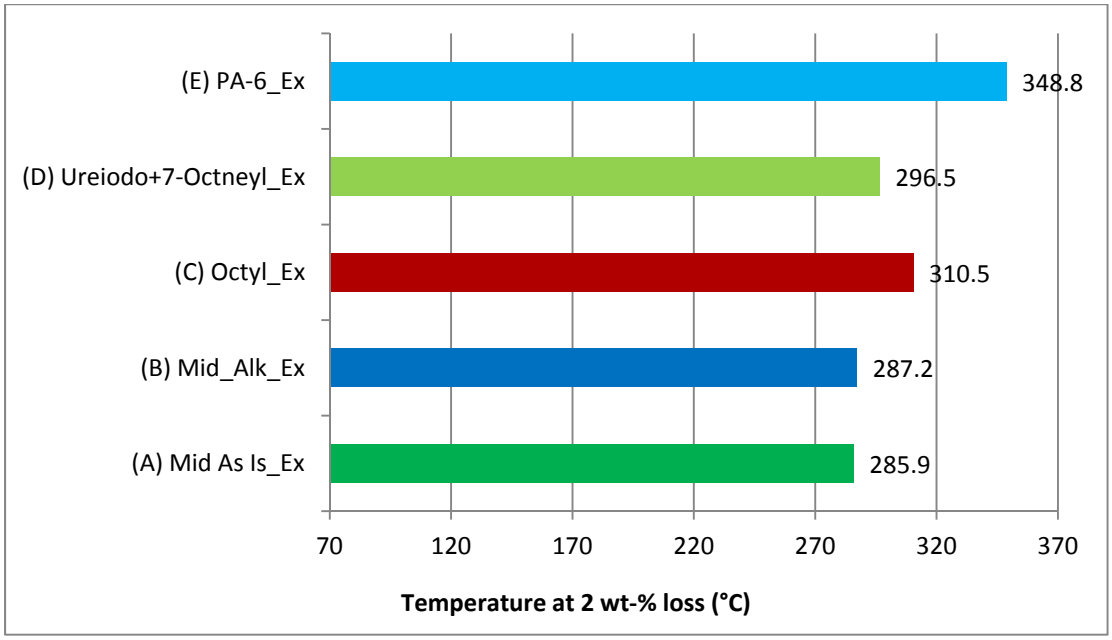

Figure 101: Temperature at 2 % weight loss for the Extruded composites set of experiments obtained from non-isothermal TGA analysis (10 °C/min heating rate and nitrogen atmosphere).

A similar behavior is observed among the injected WS/PA-6 composite samples. For example, the injected composite of untreated wheat straw and polyamide-6 (sample A in Figure 100 - As Is_Inj) displays a very intense black color indicating severe thermal degradation of the untreated WS fiber (Figure 100). On the other hand, injected composite samples with silane treated wheat straw (samples C and D in Figure 100 -Octyl_Inj and Ureiodo + 7-Octenyl_Inj, respectively) present a light golden color indicating lower thermal degradation of the silane treated wheat straw fiber samples (Figure 100).

The results of change in color are in agreement with the thermal stability presented by the injected composite samples. For example, the injected composite sample using untreated wheat straw (As Is_Inj in Figure 102) shows the poorest thermal stability (i.e., $T_{2\%}$ = 301.8 °C) and the darkest color (sample A in Figure 100). On the other hand, the injected composite containing silane treated wheat straw (Octyl_Inj in Figure 102) has the best thermal stability (i.e., $T_{2\%}$ = 328.2 °C) and exhibits a very light golden color (sample C in Figure 100).

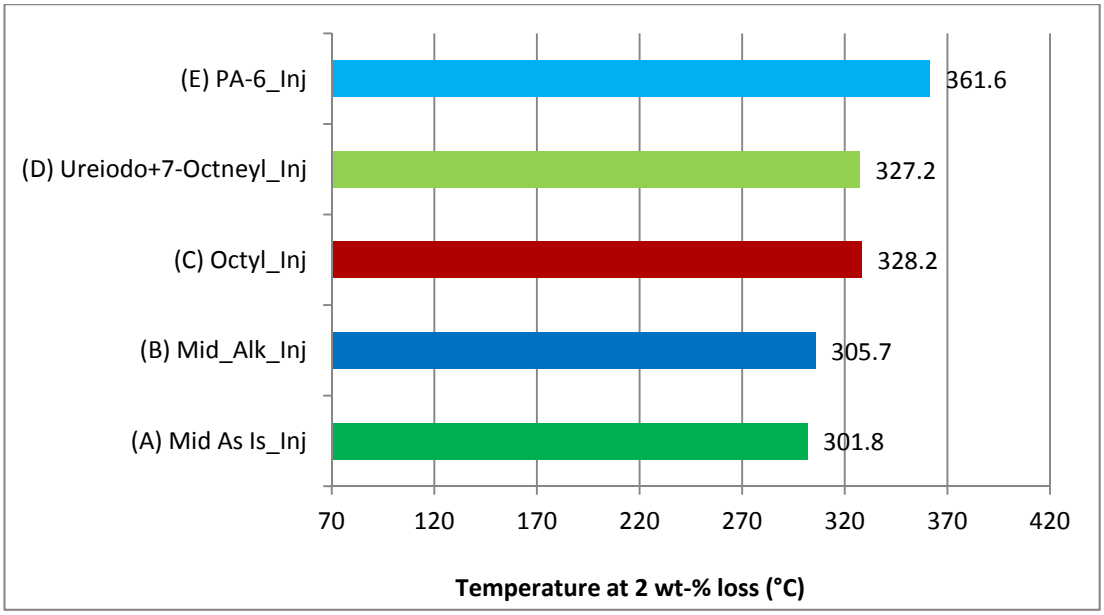

Figure 102: Temperature at 2 % weight loss for the Injected Composites set of experiments obtained from non-isothermal TGA analysis (10 °C/min heating rate and air atmosphere).

It is important to highlight that the color changes are more apparent for injection molded samples than in extruded samples. Figure 103 shows that the color of the untreated WS/PA-6 composite (sample A in Figure 103) goes from a medium dark yellow color when extruded into linear threads to very dark color after being injected into rectangular bar. Similar behavior is observed for alkali treated WS/PA-6 composite (sample B in Figure 103) which goes from medium yellow color (extruded linear threads) to a dark brown color (injected rectangular bar). In the case of silane treated WS/PA-6 composite samples, the change in the color after injection molding is less pronounced suggesting smaller thermal degradation of the silane treated wheat straw fiber samples than in the untreated or alkali treated wheat straw fiber samples.

Moreover, it is interesting to notice that even pure polyamide-6 becomes darker after the injection molding even without addition of any wheat straw fiber. Figure 103 shows that extruded polyamide-6 (linear threads) are completely white, whereas injected polyamide-6 (rectangular bar) presents a yellowish color. This color change is a sign of thermal degradation of the polymer itself during the production of injected bars.

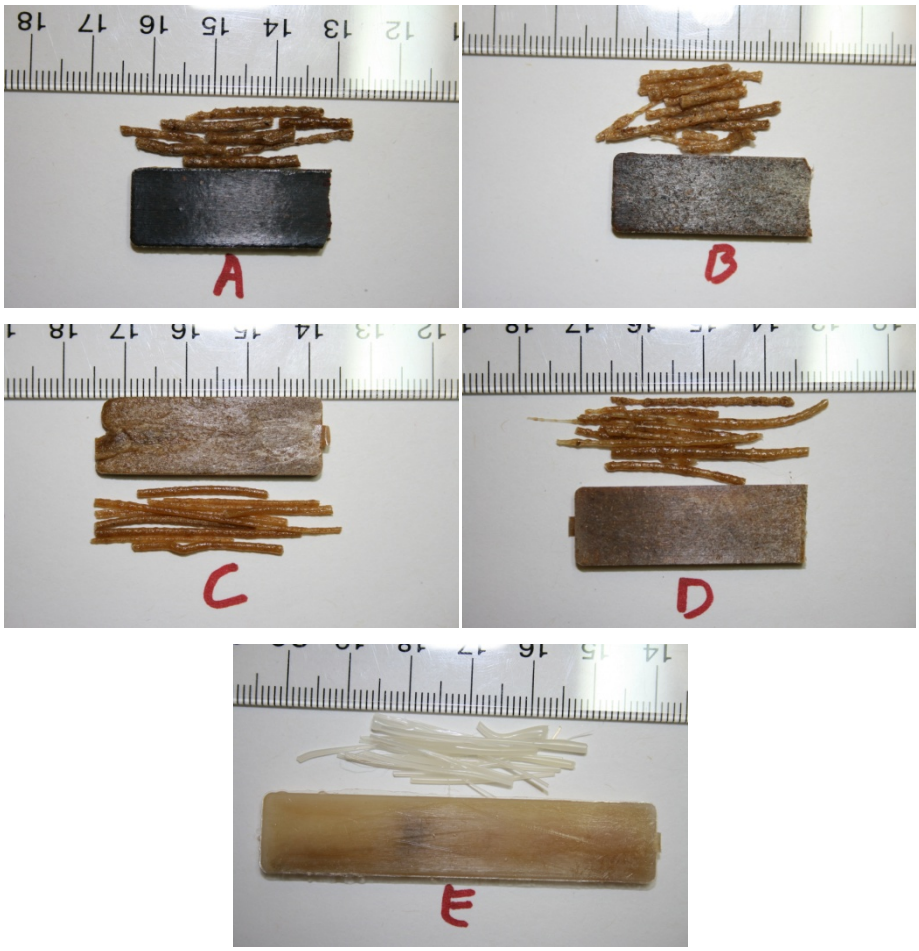

Figure 103: Extruded and injected composite samples are displayed together. Samples A = As Is_Ex and As Is_Inj, B = Alk_Ex and Alk_Inj, C = Octyl_Ex and Octyl_Inj, D = Ureiodo+7-Octenyl_Ex and Ureiodo+7-Octenyl_Inj and E = PA-6_Ex and PA-6_Inj.

It is important to note that the isothermal TGA results (Figure 104 and Figure 105) do not show a significant difference between the extruded and injection molded samples regardless of the type wheat straw sample used, i.e., silane treated, alkali treaded or untreated wheat straw samples.

More precisely, among all the extruded WS/PA-6 composite samples, the difference was not greater than 1 % between the weights of the samples after 10 minutes of exposure to 250 ^{o}C (Wt250). For example, after 10 minutes of exposure to 250 ^{o}C, the extruded composite sample Octyl_Ex retains 97.4 % of its initial weight whereas the extruded composite sample As Is_Ex exhibits 96.9 % of its initial weight (Figure 104). There is a difference of only 0.5 % between these two samples.

Similar behavior was observed for the injection molded samples. The molded samples Octyl_Inj and As Is_Inj have 98.1 % and 97.4 % of their initial weight, respectively, after 10 minutes of exposure to 250 ^{o}C (Figure 105). These samples have a weight difference of only 0.7 %.

It is possible that, after extrusion, the polymer (containing antioxidant) acts as a barrier protecting the wheat straw fiber against thermal degradation. This way, during isothermal TGA analysis (250 ^{o}C), the thermal degradation of the extruded and molded WS/PA-6 composites was significantly smaller than the thermal degradation observed for the sole wheat straw samples.

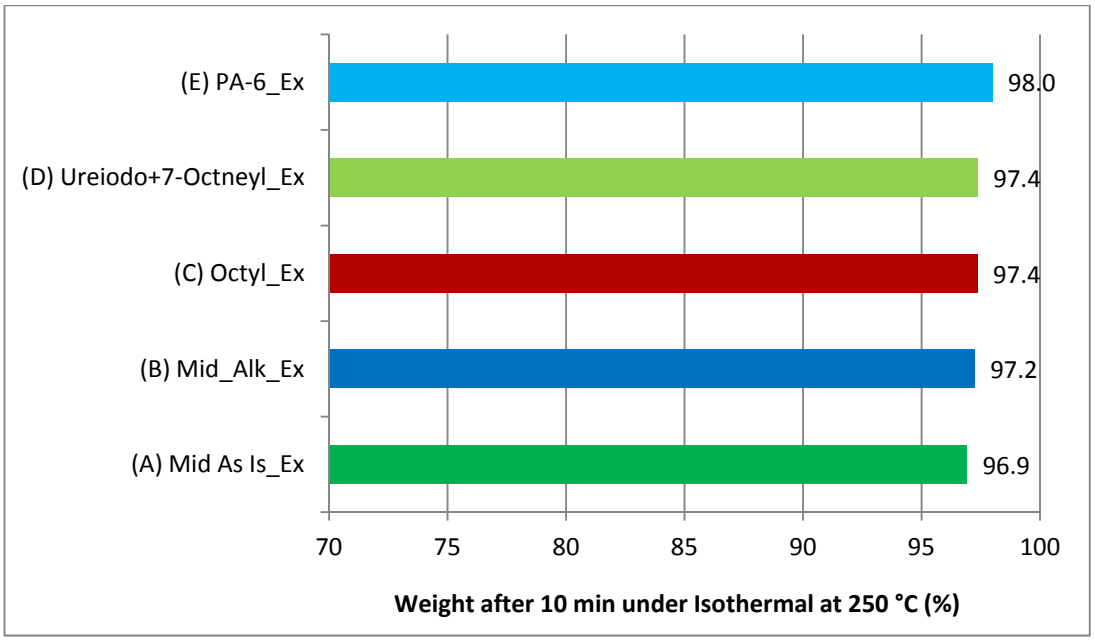

Figure 104: Percentage of the initial weight left after isothermal analysis (250 °C and nitrogen atmosphere) of the Extruded Composites set of experiments.

Furthermore, polyamide-6 represents 85 % of the WS/PA-6 composites and has a greater thermal stability than wheat straw samples which probably contributes to reduce the thermal degradation of the composite in comparison with wheat straw samples alone.

The results of the TGA analysis demonstrate that the composite samples with higher thermal stability have the lighter colors (instead of darker) after either extrusion or injection molding steps. In

addition, the extruded and injection molded composites containing silane treated wheat straw samples showed significantly smaller thermal degradation than those utilizing untreated and alkali treated wheat straw samples. It is possible to conclude that the chemical treatment of the straw fibers has a great potential for developing grades of fiber for applications in composites with engineering plastics.

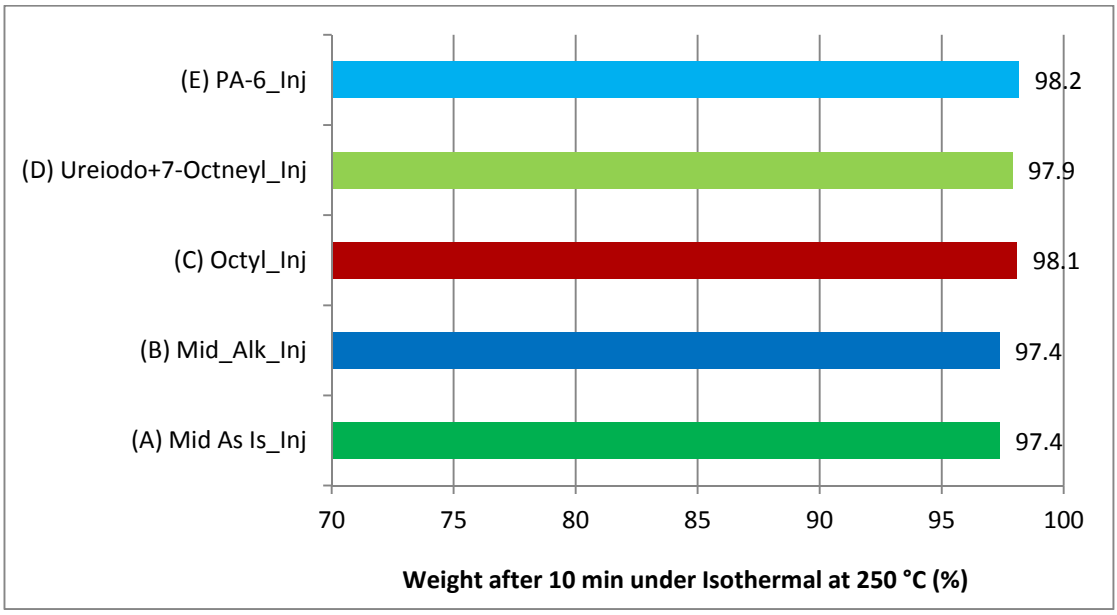

Figure 105: Percentage of the initial weight left after isothermal analysis (250 °C and nitrogen atmosphere) of the Injected Composites set of experiments.

6.4 The Effect of Silane Treatment on the Wheat Straw Samples and Mechanical Properties of Wheat Straw/Polyamide-6 Composites

The Mechanical Set of experiments has two main goals (Figure 106). The first one is to investigate the effect of the alkali and silane treatments on the chemical and physical properties of the straw

fiber, and the second one is to evaluate the effect of adding straw fiber treated with silane to the mechanical properties of polyamide-6 and its composites.

The changes on the chemical properties of the wheat straw fiber were investigated with the assistance of chemical composition and Fourier Transform Infrared (FTIR) spectroscopy analyses whereas changes on the physical properties were revealed by Scanning Electron Microscopy (SEM) and Wide angle X-ray diffraction (WXRD) tests.

The mechanical properties of the WS/PA-6 composites that were evaluated are the flexural modulus, flexural strength, and Izod impact energy. These properties were studied using the three point bending and Izod impact tests according to the ASTM international standards. These tests are described in detail in the next section.

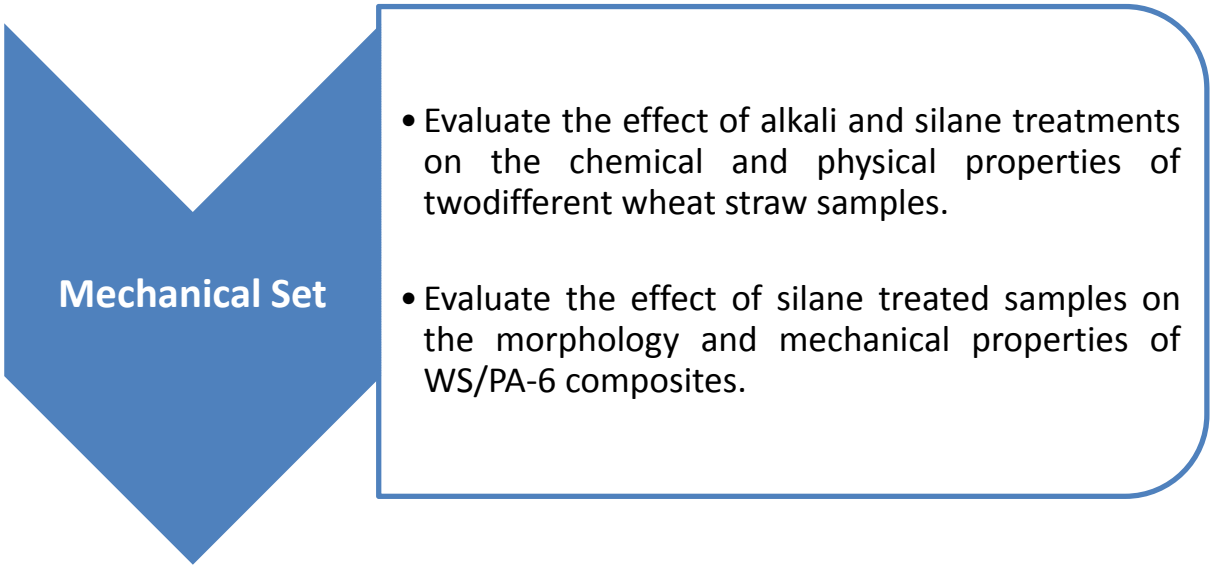

Figure 106: Diagram describing the main objectives of the Mechanical Set of experiments.

6.4.1 Silane Treatment

The alkali treatment applied to the wheat straw samples followed the procedure described in the previous section of this chapter (Thermal Set). Similarly, the procedure presented in the Thermal Set

was utilized here to perform the silane treatment of alkali treated wheat straw samples. The differences between the silane treatment used here and the one in the previous section are highlighted in Table 31. Two types of wheat straw fiber (Mid and Large) were utilized here compared to the one type (Mid) in the previous Thermal Set. The silane treatment time was reduced from 6 hours (Thermal Set) to 5 hours for this set (Mechanical Set).

In addition, two different combinations and concentrations of silane modifiers were tested in this section (Mechanical Set) as described in Table 32.

Table 31: Silane treatment parameters employed for Thermal and Mechanical Sets in comparison with Chapter 5.

Label	Wheat Straw (grams)	Wheat Straw Type	Methanol (ml)	Treatment Time (hours)	Concentration (mmole.g^{-1})
Chapter 5	0.25	Mid	50	8	1.25
Thermal Set	20	Mid	450	6	1.75 – 2.19[a]
Mechanical Set	20	Mid, Large	450	5	1.25 – 2.50[b]

a: see Table 29 for details; b: see Table 32 for details.

The first combination of silane modifiers included one alkoxysilane and two chlorosilane modifiers. As already mentioned, ureiodoalkoxy silane modifier is utilized as coupling agent for polyamides. The two chlorosilane modifiers, especially tetrachlorosilane, are extremely reactive towards hydroxyl groups and can help to hydrolyze the alkoxysilane. They are also known for promoting the formation of oligomeric (crosslinked) silanol structures.

Table 32: Silane treatment parameters used during Mechanical Set: labels, silane modifiers and concentrations, and type of wheat straw.

Label	Silane Modifiers	Reactants	Concentration ($mmole.g^{-1}$)	Wheat Straw Type
Mid_Sil_Mix	Ureiodo		1.25	20g Mid
	Octyl		0.625	
	Tetra		0.625	
		H_2O	5.0 g	
		Butylamine	5.0 g	
Large_Sil_Chloro	Octyl	None	0.625	20g Large
	7-Octenyl		0.625	
	Tetra		0.8	

For the first silane treatment (as described by Figure 107 on the left-hand side) the solution containing wheat straw, the alkoxysilane and two chlorosilane modifiers was stirred for 0.5 hour without heating in order to promote the hydrolysis of both types of silane modifiers and allow the reaction between the hydrolyzed chlorosilane and the wheat straw fiber. Then, a stoichiometric amount of water was added to the solution and heating was applied in order to further stimulate the hydrolysis of the alkoxysilane modifier. After 4.5 hours of reaction, butylamine was added to the solution with the objective of promoting the self condensation of the silane modifiers specially the ones attached to wheat straw. This could help to form a silane polymeric layer (polysiloxane) in the surface of the straw fiber and prevent this polymeric layer from being leached out during washing and filtering steps.

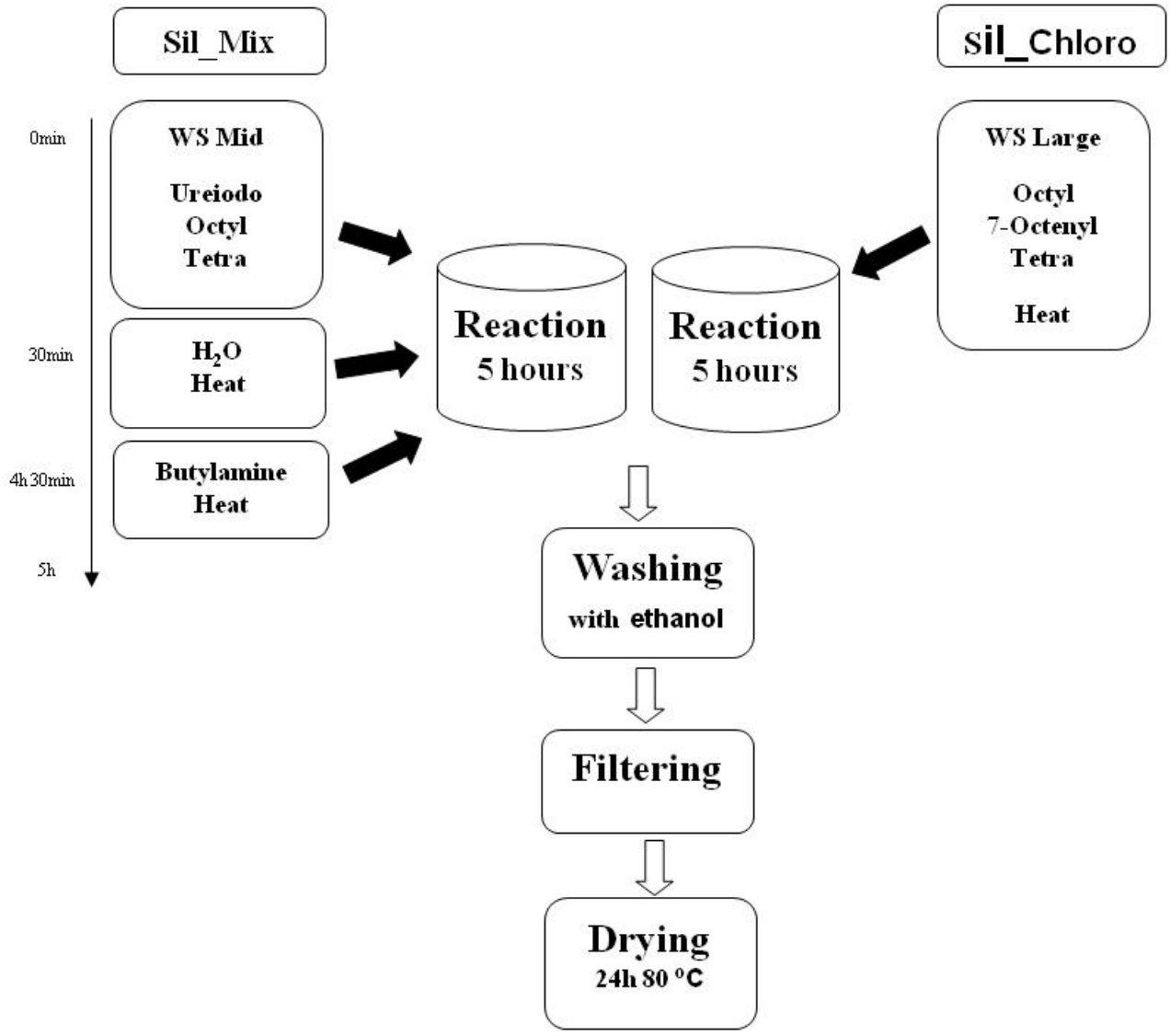

Figure 107: Schematic representation of the mains steps of the two different silane treatments (Mid_Sil_Mix and Large_Sil_Chloro) applied to wheat straw fiber.

The second silane treatment had three different chlorosilane modifiers (as described by Figure 107 on the right-hand side). For this combination, all the components (3 chlorosilane modifiers, wheat straw and methanol) were added to the system before starting the silane modification reaction (Figure 107). Unlike the first silane treatment (Mid_Sil_Mix), during the second one (Large_Sil_Chloro)

heating was applied from the beginning of the silane reaction and neither water nor butylamine were added to the system.

6.4.2 Fabrication of Wheat Straw/Polyamide-6 Composite

6.4.2.1 Extrusion

The same extrusion procedure described in the previous section (Thermal Set) was employed here to prepare the WS/PA-6 composites. In contrast with Thermal Set, the processing conditions of the extruder were set at 235 ^{o}C and 100 rpm. The increase in the screw speed (from 60 to 100 rpm) was adopted to decrease the residence time of the wheat straw inside the extruder during the composite preparation and therefore reduce the thermal degradation of these fibers.

Similar to the previous set of experiments, initially a masterbatch of polyamide-6 and antioxidant (without wheat straw fiber) was prepared in order to achieve an homogeneous dispersion of the antioxidant into the polymer matrix. After that, all the components of the composite (wheat straw fiber, masterbatch and neat polyamide-6) were hand mixed to get a uniform mixture. Finally, this mixture was fed into the extruder.

Seven different formulations were prepared according to Table 33. The same amounts of wheat straw, polyamide-6 and antioxidant (15, 84.9 and 0.1 wt-%, respectively) were used from run #1 to run #6. The main difference between these composites was the type of wheat straw utilized. While untreated, alkali and silane treated Mid wheat straw were used from run #1 to run #3, untreated, alkali and silane treated Large wheat straw were employed during runs #4 to 6. In the case of run #7, only polyamide-6 and antioxidant were utilized.

The extruded composites (Figure 108) were cut into smaller pieces by scissors and then were used to obtain bars using injection molding.

Table 33: Amount of the components utilized during extrusion of the WS/PA-6 composites. Label, wheat straw type, chemical treatment and compounding formulation for each run.

Run #	Label	WS[1] Type	WS Chemical Treatment	WS (wt-%)[2]	PA-6[4] (wt-%)	Antioxidant (wt-%)
1	Mid		None			
2	Mid_Alk	Mid	Alkali	15	84.9	0.1
3	Mid_Sil_Mix		Silane_Mix[3]			
4	Large		None			
5	Large_Alk	Large	Alkali	15	84.9	0.1
6	Large_Sil_Chloro		Silane_Chloro[3]			
7	PA-6	None	None	0	99.9	0.1

1: wheat straw; 2: weight percentage; 3: see Table 32 for detail; 4: Polyamide-6

Figure 108: WS/PA-6 composites strands obtained after extrusion with (a) untreated, (b) alkali treated and (c) silane treated Mid wheat straw.

6.4.2.2 Injection Molding

The injection molding was carried out with the assistance of our industrial partner Ford Motors Company in Dearborn, MI. The equipment used was the injection moulding machine Mini-Jector shown in Figure 109. This injection machine allowed the use of higher injection pressures in comparison with the previous laboratory injection machine (Ray-Ran RR/TSMP). In addition, it allowed different temperatures to be set in two different zones of the barrel and in the injection nozzle. This feature permits reduction of the temperature in the initial barrel zone and therefore reduces the thermal degradation of the wheat straw during the injection of the composites. The extruded pellets were fed into the injection machine. The temperature of the two barrel zones were set at 240 and 249 ^{o}C whereas the nozzle was at 253 ^{o}C according to Table 34.

After the composite was completely melted, a pressure of 750 psi was applied by a pneumatic piston and the melted composite was injected into the metallic mold. The temperature of the mold was approximately 30 ^{o}C. This pressure was held for 15 seconds for each bar to assure that the mold was completely filled. The composite was allowed to cool for 6.2 seconds and then automatically removed from the mold.

The resulting injected bars (Figure 110) were cut into half to achieve the proper dimensions (3.2 ± 0.2 mm x 12.5 ± 0.2 mm x 62 ± 0.2 mm) for mechanical testing according to the ASTM test methods for plastic composites (ASTM D 790 -07 D and ASTM 256 - 06a).

In addition, before mechanical testing, the injected bars were submitted to a procedure called annealing. Annealing is performed in order to erase the thermal history created during the cooling step of the molding process. Differences in cooling rates can lead to WS/PA-6 composites with different degrees of crystallinity which affects the mechanical properties of the composite. Therefore, it is important to remove the effect of differences in cooling rates before performing mechanical testing of thermoplastic composites.

During the annealing, injected bars were kept under vacuum (pressure of -10 psi) and temperature of 100 °C for 1 hour (Ramazani and Mousavi, 2005).

Table 34: Temperature profile employed during the injection molding of the WS/PA-6 composites.

Temperature Profile for Injection Molding (°C)			
Rear Zone	Front Zone	Nozzle	Mold Tool
240	249	253	30

Figure 109: Mini-Jector injection moulding machine (Model 55 – Wasp Series) used to obtain the injected WS/PA-6 composite bars.

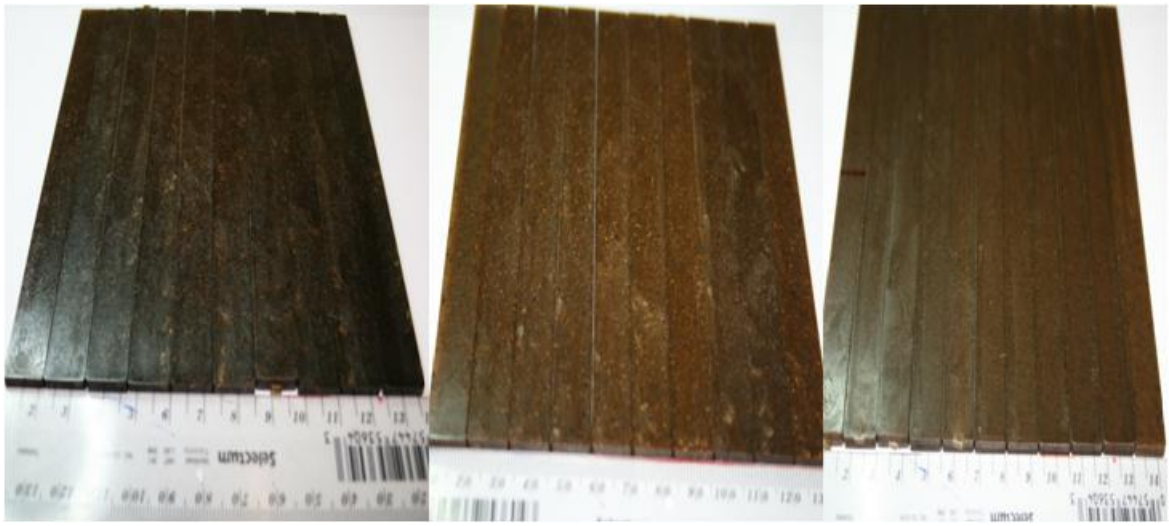

Figure 110: WS/PA-6 composite test bars obtained from injection molding process.

6.4.3 Characterization Methods

6.4.3.1 Fourier Transform Infrared (FTIR) Spectra

The Fourier-transform infrared (FTIR) analysis was carried out with the assistance of a Bruker Tensor 27 FT-IR analyzer. The samples were ground to a fine powder and mixed with potassium bromide (KBr). This mixture was compressed into thin discs using a hydraulic press. The sample/KBr discs were used to obtain IR spectra in the spectral range of 400-4000 cm^{-1} with resolution of 4 cm^{-1} and accumulation of 32 scans.

6.4.3.2 Chemical Composition Analysis

Chemical composition analysis of wheat straw as received, alkali and silane treated was carried out by AgriFood Laboratories located in Guelph, Ontario. A well-know method developed by Van Soest (Van Soest, 1963; Van Soest, 1968) was utilized to estimate the cellulose, hemicellulose and lignin content of the samples. The test uses two main indicators: Neutral Detergent Fiber (NDF) and Acid Detergent Fiber (ADF).

Neutral Detergent Fiber (NDF) indicates the total amount of cellulose, hemicellulose and lignin present in the natural fiber, that is, 100 % of cellulose, hemicellulose and lignin are recovered after NDF method; whereas during the second measurement (ADF) only cellulose and lignin are recovered, excluding hemicellulose. The subtraction of NDF and ADF indicators provides a good estimation of the hemicellulose content in the fiber.

Both Neutral Detergent Fiber (NDF) and Acid Detergent Fiber (ADF) are based on single extraction of components soluble in either neutral or acid detergents in a sequential order. First, the wheat straw is boiled in a neutral detergent solution, filtered, washed, dried and weighted. The solid fraction obtained is designated as Neutral Detergent Fiber (NDF). After that, the NDF solid fraction is submitted to the same procedure but using an acid detergent solution. This time, the solid fraction recovered after the procedure is called Acid Detergent Fiber (ADF). Then, the ADF solid fraction is treated with potassium permanganate. Lignin content is equal to the solid removed during the permanganate step (Garcia et al. 1997; Schmidt et al., 2002).

6.4.3.3 Wide Angle X-ray Diffraction (WAXRD)

Wide angle X-ray diffraction (XRD) analysis was carried out in order to determine the crystallinity of untreated, alkali and silane treated wheat straw samples. It has been reported that higher cellulose crystallinity may improve the mechanical properties, i.e., tensile strength, of plant fiber (Alemdar and Sain, 2008; Rong et al., 2001).

The XRD results that is, the intensity of amorphous and cellulose peaks (I_{am} and I_{002}, respectively), were used to calculate percentage crystallinity index (CI) of the wheat straw fiber samples according to the equation below (Cao et al., 2007; Park et al., 2010). The crystallinity index represents an estimation of the crystalline material in cellulose. Samples with higher CI values have higher degrees of crystallinity.

$$CI\ (\%) = \left(\frac{I_{002} - I_{am}}{I_{002}}\right) * 100 \qquad \textit{Equation 11}$$

Where I_{002} is the maximum peak intensity of crystalline cellulose at approximately 2θ=22° and I_{am} represents the peak intensity of the amorphous materials in the fiber at approximately 2θ=18°.

The test is performed using 0.5 grams of ground wheat straw sample which is placed inside a sample holder. The samples were analyzed with a Bruker D8 FOCUS diffractometer employing Cu Kα radiation source (λ= 1.5404Å) and operating at 40 kV and 40 mA. The XRD patterns were

recorded in the range of 5 to 45 degree (2θ values) with step size of 0.05 and each step lasting 1 second.

6.4.3.4 Annealing

Prior to mechanical testing the specimens were submitted to a controlled thermal treatment where the samples were kept under vacuum (-10 psi) at 100 °C for 1 hour. The objective of this annealing treatment was to assure that all samples will present exactly the same thermal history. This way it is avoided that different processing and cooling conditions such as variations on mould temperatures influence the data obtained. Annealing is achieved by submitting the specimens to a temperature ranging between the glass transition and melting point temperatures of the polymer. The thermal energy provided allows that the polymeric chains move slowly and pack in more favorable structures. Thus, a more perfect crystalline structure with better mechanical properties will be formed. Because this process is done under vacuum, it is also an effective method for drying the samples prior to testing the mechanical properties.

6.4.3.5 Flexural Testing

Flexural properties (modulus and strength) describe the ability of a material to resist bending when force is applied. These properties are utilized in different industries (e.g., aerospace, automotive, construction etc) to select the correct materials for building parts which must support specific loads without flexing.

The flexural modulus is obtained from the inclination of the elastic region of strain-stress curve whereas, flexural strength is defined as the maximum flexural stress supported by a specimen during a flexural test. If the sample breaks during testing, the flexural stress at break will be the flexural strength of the material. For materials that deform significantly but do not break up to the 5 % strain limit, the flexural strength can be calculated using the following equation:

$$\sigma_f = \frac{3PL}{2bd^2} \qquad \textit{Equation 12}$$

Where, σ_f represents flexural stress (MPa), P is the load at a given point on the load-deflection curve (N), L is the support span (mm), b is the width of the sample tested (mm) and d is the depth of the sample tested (mm).

Flexural properties were determined using three point bend test according to ASTM D790-07 procedure A (ASTM International 2008). Figure 111 presents a schematic representation of the three point bend test which was carried out using a load cell of 5000 N. Ten (10) samples of the composite material (wheat straw/polyamide-6) and pure polyamide-6 were tested. The rectangular injected samples with approximately 3.2 ± 0.2 mm x 12.5 ± 0.2 mm x 62 ± 0.2 mm were conditioned at 23 ± 2 °C and 50 ± 5 % of relative humidity for at least 48 hours before testing. The approximate support span-to-depth ratio is 16:1. The cross head speed was 1.3 mm per min and determined according to the specific dimensions of each specimen as described in the following equation:

$$R = \frac{Z*L^2}{6d} \qquad \textit{Equation 13}$$

Where R is equal to the cross head speed (mm/min), L is the support span (50 mm), d represents the depth of the beam (3.2 mm) and Z is the rate of straining of the testing bars (mm/mm.min) which was kept equal to 0.01, as recommended in procedure A of the ASTM D790-07.

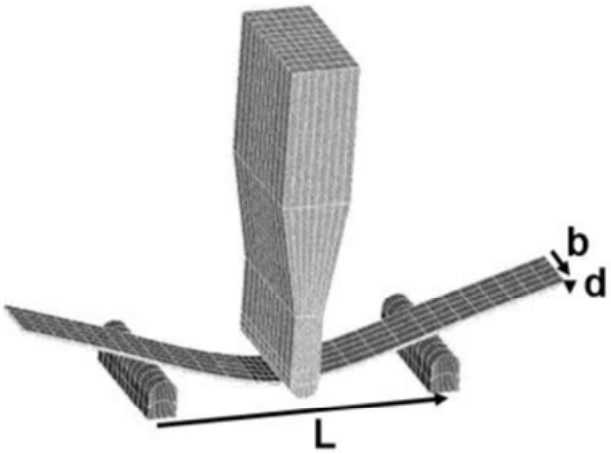

Figure 111: Schematic representation of a three-point bend test. L represents the support span (50 mm), d is the depth of the sample (3.2 mm) and b is the width of the sample (12.5 mm).

6.4.3.6 Izod Impact Testing

Izod impact test determines the energy required to break a specimen submitted to impact from a swinging pendulum. The samples were notched. The notch is utilized to induce a brittle fracture through stress concentration. The result of the impact test is usually reported in energy lost per unit of specimen thickness at the notch (e.g., J/m) and type of failure. The failure is called “complete break” when the specimen separates into two or more pieces. “Hinge break” happens when there is an incomplete break and one part of the specimen cannot support itself in less than 90 degrees when the other part is held vertically. “Partial break” occurs when there is an incomplete break which does not meet the definition for a hinge break but has fractured at least 90 % of the distance between the notch and the opposite side. The failure is named “non-break” if an incomplete break has a fracture that extends less than 90 % of the distance between the notch and the opposite side.

The impact test results indicate how tough or brittle a material is. This information is useful for product safety and liability, quality control and material selection purposes. Impact tests can be used to select the appropriate material which will support the impact energies the part can be expected to see in its lifetime. For example, certain polymeric materials are more sensitive to stress concentration and cannot be utilized in structures and designs which are submitted to high stress concentration such as sharp corners and cutouts.

Figure 112 illustrates an impact testing apparatus and the proper way to place the specimen for Izod impact testing. A Monitor Impact Tester machine (model 43-02) with a pendulum of 6.78J was utilized in this work. The specimen was clamped into the pendulum impact test fixture with the notched side facing the striking edge of the pendulum. The pendulum was released and struck through the specimen. At least 10 samples of wheat straw/polyamide-6 composites and pure polyamide-6 were tested. Dimensions of the samples were 62mm x 12.5mm x 3.2mm with a single notch of 0.25±0.05 mm and remaining width under notch of 10.16±0.05 mm. Samples were conditioned prior testing as per ASTM D256-06a.

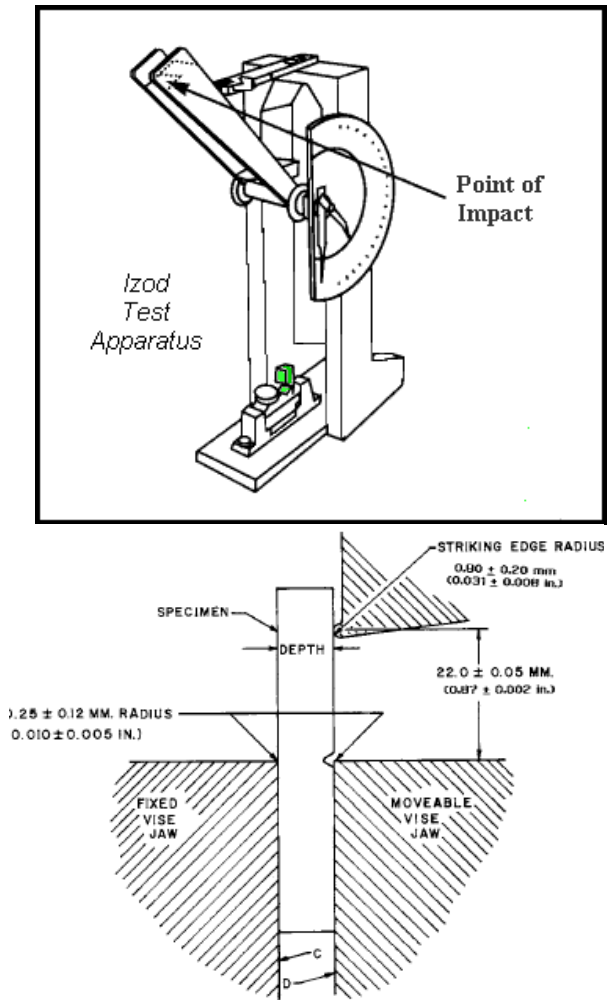

Figure 112: Examples of impact test apparatus and correct specimen clamping utilized during impact testing.

6.4.3.7 Scanning Electron Microscopy (SEM) and Energy-dispersive Spectrometry (EDS)

The morphology of wheat straw fibers and composites were investigated with a LEO 1530 field-emission scanning electron microscope equipped with Gemini field emission column (FESEM) and EDX/OIM PV9715/69 ME. Samples were placed on aluminum stubs with the assistance of double sided conductive tape. In the case of composite samples, the cross sections obtained after breaking the frozen sample in halves were utilized.

Prior to visualization with the SEM, all the samples were sputter coated for 2 minutes with gold to improve the electrical conductivity of the surface. The SEM analysis was conducted at 2.5x10-6 mbar and the current at 10 kV.

The energy-dispersive X-ray (EDX) measurements were performed for the samples and a set of X-ray maps for Si, C and O were acquired. The electron gun current was set at 20kV and the acquisition time was 2 minutes. The EDX detector and the software were from EDAX (AMETEK, Inc.).

6.4.4 Results and Discussion of the Mechanical Set

The set of experiments performed in this section, Mechanical Set, was divided into two parts. The first one (Fiber Set) was designed to investigate the effect of the alkali and silane treatments on the chemical and physical properties of wheat straw samples. The second one (Composite Set) evaluated the effect of different wheat straw treatments on the mechanical properties of the WS/PA-6 composites.

It is important to study the physical properties of the wheat straw samples because changes on the wheat straw morphology and crystallinity can affect the mechanical properties of the fiber and thereby the mechanical properties of the WS/PA-6 composite. In the same way, looking at chemical composition changes can help to understand the physical changes imposed during the alkali and silane treatments of the wheat straw samples.

6.4.4.1 The Effect of Alkali and Silane Treatments on the Chemical Properties of the Wheat Straw Samples (Fiber Set)

This section considers the chemical composition and molecular changes caused by the alkali and silane treatments on the wheat straw samples.

The chemical composition analysis of the untreated, alkali and silane treated wheat straw was performed by AgriFood Laboratories. The chemical composition analysis provides the percentage content of cellulose, hemicellulose and lignin for each one of the wheat straw samples (Figure 113 and Figure 114). In the case of Mid wheat straw sample (Mid As_Is), the percentage content of cellulose, hemicellulose and lignin obtained were 45.5, 27.0 and 9.9 wt-%, respectively. Similar

results were obtained for Large wheat straw sample (Large As_Is) which presented 45.0, 25.8 and 8.9 wt-%, of cellulose, hemicellulose and lignin, respectively.

These chemical composition results found here correspond well with the values reported by Sardashti (2009) in a different study using wheat straw from the same source (Woodrill Farms, Guelph, ON) and comparable fiber size (i.e., Mid and Large). In that study, the wheat straw with Mid size (i.e., fiber size > mesh 16) had 46.3, 28.5 and 6.9 wt-% of cellulose, hemicellulose and lignin, respectively, whereas the wheat straw with Large size (i.e., mesh 16 > fiber size > mesh 35) presented 46.6, 27.9 and 8.3 wt-% of cellulose, hemicellulose and lignin, respectively. The similarity of these two results demonstrates the reliability of the method.

Slightly different values were reported by other works. Schmidt et al., (2002) found that wheat straw from Bangor region (United Kingdom) contained 38.6 % of cellulose, 28.4 % of hemicellulose and 16.6 % of lignin. In another study, Sun et al. (1995) reported 35-40 % of cellulose, 30-35 % of hemicellulose and 14-15 % of lignin for wheat straw from Silsoe region (United Kingdom) while, Alemdar and Sain 2008 stated that wheat straw from Ontario farms (undisclosed producer) is made of 43.2, 34.1 and 22 % of cellulose, hemicellulose and lignin, respectively.

Wheat straw type (i.e., variety), maturity and growing conditions (i.e., amount of rain, temperature, type of soil etc) can account for the slight differences observed between the chemical compositions of wheat straw samples from different sources or regions.

It can also be seen from Figure 113 and Figure 114 that after the alkali and silane treatments the hemicellulose percentage is significantly decreased whereas a significant increase in the cellulose percentage is observed for both Mid and Large wheat straw. More precisely, hemicellulose was decreased by 38.7 % from 27.0 to 16.6 wt-% when Mid wheat straw is treated with alkali solution. In contrast, cellulose percentage was significantly increased by 48.3 % from 45.5 to 67.5 wt-% after alkali treatment. The increment of cellulose percentage can be explained by the removal of hemicellulose and other alkali soluble materials (e.g., silica, pectin and waxes).

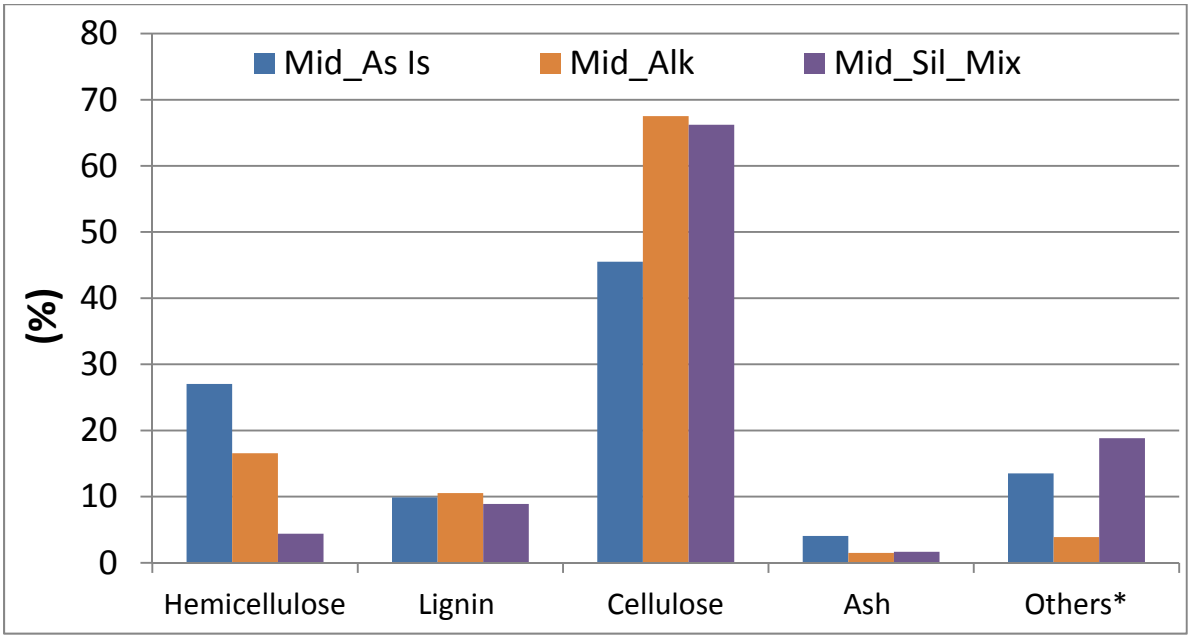

*Figure 113: Chemical composition of the untreated alkali and silane treated Mid wheat straw samples. *Others: wax, pectin, sugar and other low molecular weight compounds.*

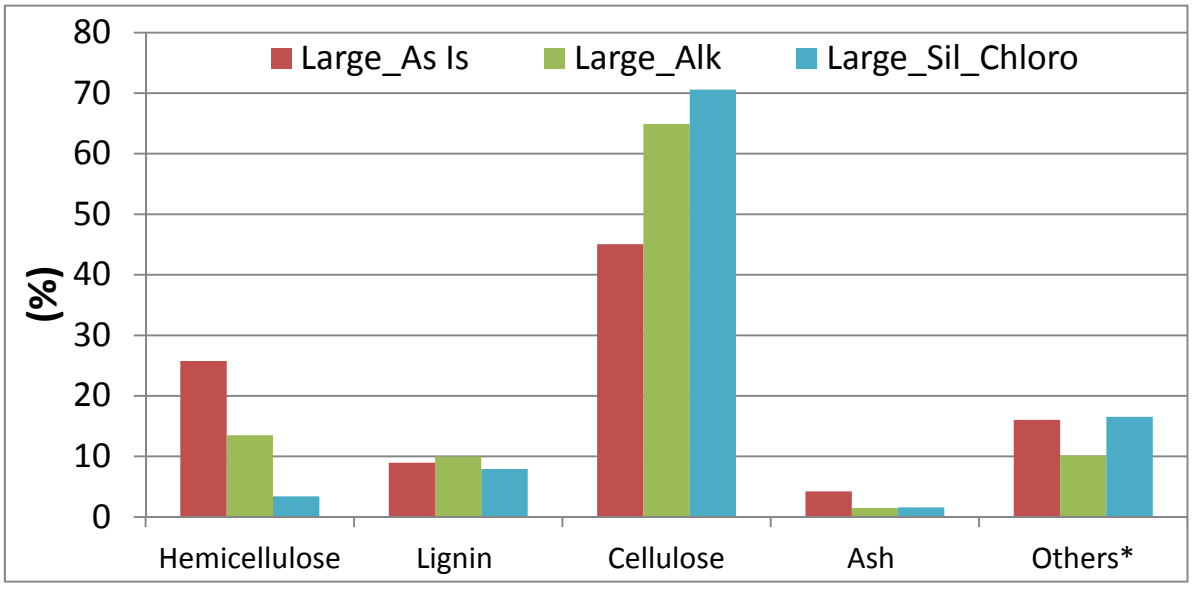

*Figure 114: Chemical composition of the untreated, alkali and silane treated Large wheat straw samples. *Others: wax, pectin, sugar and other low molecular weight compounds.*

Additional treatment with silane promotes further removal of hemicellulose which is reduced from 16.6 to 4.4 wt-%, or a total relative decrease of 83.7 % in comparison with untreated wheat straw (Mid_As Is). However, the percentage of cellulose was not affected by silane treatment. The amount of lignin was kept nearly constant after both alkali and silane treatments. In fact, lignin is very difficult to remove from plant fiber. For example, Schmidt et al. (2002) found that high temperature (185 °C) and pressure (15 bars) along with alkali treatment were necessary in order to dissolve large amounts of lignin (approximately 80 %).

Similar behavior, that is, reduction of hemicellulose and increase of cellulose percentages, was observed for Large wheat straw after alkali and silane treatments (Figure 114).

The results found in this work are consistent with the data published in the literature (Saha et al., 1991; Schmidt et al., 2002; Lawther et al., 1996; Xiao et al., 2001). It has been widely reported that alkali treatment is able to remove lignin and especially hemicellulose from plant fibers. For example, Sun et al. (1995) have found that removal of hemicellulose is significantly faster than lignin in the case of wheat straw submitted to alkali treatment (1.5 % NaOH solution at 20 °C). The authors found that after only 0.5 hour of treatment, 37.4 % of hemicellulose was removed whereas, the removal of lignin reached only 2.9 % of the original amount. In addition, with the increase of treatment time to 6 hours, the removal of hemicellulose and lignin increased to 49.8 and 20.6 %, respectively. It was also observed that lignin can be more effectively removed when higher concentration of sodium hydroxide is utilized. When the alkali concentration is increased from 0.5 to 3.0 %, the removal of lignin rose from 4.2 to 44.2 % of the initial amount, respectively.

It is well established that alkali treatment promotes the cleavage of α-benzyl ether linkages between lignin and hemicellulose, and ester bonds between hydroxycinnamic acids (i.e., p-coumaric and ferulic acids) and hemicellulose and/or lignin (Lawther et al., 1996; Xiao et al., 2001). However, reticulation between the aromatic rings of lignin makes it insoluble in almost all solvents and thereby much harder to extract or separate from hemicellulose and cellulose (Lawther et al., 1996).

Furthermore, the silane treatment caused further extraction of hemicellulose (from 16 to 4 wt-%) due to the higher temperature (around 65 °C, the boiling temperature of the solvent) and agitation applied during silane treatment. It is generally accepted that heat can induce more extensive and fast extraction of hemicellulose. Sun et al. (1995) observed larger removal of hemicellulose when temperature was increased during alkali treatment of wheat straw. Increasing the treatment

temperature from 20 to 60 °C caused the removal of hemicellulose to rise from 49.8 to 74.7 % of the initial amount. Therefore, the reaction conditions (i.e., higher temperature and agitation) utilized during silane treatment can be accounted for the additional extraction of hemicellulose (from 16 to 4 wt-%) observed in this work.

Further evidence of changes in the chemical composition of wheat straw fiber due to alkali and silane treatment can be obtained from the Fourier Transform Infrared (FTIR) spectroscopy analysis.

Figure 115 shows the FTIR spectra of Mid and Large wheat straw samples highlighting the fingerprint region located between 1800 and 800 cm^{-1}. This region contains the most important characteristic peaks of lignin, hemicellulose and cellulose. For example, the absorption bands at wavenumber of 1600, 1510, and 1265 cm^{-1} are attributed to the C=C stretching vibrations of the benzene ring occurring in lignin (Muller et al., 2003; Panthapulakkal and Sain, 2006; Hon and Chang, 1984). Hemicellulose is identified by the characteristic peak between 1720 and 1740 cm^{-1} which represent carboxyl groups, C=O (Hon and Chang, 1984; Panthapulakkal and Sain, 2006). In the same way, characteristic absorption bands of cellulose are observed at 1375, 1160, 1032-1056 and 895 cm^{-1} and are credited to the aliphatic C-H stretching in methyl and phenol OH groups, C-O-C stretching in pyranose rings and C=O stretching in aliphatic groups and C-O stretching, respectively (Chen et al., 2010; Fackler et al., 2010; Pandey and Pitman, 2003).

Molecular and chemical composition changes in the wheat straw samples can be investigated by observing variations in the intensity of these characteristic absorption bands.

A close up look of the absorption bands of hemicellulose (1720-1740 cm^{-1}) and lignin (1510 cm^{-1}) is provided in Figure 116. It is clear that the intensity of the hemicellulose and lignin peaks has systematically decreased as untreated wheat straw samples (Mid_As Is and Large_As Is) are submitted to alkali and then silane treatments.

In fact, it appears that the characteristic peak of hemicellulose between 1740 and 1720 cm^{-1} has almost disappeared after alkali treatment of Mid and Large wheat straw samples. The same peak also presented significant intensity reduction in the case of silane treated wheat straw samples (Figure 116). These observations indicate that the structure of hemicellulose molecules has been subjected to significant chemical degradation especially after alkali treatment.

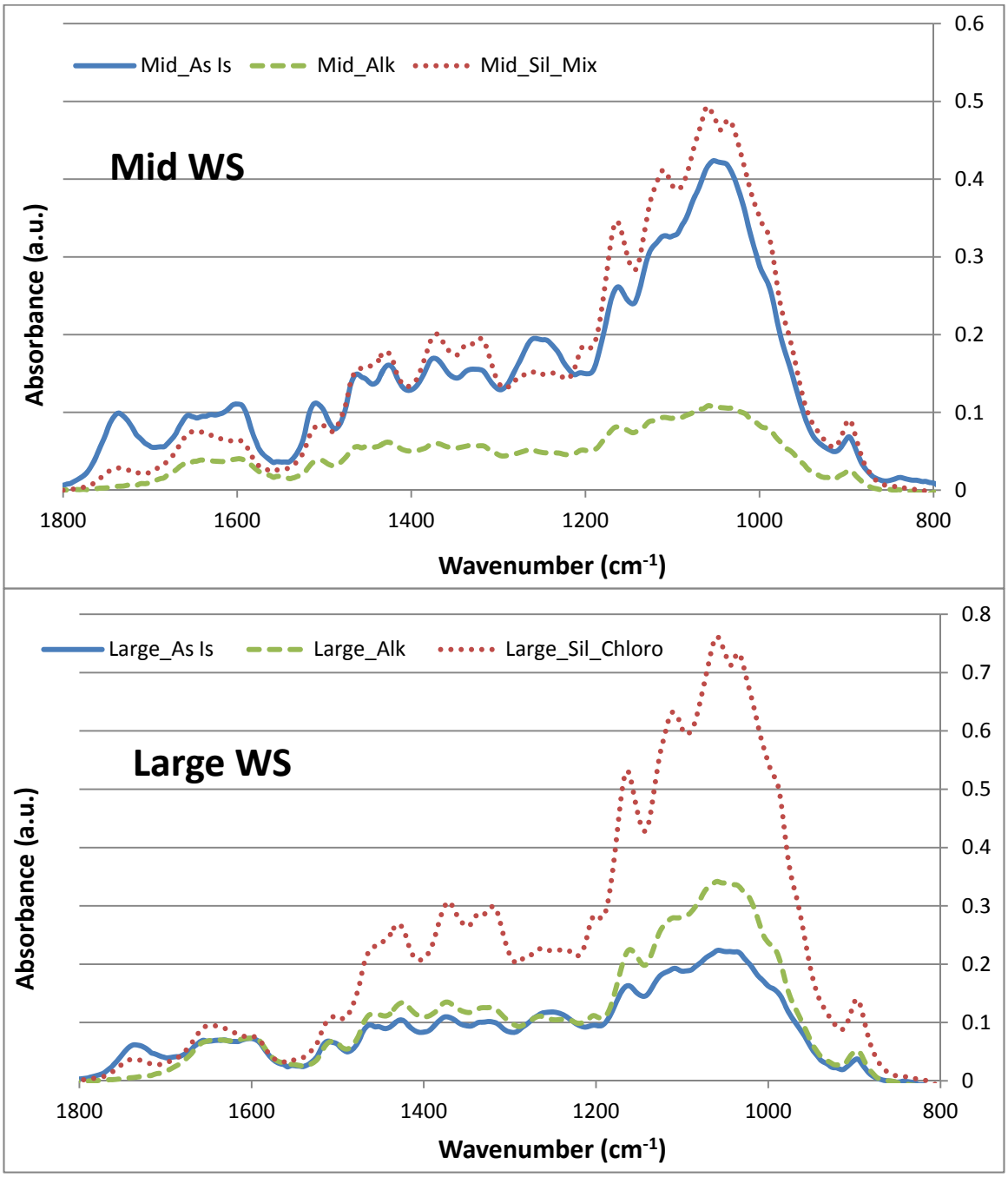

Figure 115: Infrared spectra of untreated, alkali and silane treated Mid (A) and Large (B) samples.

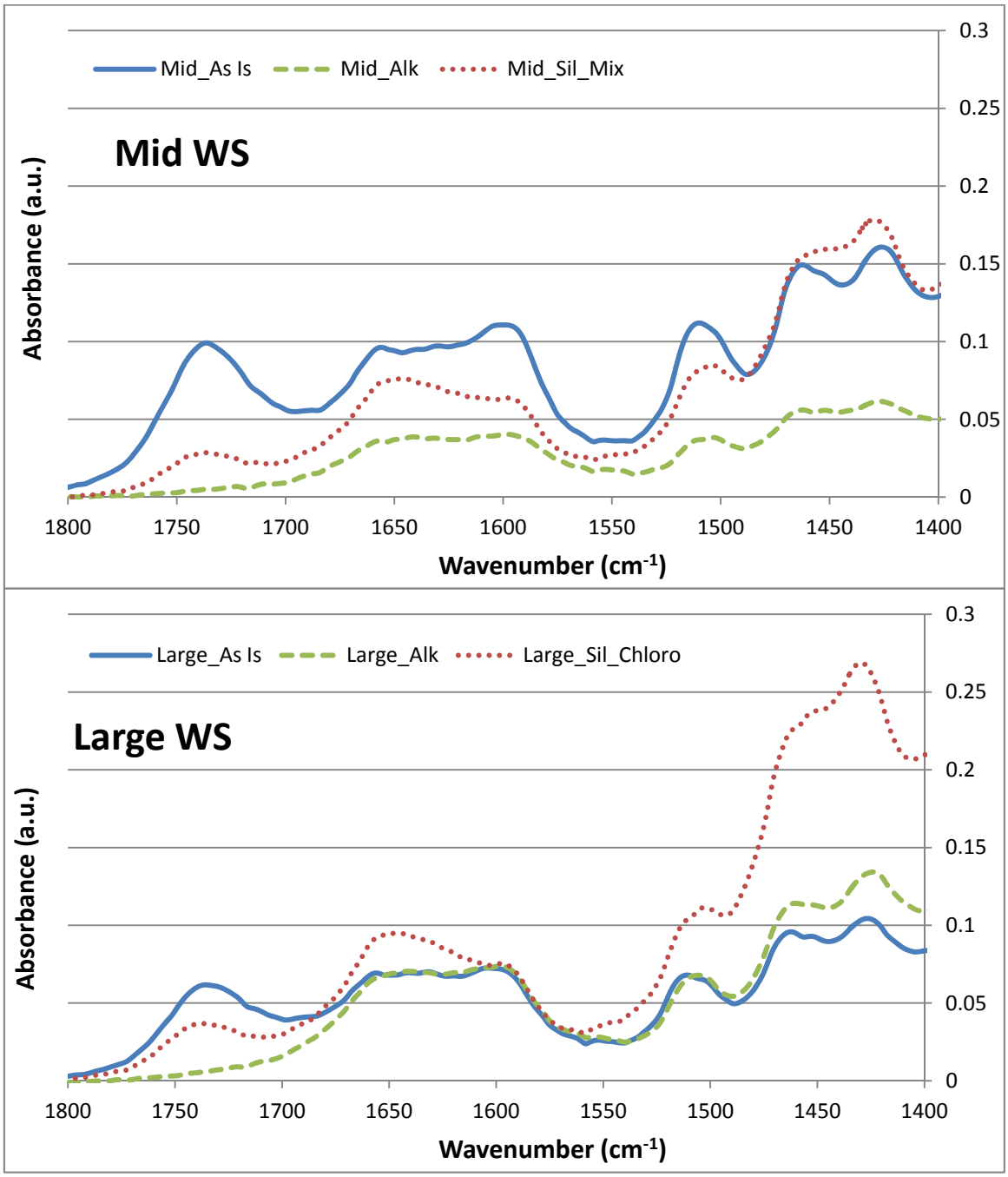

Figure 116: FTIR spectra showing the "fingerprint region" of the untreated, alkali and silane treated Mid (top) and Large (bottom) wheat straw samples.

On the other hand, even though the intensity of the characteristic peak of lignin had decreased upon alkali and silane treatments, this reduction was considerably smaller than in the case of hemicellulose.

However, it is important to highlight that only qualitative conclusions can be drawn from the changes in the intensity of the hemicellulose peak of two different wheat straw samples. The peak intensity depends on the sample mass and thickness of the potassium bromate (KBr) disc utilized during FITR analysis. Increasing the sample mass utilized for FTIR analysis increases the intensity of all peaks in this FTIR spectrum.

In order to compare two samples without the interference of these factors, the ratio between two peaks of the same FTIR spectrum is generally used. In this case, the intensity of the peak of interest (hemicellulose or lignin) is divided by the intensity of an internal reference peak from the same FTIR spectrum following the standard procedure reported in the literature (Pandey and Pitman, 2003; Pandey, 2005).

The cellulose peak at 1160 cm^{-1} was utilized as internal reference because the intensity of this peak is not significantly affected by alkali and silane treatments (Pandey and Pitman, 2003; Pandey, 2005).

In this way, it is possible to determine the rate of hemicellulose and lignin decay for each wheat straw sample and also compare the variation in the hemicellulose and lignin percentages between two different wheat straw samples by looking at the relative changes in the ratios of hemicellulose and lignin with the standard reference.

Also, the ratio between the intensities of the hemicellulose peak (1740 and 1720 cm^{-1}) and the standard peak (1160 cm^{-1}) is called here simply hemicellulose ratio. Similarly, the ratio between the intensities of the lignin peak (1510 cm^{-1}) and the standard peak are referred to as lignin ratio.

Figure 117 shows the hemicellulose ratios for untreated, alkali and silane treated wheat straw samples. It can be seen that hemicellulose decay is higher for alkali than silane treated wheat straw samples compared to untreated wheat straw. The hemicellulose ratio (Figure 117 -top) was decreased to zero after alkali treatment of Mid and Large wheat straw samples.

This is in agreement with the almost complete disappearance of the hemicellulose peak observed in the FTIR spectra (Figure 115 and Figure 116).

However, the chemical composition results (see Figure 113 and Figure 114) showed that hemicellulose was not completely removed but rather significantly reduced after the alkali treatment.

In agreement with that, after alkali and then silane treatments, the wheat straw samples (Mid_Sil_Mix and Large_Sil_Chloro) still contain small amounts of hemicellulose as indicated by FTIR (Figure 117 - top) and chemical composition (see Figure 113 and Figure 114) results. For example, FTIR results show that the hemicellulose ratio was 0.13 and 0.11 for the silane treated Mid and Large wheat straw samples, respectively.

These observations suggest that partial rather than complete removal of hemicellulose has occurred upon silane and alkali treatments.

Figure 117 (bottom) presents the changes in the lignin ratios of untreated, alkali and silane treated wheat straw samples. Overall, there is a reduction in the lignin ratio after alkali and silane treatment of Mid and Large wheat straw samples. According to the FTIR results, the lignin reduction after alkali treatment is higher for the Large wheat straw than the Mid wheat straw. For example, lignin ratio is dropped only 0.2 from 0.9 to 0.7 when Mid wheat straw is submitted to alkali treatment while, a bigger decrease (0.5, from 1.6 to 1.1) is observed upon alkali treatment of the Large wheat straw. A similar behavior was observed for silane treated samples. For example, the largest reduction in lignin ratio was observed after silane treatment of the Large (from 1.1 to 0.35) rather than Mid (from 0.7 to 0.2) wheat straw sample.

However, it is important to note that the chemical composition results show a different trend for lignin content. The chemical composition results indicate that the lignin content remains nearly constant after either alkali or silane treatment of the Mid and Large wheat straw samples.

These slight differences between the results obtained from chemical composition and FTIR analyses highlights the importance of using other methods to calibrate the FTIR data.

Because the FTIR ratio uses the intensity of only one characteristic peak (hemicellulose 1740-1720 cm^{-1} and lignin 1510 cm^{-1}) for each wheat straw component, it is possible that the measurements are not reflecting the true chemical composition of the samples.

Perhaps, the use of multiple peaks in the FTIR analysis could help to reduce these differences on the results.

In fact, the chemical composition results represent the true or absolute amount of hemicellulose and lignin in the wheat straw samples. On the contrary, the variation on the hemicellulose and lignin ratios represents relative changes in the hemicellulose and lignin in the wheat straw samples.

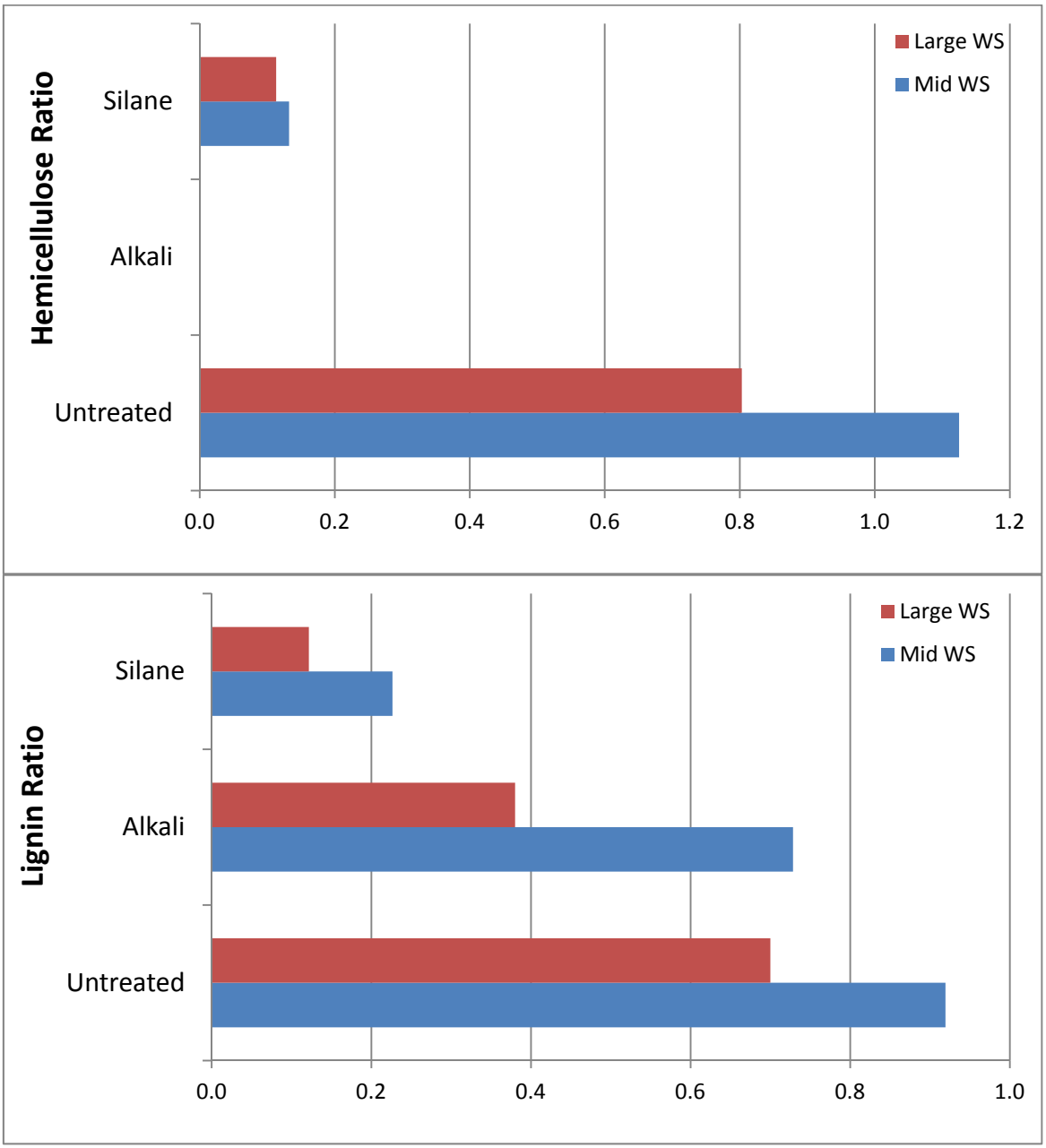

Figure 117: The hemicellulose (top) and lignin ratios (bottom) for the wheat straw samples.

For example, the amounts of hemicellulose and lignin measured with the assistance of other methods (e.g., chemical composition analysis) can be used to construct a calibration curve for FTIR data (Hon and Chang, 1984; Muller et al., 2003). This way, accurate quantitative determination of

lignin and hemicellulose can be perform with FTIR analysis. On the contrary, overestimate or underestimate values may be found. For example, Faix et al. (1991) observed that FTIR analysis predicted higher removal of lignin in comparison with values determined by other techniques. It is important to emphasize that an attempt to obtain a calibration curve for FTIR data was not part of the scope of this work and therefore it was not pursed here.

6.4.4.2 The Effect of the Alkali and Silane Treatments on the Physical Properties of Wheat Straw Samples (Fiber Set)

This section focuses on the changes caused by the alkali and silane treatments on the physical properties of the wheat straw samples, especially crystallinity and morphology. These properties are generally affected by the chemical components of wheat straw such as amount and arrangement of cellulose and lignin (Fakirov and Bhattacharyya, 2007).

The wide angle X-ray diffraction (WXRD) test was performed in order to ascertain the effect of the alkali and silane treatment on the crystallinity of wheat straw cellulose. It is believed that these treatments (i.e., alkali and silane) can improve the cellulose crystallinity which may lead to a fiber with better mechanical properties, especially tensile strength (Alemdar and Sain, 2008; Rong et al., 2001).

The intensity of amorphous and cellulose peaks (I_{am} and I_{002}, respectively) obtained from the WXRD test can be used to calculate the crystallinity index (CI) (according to procedure presented in the Characterization Methods section). The crystallinity index (CI) represents an estimation of the crystallinity of cellulose I present in the sample. Cellulose I is the part of cellulose which has highly organized chains forming crystals. Crystallinity measures the degree of organization of these crystals.

It is believed that fiber with higher crystallinity have also better mechanical properties (Alemdar and Sain, 2008; Rong et al., 2001; Sreekala and Thomas, 2003).

It can be seen from Figure 118 that the crystallinity of untreated Mid and Large wheat straw samples were 51.3 and 48.9 %, respectively. Similar values were observed by Liu et al. (2005). Those authors found that the crystallinity index of cellulose present in the epidermis and parenchyma of the wheat straw was 44.4 and 44.3 %, respectively.

Significant changes in the crystallinity of cellulose I were observed after alkali and silane treatment of the Mid and Large wheat straw samples (Figure 118). The crystallinity index of alkali treated Mid wheat straw (Mid_Alk) increased from 51.3 to 62.4 %. Similar increment was observed for Large wheat straw (Large_Alk) which had its crystallinity rising from 48.9 to 52.8 % upon alkali treatment.

Silane treatment of Mid wheat straw samples caused further increase on the crystallinity of cellulose I (Figure 118). Silane treated Mid wheat straw (Mid_Sil_Mix) presented crystallinity index of 66.9 % which represents 4.5 % increment in comparison with the alkali treated Mid sample (62.4 %). In the case of the Large wheat straw, the CI of silane treated sample (Large_Sil_Chloro) rose from 52.8 to 60.7 % in comparison with alkali treated Large sample.

The higher crystallinity observed in the alkali and silane treated wheat straw samples can be attributed to removal of non-cellulosic materials (hemicellulose, lignin and pectin) which facilitates rearrangement of cellulose chains into a better packing conformation and thus leading to higher crystallinity (Islam et al., 2011; Ray et al., 2001; Suradi et al., 2010; Yang[1] et al., 2007).

In fact, this supposition is supported by the reduction of hemicellulose percentage after alkali and silane treatment of the wheat straw samples as already demonstrated here by the chemical composition and FTIR results (Figure 113 and Figure 114).

Higher crystallinity after alkali treatment has been reported for other plant fibers including sugarcane (Yang[1] et al., 2007), jute (Ray et al., 2001), coir, and flax (Bledzki AK and Gassan J., 1999). Feng et al. (2008) observed gradual increment on crystallinity index when increasingly higher concentrations of sodium hydroxide were utilized during hot alkali treatment of hemp fiber. For example, in comparison with untreated hemp fiber, the crystallinity index of hemp fiber treated with 5 and 9 % sodium hydroxide solution (at 150 °C) increased from 40.4 to 50.4 and 53.5 %, respectively. The authors explained that the higher crystallinity of alkali treated samples is achieved through extraction of non-cellulosic components of hemp fiber. They found that, compared to untreated hemp fiber, alkali treated hemp samples had its hemicellulose percentage significantly reduced whereas the lignin percentage was only slightly decreased.

The additional increase in crystallinity of silane treated wheat straw can be explained by further extraction of non-cellulosic components and use of higher temperature. Silane treatment decreases the hemicellulose percentage of wheat straw samples as discussed before (Figure 113 and Figure 114).

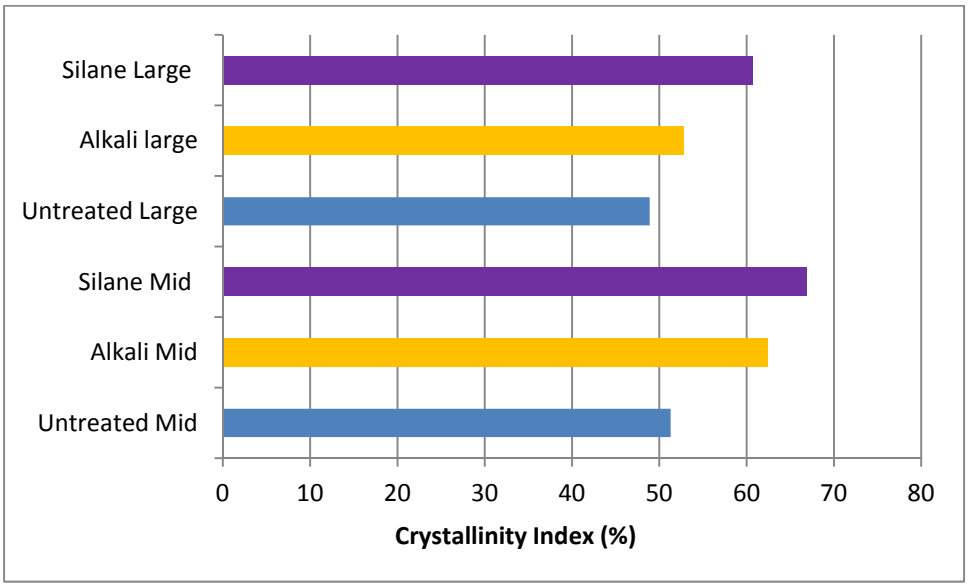

Figure 118: Crystallinity Index of the untreated, alkali and silane treated Mid and Large wheat straw samples.

In addition, the temperature utilized during silane treatment (boiling point of methanol, 65 °C) was higher than the one used by alkali treatment (around 25 °C). It is believed that heat can stimulate further rearrangement of cellulose chains into a more orderly conformation which increases the size of the crystallites (Cao et al., 2007; Feng et al., 2008; Rong et al., 2001). Heat can also induce the formation of totally new crystallites within the amorphous cellulose (Joseph et al., 2008; Rong et al., 2001).

In accordance with this, Cao et al. (2007) observed 2.5 % (from 48.7 to 51.2 %) and 7.1 % (from 48.7 to 55.8 %) increase on the crystallinity of kenaf fiber submitted to heat treatment at 130 and 140 °C, respectively, in comparison with untreated kenaf fiber. The authors attributed the higher crystallinity to improved cellulose structure.

In another study, Feng et al. (2008) found that the use of progressively higher temperatures during hot alkali treatment raised the crystallinity index of hemp fiber. Compared to untreated hemp fiber which has a CI of 40.4 %, the increment on the crystallinity index of hemp fiber treated at 100 and 150 °C rose to 46.2 and 53.5 %, respectively. When the temperature is further increased to 180 °C, additional improvement in the crystallinity is obtained and the CI of the sample reached 60.5 %. The

authors argued that the cellulose crystals suffered mild recrystallization due to high temperatures (100, 120, 150 and 180 °C) utilized during alkali treatment. They go on to say that even amorphous cellulose may undergo mild recrystallization when exposed to hydrothermal treatment above 100 °C.

The effect of the alkali and silane treatments on the morphology of wheat straw fiber was investigated with the assistance of scanning electron microscopy (SEM). It is important to study the morphological changes on the wheat straw fiber because these structural variations can extensively affect the mechanical properties of the fiber and thereby the mechanical properties of the composite (Herrera-Franco and Valadez-Gonzalez, 2005; Islam et al., 2011; Mwaikambo and Ansell, 2002).

Micrographs of outer and inner surfaces of untreated wheat straw stem (Large_As Is) are shown in Figure 119 and Figure 120, respectively. The outer layer of wheat straw shown in Figure 119 (A and B) is named epidermis and it is rich in cellulose. The cellulose is present in the form of microfibrils which are responsible for the stiffness of the straw stalk. These microfibrils of cellulose are covered by a layer of silica (approximately 1 wt-%, according to Liu et al., 2004) and wax. This outermost layer of silica and wax gives a smooth appearance to the epidermis surface as it can be seen in Figure 119 (A and B).

In contrast, the breakage of the inner structures of the wheat straw Large_As Is (i.e., sclerenchyma and parenchyma) produced a very coarse surface mainly because of the inner structure shapes (Figure 120 A and B). Sclerenchyma structures (also known as vascular bundles) have a cylindrical form resembling annular rings while parenchyma (or ground tissue) structures have different shapes according to their attributions (Hornsby[1] et al., 1997; Liu et al., 2004). These inner stem tissues are comprised of cellulose microfibrils bonded together by an amorphous matrix of lignin and hemicellulose (Hornsby[1] et al., 1997). No silica was observed in the inner surface of wheat straw stem (Hornsby[1] et al., 1997).

In addition, it is possible to observe in Figure 119 and Figure 120 the damage to the outer and inner surface of wheat straw fiber caused by the harsh grinding process which happens before alkali or silane treatment. The outer layer presents some cracks and debris whereas it seems that the inner layers are either peeled off or broken into smaller pieces.

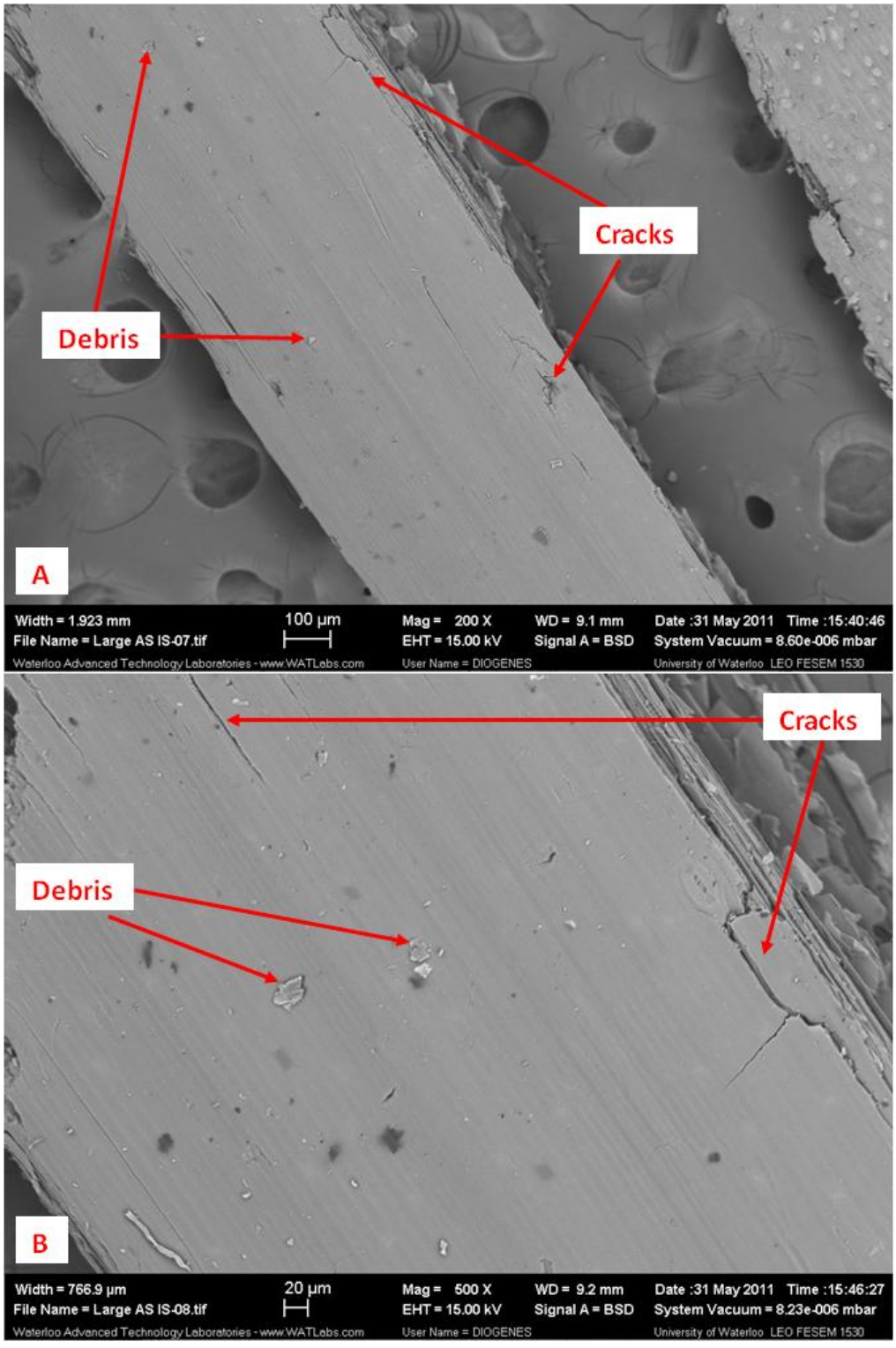

Figure 119: SEM micrograph of the outer layer of the untreated Large wheat straw (Large_As Is).

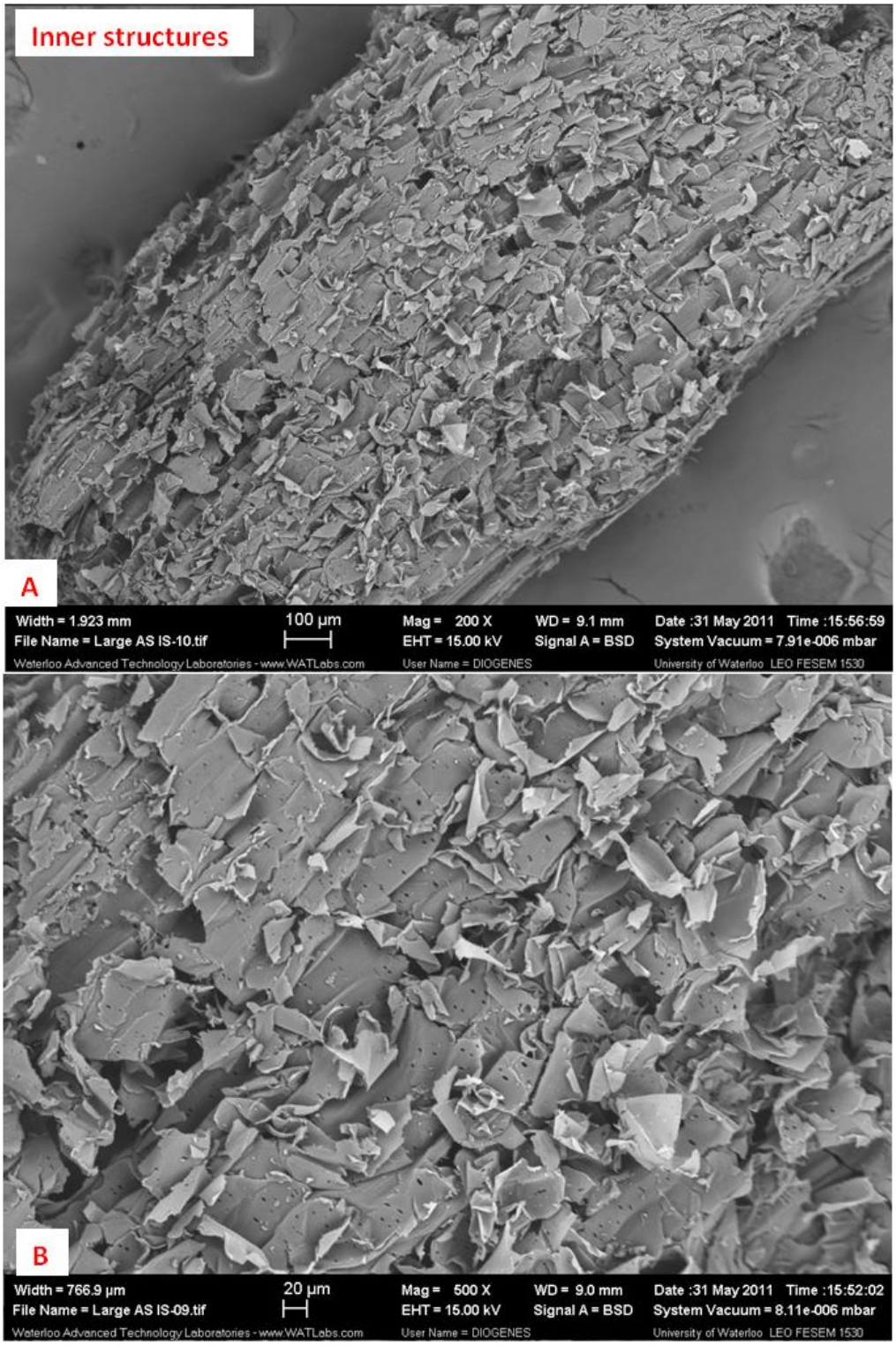

Figure 120: SEM micrograph of inner layer of the untreated Large wheat straw (Large_As Is).

The morphological features observed for the alkali and silane treated wheat straw samples are in agreement with removal of non-cellulosic material (especially hemicellulose and lignin) suggested by chemical composition and wide angle X-ray diffraction (XRD) results discussed before in this chapter.

Figure 121 (A and B) shows the epidermis of wheat straw after alkali treatment (i.e., Large_Alk sample). It is evident from the micrographs that the surface of wheat straw fiber has coarser texture in comparison with untreated wheat straw (Large_As Is).

Several authors have reported similar findings for different plant fibers. Rougher fiber surface after alkali treatment was observed in the case of sisal, hemp, wheat straw, oil palm, henequen, banana fibers by Mwaikambo and Ansell (2002), Feng et al. (2008), Liu et al. (2004), Suradi et al. (2010), Herrera-Franco and Valadez-Gonzalez (2005), Joseph et al. (2008), respectively. These authors argue that the removal of hemicellulose, lignin, wax and silica causes the exposure of the cellulose microfibrils and thereby rougher surface texture. The fiber bundle is separated into finer and smaller filaments of cellulose and lignin, referred to as microfibrils, via a process termed fibrillation. This process usually increases the roughness and porosity of the fiber surface. For example, Mwaikambo and Ansell (2002) observed fibrillation of alkali treated hemp fiber where the fiber bundles appeared more separated and with a highly serrated surface.

It has been widely reported that a coarser surface can induce both better mechanical interlocking and bonding reaction between fiber and polymer improving the mechanical properties of the composite (Herrera-Franco and Valadez-Gonzalez, 2005; Islam et al., 2011; Mwaikambo and Ansell, 2002). The improved bonding reaction is due to the removal of the surface impurities and exposure of the fiber hydroxyl groups to the polymer matrix whereas the coarser surface is responsible for inducing more fiber-polymer interpenetration at the surface.

Also, the extraction of the non-cellulosic material allows the cellulose fibers to rearrange in a compact manner leading to higher crystallinity and therefore improving the stiffness of the fiber. It is possible to observe in Figure 121 some of these microfibrils.

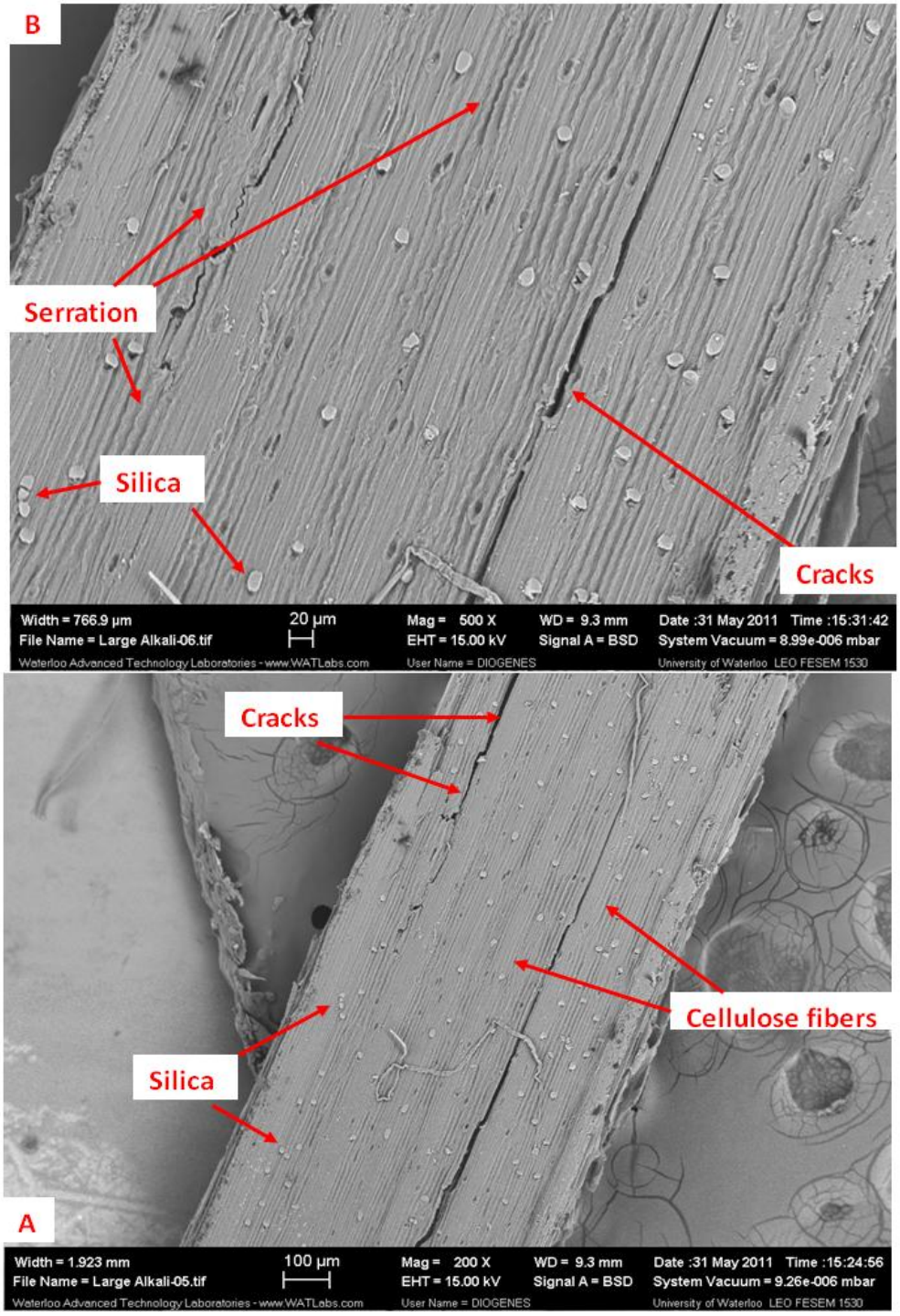

Figure 121:SEM micrograph of outer layer of the alkali treated Large wheat straw (Large_Alk). (A) 200 x magnified, (B) 500 x magnified. Arrows indicate cracks, silica and cellulose serration structure.

In addition, the presence of some cracks, cellulose fibers and white spots at the surface of the wheat straw fiber stem can be seen in Figure 121 (A and B). The cracks were caused by the wheat straw grinding process while the other two modifications were probably produced during alkali treatment. The cellulose fibers have two different shapes. Long fibers composed of several microfibrils of cellulose and short fibers with serration structure at the edge of the cells. The serration structure is responsible for connecting together the neighboring long fibers (Liu et al., 2004; Mwaikambo and Ansell, 2002). These two types of cellulose fibers are also observed in the silane treated wheat straw shown in Figure 123 and Figure 124.

The white spots are believed to be the residue of the partially removed silica layer. It is well established that alkali solution can dissolve the silica found in the epidermis of several plant fibers such as maize stems, rye straw, and rice straw (Xiao et al., 2001).

In order to confirm this assumption energy dispersive X-ray spectroscopy (EDX) was performed in the wheat straw white spots as shown in Figure 122. EDX is a microanalysis technique which allows identifying and quantifying the chemical composition based on the X-rays emitted during the scanning electron microscopy (SEM). The silica percentage found in these white spots (54.8 wt-%) was almost 100 times higher than other parts (Figure 122) of the alkali treated wheat straw fiber (0.59 wt-%).

Further evidence of silica removal from the surface of wheat straw stem (epidermis) is provided by chemical composition analysis (Figure 113 and Figure 114). The ash content after the alkali treatment decreased from 4.0 % to 1.5 % for the Mid wheat straw and from 4.2 % to 1.5 % for the Large wheat straw. The reduction of ash content indicates removal of inorganic materials such as silica. For example, Islam et al. (2011) have observed a 92 % decline in the ash content percentage after treating hemp fibers with an alkali solution.

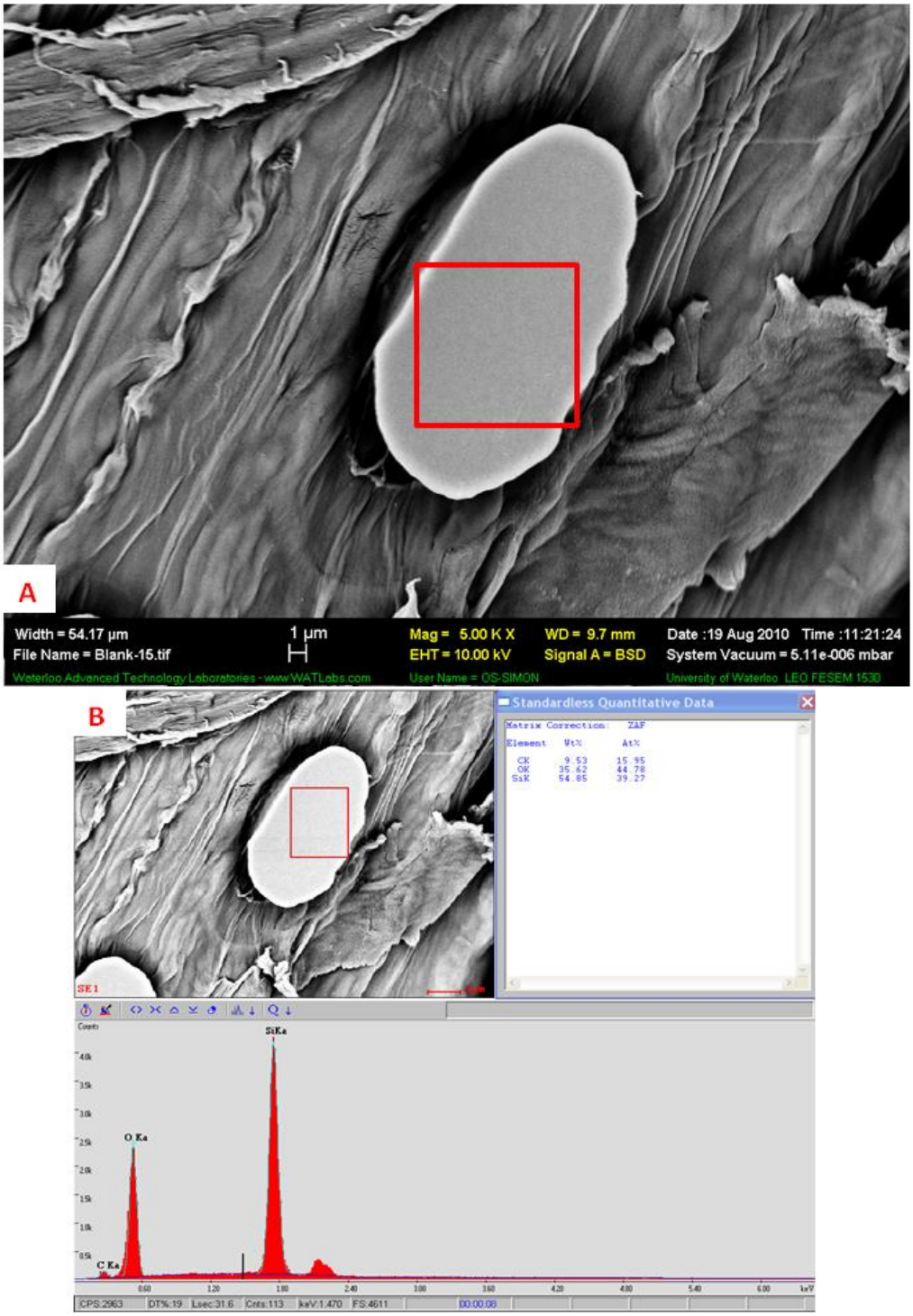

Figure 122: (A) Scanning electron micrograph of outer layer of the alkali treated Large wheat straw (Large_Alk) and (B) SEM-EDX of "white" spot on the surface of the Large_Alk WS.

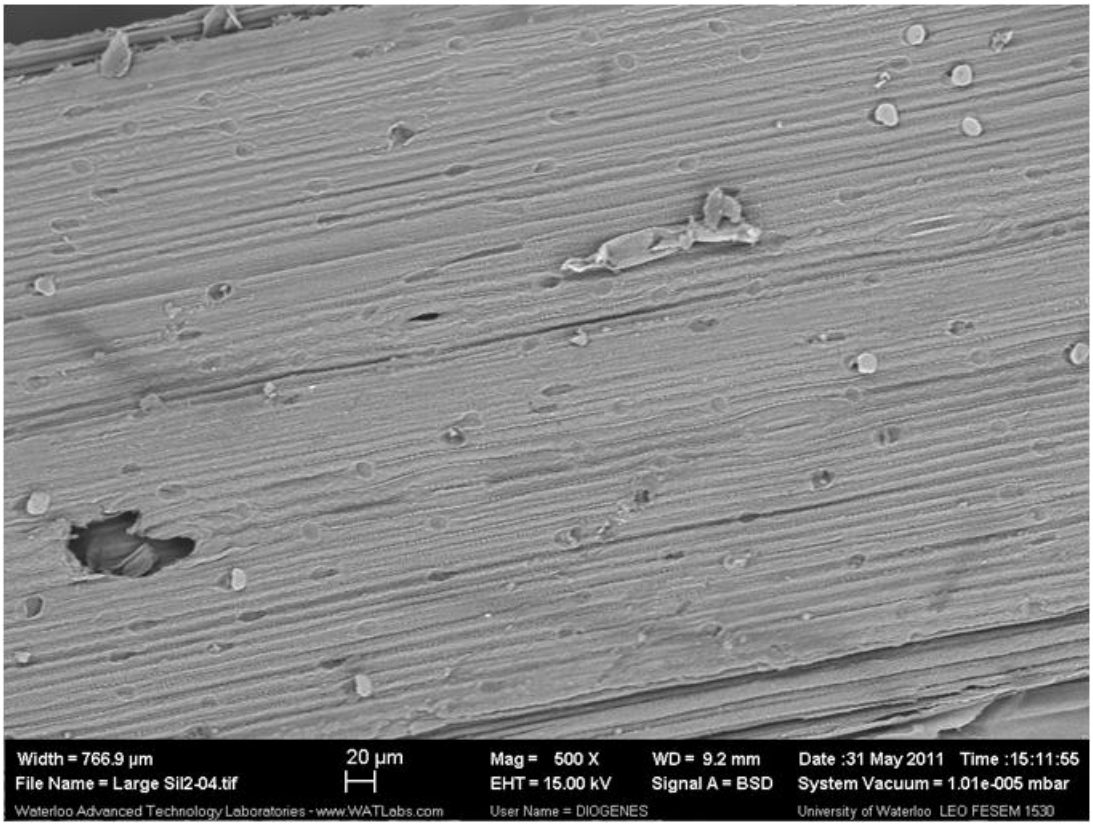

Figure 123: Scanning electron micrograph of outer layer of the silane treated Large wheat straw (Large_Sil_Chloro). (A) 500 x magnified.

Similar morphological features observed for the alkali treated wheat straw samples appear in the micrographs of the silane treated wheat straw samples. The surface texture of silane treated wheat straw (Figure 123 and Figure 124) seems as coarse as in the case of alkali treated wheat straw (see Figure 124). Cracks, silica (white spots) and cellulose fibers (long and short) are also visible. The serration structure mentioned before can be more clearly observed in Figure 124 (A and B). It is possible to see two long cellulose fibers being separated apart by disconnecting the serration structures (Figure 124, B).

In addition, there is a layer of probably non-cellulosic material (i.e., lignin and hemicellulose) being peeled off from the surface of the cellulose fibers (Figure 124, A).

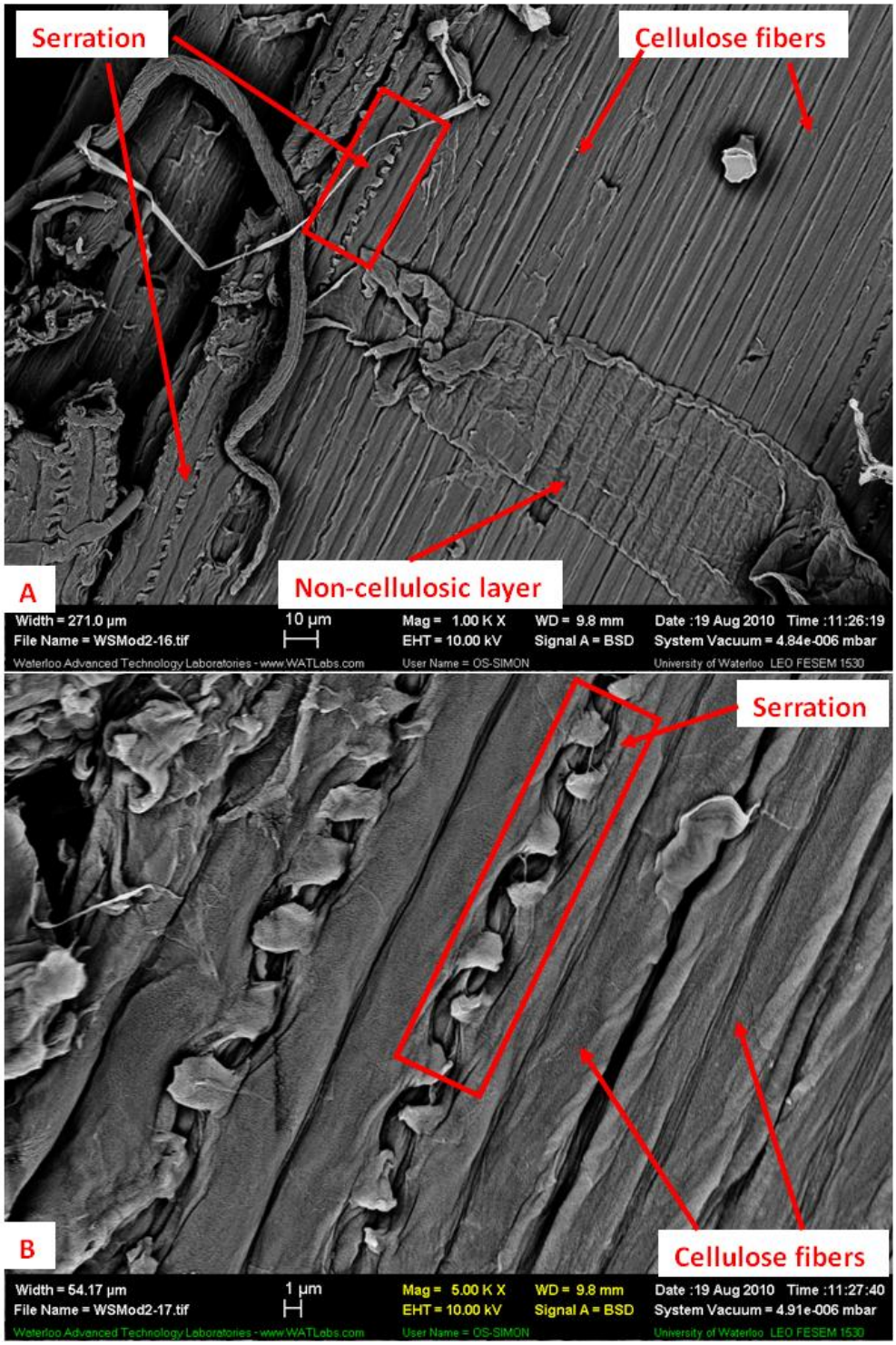

Figure 124:Scanning electron micrograph of outer layer of the silane treated Mid wheat straw (Mid_Sil_Mix). (A) 200 x magnified, (B) 500 x magnified.

The morphological features (e.g., exposure of cellulose fibers, fibrillation etc) observed for alkali and silane treated wheat straw samples correspond well with the removal of non-cellulosic material (especially hemicellulose and lignin) observed by chemical composition, FTIR and wide angle X-ray diffraction (XRD) results presented before in this chapter.

6.4.4.3 The Effect of the Alkali and Silane Treatments on the Mechanical Properties of the WS/PA-6 Composites (Composite Set)

6.4.4.3.1 Flexural Modulus

Flexural properties (modulus and strength) were determined according to ASTM D-790 and using 10 (ten) rectangular testing bars made from either pure polyamide-6 or 15 wt-% WS/PA-6 composites (see Table 33 for formulation details). All the composite samples were broken during testing whereas; the pure polyamide-6 samples were only bent.

The flexural modulus is obtained from the inclination of the elastic region of strain-stress curve and describes the ability of a material to resist bending when force is applied. Different industries (e.g., aerospace, automotive, construction, etc) use this property to select the correct materials for designing parts which must support loads without flexing. Therefore, the desirable flexural modulus will depend on the type application.

The effects of adding untreated, alkali and silane treated wheat straw samples on the flexural properties of the WS/PA-6 composites were studied here. Figure 125 presents the average flexural moduli for virgin polyamide-6 and WS/PA-6 composites prepared at 235 °C during extrusion and at 240-250 °C during injection molding. Error bars display plus and minus half of standard deviation.

Figure 125 shows that the pure polyamide-6 samples (PA-6) had lower flexural modulus (1930 MPa) than any of the composite samples which contain 15 wt-% of wheat straw. The addition of the untreated Mid wheat straw into the polymer matrix (Mid_As Is sample) increased the modulus to 2690 MPa (39 % increment), while the alkali and silane treated Mid wheat straw samples (Mid_Alk and Mid_Sil_Mix samples, respectively) raised the composite flexural modulus to 2590 MPa (34 % increment) and 2543 MPa (32 % increment), respectively.

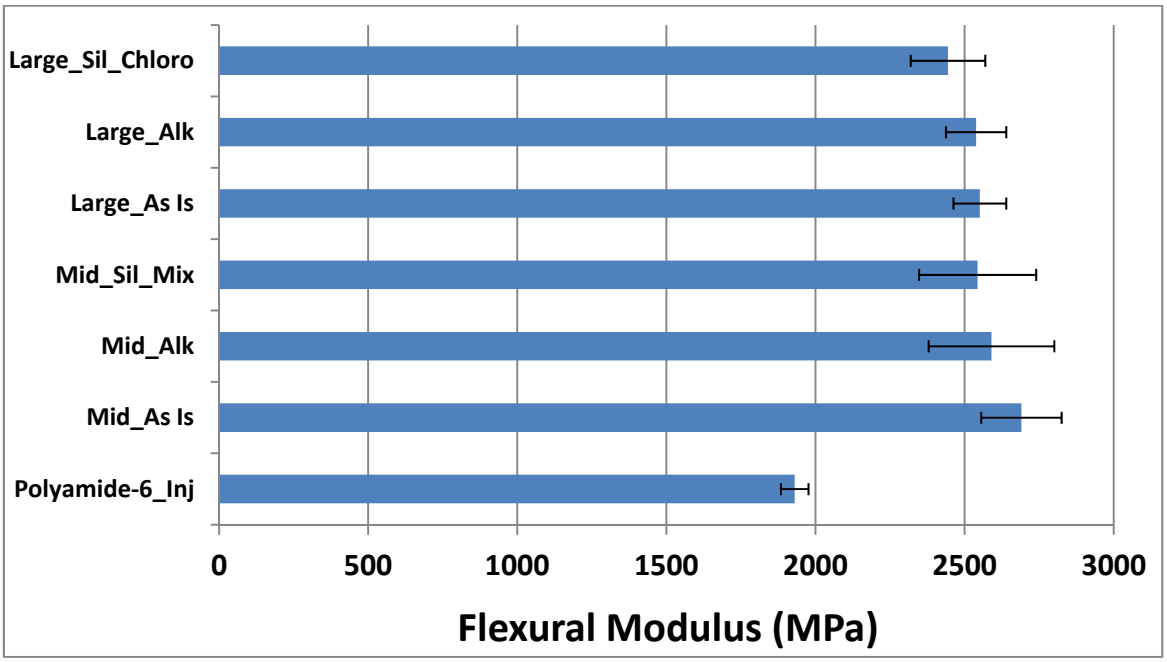

Figure 125: Flexural modulus of the polyamide-6 and its composites. The error bars show plus and minus halves standard deviation, n (number of samples)=10.

Similarly to the Mid wheat straw composites, adding Large wheat straw samples into the polymer matrix improved the flexural modulus of polyamide-6. For example, with the addition of the untreated, alkali and silane treated Large wheat straw samples into polyamide-6, i.e., Large_As Is, Large_Alk and Large_Sil_Chloro samples, the flexural modulus has increased from 1930 MPa (PA-6) to 2551, 2538 and 2444 MPa which represents 32, 31 and 27 % increment, respectively.

The increase in the composites flexural modulus in comparison with pure polyamide-6 is due to the higher stiffness of the wheat straw fiber which is added into the polymer. The increase of flexural modulus with the addition of fillers/fibers has been widely reported elsewhere. Xu (2008) observed a gradual increment on the composite flexural modulus from 1.37 GPa (pure polyamide-6) to 1.57, 2.00 and 2.60 GPa as the cellulose fiber content was increased from zero to 10, 20 and 30 wt-%, respectively. Similar behaviour was observed by Klyosov (Klyosov, 2007) when 33 wt-% of cellulose fiber were added to polyamide-6. The flexural modulus of the polymer raised almost 130 %, from 406 to 930 KPsi.

In the same fashion, addition of wheat straw fiber has also been shown to be beneficial for polypropylene flexural properties. Compared to unfilled polypropylene, the use of 10 wt-% of wheat straw was able to improve the flexural modulus of polypropylene by 50 % (Kruger, 2007). In another study, the addition of 25 wt-% of wheat straw into polypropylene caused a significant increase in the flexural modulus from 1.2 to 2.34 GPa (Hornsby[2] et al., 1997). Increment of 64 % on the polypropylene flexural modulus after addition of 30 wt-% wheat straw was also observed by Sardashti (Sardashti, 2009).

On the other hand, when comparing only the WS/polyamide-6 composites between themselves, the type of treatment applied to wheat straw fiber prior compounding seems to have no effect on the composite flexural modulus.

It appears that the alkali and silane treatments did not affect the stiffness of the alkali or silane treated wheat straw, since the composites prepared with these wheat straw samples (Mid_Alk and Mid_Sil_Mix, Large_Alk and Large_Sil_Chloro) have flexural modulus similar to the one prepared with untreated wheat straw samples (Mid_As Is and Large_As Is). For example, compared to the untreated Large wheat straw composite, the alkali and silane treated Large wheat straw composites have 0.5 % (from 2551to 2538 MPa) and 4.2 % (from 2551to 2444 MPa) smaller flexural moduli, respectively. However, these differences between the flexural modulus are smaller than the standard deviation and thus not significant.

In fact, the flexural modulus depends mostly on the amount of fiber added to the polymer composite. Because of that, the similar flexural modulus observed among the WS/polyamide-6 composites is in agreement with the fact that the amount of wheat straw fiber was kept constant at 15 wt-% for all the composites.

6.4.4.3.2 Flexural Strength

Flexural strength is defined as the maximum flexural stress supported by a specimen during a flexural test and represents the material ability to resist deformation under load. Similar to flexural modulus, flexural strength is an important parameter when selecting the correct material to design parts for different applications (e.g., automotive, consumer goods).

All the WS/polyamide-6 composite samples were broken during testing and, therefore the flexural stress at break became the flexural strength of the material. On the other hand, most of the pure polyamide-6 samples did not break before 5 % strain. Because of that the flexural strength was determined using the Equation 12 presented in the Characterization Methods section.

The effect of adding different wheat straw samples on the flexural strength of polyamide-6 is presented in Figure 126. It was found that the inclusion of different wheat straw samples did not affect the flexural strength of polyamide-6. In fact, Figure 126 shows that the average flexural strength of composites made with Mid and Large wheat straw samples is similar to pure polyamide-6 sample. For example, compared to the polyamide-6, the composites made with untreated Mid and Large wheat straw, silane treated Mid wheat straw and alkali treated Large wheat straw samples have a slight increase (1, 2, 5 and 5 %, respectively) on the flexural strength.

The good flexural strength of WS/polyamide-6 composites can be attributed to the good adhesion between the wheat straw fiber and polyamide-6 which is confirmed for all the WS/polyamide-6 composites with the assistance of SEM analysis in the next section.

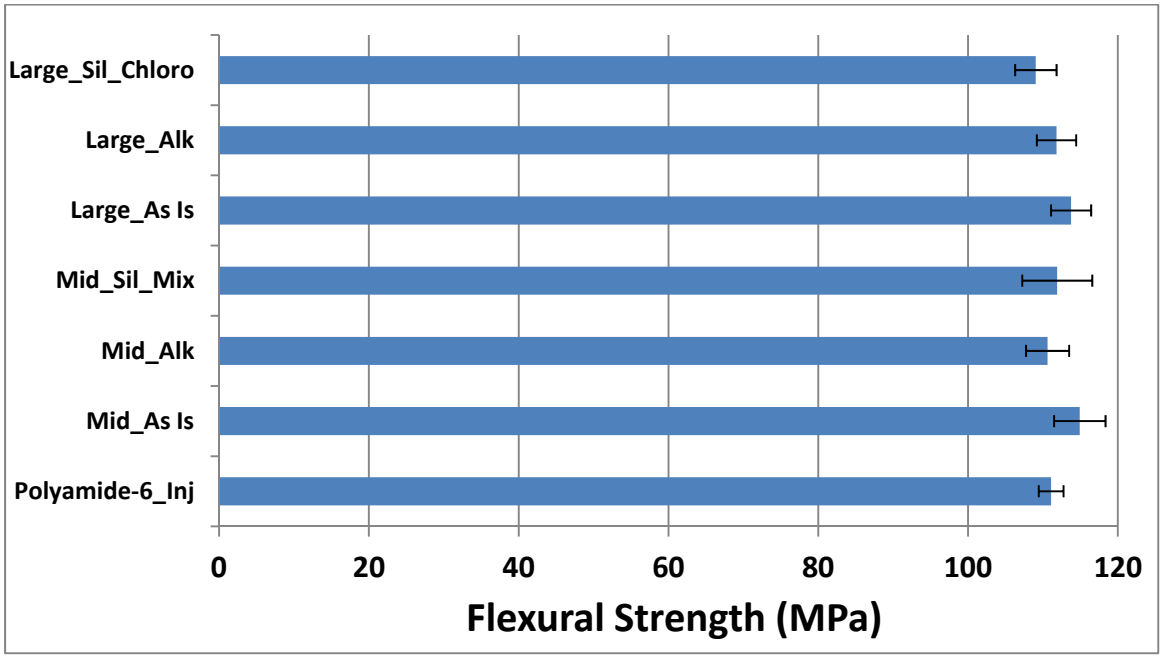

Figure 126: Flexural strength of composite samples and polyamide-6. The error bars show plus and mines half standard deviation, n (number of samples) =10.

These results represent an important achievement. In general, a significant decrease on the flexural strength is observed upon addition of natural filler or fiber into polymer. Sardashti (Sardashti, 2009) have found that the addition of wheat straw into polypropylene has significantly reduced the flexural strength of the polymer, especially when higher amounts of the fiber are utilized. For example, the polypropylene flexural strength dropped about 28 % with the addition of 30 wt-% of wheat straw. A further decrease of 46 % on the flexural strength of the composite happened when the wheat straw content is increased to 50 wt-%.

In agreement with these results, a gradual decrease on the yield strength of polypropylene was observed when the wheat straw content was increased. Addition of 30 wt-% of wheat straw into polypropylene produced a drop of 33 % on the yield strength whereas, 50 wt-% of wheat straw reduced the yield strength by 50 % compared to pure polypropylene (Kruger, 2007). Ng (Ng, 2008) has also reported that flexural strength of 40 wt-% WS/polypropylene composite was 33 % lower than virgin polypropylene.

This reduction in the flexural strength is attributed to the weak interfacial bonding between the fiber and the matrix. Yang et al. (Yang[2], 2004) explains that these weak interactions prevent the transfer of stress from the matrix to the fiber. The poor interfacial bonding becomes more important as the fiber content increases. In this case, the total interfacial area between matrix and fiber becomes bigger and microspaces (voids) between fiber and matrix may be formed. As a consequence of these voids between fiber and matrix, poor stress transfer and brittleness could occur.

6.4.4.3.3 Izod Impact Resistance

Izod impact strength is defined as the amount of energy required to fracture a material submitted to an impact loading (high strain-rate). Figure 127 presents the average Izod impact resistance values for virgin polyamide-6 and WS/polyamide-6 composites. Error bars display plus and minus half of standard deviation. The pure polyamide-6 samples have average impact energy of 54 J/m and partially break during testing. High impact resistance is expected from polyamide-6.

It has been reported by other authors that the addition of fiber leads to a reduction of the izod impact resistance of the polymer (Hornsby[2] et al., 1997; Panthapulakkal and Sain, 2006; Xu, 2008; Wu et al., 2001). For example, a decrease in impact resistance was observed when cellulose fiber or

even glass fiber were added to polyamide-6 (Xu, 2008; Wu et al., 2001). The addition of only 10 wt-% of cellulose fiber decreased the Izod impact of polyamide-6 by 58.7 % from 8.94 to 3.69 KJ/m^2 (Xu, 2008). Similar findings are reported for other polymers. The impact resistance of neat polypropylene decreased 9.8 % (from 2.46 to 2.22 KJ/m^2) when 25 wt-% of wheat straw is added to the polymer matrix (Hornsby^2 et al., 1997).

The same behavior was observed for the WS/PA-6 composites presented here. The introduction of the wheat straw fiber into the polyamide-6 has considerably decreased the Izod impact strength of the polyamide. It also changed the mechanism of fracture, since a complete break of the bar happened during the impact test. For example, the addition of the untreated Mid wheat straw sample decreases the composite (Mid_As Is) impact strength from 54 to 30 J/m, or 44%.

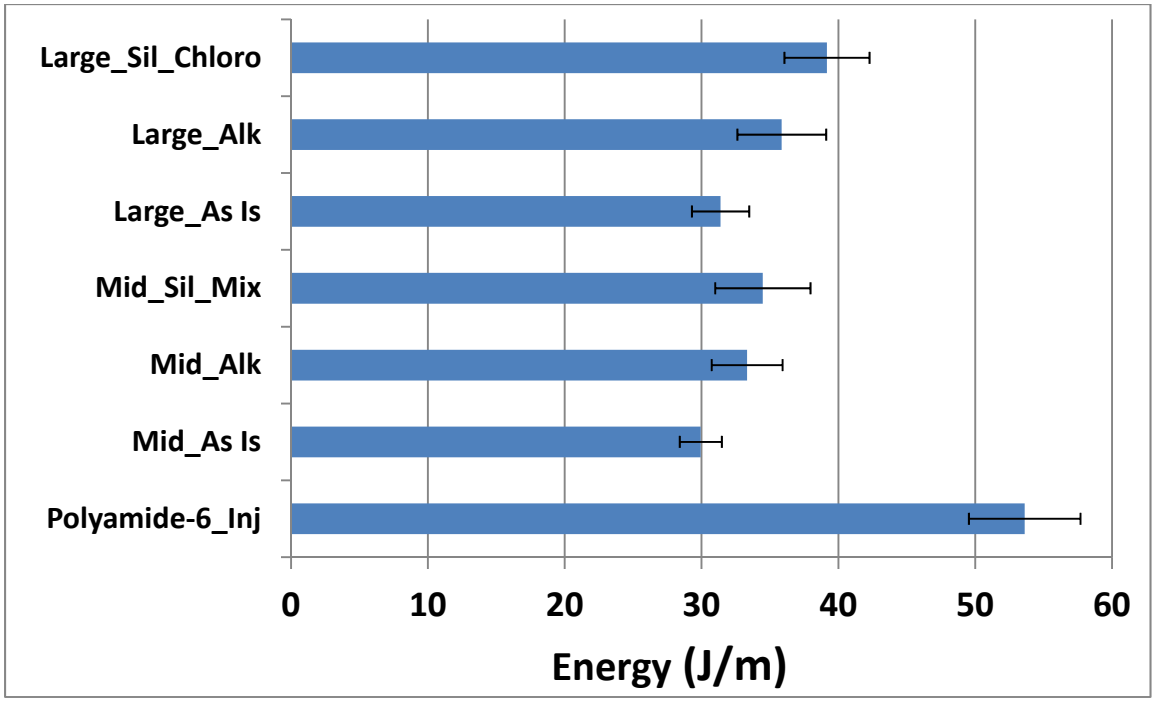

Figure 127: Izod impact resistance of composite samples and polyamide-6. The error bars show plus and mines half standard deviation, n (number of samples) =10.

In contrast, compared to the untreated wheat straw composites, the silane treated wheat straw composites (Mid_Sil_Mix and Large_Sil_Chloro) had higher Izod impact resistance. For example, among all the WS/polyamide-6 composites, the best result was achieved when the treated silane Large wheat straw was utilized. In this case, the impact strength of the composite sample (Large_Sil_Chloro) dropped 28 % from 54 to 39 J/m in comparison with the pure polyamide-6.

On the other hand, when comparing only the WS/PA-6 composites between themselves, it seems from Figure 127 that there is a trend of increasing the impact strength of the composites. For example, compared to the untreated wheat straw composites (Mid_As Is and Large_As Is), the silane treated wheat straw composites (Mid_Sil_Mix and Large_Sil_Chloro) have a 15.2 % (from 29.9 to 34.5) and 24.8 % (from 31.4 to 39.2), respectively, increase on the impact strength.

It is possible that additional study focus on finding the right silane combination and reaction conditions could provide wheat straw composites with even better impact resistance. However, a more extensive study focusing on the composites mechanical properties would be necessary. Such study was not part of the scope of this work due to time limitation.

The addition of fiber into polymer may or may not be beneficial for the polymer impact strength depending on the quality of the fiber and the bond strength between matrix and fiber. Poor bonding between the fiber and the matrix and/or poor fiber properties (e.g., strength, length, volume fraction and aspect ratio) will lead to decrease in the impact strength. In this case, the fibers will introduce voids and flaws into the polymer matrix which generate stress concentration and facilitate crack propagation.

On the other hand, proper bond strength and aspect ratio can cause enhancement of the polymer impact strength, especially in the case of brittle matrices. In this case, the presence of fiber acts as a barrier for the crack propagation, forcing the cracks to divert around the fibers (Xanthos, 2010).

It is important to clarify that the scope of this work was not searching for the best set of parameters to produce WS/PA-6 composites (e.g., percentage of filler, use of additive, extrusion and injection temperature etc). The objective was rather to evaluate the hypothesis that improving the thermal stability of wheat straw samples, with alkali and silane treatments, will not negatively affect other properties of the fiber and composite such as mechanical properties.

Based on the results presented here, it is possible to conclude that the different treatments applied to wheat straw samples (i.e., alkali and silane) are not negatively impacting (i.e., decreasing) the flexural modulus and strength of the WS/polyamide-6 composites.

In fact, compared to the pure polyamide-6 samples, the WS/PA-6 composites (containing 15 wt-% of wheat straw) have better flexural properties regardless of the wheat straw sample (i.e., untreated, alkali and silane) utilized to prepare the composite.

Even though there is an overall decrease on the Izod impact resistance, there is potential for increasing the impact resistance of composites as we move from the untreated to the alkali and then the silane treated wheat straw composites. Further investigation could determine whether or not these treatments (i.e., alkali and silane) could actually promote improvements on the impact resistance of the WS/PA-6 composites.

6.4.4.4 The Effect of the Alkali and Silane Treatments on the Morphology of the WS/PA-6 Composites (Composite Set)

The morphology of the wheat straw/polyamide-6 (WS/PA-6) composites and wheat straw fiber were investigated with field emission scanning electron microscopy (SEM). The surface of the composites was analyzed after Izod impact test.

The SEM images in low magnification can reveal overall dispersion, wetting and indications of fiber pull-out such as voids and spots. Images made in high magnification are useful to observe the quality of interface between filler and matrix. Better fiber-matrix adhesion usually is translated into enhanced mechanical properties. These images may also provide information about the fracture mechanisms such as crack propagation and load transfer between filler and matrix.

All the WS/PA-6 composites show good wetting of the fiber by the polymer, good dispersion of the fiber in the matrix and strong fiber-matrix interaction. In addition, very few voids and fiber pull-outs were observed. On the other hand, the fracture surface was brittle for all the composites. The addition of the wheat straw samples introduces flaws which are responsible for the brittle behavior of these composites. It seems that the type of wheat straw fiber (e.g., Mid or Large) and the fiber treatment (e.g., alkali, silane) did not affect the interfacial bonding between wheat straw and polyamide-6.

These observations are illustrated in Figure 128 to Figure 132. They show the surface fracture after Izod impact test of the Large_Sil_Chloro and Mid_As Is, Mid_Sil_Mix, Large_Sil_Chloro, Large_Sil_Chloro, Mid_Alk and Large_As Is wheat straw/polyamide-6 composites, respectively.

It can be seen that the wheat straw fibers are oriented in different directions on the surface fracture. The fiber indicated by the box 1 (in Figure 128, 41 and 42) is perpendicular (i.e., 90 degrees angle) to the fracture surface while, the fiber highlighted by the box 2 (in Figure 128, 41 and 42) is almost parallel (low angle) to the fracture surface. These findings suggest that wheat straw fiber is only partially oriented during injection molding.

Fiber orientation is especially important in the case of short fiber reinforced composites. Short fibers may be completely oriented, randomly oriented or partially oriented. Completely oriented fibers are all aligned parallel to each other and towards a single direction while randomly oriented fibers are neither aligned parallel to each other nor in one single direction. The arrangement of partially oriented fibers lay in between the ones of completely oriented and randomly oriented fibers.

In fact, it is very difficult to obtain completely oriented composites when using short fibers. Typically, composites with short fibers are either random or partially oriented. For example, when preparing 30 and 40 wt-% wheat straw-polypropylene composites, Sardashti (2009) obtained part of the fibers aligned parallel to the fracture surface of the composite. It is believed that injection moulding promotes the alignment of the fibers in the direction of the polymer flow (Hornsby[2] et al., 1997; Sardashti, 2009).

The desirable fiber orientation depends on the direction of the load. When the load is applied in only one direction (e.g., longitudinal) of the composite, fibers oriented in that direction provide better reinforcement effect. On the other hand, if the load is applied in the transverse direction of the composite or multiple directions at the same time, it is preferable random or partially oriented fibers (Callister, 2000).

The good adhesion fiber-polymer is evident in Figure 128, 129, 130 and 131. It can be observed that the wheat straw fiber was broken instead of being pulled out of the matrix. For example, the fiber perpendicular to the fracture surface (box 1, Figure 128, 129 and 130) was completely cut into two parts whereas; the fiber with low angle with respect to the fracture surface (box 2, Figure 128, 129 and 130) was partially damaged.

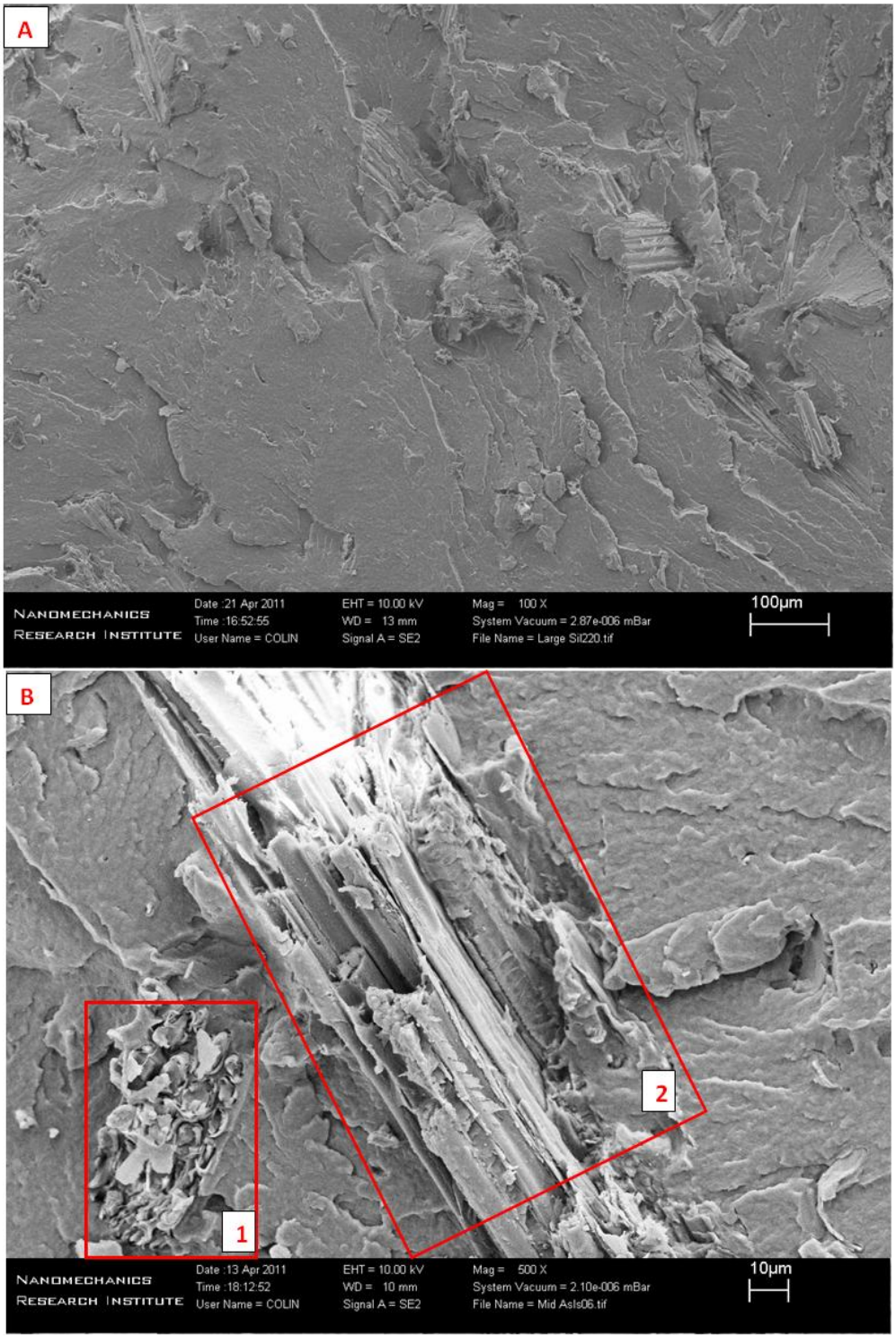

Figure 128: SEM micrograph of a cross-section from (A) the silane treated WS/PA-6 composite (Large_Sil_Chloro) and (B) the untreated WS/PA-6 (Mid) composite.

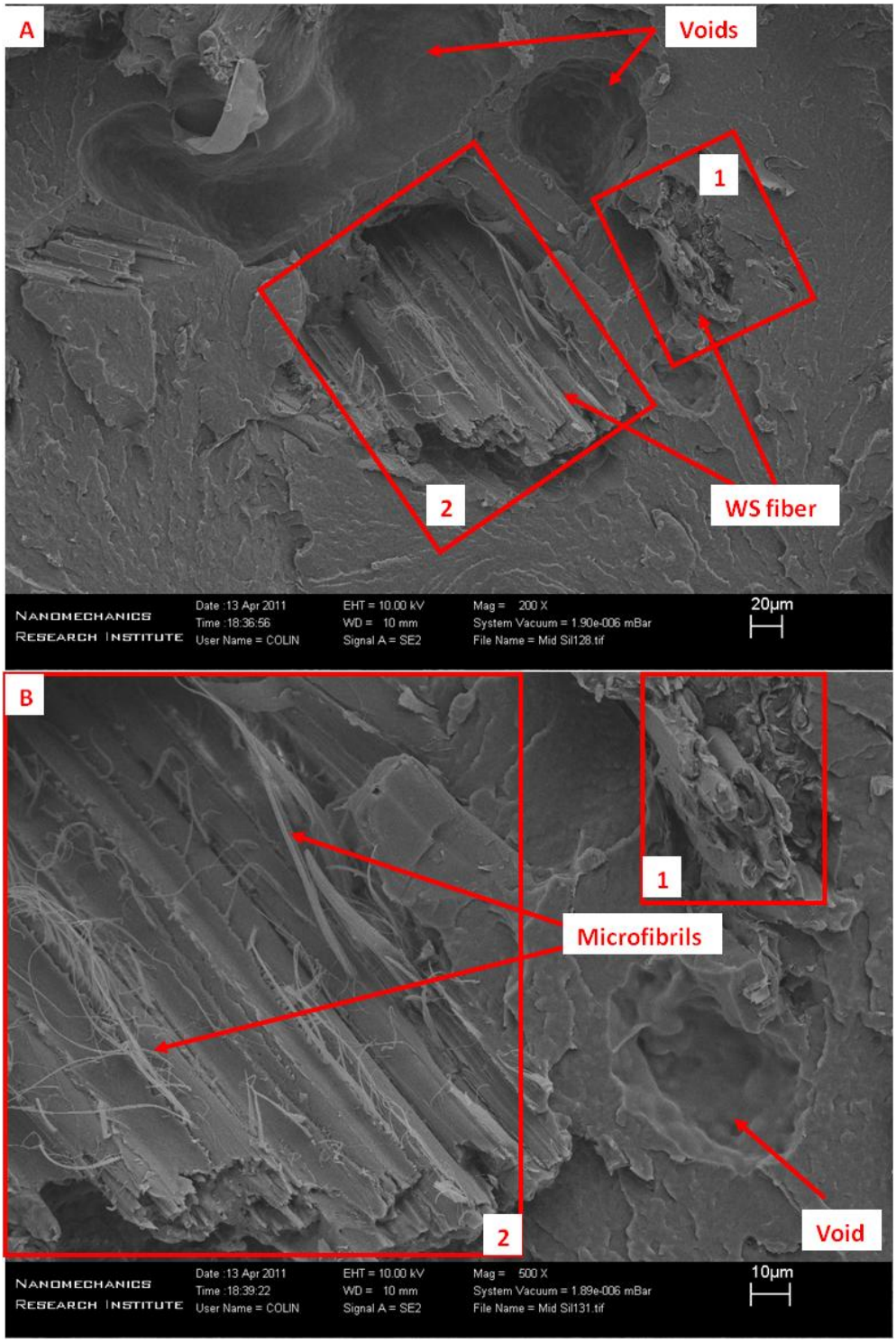

Figure 129: Scanning electron micrograph of a cross-section from the silane treated WS/PA-6 composite (Mid_Sil_Mix magnified (A) 200x and (B)500x.

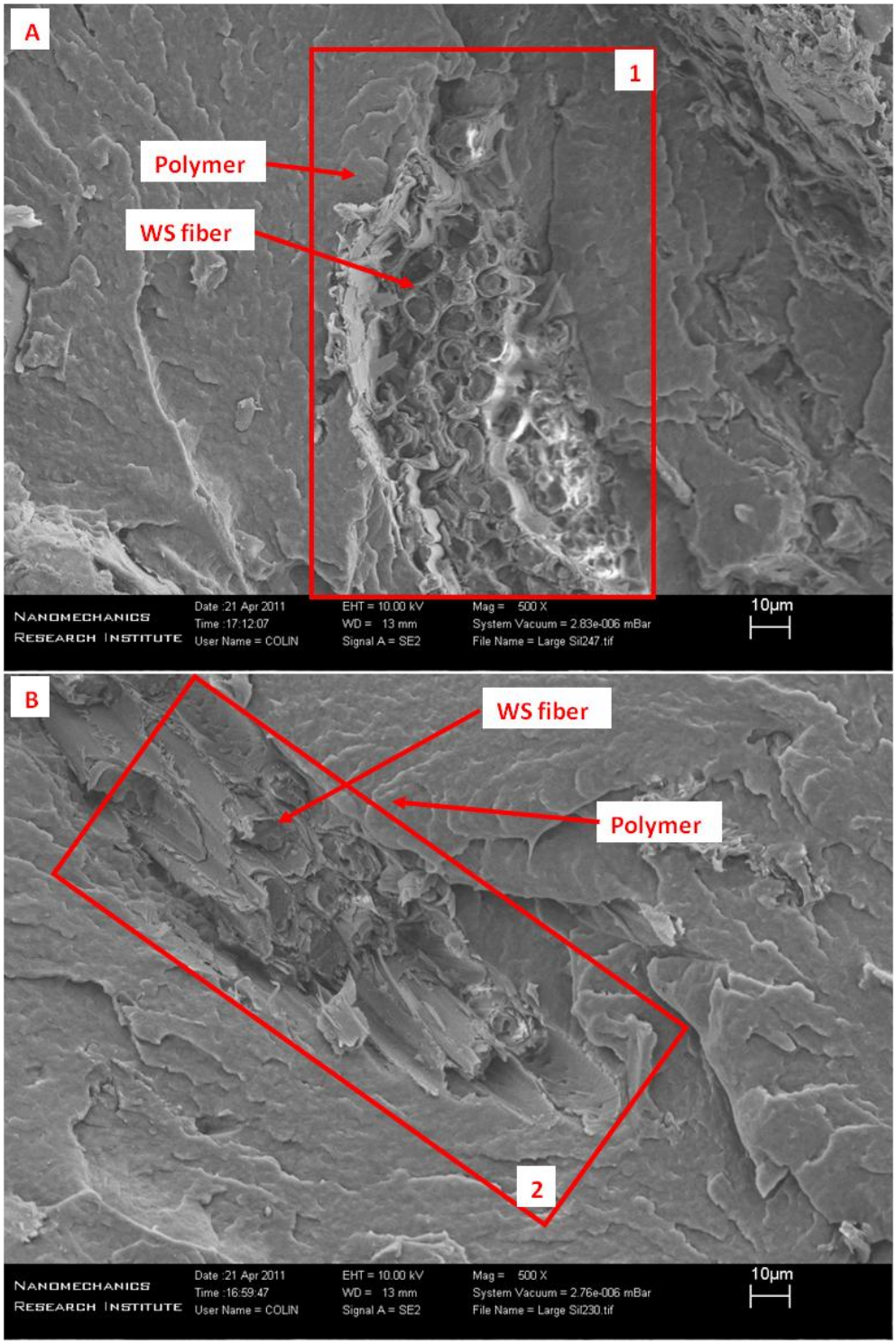

Figure 130: Scanning electron micrograph of a cross-section from the silane treated WS/PA-6 composite (Large_Sil_Chloro) magnified (A) 500x and (B 500x.

Figure 129 (B) shows in detail these behaviors. It can be seen that there was extensive fiber breakage when the fiber was parallel to the fracture surface (box 2). In this case, the outer structural wall of the fiber was peeled off leaving the internal structure and microfibrils exposed (as indicated by arrows). On the other hand, the fiber perpendicular to the fracture surface does not present damage in the fiber surface but rather a transverse cut (box 1 in Figure 129 (B)).

Another example of good fiber-matrix adhesion is shown in Figure 131. The Figure 131 (A) shows that, even after the surface fracture, the top of wheat straw fiber is still completely covered by the polymer (arrow 1). It is possible to observe in Figure 130 (A) and Figure 131 (B) that there is no visible space in the interface matrix-fiber. In fact, it is very difficult to determine where is the end of the matrix surface and the beginning of the fiber surface. These observations indicate very good adhesion between the wheat straw fiber and the polyamide-6.

Several authors have reported good interfacial bonding between natural fibers and polar polymers. Xu (2008) observed very good compatibility between cellulose fiber and polyamides which formed composites with no obvious separation in the matrix-fiber interface. Similarly, Amintowlieh (2010) have prepared wheat straw-polyamide-6 composites and reported good wetting and bonding between the matrix and fiber. However, when non-polar polymers (e.g., polypropylene) are combined with wheat straw, the use of a coupling agent (e.g., maleic anhydride) is usually required in order to achieve good interfacial bonding (Guettler, 2009; Hornsby[2] et al. 1997; Kruger, 2007; Panthapulakkal and Sain, 2006; Sardashti, 2009).

Therefore, the good adhesion between wheat straw fiber and polyamide-6 can be attributed to their polar character which increases the fiber-matrix compatibility and thereby justifies the improved flexural properties of the WS/PA-6 composites in comparison with neat polyamide-6 as discussed previously.

In addition, the anisotropic nature of the wheat straw fiber is illustrated in the previous figures. The mechanical properties of natural fibers are generally anisotropic, that is, the fiber is weaker when the stress is applied in the transverse direction rather than along of the main dimension of the fiber (lengthwise direction) (Callister, 2000).

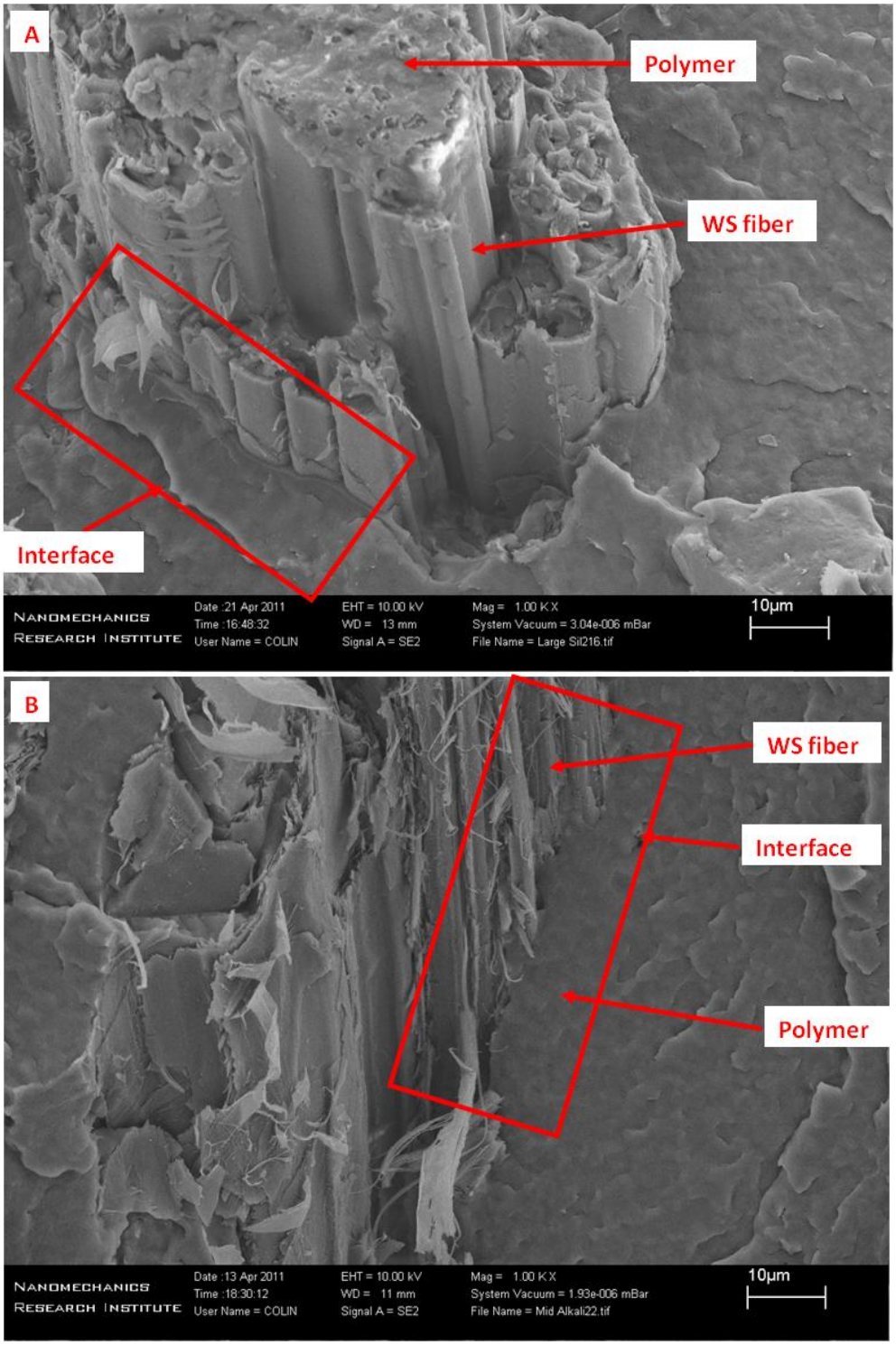

Figure 131: SEM of a cross-section from (A) the silane treated WS/PA-6 composite (Large_Sil_Chloro) and (B) the alkali treated WS/PA-6 (Mid_Alk) composite. Magnified 1000x.

Therefore, in the case of the fiber perpendicular to the fracture surface (box 1 indicated in Figure 129 (A) and (B) and Figure 130 (A)) the stress was applied in the weakest (transverse) direction of the fiber which caused the cut of the fiber into two parts. On the contrary, the fiber at low angle with the fracture surface (box 2 indicated in Figure 129 (A) and (B) and Figure 130 (B)) has the stress applied to the strongest direction of the fiber which resulted in fiber damage but not total fracture of the fiber. Because of that, only the fibers aligned in the same direction of the stress being applied will provide reinforcement effect.

Additionally, it is noticeable in Figure 129 (A) and (B) the presence of voids (as indicated by arrows). These voids do not represent fiber pull-out but rather bubbles which are formed during composite preparation. These voids can be the result of the evaporation of water and/or decomposition of low molecular weight components of the wheat straw fiber (Amintowlieh, 2010; Kruger, 2007). The presence of these defects (i.e., bubbles, voids) facilitates crack propagations and contributes to reduce the mechanical properties of the composite. It should be highlighted that very few bubbles or voids were observed in all the WS/PA-6 composites, independently of the fiber type (e.g., Mid and Large) or treatment (e.g., untreated, alkali and silane).

Furthermore, it was expected that the alkali and silane treatments could improve the interfacial bonding between fiber and polymer matrix. First, alkali treatments can produce fiber with rougher surface which facilitates the mechanical interlocking between the fiber and matrix. In the same way, silane treatments can introduce functional groups in the wheat straw surface that would promote better fiber-polymer bonding.

Therefore, both treatments can potentially improve the adhesion between fiber and matrix. In this case, an increment on the flexural strength of the composites would be observed, because the flexural strength is especially affected by the quality of the interface between matrix and fiber.

However, from figures previously presented, it appears that the matrix-fiber interface of the treated wheat straw (alkali and silane) composites is similar to the one presented by the untreated wheat straw composites. This corresponds well with the flexural strength results which indicate that no further increment on the flexural strength was observed for composites using the alkali and silane treated wheat straw samples.

It has been reported that the mechanical properties depend not only on the fiber-matrix adhesion but also on the volume of fiber, critical fiber length, fiber strength and orientation. For example, the

length of the fiber has to be at least equal to the critical length in order that the fiber reinforcement becomes effective. In this case, the fiber will actually support part of the stress applied to the composite. Increasing the fiber length will increase the effect of fiber reinforcement.

In order to verify if the composite fabrication steps (i.e., extrusion and injection molding) and/or the alkali and silane treatments are affecting the aspect ratio of the wheat straw samples, it is suggested that additional research could be done to study the aspect ratio of the wheat straw samples after the alkali and silane treatments as well as the fabrication of the WS/PA-6 composites. However, due to time limitation this study was not conducted here.

Furthermore, Figure 132 presents the cross section of the surface fracture of the WS/PA-6 composite using the Large wheat straw without treatment. Figure 132 (B) shows a close up of the region indicated by the box in Figure 132 (A). Crack pinning mechanisms, crack pinning and bow out, can be observed.

Crack pinning occurs when a fiber acts as an obstacle and impedes, or pins, the growth of a crack. The crack is then forced to bow out the obstacle which leads to an increase fracture energy (Amintowlieh, 2010; Spanoudakis and Young, 1984). This is exactly the behavior observed in the images. The crack initially propagates straight through the matrix (arrow 1 in Figure 132 (A) and (B)) until the crack is forced to go around the fiber (arrow 2, Figure 132 (A) and (B)). This “detour”, which is called crack bow out, increases the distance covered by the crack and is believed to raise the energy absorption during fracture (Spanoudakis and Young, 1984). The fiber was also damaged but not completely cut into two parts. This suggests that the fiber was strong enough to impede the crack progress.

It was observed for all the WS/PA-6 composites good wetting of the wheat straw fiber by the polyamide-6 polymer, good dispersion of the fiber in the matrix and strong adhesion between fiber and matrix. Overall, very few voids and fiber pull-outs were observed. However, the addition of wheat straw fiber introduces flaws which are responsible for the brittle behavior observed for the WS/PA-6 composites. It seems that the type of wheat straw fiber (e.g., Mid or Large) and the fiber treatment (e.g., alkali, silane) did not affect the interfacial bonding between wheat straw and polyamide-6.

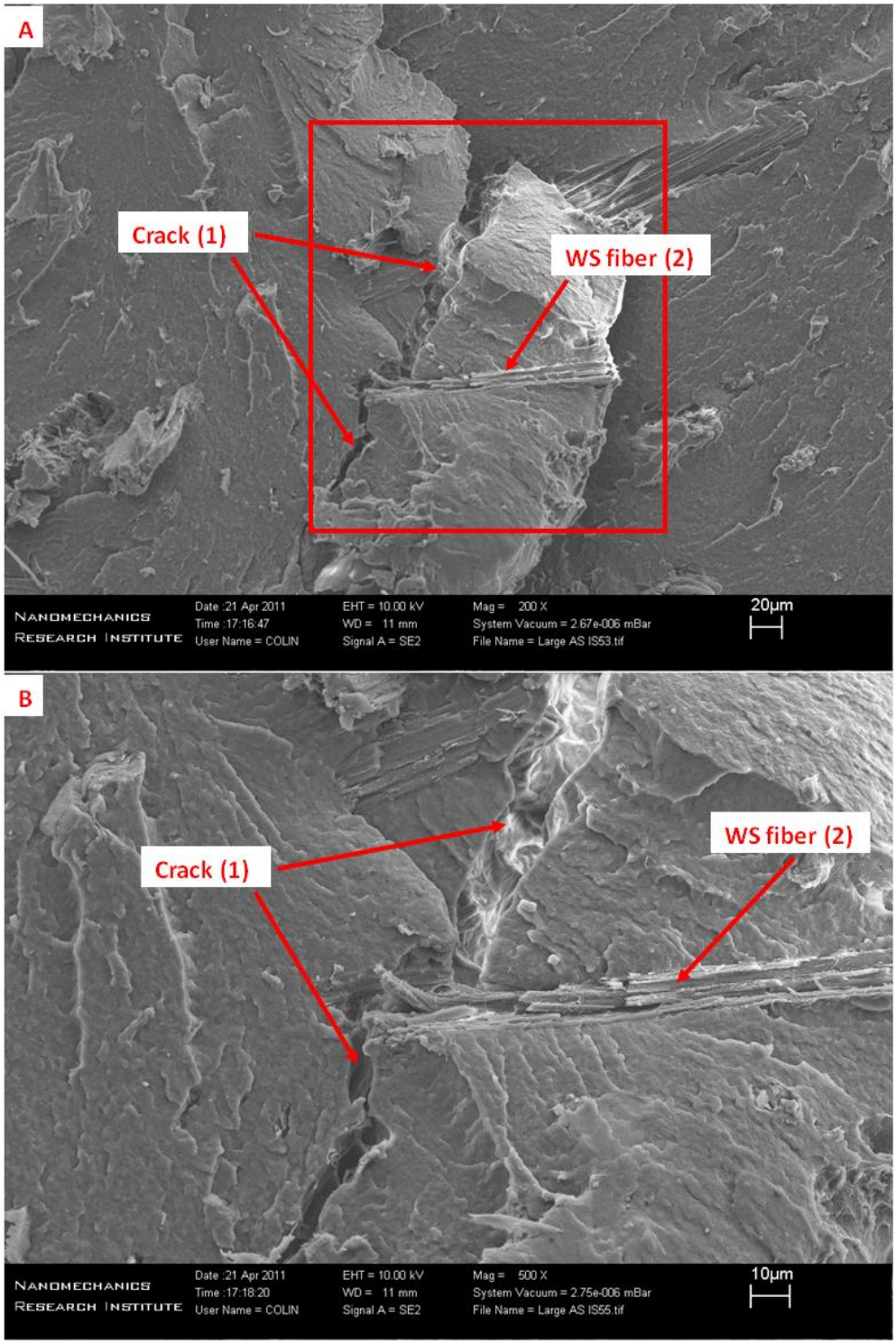

Figure 132: Scanning electron micrograph of a cross-section from the untreated WS/PA-6 composite (Large) magnified (A) 200x and (B) 500x.

6.5 Conclusions

In this chapter, the knowledge obtained in Chapter 4 is applied to select different combinations of alkoxysilane and chlorosilane modifiers to increase both the thermal stability and the compatibility of wheat straw with polyamides via silane modification.

The TGA analysis indicates that the extruded and injection molded composites containing silane treated wheat straw samples have significantly smaller thermal degradation than those utilizing untreated and alkali treated wheat straw samples. In addition, the composites with the highest thermal stability (which contain silane treated samples) have the lighter colors after the extrusion and injection molding steps.

Besides evaluating the thermal stability, the effect of the silane treatments on the wheat straw samples (chemical composition, crystallinity and morphology) and mechanical properties (flexural modulus and strength, and Izod impact strength) of the WS/polyamide 6 composites were also considered.

The silane treatments considerably decrease the hemicellulose content whereas a significant increase on the cellulose content is observed (because of alkali pre-treatment). As a consequence of this removal of non-cellulosic materials (hemicellulose, lignin and pectin), the crystallinity of the silane treated samples is increased. The removal of non-cellulosic materials is also present in the morphological features (e.g., exposure of cellulose fibers, fibrillation etc) observed for silane treated wheat straw samples.

Additionally, it appears that the silane treatment did not affect the stiffness of the silane treated wheat straw, since the composites prepared with these wheat straw samples have flexural properties similar to the one prepared with untreated wheat straw samples.

Overall, it was also observed that the WS/polyamide-6 composites possess good flexural properties which can be attributed to the good adhesion between the wheat straw fiber and polyamide-6. This good adhesion was confirmed with the assistance of SEM analysis. In fact, all the WS/PA-6 composites show good wetting of the fiber by the polymer, good dispersion of the fiber in the matrix and strong fiber-matrix interaction. For example, very few voids and fiber pull-outs were observed.

On the other hand, the fracture surface was brittle for all the composites. The addition of the wheat straw samples introduces flaws which are responsible for the brittle behavior of these composites and

an overall decrease on the Izod impact strength. However, this is something almost unavoidable when plant fibers are compounded with polyamide.

Despite this, silane treatment shows potential for increasing the impact resistance of WS/PA-6 composites. The impact strength increases when silane treated samples are added to the composites. Further investigation could determine whether or not other silane treatments could promote additional improvements in the impact resistance of the WS/PA-6 composites.

It is shown here that the selected combinations of silane modifiers successfully increased the thermal stability of wheat straw using large scale treatment. Moreover, this enhancement in the thermal stability of straw fiber is sufficient to allow the fabrication of wheat straw/polyamide-6 (WS/PA-6) composites with reduced thermal degradation of the wheat straw fiber. Furthermore, the mechanical properties of these composites do not seem to be compromised for the use of silane treated straw compared to untreated straw.

The results obtained in this chapter indicates that the chemical treatment of the straw fibers has a great potential for developing grades of fiber for applications in composites with engineering plastics.

Chapter 7- Novel Use of Ultraviolet Irradiation to Improve the Thermal Stability of the Wheat Straw Fiber

7.1 Introduction

In this chapter, a novel, fast and cost-effective technique capable of improving the thermal stability of wheat straw was developed. High intensity (1800W) ultraviolet (UV) irradiation was utilized to potentially remove or alter the lignin and hemicellulose present in wheat straw.

Various reports have demonstrated that long time or wavelenght UV irradiation exposure can selectively reduce the lignin content in different kinds of woods, e.g., European spruce veneer, coniferous southern yellow pine, lime wood, rubber wood etc (Deka et al., 2008; Feist and Hon, 1984; Fengel and Wegener, 1989; Hon and Chang, 1984; Muller et al., 2003). Similar to lignin, hemicelluloses can also be affected by UV radiation (Deka et al., 2008; Norrstrom, 1969).

Surprisingly, to the best of our knowledge, the ultraviolet light has not been employed in any attempt to enhance the thermal stability of agro-based fibers. Thus, the main objective of this chapter is to develop a novel chemical-free ambient temperature processing technique that can remove or alter lignin and hemicellulose. Hence, high intensity ultraviolet irradiation was utilized to increase the temperature of thermal degradation of wheat straw fiber.

The success of the ultraviolet irradiation treatment was assessed by comparing improvements on the thermal stability measured by thermogravimetry (TGA) analysis and yield. Chemical composition and Fourier-transform infrared (FTIR) spectroscopy were used to obtain insights on the mechanisms.

Thermogravimetry analysis (TGA) results show that the UV irradiation is a very effective method to improve the thermal stability of wheat straw fiber. Only 15 minutes of the UV light treatment was able to raise by 40 ºC the temperature at 2% of weight loss, from 230 to 270 ºC. Changes in the lignin molecular structure and removal of hemicellulose are believed to be responsible for the enhancement of the thermal stability of the ultraviolet treated wheat straw samples.

7.2 Materials and Methods

7.2.1 Materials

The Mid wheat straw fiber used in this chapter is described in details in Chapter 3, Materials section.

7.2.2 Pre-treatment

Four sets of samples were submitted to the UV treatment. Two of these sets were submitted to two independent pre-treatments, alkali and acetone, prior to the UV treatment.

Alkali treatment is a widely used technique to remove waxes as well as hemicellulose and lignin from plant fibers. Acetone is a commonly used solvent and can also remove waxes in the outer surface of plant fibers. The first reason for the inclusion of these two pre-treatments was to compare the thermal stability of the sole alkali and acetone samples with the UV treated wheat straw samples. The second objective was to investigate the possibility of further increasing the thermal stability of the alkali or acetone treated samples by applying subsequently UV treatment.

The 1 molar alkali pre-treatment applied to the wheat straw samples is described in detail in Chapter 5 (in the Methods section).

The acetone pre-treatment of the wheat straw samples was performed under reflux condition using acetone as solvent. Initially, 10 grams of wheat straw fibers and 150 ml of solvent were placed inside a round bottle flask. The system was refluxed under gentle heating and stirring for 24 hours. After this period of time, the heating was stopped. Then, the mixture was filtered using filter paper and washed twice with ethanol to remove any extracted organic compound present in the solution. Finally, the pre-treated fibers were dried in an oven for 12 hours at 80 ^{o}C.

7.2.3 The Ultraviolet Treatment of the Wheat Straw Samples

A custom built UV radiation treatment system was used in this study to modify the molecular structures of the wheat straw samples. This instrument has the capability to irradiate specimens in a controlled environmental condition. The UV light source incorporated in this system is a 1.8 kW

Fusion UV System F300S unit equipped with a 6 inch microwave-powered electrodeless lamp. The spectral output of this radiation source is shown in Figure 133. This figure shows that the light source emits radiation with wavelengths in the range of 210 and 590 nm. In addition, the output power is the highest for radiation with wavelengths of 380 – 390 nm. Therefore, it is expected that significant chemical alterations on the wheat straw samples can be achieved not only in the surface but also inside the sample. It should be noted that this UV light treatment is fast, chemical-free and performed at room temperature which are advantages in comparison with other methods.

Four sets of experiments using the ultraviolet treatment were conducted. Each batch of irradiated wheat straw sample consists of an initial mass of 1 gram. In order to characterize the effect of UV light intensity, one set of samples (High Set) was exposed to the UV radiation directly (high-intensity group) whereas three sets of samples (Low, Alkali and Acetone Sets) were covered with a thin optical glass slide before the UV treatment (low-intensity groups). Four UV exposure times were studied in each set of samples: 0, 5, 10, and 15 minutes. This range of time was chosen based on the preliminary trials where it was observed that longer periods of exposure to the UV light severely degraded the wheat straw samples (i.e., it produced charred samples). Nitrogen atmosphere was utilized for all the four sets of experiments. After the UV treatment, the samples were removed from the chamber and stored for further analysis. The mass of each sample was recorded before and after the UV irradiation treatment.

The nomenclature used to label all the samples and the treatment conditions are presented in Table 35. The type of wheat straw used, i.e. with or without pre-treatment, is represented in the first part of the label, while the time of the UV treatment is presented in the second part of the label. For example, the label Low_10 min indicates that untreated wheat straw was exposed to the UV treatment during 10 minutes.

Table 35: Table shows the UV treatment conditions, i.e., time, pre-treatment and UV intensity as well as the labels of the samples.

Set of Experiment	Run #	Label	UV exposure (min)	Pre-treatment	UV Intensity
Low Set	1	Low_0min	0	None	Low
	2	Low_5min	5	None	
	3	Low_10min	10	None	
	4	Low_15min	15	None	
Alkali Set	5	Alkali_0min	0	Alkali	Low
	6	Alkali_5min	5	Alkali	
	7	Alkali_10min	10	Alkali	
	8	Alkali_15min	15	Alkali	
Acetone Set	9	Acetone_0min	0	Acetone	Low
	10	Acetone_5min	5	Acetone	
	11	Acetone_10min	10	Acetone	
	12	Acetone_15min	15	Acetone	
High Set	13	High_0min	0	None	High
	14	High_5min	5	None	
	15	High_10min	10	None	
	16	High_15min	15	None	

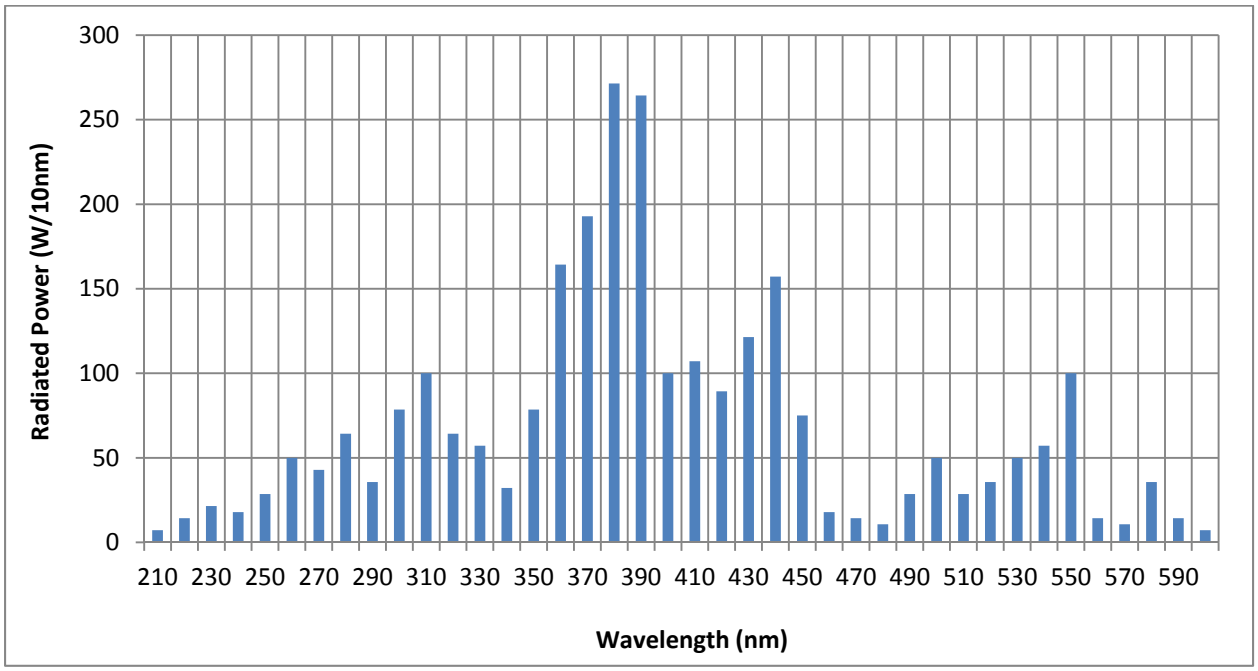

Figure 133: UV emission spectrum of the UV lamp used in the UV treatment (Fusion Systems Inc., 2010).

7.2.4 Thermogravimetry Analysis (TGA)

The thermogravimetry analysis (TGA) of the wheat straw samples was performed under non-isothermal and isothermal conditions. In the case of non-isothermal analysis, the temperature is increased from 35 to 700 °C using a heating rate of 10 °C/min under nitrogen atmosphere. The isothermal analysis was carried out by increasing the temperature from 35 to 250 °C using a heating rate of 50 °C/min (maximum allowed by the instrument). After achieving the target temperature, the wheat straw samples were kept at 250 °C for 30 minutes under nitrogen atmosphere.

7.2.5 Yield

The mass of the wheat straw samples was measured before (W_i) and after (W_f) the UV treatment using an analytical balance. These values were utilized to calculate the yield according with the following equation.

$$\text{Yield (\%)} = \left[1 - \left(\frac{W_i - W_f}{W_i}\right)\right] * 100 \qquad \textit{Equation 14}$$

7.2.6 Fourier Transform Infrared (FTIR) Spectra

The Fourier-transform infrared (FTIR) analysis was carried out with the assistance of a Bruker Tensor 27 FT-IR analyzer. The samples were ground to a fine powder and mixed with potassium bromide (KBr). This mixture was compressed into thin discs using a hydraulic press. These discs were used to obtain the infrared spectrum in the spectral range of 400-4000 cm^{-1}. Thirty-two (32) scans per sample were collected with spectral resolution of 4 cm^{-1}. Baseline correction was performed for all samples spectra using OPUS program.

In order to compare the relative changes in the chemical composition of two different samples, the ratio between two peaks of the same FTIR spectrum it is generally utilized. This way, the sample mass and thickness of the potassium bromate (KBr) disc do not affect the peak intensity. Thus, the intensity of the peak of interest (hemicellulose or lignin) was divided by the intensity of an internal reference peak from the same FTIR spectrum for each sample following the standard procedure reported in the literature (Pandey and Pitman, 2003; Pandey, 2005). The cellulose peak at 1160 cm^{-1} was utilized as internal reference because the intensity of this peak is not significantly affected by alkali and silane treatments (Pandey and Pitman, 2003; Pandey, 2005).

The peak heights were measured from the baseline which was constructed by connecting the lowest data points on either side of the peak. The vertical line between the top of the peak and the baseline represents the peak height.

7.2.7 Chemical Composition Analysis

Chemical composition analysis of the wheat straw samples was carried out by AgriFood Laboratories. This analysis is explained in detail in the Materials and Methods section of the Chapter 3.

7.3 Results and Discussion

7.3.1 The Effect of the Ultraviolet Treatment on the Thermal Stability of the Wheat Straw Samples

The thermal stability of the wheat straw samples was investigated under nitrogen atmosphere using a heating rate of 10 °C/min. Figure 134 shows the TGA curves, for the four sets of experiments Low, Acetone, Alkali and High samples before and after ultraviolet modification. Overall, it is difficult to quantify the starting point of the degradation of the wheat straw samples (i.e. temperature in the TGA curve where the mass starts to drop). However, it is possible to notice in the plots that the starting point of the degradation was shifted to higher temperatures as the time of the UV treatment was increased. The higher gain on thermal stability was achieved when a higher UV radiant power was applied which was the case of the High samples. For example, in Figure 134-D it can be observed that the curve High_15min was displaced 35 °C to the right in comparison with the curve High_0min. This trend was observed for the other three sets of experiments, Low, Alkali and Acetone wheat straw samples, although the gain on thermal stability was more moderate with smaller difference between the starting point of the degradation of the wheat straw samples.

The quantitative comparison of the starting point of the degradation was done by calculating and comparing the temperatures that correspond to 2 % of the weight loss ($T_{2\%}$) of these wheat straw samples. The results are summarized in Figure 135. The $T_{2\%}$ can be obtained from the TGA curves following procedure previously described (Chapter 3).

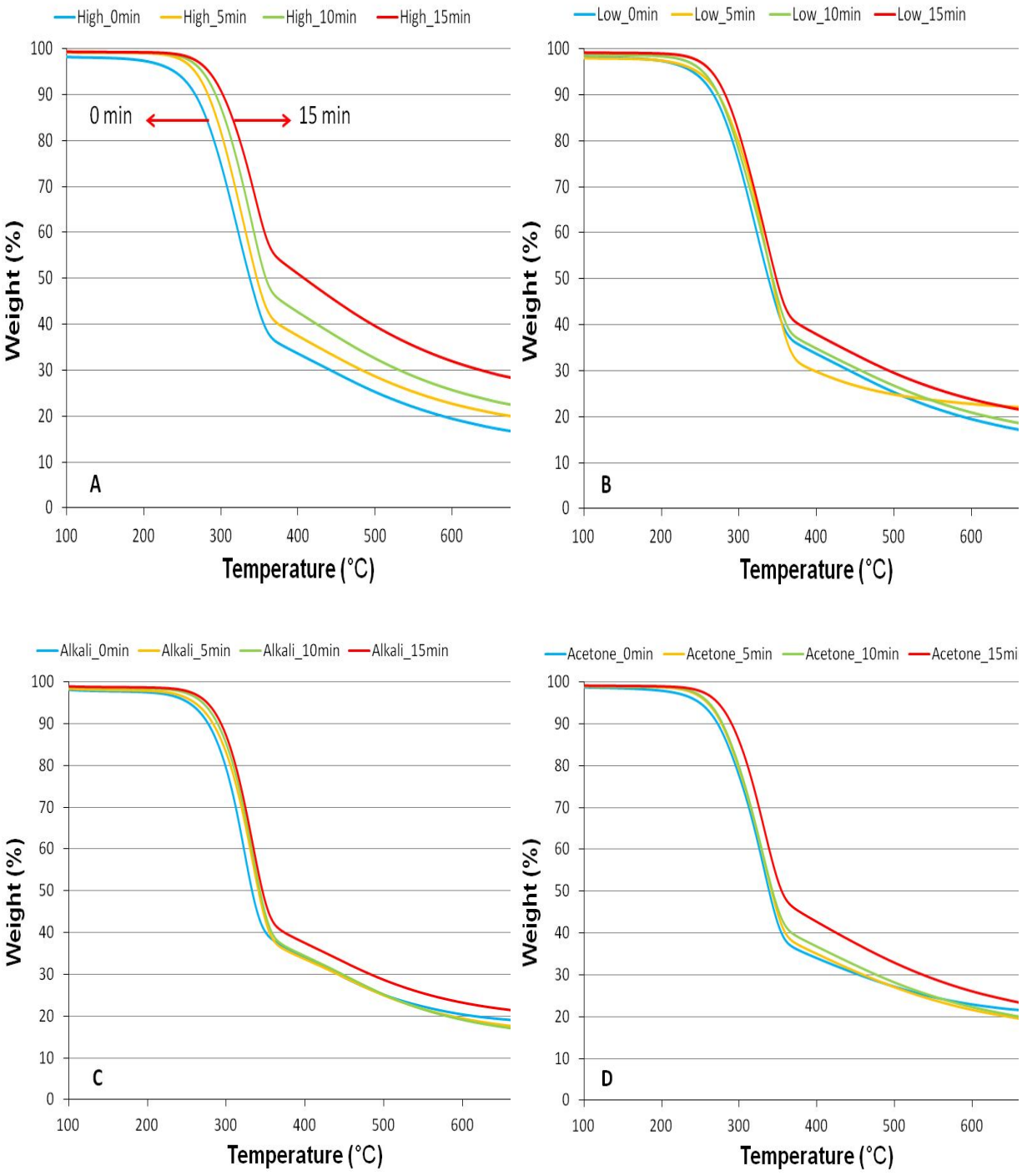

Figure 134: TGA curves for: (A) High, (B) Low, (C) Alkali and (D) Acetone wheat straw samples submitted to 0, 5, 10 and 15 minutes of the UV treatment.

Figure 135 displays the $T_{2\%}$ as function of the UV treatment time for the four sets of experiments. It can be seen that the temperature at 2% weight loss increased as the time of the UV treatment was increased. This temperature increment indicates that the thermal stability of the wheat straw samples was improved by the UV treatment. For example, the Acetone and High samples without any UV treatment (Acetone_0min and High_0min) had the 2 % of the weight lost at 234 and 229 °C, respectively; whereas, the same samples treated during 15 minutes with UV light (Acetone_15min and High_15min) showed the 2 % of weight loss at considerably higher temperatures, 258 and 269 °C, respectively. This represents an enhancement on the thermal stability of 10.2 and 17.5 % for the UV treated Acetone and High samples, respectively. In the case of the Alkali and Low wheat straw samples the gain after 15 minutes of UV treatment was more modest. While the first sample has the thermal stability increased by 7.6 % (from 245 to 263.7 °C), the second one displays an increment of 9.5 % (from 229 to 250.7 °C) in the temperature at 2 % of weight loss.

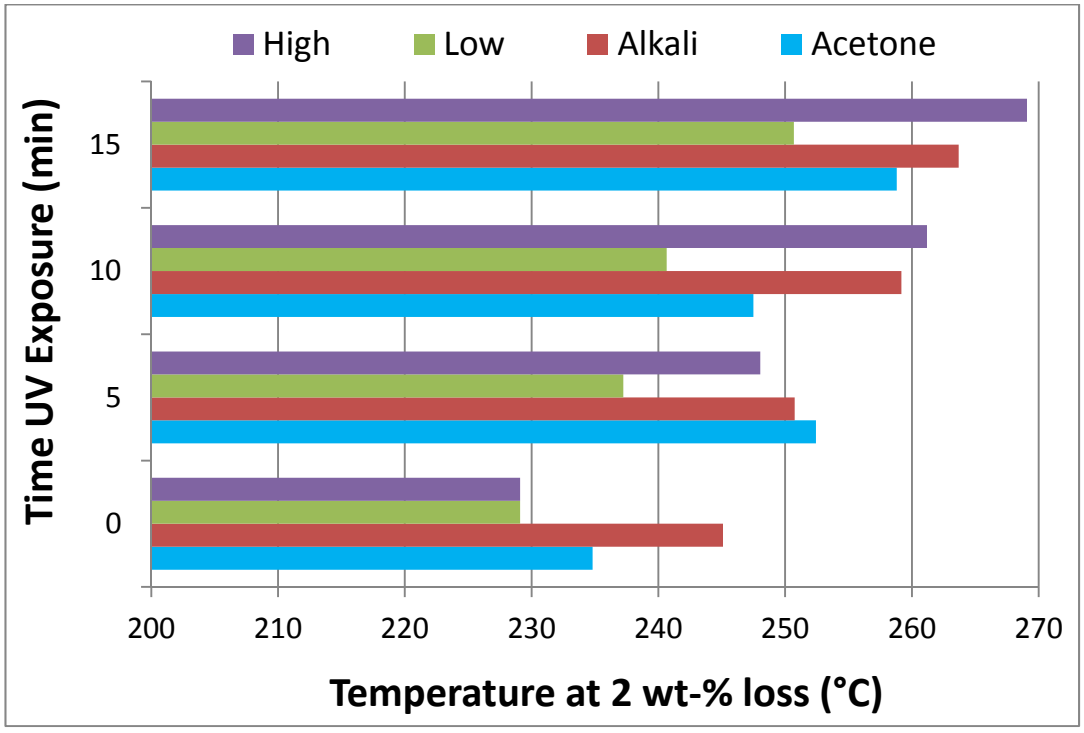

Figure 135: Temperature at 2 % weight loss as a function of the UV treatment time for all the four sets of experiments.

Another way to evaluate the thermal stability is to consider the temperatures at which the degradation starts (called onset temperature), the temperature at which the rate of degradation is maximum (referred as maximum temperature) and the temperature at which the degradation ends (named finishing temperature). These temperature peaks can be obtained from the derivative thermogravimetry curves (DTGA) in Figure 136, following the procedure depicted in Figure 137. Table 36 summarizes these peaks temperatures for the untreated and UV treated samples. The peak onset, peak maximum and peak finishing temperatures at which weight losses have occurred are consistently higher for the UV treated samples compare to the untreated samples. For example, when the UV treatment is not applied, the High and Alkali samples (High_0min and Alkali_0min) have the onset peak temperature at 135 and 175 °C, respectively; while, the same samples after 15 minutes of the UV treatment (High_15min and Alkali_15min) display the onset peaks at higher temperature, 195 °C.

The same trend of increasing the onset peak temperature is observed for Low and Acetone samples. When the UV treatment is applied for 15 minutes to the Low and Acetone samples (Low_5min and Acetone_15min), the onset peak temperature is increased by 30 and 45 °C, respectively.

Although no report on the literature was found regarding the use of UV irradiation to improve the thermal stability of plant fibers, there are several reports in the literature dealing with UV irradiation of wood products in general. Different studies have reported the effects of the UV light on wood and its components. For example, Hon and Chang (1984) have found that UV light degradation of yellow pine wood occurs through removal of lignin. After 40 days of exposure to UV light, the lignin content was decreased from 28 to 14.5 % which represents a reduction of 48 % in the original amount of lignin. In agreement with that, Muller et al. (2003) have observed that only 72 hours of exposure to the UV irradiation with intensity of 50 $mW.cm^{-2}$ and wavelength higher than 300 nm was sufficient to decrease the lignin content of spruce wood by up to 20 % of the initial value.

In addition, the results presented by Deka et al. (2008) suggest that, not only lignin, but also hemicellulose is affected by UV light. This conclusion was based on the fact that the intensities of the absorption bands at 1508 and 1264 cm^{-1} (due to lignin) and 806 cm^{-1} (credited to hemicellulose) were reduced.

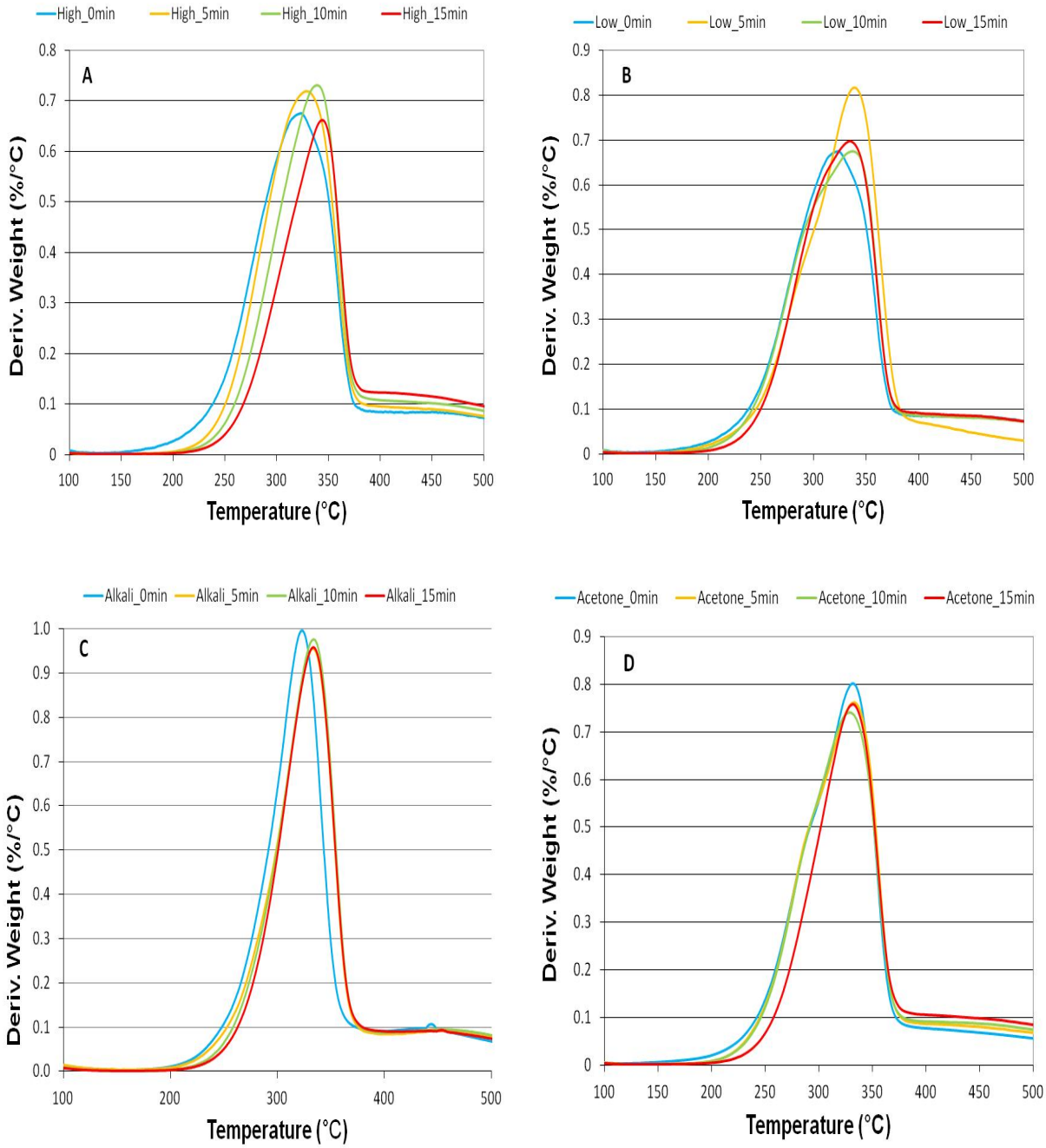

Figure 136: DTGA curves for: (A) High, (B) Low, (C) Alkali and (D) Acetone wheat straw samples submitted to 0, 5, 10 and 15 minutes of the UV treatment.

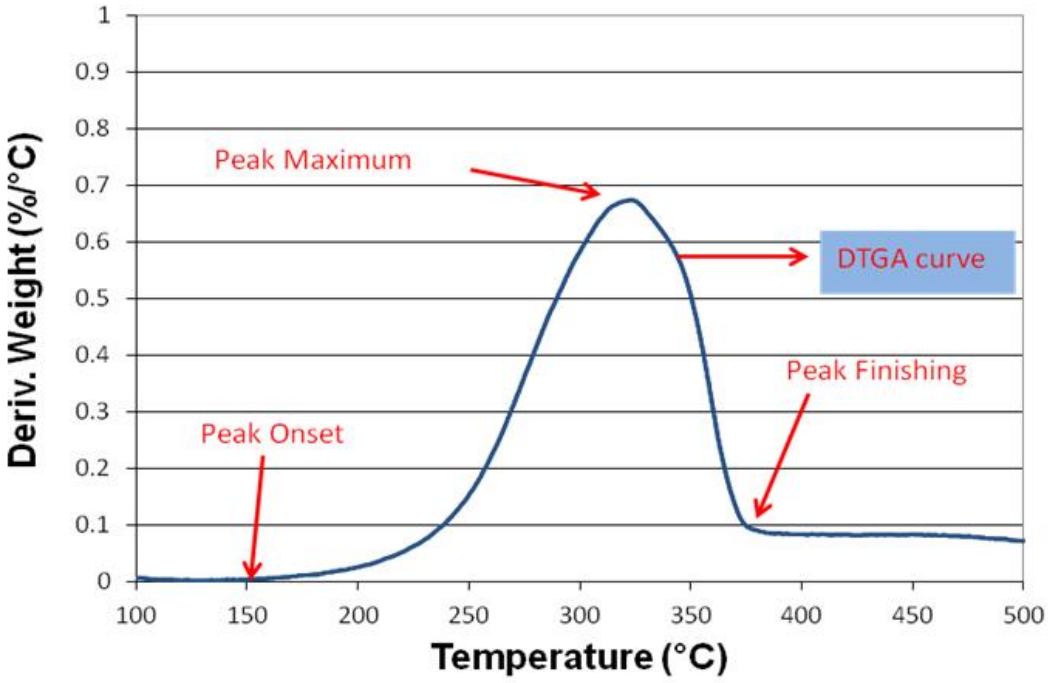

Figure 137: Procedure utilized to obtain the peak onset, peak and peak finishing temperatures from DTGA curves.

Some researchers have suggested that the removal of (or changes to) hemicellulose and lignin might lead to better thermal stability. Zhang et al. (2008) have studied the effect of the combination of steam explosion and biodegradation on the wheat straw fiber. They achieved different lignin content removal and consequently different degrees of thermal stability improvement. The highest enhancement on the temperature of degradation of the wheat straw was accomplished by the sample with the highest lignin elimination, 55.4 %. In the same fashion, Feng et al. (2008) claim that removing pectin, hemicellulose and lignin from hemp fiber has great efficacy on shifting to higher temperatures the beginning of the degradation of hemp fiber. Similarly, Alemdar and Sain (2008) argue that alkali treated wheat straw presented a 17 °C improvement in its temperature of degradation in comparison with untreated wheat straw. Once more, the higher thermal stability is attributed to the lower lignin content obtained after the alkali treatment. Therefore, it is reasonable to suggest that in the present study, the UV treated wheat straw samples demonstrate better thermal stability due to the

reduction or modification of the lower thermal stable components, most probably lignin and hemicellulose.

Table 36: The peak onset, peak and peak finishing temperatures for the High, Low, Alkali and Acetone samples obtained from DTGA thermograms.

Label	UV Exposure (min)	Onset Temperature (°C)	Peak Temperature (°C)	Finishing Temperature (°C)
High_0min	0	135	323	375
High_5min	5	170	333	380
High_10min	10	190	338	385
High_15min	15	195	344	385
Low_0min	0	135	323	375
Low_5min	5	155	339	390
Low_10min	10	155	336	385
Low_15min	15	165	334	380
Alkali_0min	0	175	322	370
Alkali_5min	5	185	333	380
Alkali_10min	10	185	334	380
Alkali_15min	15	195	333	380
Acetone_0min	0	135	330	375
Acetone_5min	5	170	332	380
Acetone_10min	10	175	328	380
Acetone_15min	15	180	331	380

Another indication that organic material has been removed or modified is given by the ash content analysis. This analysis measures the amount of inorganic material left at 600 °C under air atmosphere. In the case of wheat straw and other plant fibers, the percentage of ash content reflects mostly the amount of silica present. The typical ash content of the wheat straw fiber is in the range of 4.5 and 9 % and from this percentage between 3 to 7 % is silica. The actual values of ash and silica content vary

depending on factors such as variety, age and region of cultivation of the wheat crop (James et al., 1997 or Hornsby[1] et al., 1997).

Figure 138 shows that the amount of inorganic material has slightly increased as time of the UV treatment is increased. One plausible explanation for this observation is that the UV treatment has extracted a small amount of organic materials from the wheat straw samples. Even though, the ash content analysis cannot identify the organic materials being removed, lignin and hemicellulose are the most likely candidates based on the literature reports (Deka et al., 2008; Hon and Chang, 1984; Muller et al., 2003).

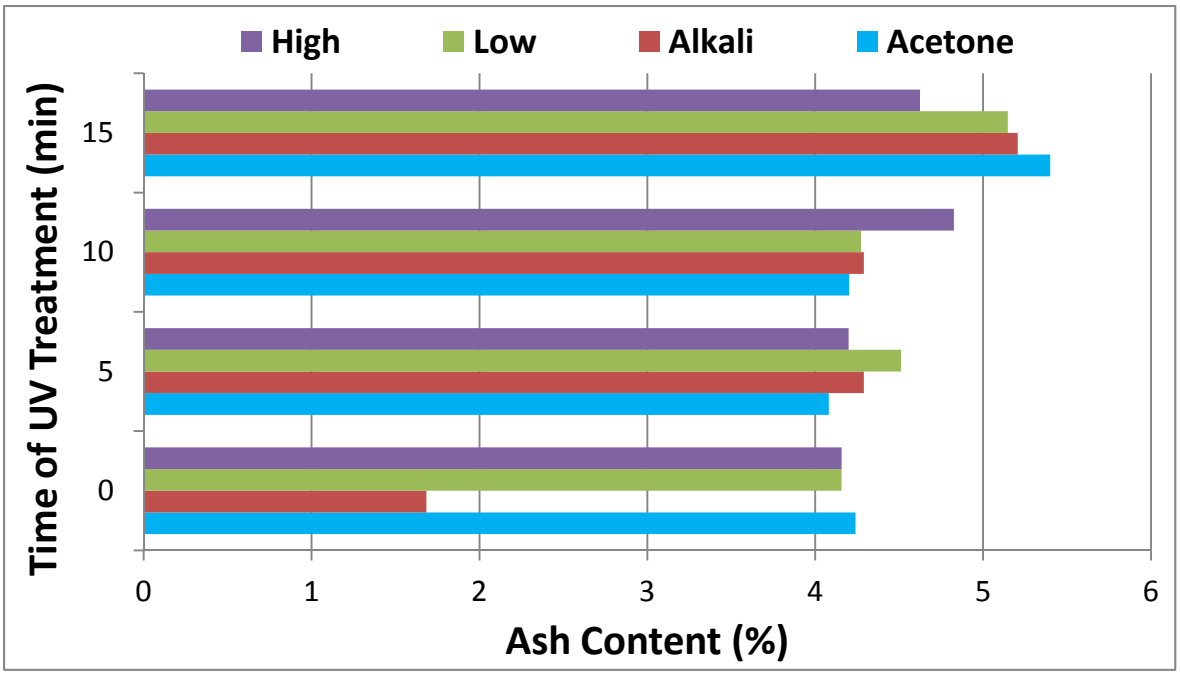

Figure 138: Ash content (weight left at 600 °C under air atmosphere) as a function of the UV treatment time.

This behavior has also been described by others researchers. Feng et al. (2008) have reported that treating hemp fibers with an alkali solution at 150 °C removes hemicellulose and lignin up to 79.1 and 83.5 %, respectively. In agreement with that, Ray et al. (2002) have found that alkali treated jute fiber have a 41% decrease on the hemicellulose content, while the ash content of these alkali treated

fibers has considerably increased from 15 to 22 %. In the same way, Saha et al. (1991) have observed that alkali treatment significantly decreases the hemicellulose content of pineapple leaf fibers. According to the authors, the removal of hemicellulose caused the formation of a lignin-cellulose complex with higher thermal stability which is translated in increased ash content.

Different studies have suggested that alkali treatments extract both organic and inorganic material from plant fibers. It is reported by Xiao et al. (2001) that 1 M NaOH solution was able to eliminate roughly 90 % of the original silica from maize stems, rye straw and rice straw. Likewise, Islam et al. (2011) have observed a 92 % decline in the ash content percentage after treating hemp fibers with an alkaline solution. These findings are in agreement with our study. The alkali wheat straw samples displays the highest increment on ash content increasing from 1.7 to 5.2 % for the untreated (Alkali_0min) and 15 minutes UV treated (Alkali_15min) samples, respectively. The lower initial ash content value of the Alkali_0min sample might be due to removal of silica during the alkali treatment.

Figure 139 displays the results for isothermal gravimetric analysis, where the samples were kept at the constant temperature of 250 °C for 30 minutes under nitrogen atmosphere. The main objective of this analysis was to mimic the thermal conditions to which the fibers will be exposed during the composite preparation and observe the thermal degradation behavior of the wheat straw samples.

It can be seen from Figure 139 that overall, increasing the time of the UV treatment decreases the weight loss due to thermal degradation. The curves representing 15 minutes of UV treatment (High_15min, Low_15min, Alkali_15min and Acetone_15min - curves in red color) are depicted at the top of the graphs, where the degradation is smaller. This behavior is more pronounced in the case of the High samples. The untreated wheat straw sample (High_0min) shows a steep decline of the weight when exposed to the temperature of 250 °C (Figure 139-D). While the initial weight has decreased to 89.6 % in the first 5 minutes, after 30 minutes of exposure to 250 °C, only 78.5 % of the initial weight is left. This drop of 22.5 % in the initial weight represents a major thermal degradation.

In contrast, treating the wheat straw fiber with UV irradiation for 15 minutes (High_15min) was able to dramatically reverse this trend. The first 5 minutes at 250 °C decreased the initial weight to 96.5 % which represents a weight loss of only 4.5 %. Even after 30 minutes of heating, the weight left is 91.04 % which gives a weight loss of only 9 %. These numbers demonstrate the great potential of the UV treatment for improving thermal stability of plant fibers.

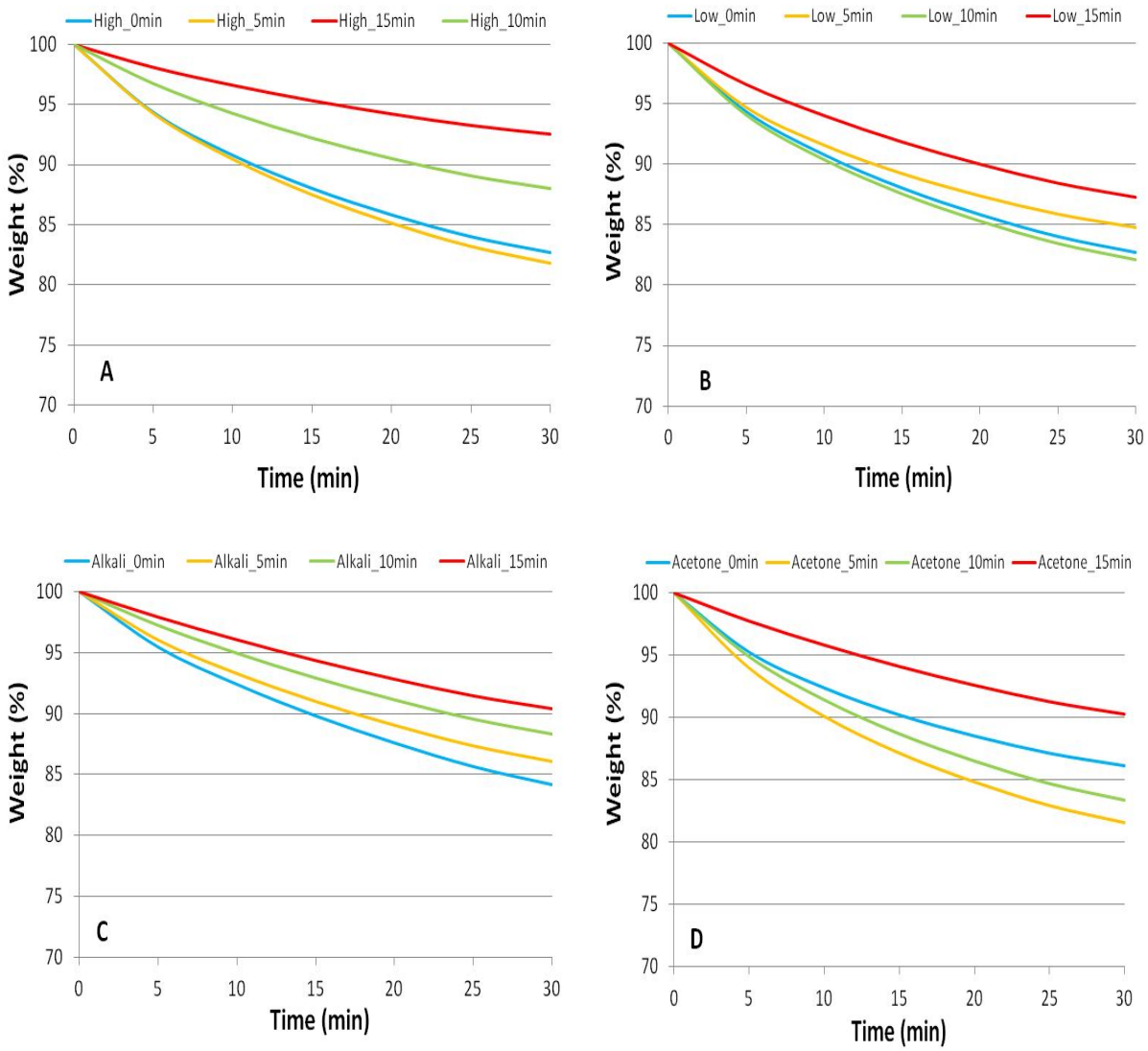

Figure 139: Isothermal curves obtained at 250 °C under nitrogen atmosphere for: (A) High, (B) Low, (C) Alkali, and (D) Acetone samples submitted to 0, 5, 10 and 15 minutes of UV treatment.

It is important to bring this study in the context of manufacturing thermoplastic composites. The time that wheat straw fiber remains inside the polymer processing equipment (extruder and injection molding machines), or residence time, is an important parameter to determine how long the fibers have to resist to thermal degradation in order to be employed in commercial applications. In the case of small car parts such as interior storage bin, door trim panel components and armrest liners, the

estimated total time that the material remains at elevated temperatures is less than 10 minutes (including the time for extrusion compounding, injection molding and cooling). In an attempt to estimate the degradation of wheat straw fiber during comparable time, the weight percentage at 10 minutes under isothermal conditions was obtained from the plots in Figure 139 (as illustrated in the Materials and Methods section of Chapter 3).

Figure 140 exhibits the performance of the different pre-treatments and the UV treatment. Overall, the samples without the UV treatment have a steeper decrease on the weight in comparison with the samples treated with UV irradiation. Also, it is important to highlight that the UV treatment alone is able to deliver better thermal stability enhancement within shorter treatment time than sole alkali or any other pre-treatments. For example, the enhancement on the thermal stability of the sample High_15min is enough to allow this sample to be processed at 250 °C for 10 minutes (5 minutes non-isothermal + 10 minutes isothermal) with a weight loss of only 4.9 %. In contrast, when only the alkali treatment is applied, the wheat straw sample (Alkali_0min) has a severe thermal degradation after 10 minutes of exposure to 250 °C with a weight loss of 11.3 %. Note that the total treatment time for the UV treated sample (High_15min) was 15 minutes; whereas, the treatment time required by the alkali treated sample (Alkali_0min) was 24 hours.

In addition, the thermal stability of the alkali pre-treated wheat straw sample was further improved upon application of the UV treatment. The alkali sample submitted to UV irradiation for 5 minutes, Alkali_5min, showed a weight loss of 9.1 %; whereas, 15 minutes of UV treatment reduced the weight loss of the Alkali_15min sample to only 5.2 %.

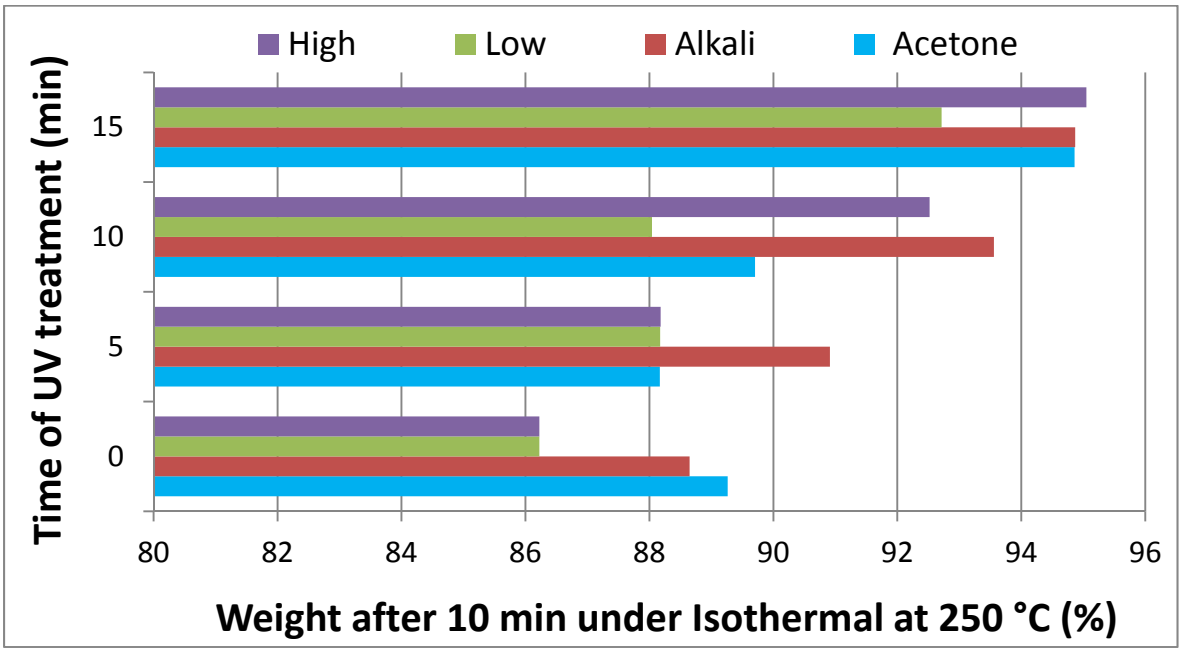

Figure 140: The weight percentage left after 10 minutes under isothermal heating at 250 °C is plotted against the time of UV treatment.

3.1 Yield and Color Changes after the Ultraviolet Treatment

The yield is defined here as the mass obtained after a treatment and calculated according to the equation presented before (in the Materials and Methods section). When evaluating the feasibility of implementing a specific thermal, physical or chemical treatment for commercial applications, the yield is valuable information. The higher the yield is the higher will be the productivity of this process.

Therefore, the yield obtained after the UV treatment is presented as a function of the UV exposure time in Figure 141.The figure reveals that there is a trend to reduce the yield with the increasing of the time of the UV treatment for all the samples. This reduction is more apparent after 10 and 15 minutes of UV exposure. The decline in the yield is more severe for the High samples, followed by Acetone and Low samples. For example, after 15 minutes of the UV treatment, the yield is 68.2, 75.1 and 82.3 % of the initial mass for High_15min, Acetone_15min and Low_15min samples, respectively. When considering only the UV treatment, the smallest drop in the yield is achieved by the Alkali_15min sample which presents a yield of 84.4 %. This high yield of the alkali pre-treated

samples after the UV treatment is likely due to the alkali pre-treatment which removed great amounts of the hemicellulose and lignin present in the wheat straw. When the UV treatment is applied, the remaining amount of organic material (possibly lignin and hemicellulose) that may be extracted is smaller and therefore, there is a smaller mass reduction.

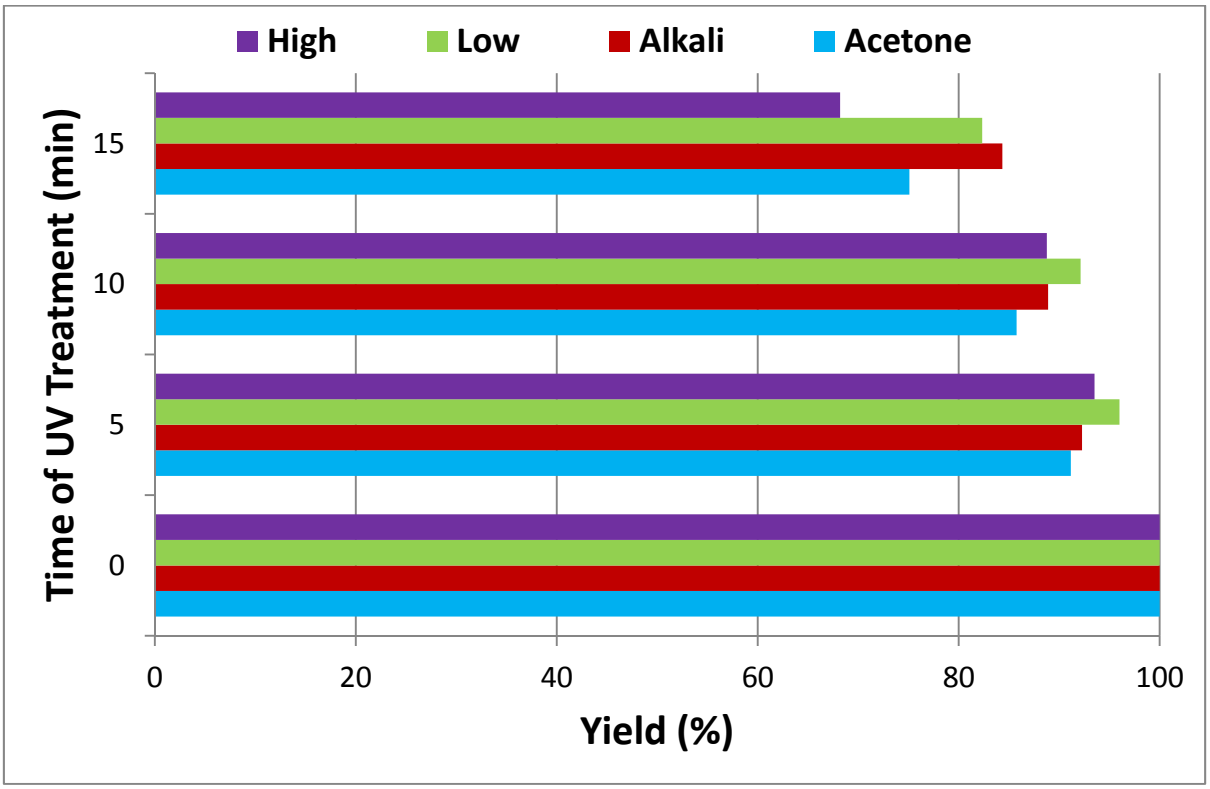

Figure 141: Yield percentage obtained after the UV treatment as a function of the UV exposure time.

The reduction in yield with chemical treatment has been well documented. Varma et al. (1984) reported that 3 hours of treatment with a solution of sodium hydroxide (10 %) at 30 °C removed 9.3 % of the original mass of coir fiber. However, if more severe conditions are used, the mass reduction is even higher. Xiao et al. (2001) have treated maize stems, rye straw and rice straw with 1 M of sodium hydroxide at 30 °C for 18 hours and obtained 49, 53.7 and 32 % of the original mass, respectively. They attributed this small yield to the dissolution of most of the lignin and hemicellulose of maize stem, and rye and rice straws.

Similarly, during the research conducted for this thesis, the pre-treatment of the wheat straw fiber with alkali solution yielded 45 % of the initial mass. Taking into account the additional mass loss during the UV treatment (yield of 84.4 %), the combination of the alkali and UV treatments yielded only 38 % of the initial mass in the case of the Alkali_15min sample. Therefore, the sole UV treated samples High_15min and Low_15min have a higher yield (68.2, and 82.3 % of the initial mass, respectively) than the Alkali_15min sample (38 % of the initial mass).

In addition, the changes in the yield can directly be related to the changes in color. In Figure 142, it is possible to note that the highest shift to darker color is shown by High_15min and Acetone_15min samples which also exhibited the lowest yield among all the samples: 68.2 and 75.1 %, respectively. On the other hand, the samples Low_5min and Alkali_5min kept their original light yellow color almost intact and are among the highest yields obtained with 96 and 92.3 %, respectively. Thus, it is possible to conclude that as the wheat straw fiber degrades, the color tends to get darker with concomitant reduction of the yield.

Moreover, Figure 142 shows that the samples become systematically darker as the UV treatment time increases. The trend for change in color (perhaps towards darker shades of the same colors) is more apparent after 10 and 15 minutes of UV exposure and implies more severe photodegradation of the wheat straw samples. These observations are consistent with the findings of Muller et al. (2003) which describe the tendency of spruce wood to change its color from light to dark yellow with increasing UV irradiation time. The authors argued that the color changes, especially photoyellowing, of the UV irradiated samples can be correlated to lignin degradation. Similarly, Deka et al. (2008) studied the effect of long term exposure to UV light on untreated as well as chemically and thermally treated spruce wood. It was found that rapid and drastic color changes occurred for all three samples in the first 100 hours of UV exposure. However, this change was more apparent in the case of untreated wood which presented an overall color change value 77 and 45 % bigger than the value for thermally and chemically treated wood, respectively. Once more those authors attributed the color changes to depolymerisation and oxidation of lignin and other non-cellulosic polysaccharides such as hemicellulose.

(A-1) High_0min **(A-2) High_5min** **(A-3) High_10min** **(A-4) High_15min**

(B-1) Low_0min **(B-2) Low_5min** **(B-3) Low_10min** **(B-4) Low_15min**

(C-1) Acetone_0min **(C-2) Acetone_5min** **(C-3) Acetone_10min** **(C-4) Acetone_15min**

(D-1) Alkali_0min **(D-2) Alkali_5min** **(D-3) Alkali_10min** **(D-4) Alkali_15min**

Figure 142: Photos of the High (A), Low (B), Acetone (C) and Alkali (D) wheat straw samples submitted to 0, 5, 10 and 15 minutes of the UV treatment.

The mechanism of removal of lignin and hemicellulose by UV has been discussed in the literature. It is comprised of complex photochemical reactions. Initially, UV light is absorbed by the plant fiber

components generating free radical species. Then, these species react with oxygen causing oxidation and ultimately photo-degradation of lignin and hemicellulose. The lignin decay can be confirmed by observing the steep decrease on the characteristic aromatic of lignin band at 1510 cm^{-1} and the formation of carbonyl groups. These new carbonyl bands in the region below 1700 cm^{-1} and region between 1700 and 1750 cm^{-1} indicate that there is oxidation of the plant fiber components (Deka et al., 2008; Muller et al., 2003; Hong and Chang, 1984).

When evaluating the potential of the alkali, acetone and UV treatments for developing new technology, it is important to consider three factors together: a) improvement on thermal stability, b) yield and c) time of treatment. Table 37 presents the samples label, the time of pre-treatment and/or UV treatment, the yield, the temperature at 2 % of weight loss ($T_{2\%}$), the weight at after 10min at 250 °C and the onset temperature for the Low_0min, Alkali_0min, Acetone_0min, High_15min and Low_15min samples.

Table 37: Time of treatment, yield and thermal stability ($T_{2\%}$, Wt250 and Onset temperature) of Low_0min, Alkali_0min, Acetone_0min, High_15min and Low_15min samples.

Sample	Pre-treatment	UV Treatment	Yield (%)	$T_{2\%}$ [1] (°C)	Wt250 [3] (%)	Onset Temp. [4] (°C)
Low_0min	Zero	Zero	NA [2]	229.1	86.2	135
Alkali_0min	24 hours	Zero	45	245	88.3	175
Acetone_0min	8 hours	Zero	70	234	89.3	135
High_15min	Zero	15 minutes	68.2	269	95	195
Low_15min	Zero	15 minutes	82.3	250.7	92.7	165

1: the temperature at 2 % weight loss; 2: Not Applicable; 3: Weight after 10minutes at 250 °C 4: Temperature from DTGA curves.

The comparison between the two pre-treatments utilized in this study, reveals that alkali pre-treatment presents higher improvement on the thermal stability of wheat straw fiber than acetone pre-treatment. The results show (Table 37) that the temperature at 2 % of weight loss ($T_{2\%}$) increases from 229.1 (Low_0min) to 245 and 234 °C in the case of alkali and acetone pre-treatments, respectively. Similarly, the weight percentage after 10 min under 250 °C has improved from 86.2 (Low_0min) to

88.3 and 89.3 % (alkali and acetone samples, respectively). Although the improvement on thermal stability is higher applying the alkali pre-treatment, the alkali yield is considerably lower than the acetone yield and the time employed for the alkali pre-treatment is greater than the time for acetone pre-treatment. Whereas 24 hours of the alkali pre-treatment yields 45 % of the initial mass, the acetone pre-treatment requires 8 hours to deliver 70 % of the starting mass.

In contrast, the sole UV treatment can provide higher thermal stability and yield within shorter time than the sole alkali pre-treatment. Whereas UV treatment (High_15min) was able to increase by 40 °C the $T_{2\%}$ of the wheat straw fiber from 229 to 269 °C, the alkali pre-treatment (Alkali_0min) raised by 16 °C the $T_{2\%}$ of the wheat straw fiber from 229 to 245.1 °C (Table 37). Furthermore, the UV treated sample (High_15min) presented 6.7 % lesser weight loss after 10 minutes at 250 °C and 20 °C higher onset temperature of degradation than in the case of alkali treated sample (Alkali_0min), as illustrated by Table 37. Besides the lower improvement on thermal stability, the alkali treated sample (Alkali_0min) also exhibited 23.2 % lower yield than the UV treated sample (High_15min). While the alkali treated sample presented 45 % of yield, the UV treated sample showed 68.2 %. However, the most remarkable advantage of the UV over the alkali treatment is the difference in the time necessary for each one of these treatments. Whereas the alkali pre-treatment requires more than 24 hours, the UV treatment takes only 15 minutes.

The experimental results for the Low_15min and High_15min samples also reveal that the higher UV intensity can provide greater thermal stability at the expense of lower yield. Table 37 shows that the $T_{2\%}$ and onset temperature of degradation of the High_15min sample were improved by 18.3 °C (from 250.7 to 269 °C) and 30 °C (from 165 to 195 °C) with respect of the Low_15min sample. In the same fashion, the weight percentage after 10 min under 250 °C had a greater enhancement when the higher UV intensity was used. While the Low_15min sample has a weight of 92.7 %, the High_15min keeps 95 % of the initial mass. Despite the better thermal stability, the yield obtained for the higher UV intensity treatment (High_15min) is 14.1 % lower than in the case of the lower UV intensity treatment (Low_15min). While the yield after the higher UV intensity treatment (High_15min) was 68.2 %, the yield for the lower UV intensity treatment (Low_15min) reached 82.3 %.

This research has shown that there are significant differences in the thermal stability and yield of straw produced by chemical or UV treatments. It has also investigated some of the variables

associated with this process. It was not the objective of this study to optimize the processing conditions, but rather to evaluate and compare new methodologies for improving the thermal stability. An optimization study would require a target set of attributes or properties, which unfortunately do not exist yet because this is a new technology.

7.3.2 The Effect of the Ultraviolet Treatment on the Chemical Composition of the Wheat Straw Samples

Fourier Transform Infrared (FTIR) spectroscopy is a well established technique used to obtain qualitative and quantitative information about the functional groups present in a material. The FTIR spectrum consists of a plot of wavelength (in the range of 400 to 4000 cm^{-1}) versus transmittance or absorbance.

The chemical bonds belonging to a molecule absorb infrared light in different regions of the FTIR spectrum, depending on the elements and the type of bonds present in this molecule. The position (wavelength) and height of these peaks will change if a chemical modification in a material occurs. By comparing the position (wavelength) and/or the intensity (height) of the peaks in the FTIR spectra of the wheat straw fiber before and after the UV treatment, it is possible to identify changes in the chemical composition of the sample.

Figure 143 shows the typical FTIR spectrum for wheat straw which is very complex because of the overlapping of the peaks. The highlighted region (1400-1900 cm^{-1}) is called carbonyl zone or fingerprint region. The 1400-1900 cm^{-1} region contains most of the characteristic peaks of lignin and hemicellulose. For example, the absorption peaks at wavenumber of 1600, 1510, and 1265 cm^{-1} are attributed to the C=C stretching vibrations of the benzene ring occurring in lignin (Muller et al., 2003; Panthapulakkal et al., 2006; Hon and Chang, 1984). In the same way, hemicellulose is identified by the characteristic peaks at 900 and between 1720 and 1737 cm^{-1} which represent carboxyl groups (Hon and Chang, 1984; Panthapulakkal et al., 2006). Molecular and chemical changes of lignin and hemicellulose can be investigated by observing variations on these characteristic bands.

Figure 144 shows the carbonyl zone (1400-1900 cm^{-1}) of the FTIR spectra of the wheat straw samples before and after the UV treatment. Overall, it can be seen in Figure 144 that the intensity of the absorption bands (i.e. height of the peaks) of hemicellulose and lignin has systematically decreased as the time of the UV treatment is increased.

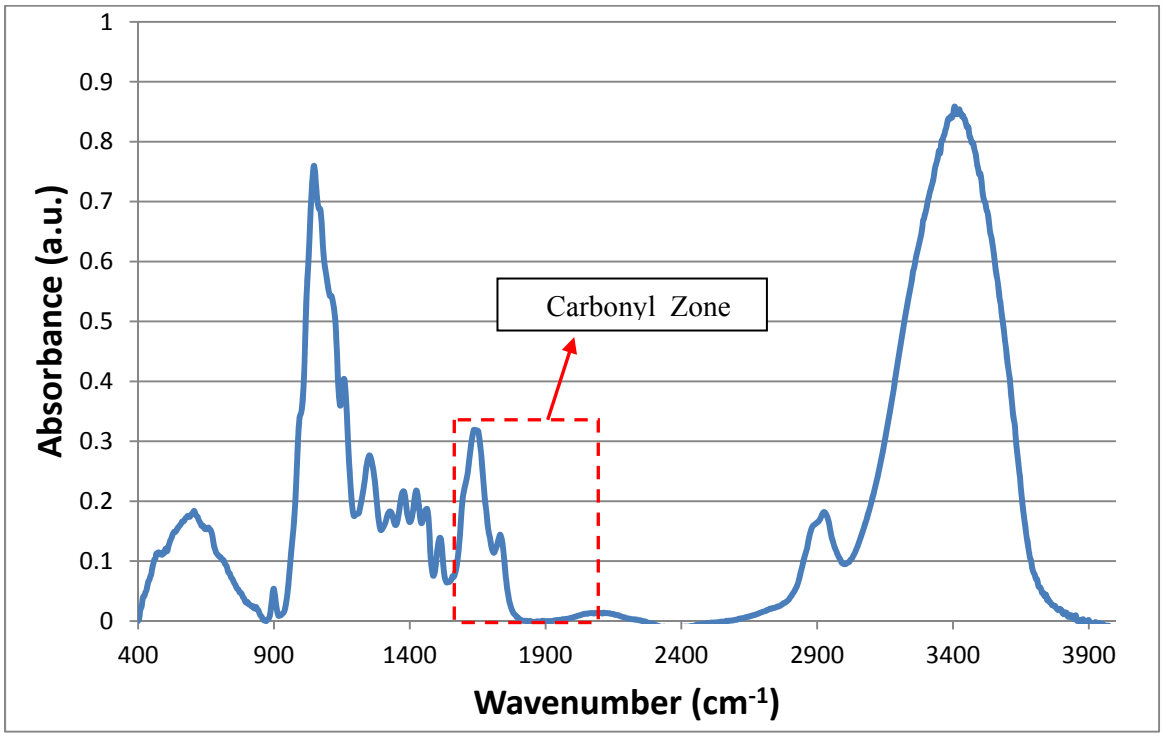

*Figure 143: FTIR spectrum of the untreated wheat straw (*Low_*0min) highlighting the carbonyl zone (1400-1900 cm^{-1}).*

In the case of the Alkali samples, Figure 144 (bottom) shows that the characteristic absorption bands of hemicellulose between 1735 and 1720 cm^{-1} had disappeared. This suggests the removal of a high amount of hemicellulose. This supposition was already confirmed with chemical composition analysis in the previous chapter (Results and Discussion of the Mechanical Set section). However, it seems that the hemicellulose removal is due to the alkali treatment rather than the UV treatment because the alkali treated sample not submitted to the UV treatment (Alkali_0min) already does not have the hemicellulose peak (1735 and 1720 cm^{-1}).

Compared to the Alkali samples set, the Low, High, and Acetone samples sets have only a decrease in the intensity of the hemicellulose peaks (between 1735 and 1720 cm^{-1}) rather than complete disappearance of this peak. In addition, the hemicellulose peak decrease was caused by the UV treatment in the case of the Low, High, and Acetone samples sets. For example, the hemicellulose peak intensity is higher for the untreated wheat straw samples (Low_0min and Acetone_0min) than for any of the UV treated samples, e.g., samples Low_5min, High_5min and Acetone_5min.

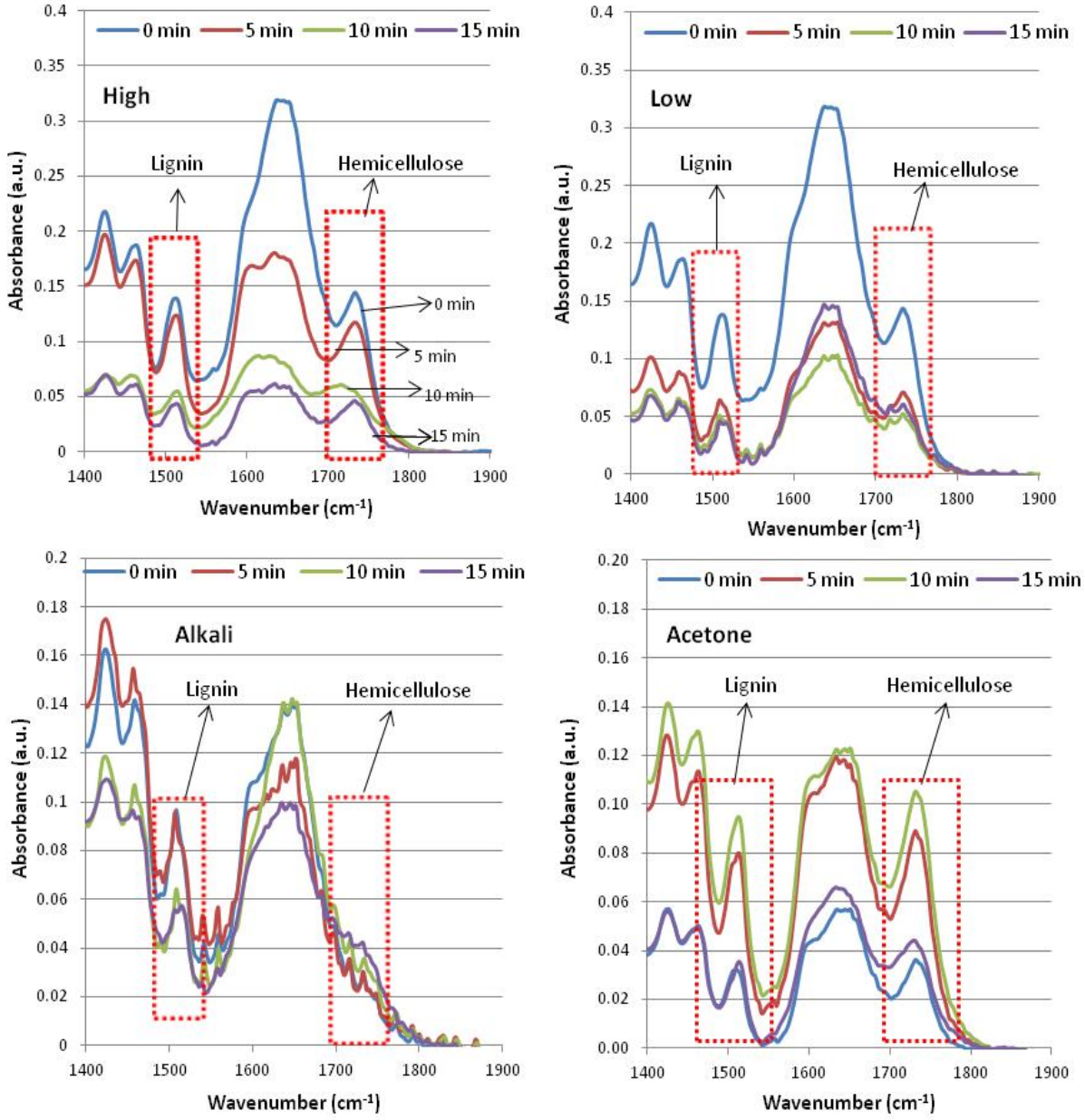

Figure 144: FTIR spectra of samples Acetone, Alkali, High and Low sets of wheat straw samples exposed to the UV treatment for various periods.

Figure 144 also shows that there is intensity (i.e. height) reduction of the lignin characteristic peak at 1510 cm^{-1} after the UV treatment for all the samples (i.e., Alkali, Acetone, Low and High). This

observation could indicate that lignin has been partially removed or perhaps transformed into another chemical compound. In fact, lignin is the most affected compound by UV light according to many reports in the literature (Hon and Chang, 1984; Muller et al., 2003; Deka et al., 2008).

In addition, it appears from Figure 144 (Low and High) that the peak around 1650 cm^{-1} (between 1600 and 1700 cm^{-1}) has its intensity decreased and shape changed to multiple sub-peaks with increasing time of UV exposure. These observations suggest that some of the chemical bonds are disappearing and perhaps new ones are being formed. For example, the photo-induced oxidation of lignin can produce quinone compounds which have a characteristic peak between 1650-1690 cm^{-1} (Agarwal, 1998; Muller et al., 2003).

In order to confirm these observations, the ratio between the intensities of the peaks of interest (hemicellulose, lignin and 1650 peak which could indicate quinone structures) and one internal reference peak (1160 cm^{-1}) was used to compare the samples.

As discussed before in the previous chapter (Results and Discussion of the Mechanical Set), it is more representative and common practice to compare different samples by using the ratio between a characteristic peak and an internal reference peak instead of comparing the intensities of only one characteristic peak. The peak at 1160 cm^{-1} was utilized as internal reference because the intensity of this peak is not significantly affected by UV irradiation according to reports in the literature (Pandey and Pitman, 2003; Pandey, 2005).

Figure 145 shows the hemicellulose, lignin and 1650 peak ratios for the Low and High UV treated wheat straw samples. It can be seen in Figure 145 that the hemicellulose ratio has a mild decrease especially after 15 minutes of exposure to the Low UV treatment. On the other hand, the lignin ratio is slightly increasing up to 10 minutes and then has a small decrease at 15 minutes of Low UV treatment. Similarly, when High intensity UV treatment is used, the hemicellulose and lignin ratios seem to slightly increase up to 10 minutes. However, after that, the lignin ratio continues to increase whereas there is a very small decrease in the hemicellulose peak at 15 minutes of exposure to the High UV treatment.

However, these changes on the hemicellulose and lignin ratios of the Low and High samples are very small which could indicate that overall hemicellulose and lignin content are nearly constant. These observations are partially confirmed by the chemical composition results of the untreated and two UV treated samples (Low_10min and High_10min) presented in Figure 146.

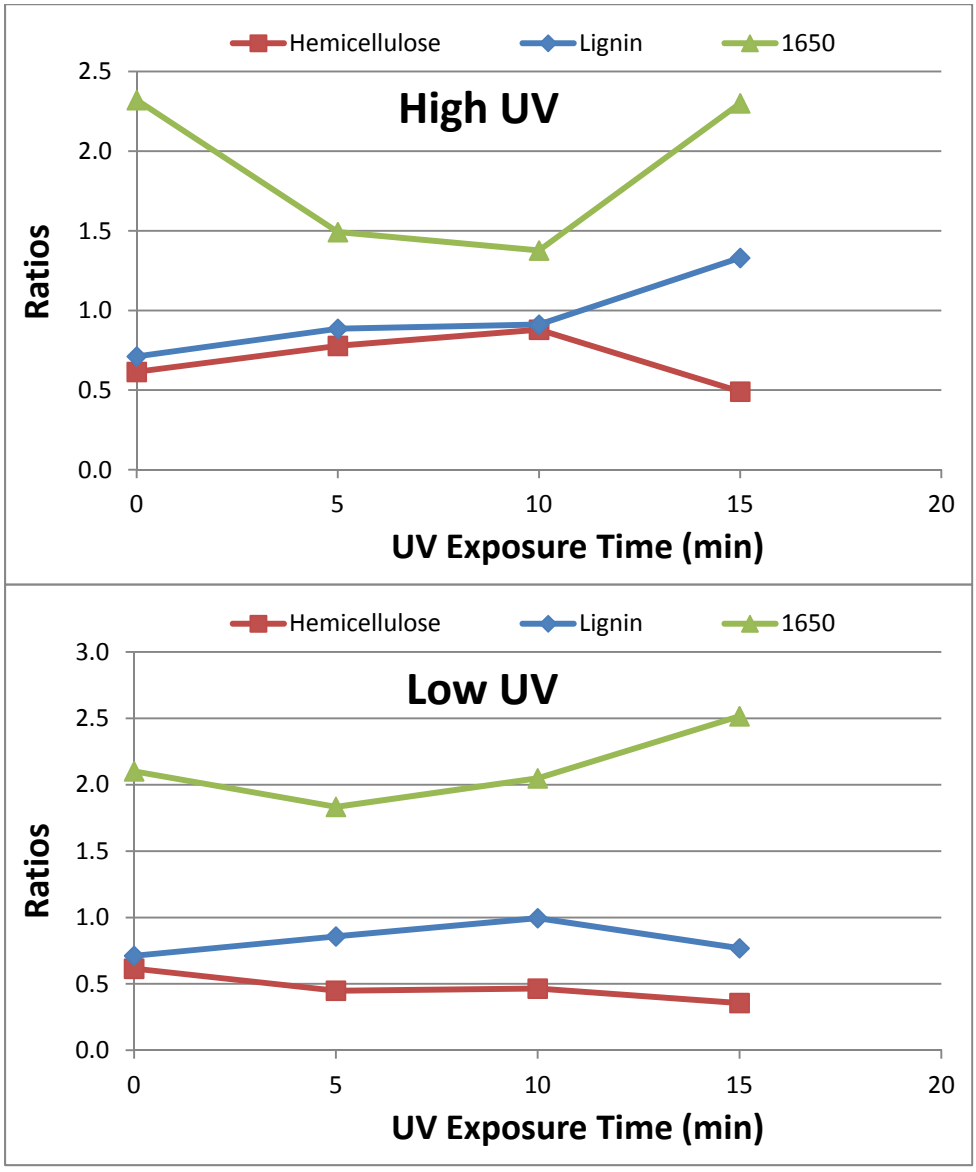

Figure 145: Hemicellulose, lignin and 1650 peak ratios for the High (top) and Low (bottom) set of wheat straw samples. The peak at 1160 cm^{-1} was used as internal reference.

The chemical composition analysis (Figure 146) shows that the lignin content is slightly increased after the Low UV treatment (from 9.88 to 11.7 wt-%) and High UV treatment (from 9.88 to 13.3 wt-

%). This increase was also suggested by the lignin ratio which is especially higher after the High UV treatment.

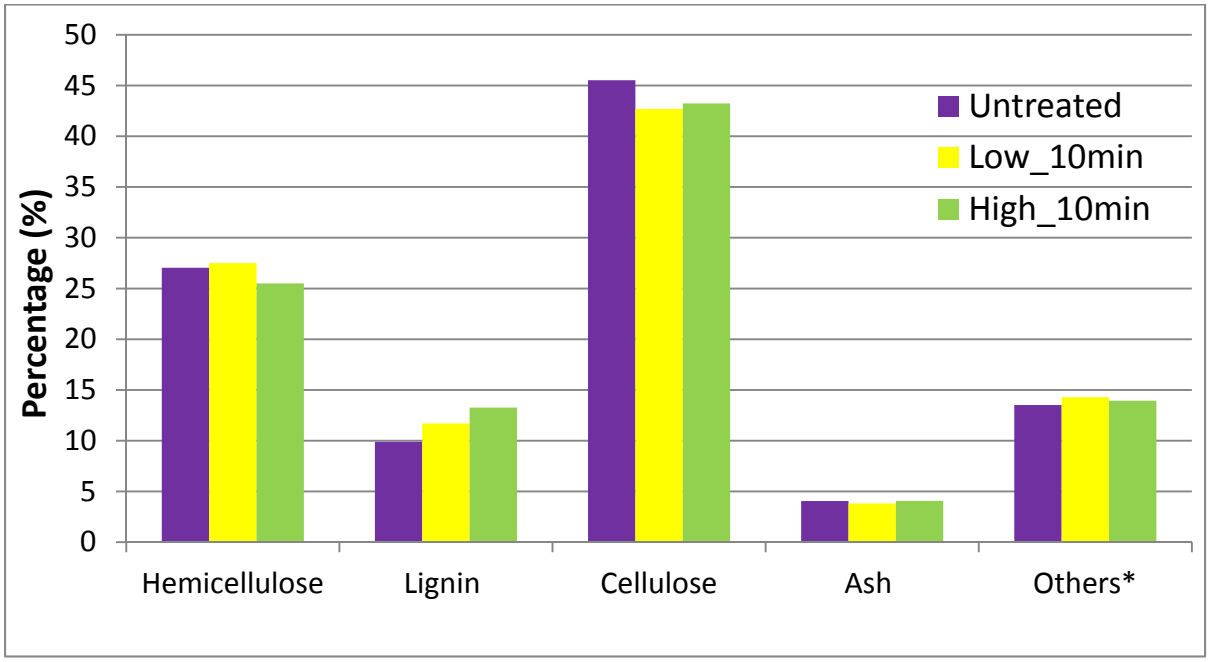

Figure 146: Chemical composition of the untreated, Low and High (10 min) UV treated wheat straw samples. Others: wax, pectin, sugar and other low molecular weight compounds.*

On the other hand, Figure 146 indicates that the hemicellulose content remains virtually unchanged or slightly declines after the wheat straw sample is submitted to the Low or High UV treatments. For example, the hemicellulose content increases from 27.0 to 27.5 wt-% after the Low UV treatment and slightly decreases from 27.0 to 25.5 wt-% upon the application of the High UV treatment. However, it was not possible to identify these changes using the hemicellulose ratio (Figure 145).

In addition, it seems that increasing the UV radiant power (from Low to High) affected more lignin than hemicellulose. For example, increasing the intensity of the UV treatment from Low to High caused the lignin content to increase 13.3 % (or 1.56 wt-%, from 11.7 to 13.3 wt-%) whereas the hemicellulose content decrease only 7.3 % (or 2 wt-%, from 27.5 to 25.5 wt-%.

The formation of quinone structures and the small decrease of cellulose content may be responsible for the mild and unexpected increase on the lignin content observed in this work. The quinone

compounds are usually formed as result of lignin degradation via UV irradiation (Hon and Chang, 1984; Muller et al., 2003). Because the quinone compounds have aromatic structures similar to the ones presented by lignin, it is likely that the chemical composition analysis cannot differentiate between these two compounds. Therefore, the increase of the lignin content may be due actually to the formation of quinone.

In agreement with that, Figure 145 shows that the Low intensity UV treatment 1650 peak ratio caused a slight increase on the 1650 peak ratio. Similarly, after a small decrease up to 10 minutes, the High intensity UV treatment produced a sharp increase on the 1650 peak ratio at 15 minutes.

Additionally, the small decrease of cellulose content may be also responsible for the mild and unexpected increase on the lignin content observed in this work. Figure 146 shows that there is a 2.8 wt-% drop (from 45.5 to 42.7 wt-%) in the cellulose content after the Low UV treatment (Low_10min sample), while a smaller drop (2.3 wt-% from 45.5 to 43.2 wt-%) is observed after the High UV treatment (High_10min sample). Therefore, the decrease of cellulose content may partially explain the mild increase on the lignin content. In agreement with these results, the ash content results obtained before have already suggested the removal of small amounts of organic materials from the UV treated samples.

It is possible to conclude from these results that the lignin content is slightly increased after the UV treatments, especially when the High UV treatment (higher radiant power) is applied to the wheat straw samples whereas, the hemicellulose content has slightly decreased.

Furthermore, the lignin content increase may be explained by the slight decrease of the cellulose content which was proportional to the lignin increase. However, this content increase does not mean that lignin was not affected by the UV treatments. It is plausible that lignin was changed into quinone structures which are not differentiated by the chemical composition analysis utilized here.

7.4 Conclusions

A novel, fast and cost-effective method based on ultraviolet irradiation was successfully utilized to increase the temperature of thermal degradation of wheat straw fiber. This approach has never been reported before in the literature. Wheat straw samples with and without pre-treatment (acetone and alkali pre-treatments) were exposed to the UV light treatment during different periods of time.

Thermal gravimetric analysis (TGA) proves that the UV light treatment is an effective method to improve the thermal stability of the wheat straw samples. Overall, increasing the time of the UV treatment improved the thermal stability of all the samples. In spite of the fact that the UV treatment was able to further increase the thermal stability of alkali and acetone pre-treated fibers, the sole UV treated samples, especially using a higher UV power (High set), showed the highest increment on thermal stability.

More important, the improvement on thermal stability provided by the use of alkali and acetone pre-treatments is not satisfactory enough to overcome the low yield obtained and the extra time invested during these two pre-treatments (especially if the added costs would be consider). In contrast, the sole UV treatment can provide higher thermal stability and yield within shorter time. In fact, the most remarkable advantage of using sole UV treatment over the alkali or acetone pre-treatments is the enormous difference in the time of treatment. Whereas, the alkali and acetone pre-treatment require 24 and 8 hours, respectively, the application of the UV treatment takes only 15 minutes. Although, there is a decrease in the yield when higher UV intensity (case of the samples in the High set) instead of Low UV intensity (case of the samples in the Low set) is utilized, this yield reduction is not severe enough to cancel the gains on thermal stability achieved with the higher UV intensity treatment.

The UV treatment presented here proved to be a fast, chemical-free and cost-effective method to improve the thermal stability to wheat straw fiber. In addition, this method may successfully be extended to other plant fibers.

Chapter 8 - Concluding Remarks, Main Contributions and Future Work

8.1 Conclusions

The utilization of plant fibers in the production of thermoplastic composites has been explored for applications in different industries (such as automotive and construction). Currently, it is possible to use plant fibers to produce composites with thermoplastics that require low processing temperatures.

For example, wheat straw polypropylene composite has been used in the fabrication of the quarter trim bin in the Ford Flex vehicle model 2010. This represents a major accomplishment which was achieved thanks to the contribution of many researchers (Erickson, L.; Fatoni, R.; Kruger, P; Lee, E.; Golbabaie, M.; Ng, Z.; Sardashti, A.; Simon, L.) including our research group.

Composition of Wheat Straw

However, in order to extend wheat straw use to other polymers such as the ones with higher processing temperatures and therefore to other thermoplastics and products, the low thermal stability of wheat straw has to be overcome. During the fabrication of composites with engineering thermoplastics (such as polyamide-6 processed at 250 °C), wheat straw fiber suffers considerable thermal degradation which can affect the physical and mechanical properties of the composite.

To exploit the full potential that wheat straw could offer, in this thesis the problem of enhancing the thermal stability of wheat straw was addressed. To increase the low thermal stability of wheat straw, it is necessary first to have a better understanding of the degradation process of wheat straw. Hence, in this thesis, the chemical composition and thermal stability of several wheat straw samples from different regions of North America (Chapter 3) were investigated.

The analysis indicates that the beginning of the wheat straw thermal degradation does not significantly vary with wheat straw type and cultivation region. The main thermal degradation of wheat straw samples starts in a narrow window of temperature which goes from 220.8 to 237.8 °C and from 224.8 to 238.1 °C for air or nitrogen atmospheres, respectively. Therefore, if large scale wheat straw utilization is required, wheat straw samples from different types and regions can be used together without significantly affecting the thermal stability of the entire batch of wheat straw. Although it is important to note that different sources of wheat straw may have different thermal stability.

In addition, chemical composition results reveal relatively small variation on the wheat straw components. For example, among all the components, lignin and inorganic material were the ones with the highest relative variation (around 35.8 % and 66.2 %, respectively), followed by hemicellulose and cellulose. This implies that treatment methods targeted towards modifying different chemical components of wheat straw will be effective regardless of the wheat straw type or cultivation region. Equally important is the fact that the most effective treatments could be applied to other plant fibers because similar chemical components are found throughout plant fibers including wheat straw.

Thermochemical Treatment

On the other hand, the thermal degradation of wheat straw depends on the atmosphere (air or nitrogen) and temperature when under isothermal conditions. More precisely, wheat straw fibers degrade faster under air atmosphere than under nitrogen atmosphere at 250 °C. Because of that, it would be advisable to utilize nitrogen atmosphere when processing wheat straw fiber with polyamide-6 or other thermoplastics that have higher melting temperatures.

In this thesis, three different methods were developed to improve the thermal stability of wheat straw fiber. The first approach to increase the thermal stability of wheat straw utilizes thermochemical treatments (Chapter 4). This thermochemical treatment is based on the first step of carbon fiber fabrication using rayon or cellulose fibers as precursors (in a process called stabilization). Initially, the samples are chemically pre-treated using ammonium chloride. After that, the ammonium chloride pre-treated fibers are submitted to different thermal treatments under oxidative atmosphere.

When this strategy was applied to enhancing the thermal stability of the wheat straw, the results obtained here indicated that significant thermal stability enhancement is achieved at the expense of the samples mechanical properties, especially after treatments utilizing high temperatures. For example, the samples with the best thermal stability enhancement could be significantly damaged using bare hands. Another limitation of this method is the low yield. The mass obtained after the thermochemical treatment was lower than 40 wt-% for the samples with significant enhancement on its thermal stability.

On the other hand, reducing the temperature and time during the thermal treatment increases the thermal stability with smaller removal of organic material. However, these samples still exhibit moderately fragile structure. It is possible that further investigation exploring these regions of temperature and time could lead to straw fibers with better thermal stability without compromising the yield or mechanical properties.

Silane Modification

To overcome the disadvantages of the thermochemical treatment, a second alternative, silane modification, was explored in this thesis to improve the thermal stability. Two classes of silane modifiers, alkoxysilane and chlorosilane, along with different reaction conditions (such as different solvents and pH) were evaluated for silane modification of wheat straw.

Promising thermal stability improvement was achieved after silane modification of wheat straw utilizing chlorosilane modifiers. The size of the chlorosilane modifiers molecules seems to be of crucial importance in the success of the silane modification. The highest thermal stability enhancement was obtained utilizing Acryloxy, Ethyl and 7-Octenyl chlorosilane modifiers. The starting temperature of the thermal degradation of the sample treated with Acryloxy is increased by 15 % (from 238 to 273.7 ^{o}C) in comparison with the untreated sample.

More important, the silane treated samples have lower thermal degradation during the fabrication of composites with polyamide-6. TGA analysis indicates that the extruded and injection molded composites containing silane treated wheat straw samples have significantly smaller thermal degradation than those utilizing untreated wheat straw samples. In addition, the composites with the highest thermal stability (which contain silane treated samples) have the lighter colors after the extrusion and injection molding steps.

Equally important is the fact that the silane treatment did not compromise the flexural properties of the wheat straw/polyamide-6 composites. In fact, this treatment shows capability for increasing the impact strength of these composites.

Silane treatment of the straw fibers has a great potential for developing grades of fiber for applications in composites with engineering plastics. However, it is necessary in the future work to evaluate the economic cost of implementing this method for commercial applications. It may be

necessary to reduce the time and increase the yield of the treatment in order to make the silane modification a cost-effective alternative to improve the thermal stability of wheat straw.

Ultraviolet (UV) Light Treatment

A third treatment method using ultraviolet light was developed in this thesis. This is a novel application for ultraviolet light which, to the best of our knowledge, has not been reported in the literature before. Wheat straw samples with and without pre-treatment (acetone and alkali pre-treatments) were exposed to the UV light treatment during different periods of time.

The results obtained in this work demonstrate that the ultraviolet light treatment can increase the thermal stability of wheat straw. Overall, increasing the time of the UV treatment improved the thermal stability of all the samples. In spite of the fact that the UV treatment was able to further increase the thermal stability of alkali and acetone pre-treated fibers, the sole UV treated samples, especially using a higher UV power, showed the highest increment on thermal stability. More precisely, only 15 minutes of the high intensity UV light treatment is able to raise by 40 ºC the temperature of 2% of weight loss, from 230 to 270 ºC.

In the case the sole UV treatment (without pre-treatment), the high yield, the short treatment time and the relative low cost are the most attractive advantages of the ultraviolet light treatment compared to other methods presented here and in the literature.

In addition to that, the UV treatment offers additional economical and environmental benefits because this treatment is chemical-free and performed at ambient temperature. In the future work, compounding of UV treated wheat straw with polyamides should be performed to confirm if the thermal stability gains will be translated into lower thermal degradation during composite fabrication.

Comparison of Treatments

Table 38 summarizes selected results. It shows some of the most thermal stable wheat straw samples obtained after the application of one of the three treatments described in this thesis.

Table 38: Selected wheat straw samples obtained after thermochemical, silane and ultraviolet treatments.

Method	Treatment Time	Yield (%)	$T_{2\%}$ [a] (°C)	Wt250[b] (%)	Color of the samples[c]
None	Zero	NA[d]	229.1	86.2	Light Yellow
Thermochemical	6 min	62.1	265.3	---	Black
Thermochemical	30 min	46.41	268.0	---	Black
Silane	5 hours	80[e]	273.7	95.2	Yellow
Silane	5 hours	80[e]	270.9	95.3	Yellow
Ultraviolet	15 min	68.2	269.0	95.0	Dark Brown
Ultraviolet	15 min	82.3	250.7	92.7	Brown

a: The temperature at 2 % weight loss; b: Weight after 10 minutes at 250 °C; c: Visual inspection; d: Not applicable; e: Pre-treatment not included.

8.2 Main Contributions

- This thesis provides a better understanding of the wheat straw thermal degradation under non-isothermal and isothermal conditions utilizing air and nitrogen atmospheres. The experimental investigation shows that the degradation can start at different temperatures depending on the atmosphere (air or nitrogen) whereas the beginning of this degradation does not significantly vary with wheat straw type and cultivation region.

- It is demonstrated here for the first time that silane treatment can be used to significantly increase the thermal stability of wheat straw. It is presented a comprehensive study of different chlorosilane and alkoxysilane modifiers along with different reaction conditions. Also, it is shown that the best option for increasing the thermal stability of wheat straw fiber is the utilization of chlorosilane modifiers. The methodology described in this work can be used as a guideline for silane modification of other plant fibers.

- To evaluate the potential of silane modification, wheat straw was compounded with polyamide-6. The results showed that the thermal stability of the straw fiber samples

influences the thermal stability of the extruded and injected wheat straw/polyamide-6 composite samples. When wheat straw samples with higher thermal stability (silane treated) are used to produce the composite, the extruded and injected composite samples obtained have less signs of thermal degradation (such as dark colors) and higher thermal stability (measured by TGA analysis). In addition, these observations confirmed that TGA analysis is a powerful tool in predicting the thermal degradation that plant fibers could experience during the real composite fabrication conditions.

- A novel, fast and cost-effective method based on ultraviolet light was successfully utilized to enhance the thermal stability of wheat straw. The methodology developed here requires only 15 minutes of treatment to significantly reduce the thermal degradation of wheat straw without sacrificing the yield. In addition to that, the UV treatment offers additional environmental benefits because the treatment is chemical-free and performed at ambient temperature. Overall this treatment shows potential to develop commercial grades of fibers.

8.3 Future work

Thermal Degradation Process

- Formulate a mathematical model that represents the connection between chemical composition and thermal degradation of the wheat straw, if it exists.
- Develop a chemical kinetic model that explains the reaction mechanism responsible for the thermal degradation of wheat straw fiber under air atmosphere and isothermal temperatures around 250 °C. Based on the findings obtained in Chapter 3, it is suggested that this chemical kinetics study uses a two-step reaction mathematical model.

Silane Modification

- Optimize the silane modification to obtain the highest thermal stability in a cost-effective way. This optimization could include reducing the treatment time to achieve higher yield or using oligomers silane modifiers as an alternative to further increase on the thermal stability gain.
- Explore new combinations of Chlorosilane and Alkoxysilane modifiers to promote further improvement on the impact strength of wheat straw/polyamide-6 composites.

- Utilize other characterization techniques such as Raman spectroscopy, Si-NMR and H-NMR (nuclear magnetic resonance), electron spectroscopy for chemical analysis (ESCA), and Pyrolysis-gas Chromatography to further understand the silane modification and the nature of the bonding between the silane modifier and wheat straw.

Producing Wheat Straw/Polyamide-6 Composites

- Investigate the effect of shear during composite fabrication on the aspect ratio of the wheat straw fiber. In this case, the fibers have to be extracted from the composite to perform the analysis of the aspect ratio.
- Optimize the formulation and processing conditions utilized during composite fabrication (e.g., percentage of fiber, use of additive, extrusion and injection temperature, etc.) to further reduce the thermal degradation and breakage of the fiber as well as increase the mechanical properties of the composite.
- Use other characterization methods (such as Heat distortion temperature, HDT, and Dynamic mechanical thermal analysis - DMTA) to determine the potential of the wheat straw-polyamide 6 composites for under the hood applications.

Ultraviolet Light Treatment

- Employ other characterization techniques (such as Ultraviolet visible spectroscopy and Raman spectroscopy) to evaluate the effect of the UV treatment on the chemical structure of wheat straw.
- Compound the UV treated samples with polyamide-6 to evaluate the thermal stability of wheat straw during the actual composite fabrication conditions such as higher temperature, sheer and residence time.

References

Abdelmouleh, M., Boufi, S., Ben Salah, A., and Belgacem, M.N. (2002). "Interaction of silane coupling agents with cellulose", *Langmuir*, 18(8), 3203-3208.

Agarwal, P. U. (1998). "Assignment of the Photoyellowing-related 1675 cm^{-1} Raman/IR band to p-Quinones and its Implications to the Mechanism of Color Reversion in Mechanical Pulps", *Journal of Wood Chemistry and Technology*, 18(4), 381-402.

Ahemed, A. (2008). "Wheat production to drop slightly: FAO" Retrieved in 2008 from http://www.dawn.com/2008/05/23/nat10.htm

Alemdar, A., and Sain, M. (2008). "Biocomposites from wheat straw nanofibers: Morphology, thermal and mechanical properties", *Composites Science and Technology*, 68(2), 557–565.

Amintowlieh, Y. (2010). "Nylon-6/Agricultural Filler Composites", M.Sc. Thesis, Department of Chemical Engineering, University of Waterloo, Ontario, Canada.

ASTM International (2008)b. ASTM D 256 - 06a Standard Test Methods for Determining the Izod Pendulum Impact Resistance of Plastics.

ASTM International (2008). ASTM D 618-08 Standard Practice for Conditioning Plastics for Testing.

ASTM International 2008a. ASTM D 790 - 03 Standard Test Methods for Flexural Properties of Unreinforced and Reinforced Plastics and Electrical Insulating Materials.

ASTM International (2008)b. ASTM D 790 - 07 Standard Test Method for Flexural Properties of Unreinforced and Reinforced Plastics and Electrical Insulating Materials.

ASTM D-790 – 03 (2003), Standard test method for flexural properties of unreinforced and reinforced plastics and electrical insulating materials, USA.

Avella, M., Bozzi, C., Dell'Erba, R., Focher, B., Marzetti, A., and Martuscelli, E. (1995). "Steam exploded wheat straw fibers as reinforcing material for polypropylene-based composites", *Die Angewandte Makromolekulare Chemie*, 233(1), 149-166.

Bartkiwiak, M., and Zakrzewski, R. (2004). "Thermal Degradation of Lignins Isolated from Wood", *Journal of Thermal Analysis and Calorimetry*, 77(1), 295–304.

Bashar, A. S., Khan, M. A., and Idriss Ali, K. M. (1997). "Modification of Cotton, Rayon, and Silk with Urethane Acrylate under Ultraviolet Radiation", *Journal of Applied Science*, 63(13), 1703-1711.

Beari, F., Brand, M., Jenkner, M., Lehnert, R., and Metternich, H. J. (2001). "Organofunctional alkoxysilanes in dilute aqueous solution: new accounts on the dynamic structure mutability", *Journal of Organometallic Chemistry*, 625(2), 208-16.

Bengisu, M., and Yilmaz, E. (2002). "Oxidation and pyrolysis of chitosan as a route for carbon fiber derivation", *Carbohydrate Polymers*, 50(2), 165-175.

Bledzki A. K., and Gassan J. (1999). "Composite reinforced with cellulose based fibres", *Progress in Polymer Science*, 24(2), 221–274.

Bledzki, A. K., Mamun, A. A., and Faruk, O. (2007). "Abaca fibre reinforced PP composites and comparison with jute and flax PP composites", *Express Polymer Letters*, 1(11), 755-762.

Blum, F. D., Meesiri, W., Kang, H., and Gambogi, J. E. (1991). "Hydrolysis, adsorption, and dynamics of silane coupling agents on silica surfaces", *Journal of Adhesion Science Technology,* 5(6), 479-496.

Bogan, R. T., and Brewer, R. J. (2002). "Cellulose esters" in Encyclopedia of Polymer Science and Technology. (2nd ed.): John Wiley and Sons Inc.

Borup, B., and Weissenbach, K. (2010). "Silane Coupling Agents in Functional Fillers for Plastics", Wiley-VCH, (2nd ed.): edited by Marino Xanthos.

Brauns, F. E., and Brauns, D. E. (1952). The chemistry of lignin. Academic Press.

Cai, J. M., and Bi, L. S. (2009). "Kinetic analysis of wheat straw pyrolysis using isoconversional methods", *Journal of Thermal Analysis and Calorimetry*, 98(1), 325-330.

Callister, W. D. Jr. (2000). Materials Science and Engineering, an introduction. (5th ed.): John Wiley & Sons.

Cao, Y., Sakamoto, S., and Goda, K. (2007). "Effects of heat and alkali treatments on mechanical properties of kenaf fibers", *16th International Conference on Composite Materials*, Kyoto, Japan.

Castellano, M., Gandini, A., Fabbri, P., and Belgacem, M. N. (2004). "Modification of Cellulose Fibres with Organosilanes: Under What Conditions does Coupling Occur?", *Journal of Colloid and Interface Science*, 273(2), 505-511.

CEN-Chemical and Engineering News (2008). Retrieved in December, 2008 from: http://pubs.acs.org/cen/coverstory/86/8649cover2.html

Cella, J. A., and Carpenter, J. C. (1994). "Procedures for the Preparation of Silanols", *Journal of Organometallic Chemistry*, 480(1-2), 23-26.

Chawla, K. K. (1998). Composite Materials: Science and Engineering. (2nd ed.): Springer-Verlag New York Inc.

Chen, H., Ferrari, C., Angiuli, M., Yao, J. Raspi, C., and Bramanti, E. (2010). "Qualitative and quantitative analysis of wood samples by Fourier transform infrared spectroscopy and multivariate analysis", *Carbohydrate Polymers*, 82(3), 772-778.

Dean, K. M., Bateman, S. A., and Simons, R. (2007). "A Comparative Study of UV Active Silane-grafted and Ion-exchanged Organo-clay for Application in Photocurable Urethane Acrylate Nano- and Micro-composites", *Polymers*, 48(8), 2231-2240.

Deka, M., Humar, M., Rep, G., Kricej, B., Sentjurc, M., and Petric, M. (2008). "Effects of UV light irradiation on colour stability of thermally modified, copper ethanolamine treated and non-modified wood: EPR and DRIFT spectroscopic studies", *Wood Science Technology*, 42(1), 5-20.

Di Blasi, C., and Lanzetta, M. (1997). "Intrinsic kinetics of isothermal xylan degradation in inert atmosphere", *Journal of Analytical and Applied Pyrolysis*, 40-41, 287-303.

Dobele, G., Rossinskaja, G., Telysheva, G., and Meier, D. (1999). "Cellulose dehydration and depolymerization reactions during pyrolysis in the presence of phosphoric acid". *Journal of Analytical and Applied Pyrolysis* 49(1-2), 307-317.

Domburg, G. E., Sergeeva, V. N. and Zheibe, G. A. (1970). "Thermal Degradation of some Lignin Model Compounds", *Journal of Thermal Analysis and Calorimetry*, 2(4), 419-428.

Donath, S., Militz, H., and Mai, C. (2004). "Wood modification with alkoxysilanes", *Wood Science and Technology*, 38(7), 555-566.

Ehrenstein, G. W., Riedel, G., and Trawiel, P. (2004). Thermal Analysis of Plastics: Theory and Practice. Hanser Gardner Publications.

Fackler, K., Stevanic, J.S., Ters, T., Hinterstoisser, B., Schwanninger, M., and Salmen, L. (2010). "Localisation and characterization of incipient brown-rot decay within spruce wood cell walls using FT-IR imaging microscopy", *Enzyme and Microbial Technology*, 47(6), 257-267.

Fakirov, S., Bhattacharyya, D. (2007). Handbook of Engineering Biopolymers: Homopolymers, blends and composites. Hanser Publications.

Faix, O., Bremer, J., Schmidt, O., and Stevanovic, T. (1991). "Monitoring of chemical changes in white-rot degraded beech wood by pyrolysis-gas chromatography and Fourier transform infrared spectroscopy", *Journal of Analytical and Applied Pyrolysis*, 21(1-2), 147-162.

Feist, W. C. and Hon, D. N. S. (1984). “Chemistry of Weathering and Protection”. In: The Chemistry of Solid Wood, R.M. Rowell, ed. Advances in Chemistry Series N^{o}. 207. American Chemical Society, Washington, DC.

Feng, X. X., Chen, J. Y., and Zhang, H. P. (2008). “Effect of high temperature alkali cooking on the constituents, structure and thermal degradation of hemp fiber.” *Journal of Applied Polymer Science,* 108(6), 4058-4064.

Fengel, D., and Wegener, G. (1989). “Wood: Chemistry, Ultrastructure, Reactions”. Walter de Gruyter Berlin, New York.

Fusion Systems Inc. (2010). UV Curing from Fusion UV. Retrieved in May, 2011 from: http://www.fusionuv.com/uploadedFiles/PDF_Library/SB661%20Fusion%20Difference.pdf

Garcia, O. E., Infante, R. B., and Rivera, C. J. (1997). “Determination of total, soluble and insoluble dietary fibre in two new varieties of Phaseolusvulgaris L. using chemical and enzymatic gravimetric methods”. *Food Chemistry*, 59 (1), 171-174.

Gassan, J., and Gutowski, V. S. (2000). “Effects of corona discharge and UV treatment on the properties of jute-fibre epoxy composites”, *Composites Science and Technology*, 60(15), 2857-2863.

George, J., Bhagawan, S. S., Prabhakaran, N., and Thomas, S. (1995). “Short pineapple-leaf-fiber-reinforced low-density polyethylene composites”. *Reinforced Plastics*, 22, 28-32.

Giessler, S. and Mack, H. (2003). “Organofunctional silanes – molecular bridges for glass fibre reinforced polyamides”, *Journal of Applied Polymer Science*, 85 (12), 2485–2490.

Golbabaie, M. (2006). "Characterization of Ontario crop fibers for use in biocomposites (wheat and soybean)", M.Sc. Thesis, University of Guelph, Ontario, Canada – personal communication.

Good, D. (2007). "Purdue Outlook: Will world wheat production rebound?" Retrieved in 2008 from http://www.cattlenetwork.com/content.asp?contentid=114684

Guettler, B. E. (2009). "Soy-Polypropylene Biocomposites for Automotive Applications", M.Sc. Thesis, University of Waterloo, Ontario, Canada.

Haynes, W. M., (2012) CRC Handbook of Chemistry and Physics. (93rd ed.). CRC Press.

Hansen, N. M. L., and Plackett, D. (2008). "Sustainable films and coatings from hemicelluloses: a review", *Biomacromolecules*, 9(6), 1493-1505.

Herrera, N., Letoffe, J. M., Putaux, J. L., David, L., and Bourgeat-Lami, E. (2004). "Aqueous Dispersions of Silane-Functionalized Laponite Clay Platelets. A First Step toward the Elaboration of Water-Based Polymer/Clay Nanocomposites". *Langmuir*, 20(5), 1564-1571.

Herrera-Franco, P. J., and Valadez-Gonzalez, A. (2005). "A study of the mechanical properties of short natural-fiber reinforced composites", *Composites: Part B*, 36(8), 597–608.

Hill, C. A. S., Abdul Khalil, H. P. S., and Hale, M. D. (1998). "A study of the potential of acetylation to improve the properties of plant fibres". *Industrial Crops and Products*, 8(1), 53-63.

Hill, C. A. S., Mastery Farahani, M. R., and Hale, M. D. C. (2004). "The use of organo alkoxysilane coupling agents for wood preservation", *Holzforschung*, 58(3), 316-325.

Hon, D. N. S., and Chang, S. T. (1984). "Surface Degradation of Wood by Ultraviolet Light", *Journal of Polymer Science*, 22(9), 2227-2241.

Hornsby[1], P. R., Hinrichsen, E., and Travedi, K. (1997). "Preparation and properties of polypropylene composites reinforced with wheat and flax straw fibers, Part I. Fiber characterization." *Journal of Material Science*, 32(2), 443-449.

Hornsby[2], P. R., Hinrichsen, E., and Travedi, K. (1997). "Preparation and properties of polypropylene composites reinforced with wheat and flax straw fibers, Part II Analysis of composite microstructure and mechanical properties", *Journal of Material Science*, 32(4), 1009-1015.

Hozumi, A., Inagaki, H., and Kameyama, T., (2004). "The hydrophilization of polystyrene substrates by 172-nm vacuum ultraviolet light", *Journal of Colloid and Interface Science*, 278(2), 383-392.

Islam, N., Rahman, R. Haque, M. and Huque, M., (2010). "Physico-mechanical properties of chemically treated coir reinforced polypropylene composites", *Composite Part A: Applied Science and Manufacturing*, 41(2), 192–198.

James, S., Rowell, H. S., and Rowell, J. S. (1997). "Chemical composition of fibers", In: Rowell, R.M., Young, R.A., Rowell, J.K., (Eds.), "Paper and composites from agro-based resources", CRC Press Inc. 83-107.

John, M. J., and Thomas, S. (2008). "Biofibres and biocomposites", *Carbohydrate Polymers*, 71(3), 343-364.

Joseph, S., Sreekala, M. S., and Thomas, S. (2008). "Effect of chemical modifications on the thermal stability and degradation of banana fiber and banana fiber-reinforced phenol formaldehyde composites", *Journal of Applied Polymer Science*, 110(4), 2305–2314.

Khan, M. A., Shehrzade, S., and Hassan, M. M. (2004). "Effect of Alkali and Ultraviolet (UV) Radiation Pretreatment on Physical and Mechanical Properties of 1,6-Hexanediol Diacrylate-Grafted Jute Yarn by UV Radiation", *Journal of Applied Polymer Science*, 92(1), 18-24.

Kiran, D. (1986). "Thermal decomposition of wood pulps at different degrees of delignification" in Cellulose – structure, modification and hydrolysis, Young, R. A., Rowell, R. M., A Wiley-interscience Publication, Madison, Wiconsin.

Klysov, A. A. (2007). Wood-plastic composites, John Wiley & Sons, Inc.

Kruger, P. K. (2007). "Wheat straw-polypropylene composites". M.Sc. Thesis, University of Waterloo, Ontario, Canada.

Lanzetta, M., and Di Blasi, C. (1998). "Pyrolysis kinetics of wheat and corn straw", *Journal of Analytical and Applied Pyrolysis*, 44(2), 181–192.

Lawther, J. M., Sun, R., and Banks, W. B. (1996). "Fractional characterization of alkali-labile lignin and alkali-insoluble lignin from wheat straw", Industrial Crops and Products, 5(4), 291-300.

Li, X., Tabil, L. G., and Panigrahi, S. (2007). "Chemical treatments of natural fiber for use in natural fiber-reinforced composites: a review", *Journal of Polymers and the Environment*, 15(1), 25-33.

Liu, R., Yu, H., and Huang, Y. (2005). "Structure and morphology of cellulose in wheat straw", *Cellulose*, 12(1), 25-34.

Love, K. T., Nicholson, B. K., Lloyd, J. A., Franich, R. A., Kibblewhite R. P., and Mansfield, S. D. (2008). "Modification of kraft wood pulp fibre with silica for surface functionalisation". *Composites Part A*, 39(12), 1815-1821.

Lowry, T. H. and Richardson, K. S. (1987). "Mechanism and Theory in Organic Chemistry", (3rd ed.) Harper & Row Publishers, New York.

Media.Ford (2009). "Ford teams up to develop wheat straw-reinforced plastic; New biomaterial debuts in 2010 Ford Flex". Retrieved in May, 2011 from http://media.fordvehicles.com/article_display.cfm?article_id=3139.

Mishra, S., Mohanty, A. K., Drzal, L. T., Mishra, M., Parija, S., Nayak, S. K., and Tripathy, S. S. (2003). "Studies on mechanical performance of biofibre/glass reinforced polyester hybrid composites", *Composites Science and Technology*, 63(10), 1377-1385.

Mohanty, A. K., Misra, M., and Drzal, L. T. (2005). "Natural Fibers, Biopolymers, and Biocomposites", Published by CRC Press and Taylor & Francis Group.

Mukhopadhyay, S., and Fangueiro, R. (2009). "Physical Modification of Natural Fibers and Thermoplastic Films for Composites – A Review", *Journal of Thermoplastic Composite Materials*, 22(2), 135-162.

Muller, U., Ratzsch, M., Schwanninger, M., Steiner, M., and Zobl, H. (2003). "Yellowing and IR-changes of spruce wood as result of UV-irradiation", *Journal of Photochemistry and Photobiology B: Biology*, 69(2), 97–105.

Mwaikambo, L. Y., and Ansell, M. P. (2002). "Chemical modification of hemp, sisal, jute, and kapok fibers by alkalization". *Journal of Applied Polymer Science*, 84(12), 2222-2334.

Nair, K. C. M., Thomas, S., Groeninckx, G. (2001). "Thermal and dynamic mechanical analysis of polysterene composites reinforced with short sisal fibers", *Composites Science and Technology*, 6(16), 2519-2529.

Ng, Z. S. (2008). "Bulk Orientation of Agricultural Filler-Polypropylene Composites", M.Sc. Thesis, University of Waterloo, Ontario, Canada.

Norrstrom, H. (1969). "Light absorption properties of pulp and paper components". *Svensk Paperstidn*, 72, 25-38.

NUE (2007). "The story of wheat". Retrieved in 2008 from http://nue.okstate.edu/Crop_Information/World_Wheat_Production.htm.

Onyiriuka, E. C. (1993). "The Effects of High-Energy Radiation on the Surface Chemistry of Polystyrene: A Mechanistic Study", *Journal of Applied Polymer Science*, 47(12), 2187-2194.

Ouajai, S., and Shanks, R. A. (2005). "Composition, structure and thermal degradation of hemp cellulose after chemical treatments". *Polymer Degradation and Stability*, 89(2), 327-335.

Pandey, K. K., and Pitman, A. J. (2003). "FTIR studies of the changes in wood chemistry following decay by brown-rot and white-rot fungi", *International Biodeterioration & Biodegradation*, 52(3), 151-160.

Pandey, K. K. (2005). "Study of the effect of photo-irradiation on the surface chemistry of wood", *Polymer and Degradation and Stability*, 90(1), 9-20.

Pantano, C. G., Carman, L. A., and Warner, S. (1992). "Glass fiber surface effects in silane coupling", *Journal of Adhesion Science and Technology*, 6(1), 49.

Panthapulakkal, S., and Sain, M. (2006). "Injection molded wheat straw and corn stem filled polypropylene composites", *Journal of Polymers and the Environment*, 14(3), 265-272.

Panthapulakkal, S., and Sain, M. (2007). "Agro-residue reinforced high-density polyethylene composites: Fiber characterization and analysis of composite properties", *Composites Part A: Applied Science and Manufacturing*, 38(6), 1445-1454.

Panthapulakkal, S., Zereshkian, A., and Sain, M. (2006). "Preparation and characterization of wheat straw fibers for reinforcing application in injection molded thermoplastic composites", *Bioresource Technology*, 97(2), 265-272.

Park S., Baker1, J. O., Himmel, M. E., Parilla, P. A., and Johnson, D. K. (2010). "Cellulose crystallinity index: measurement techniques and their impact on interpreting cellulose performance". *Biotechnology for Biofuels*, 3, 10.

Pervaiz, M., and Sain, M. (2004). “High performance natural fiber thermoplastics for automotive interior parts”. *SAE* Paper No. 2004-01-0729.

Pickering, K. L., Abdalla, A., Ji, C., Mcdonald, A. G., and Franich, R. A., (2003). “The effect of silane coupling agents on radiate pine fibre for use in thermoplastic matrix composites”. *Composites Part A*, 34(10), 915-926.

Plueddemann, E. P. (1991). Silane Coupling Agents, (2nd ed) Plenum Press.

Prasad, B. M., Sain, M. M., and Roy, D. N. (2004). “Structure property correlation of thermally treated hemp fiber”, *Macromolecule Materials and Engineering*, 289(6), 581-592.

Preston, R. D. (1986). “Natural celluloses” in “Cellulose – structure, modification and hydrolysis,” Young, R. A., Rowell, R. M., A Wiley-interscience Publication, Madison, Wiconsin.

Rachini, A., Troedec, M. L., Peyratout, C., and Smith, A. (2009). “Comparison of the thermal degradation of natural, alkali-treated and silane-treated hemp fibers under air and an inert atmosphere”. *Journal of Applied Polymer Science*, 112(1), 226-234.

Ramazani, S.A. A. and Mousavi, S. SA. (2005). “Investigation of vacuum annealing effects on physical-mechanical properties of thermoplastic parts”, *Materials and Design*, 26(1), 89-93.

Ramos, L. P. (2003). “The chemistry involved in the steam treatment of lignocellulosic materials”. *Quimica Nova*, 26(6), 863-871.

Ray, D., Sarkar, B. K., Basak, R. K., and Rana, A. K. (2002). "Study of the Thermal Behavior of Alkali-Treated Jute Fibers". *Journal of Applied Polymer Science*, 85(12), 2594–2599.

Ray, D., Sarkar, B. K., Rana, A. K., and Bose, N. R. (2001). "The mechanical properties of vinylester resin matrix composites reinforced with alkali-treated jute fibers". *Composites Part A: Applied Science and Manufacturing*, 32(1), 119-127.

Reddy, C. R., Sardashti, A. P., and Simon, L. C. (2010). "Preparation and characterization of polypropylene–wheat straw–clay composites", *Composites Science and Technology*, 70(12), 1674-1680.

Reddy, C. R., and Simon, L. C. (2010). "Surface Modification of Wood Fiber and Preparation of a Wood Fiber-Polypropylene Hybrid by In situ Polymerization", *Macromolecular Materials and Engineering*, 295(10), 906-914.

Reddy, N., and Yang, Y. (2009). "Natural cellulose fibers from soybean straw", *Bioresource Technology*, doi:10.1016/j.biortech.2008.09.063.

Rong, M. Z., Zhang, M. Q., Yang, G. C., and Zeng, H. M. (2001). "The effect of fiber treatment on the mechanical properties of unidirectional sisal-reinforced epoxy composites", *Composites Science and Technology*, 61(10), 1437-1447.

Rosas, J. M., Bedia, J., Rodriguez-Mirasol, J., and Cordero, T. (2009). "Hemp-derived activated carbon fibers by chemical activation with phosphoric acid", *Fuel*, 88(1), 19-26.

Rouison, D., Couturier, M., and Sain, M. (2004). "The effect of surface modification on the mechanical properties of hemp fiber/polyester composites". *SAE* Paper No. 2004-01-0728.

Saha, S. C., Ray, P. K., Pandey, S. N., and Goswami, K. (1991). "IR and X-ray diffraction studies of raw and chemically treated pineapple leaf fiber (PALF)", *Journal of Applied Polymer Science*, 42(10), 2767-2772.

Salon, M. C. B., Gerbaud, G., Abdelmouleh, M., Bruzzese, C., Boufi, S., and Belgacem, M. N., (2007). "Studies of Interaction between Silane Coupling Agents and Cellulose Fibers with Liquid and Solid-state NMR", *Magnetic Resonance in Chemistry*, 45(6), 473-483.

Sain, M., and Panthapulakkal, S. (2006). "Bioprocess preparation of wheat straw fibers and their characterization", *Industrial Crops and Products*, 23(1), 1-8.

Santos, P. A., Spinace, M. A. S., Fermoselli, K. K. G., and De Paoli, M. A. (2007). "Polyamide-6/vegetal fiber composite prepared by extrusion and injection molding", *Composite Part A:Applied Science and Manufacturing*, 38(2), 2404-2411.

Sardashti, A. (2009). "Wheat straw-clay-polypropylene hybrid composites", M.Sc. Thesis: University of Waterloo, Ontario, Canada.

Sarkanen, K. V., and Ludwig, C. H. (1971). "Lignins, Occurrence, Formation, Structure and Reactions", Wiley-Interscience, New York, USA.

Savage, G. (1993). "Carbon-carbon composites", (1st ed.) Chapman and Hall, London.

Schmidt, A. S., Mallon, S., Thomsen, A. B., Hvilsted, S., and Lawther, J. M. (2002). "Comparison of the chemical properties of wheat straw and beech fibers following alkaline wet oxidation and laccase treatments", *Journal of Wood Chemistry and Technology*, 22 (1), 39-53.

Silanes & Silicones (2008) Gelest Catalog 4000-A.

Simon, P. (2004). "Isoconversional Methods – Fundamentals, meaning and application", *Journal of Thermal Analysis and Calorimetry*, 76(1), 123-132.

Sjöström, E. (1993). "Wood Chemistry: Fundamentals and Applications", (2nd ed.), Academic Press Inc, St Louis, Missouri, USA.

Spanoudakis, J., and Young, R. J. (1984). "Crack propagation in a glass particle-filled epoxy resin", *Journal of Materials Science*, 19, 473-486.

Sreekala, M. S., and Thomas, S. (2003). "Effect of fibre surface modification on water-sorption characteristics of oil palm fibres", *Composites Science and Technology*, 63(6), 861-869.

Stark, N. M., and Matuana L. M. (2004). "Surface chemistry changes of weathered HDPE/wood-flour composites studied by XPS and FTIR spectroscopy", *Polymer Degradation and Stability*, 86(1), 1-9.

Stark N. M., Matuana L. M., Clemons C. M. (2004). "Effect of processing method on surface and weathering characteristics of wood-flour/HDPE composites", Journal of Applied Polymer Science, 93, 1021-1030.

Stark, N. M., and Matuana L. M. (2006). “Influence of photostabilizers on wood flour-HDPE composites exposed to xenon-arc radiation with and without water spray”, *Polymer Degradation and Stability*, 91(12), 3048-3056.

Sun, R. C., Fang, J. M., Rowlands, P., and Bolton, J. (1998). “Physicochemical and thermal characterization of wheat straw hemicelluloses and cellulose”, *Journal of Agricultural and Food Chemistry*, 46(7), 2804-2809.

Sun, R., Lawther, J. M., and Banks, W. B. (1995). “Influence of alkaline pre-treatments on the cell wall components of wheat straw”, *Industrial Crops and Products*, 4(2), 127-145.

Suradi, S. S., Yunus, R. M., and Beg, M. D. H. (2010). “Oil palm bio-fiber-reinforced polypropylene composites: effects of alkali fiber treatment and coupling agents”, *Journal of Composite Materials*, 45(18), 1853–1861.

Valadez-Gonzalez, A., Cervantes-Uc, J. M., Olayo, R., and Herrera-Franco, P. J. (1999). “Effect of fiber surface treatment on the fiber-matrix bond strength of natural fiber reinforced composites”, *Composites Part B – Eng*, 30, 309-20.

Van Soest, P. J. (1963). “Use of detergents in the analysis of fibrous feeds. I. Preparation of fiber residues of low nitrogen content”, *Association of Official Analytical Chemists*, 46, 825–829.

Van Soest, P. J., and Wine, R. H. (1968). “Determination of lignin and cellulose in acid detergent fiber with permanganate”. *Association of Official Analytical Chemists*, 51, 780–785.

Varma, D. S., Varma, M., and Varma, I. K. (1984). "Part I: Effect of physical and chemical treatments on Properties", Textile Research Journal, 54(12), 827-832.

Vyazovkin S. V., and Lesnikovich A. I. (1990). "Reaction Kinetics from Thermal Analysis", *Thermochimica Acta*, 165:273–80.

Vyazovkin S. V., and Wight, C.A. (1997). "Kinetics in Solids". *Annual Review of Physical Chemistry*, 48. 125–49.

Wang, B., and Sain, M. (2007). "Dispersion of soybean stock-based nanofiber in a plastic matrix". *Polymer International*, 56(4), 538-546.

Wang, H.M., Postle, R., Kessler, R.W., and Kessler, W. (2003). "Removing pectin and lignin during chemical processing of hemp for textile applications". *Textile Research Journal*, 73(8), 664-669.

Wesson, S. P., Jen, J. S., and Nishioka, G. M. (1992). "Acid-base characteristics of silane-treated E glass fiber surfaces", Journal of Adhesion Science Technology, 6(1), 151-169.

White, R. H., and Dietenberger, M. A. (2001). "Wood Products: Thermal Degradation and Fire," Encyclopedia of materials: science and technology, Elsevier Science Ltd: 9712-9716

White, N. M., and Ansell, M. P. (1983). "Straw reinforced polyester composites" *Journal of Material Science,* 18(5), 1549-1556.

Wikipedia, 2009. "Grain Market Report". Retrieved in May 2011 from: http://en.wikipedia.org/wiki/International_wheat_production_statistics

Wong A. (2004). "Politics and economics of using wheat straw for the co-manufacture of paper and energy". Retrieved in 2008 from www.agripulp.com/econ.html#dakota.

Woodhams, R. T., Thomas, G., and Rodgers, D. K. (1984). "Wood fibers as reinforcing fillers for polyoefins", *Polymer Engineering & Science*, 24(15), 1166–1171.

Wu, S., Wang, F., Ma, C. M., Chang, W., Kuo, C., Kuan, H. and Chen, W. (2001). "Mechanical, thermal and morphological properties of glass fiber and carbon fiber reinforced polyamide-6 and polyamide-6/clay nanocomposites", *Materials Letters*, 49(6), 327-333.

Xanthos, M. (2010). "Functional Fillers for Plastics". (2nd ed.) Wiley-Vhc Verlag GmbH & Co.

Xiao, K. B., Sun, X. F., and Sun, R. C. (2001). "Chemical, structural and thermal characterization of alkali soluble lignins and hemicelluloses and cellulose from maize stems, rye straw and rice straw," *Polymer Degradation and Stability*, 74(2), 307-319.

Xiao-feng, S., Bin, X., and Baird, M.S. (2006). "Modification and characterization of fibers of three sandy willow shrub species", *Forestry Studies in China*, 8(3), 16-21.

Xie, Y., Hill C. A. S., Xiao, Z., Militz, H., and Mai, C. (2010). "Silane coupling agents used for natural fiber/polymer composites: A review", *Composites: Part A: Applied Science and Manufacturing,* 41(7), 806-819.

Xu, X., (2008). “Cellulose fiber reinforced nylon 6 or nylon 66 composites”, PhD Thesis, Georgia Institute of Technology.

Yang[1], H., Yan, R., Chen, H., Lee, D. H., and Zheng, C. (2007). “Characteristics of hemicellulose, cellulose and lignin pyrolysis”, *Fuel*, 86(12-13), 1781-1788.

Yang[2] H. S., Wolcott M. P., Kim H. S., Kim S., and Kim H.J. (2007). “Effect of different compatibilizing agents on the mechanical properties of lignocellulosic material filled polyethylene bio-composites”, *Composite Structures*, 79(3), 369–375.

Zhang, D., Dougal, S. M., and Yeganeh, M. S. (2000). “Effects of UV Irradiation and Plasma Treatment on a Polystyrene Surface Studied by IR−Visible Sum Frequency Generation Spectroscopy”, *Langmuir*, 16, 4528-4532.

Zhang, L. H., Li, D., Wang, L. J., Wang, T. P., Zhang, L., Chen, X. D., and Mao, Z. H. (2008). “Effect of steam explosion on biodegradation of lignin in wheat straw”, *Bioresource Technology*, 99(17), 8512-8515.

Appendix

Chapter 3 – Understanding the Thermal Degradation and Chemical Kinetics of Wheat Straw Fiber

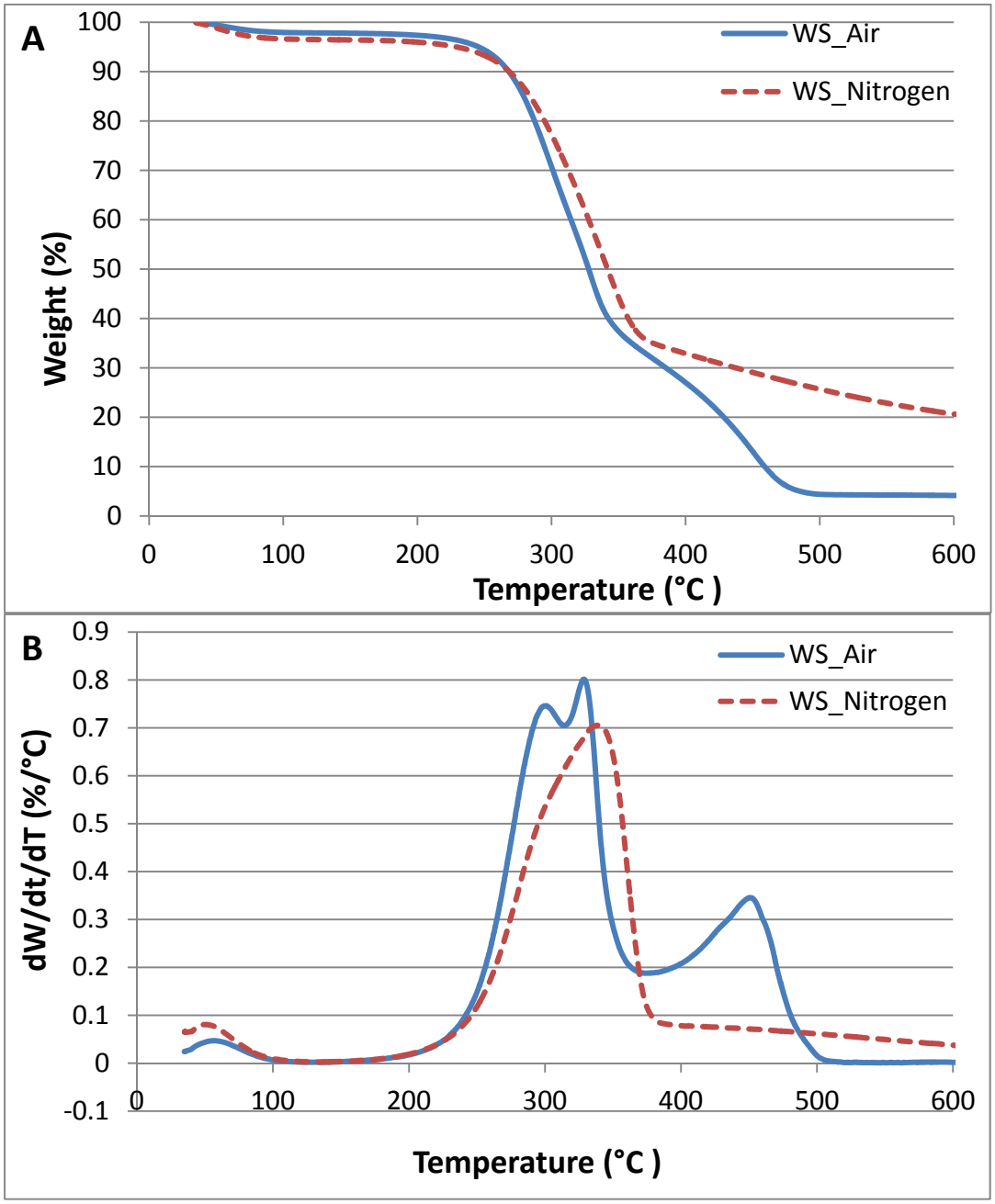

Figure 147: Comparison between TGA curves (A) and DTGA curves (B) obtained under air and nitrogen atmospheres for Mid sample.

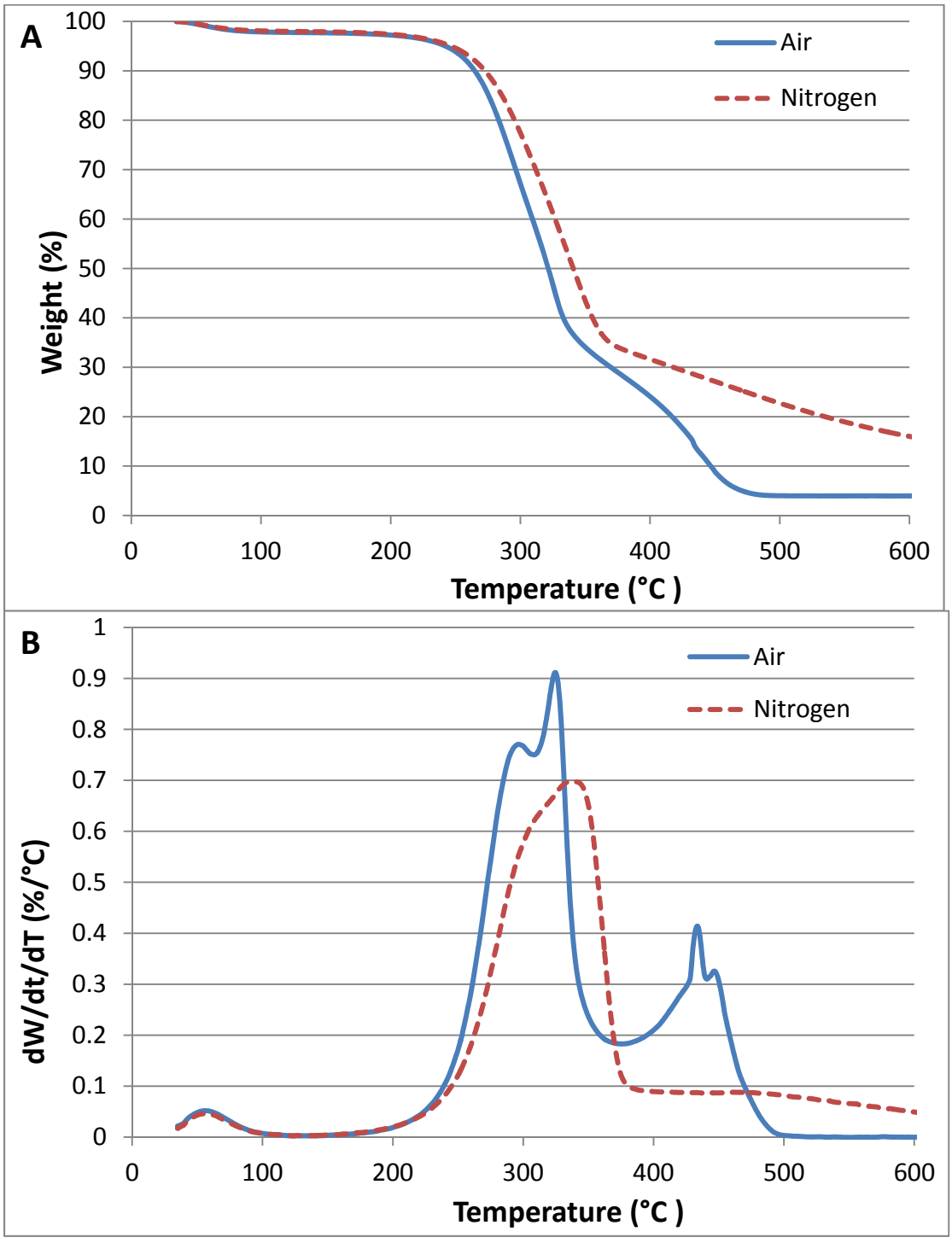

Figure 148: Comparison between TGA curves (A) and DTGA curves (B) obtained under air and nitrogen atmospheres for Large sample

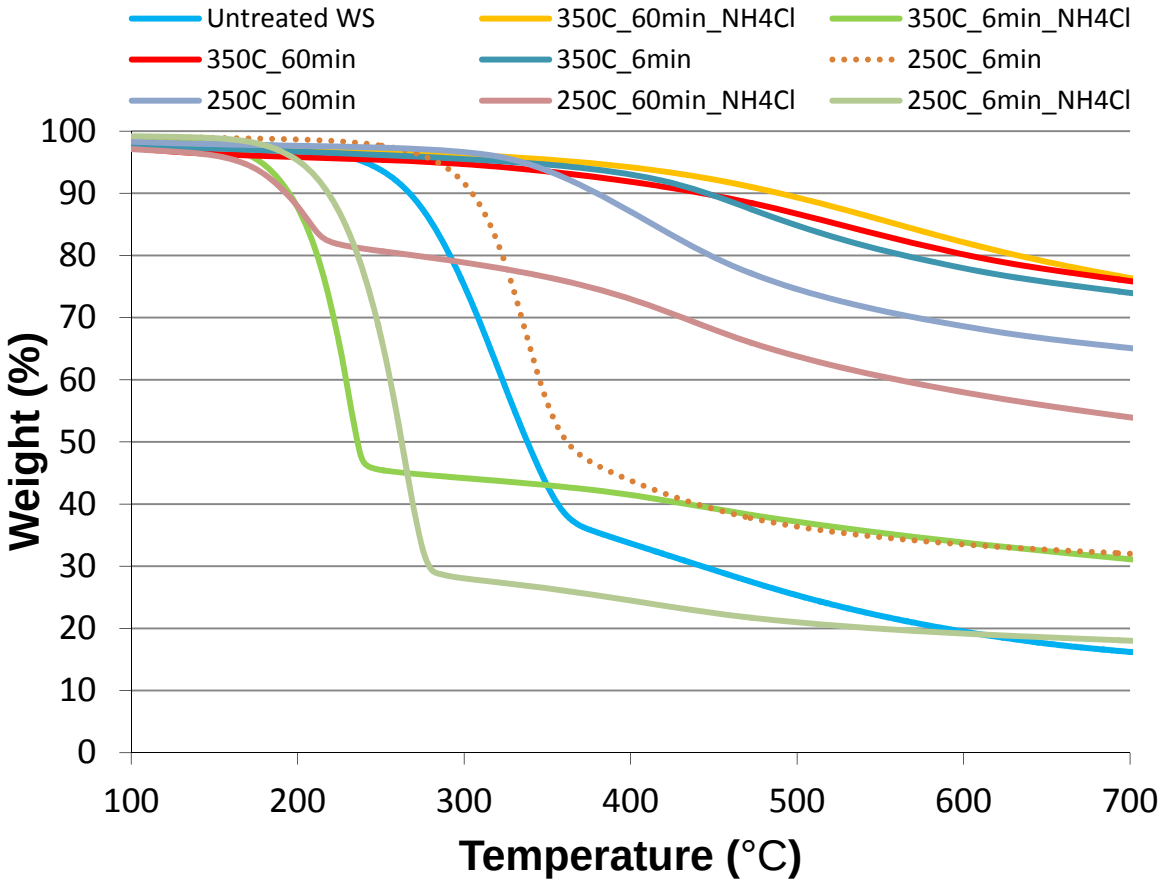

Figure 149: TGA curves used to obtain the $T_{2\%}$ and weight loss at 250 and 275 °C for the samples in Experiment #01.

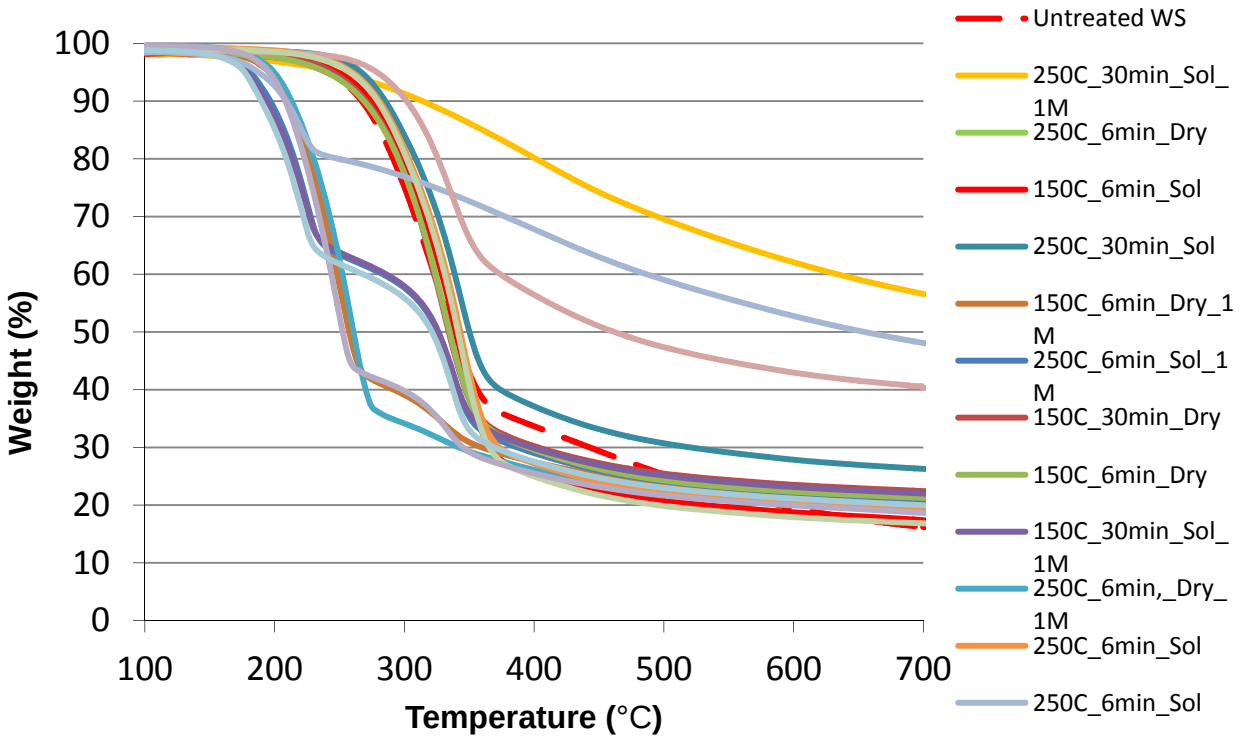

Figure 150: TGA curves used to obtain the $T_{2\%}$ and weight loss at 250 and 275 °C for the samples in Experiment #02.

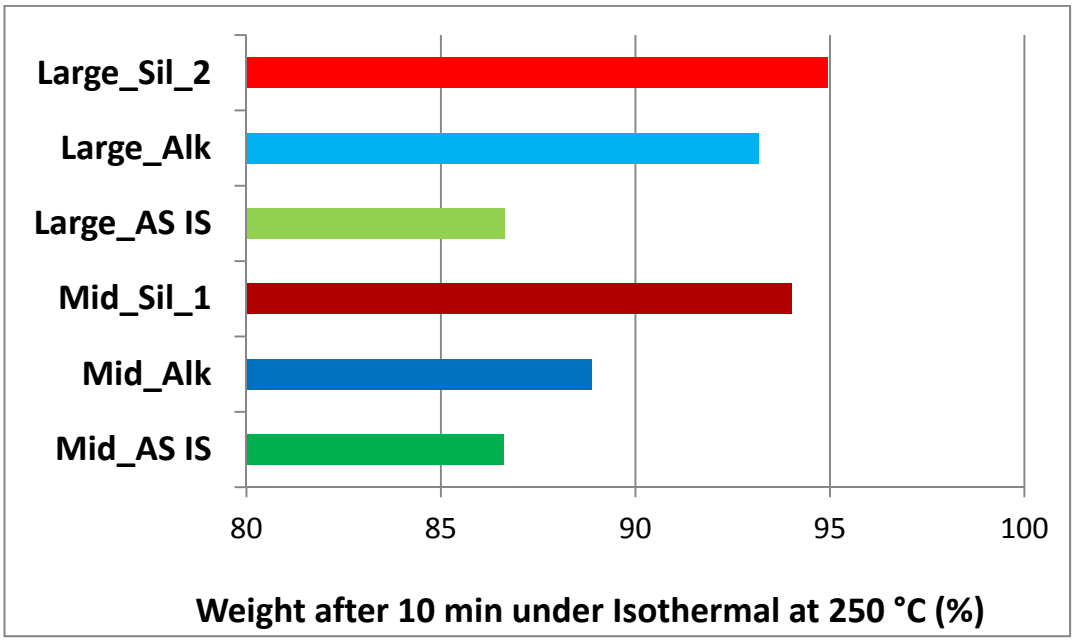

Figure 151: Weight percentage left after 10 minutes under isothermal at 250 °C and nitrogen atmosphere for "AS IS", "Alkali" and "Silane" "Mid" and "Large" samples.

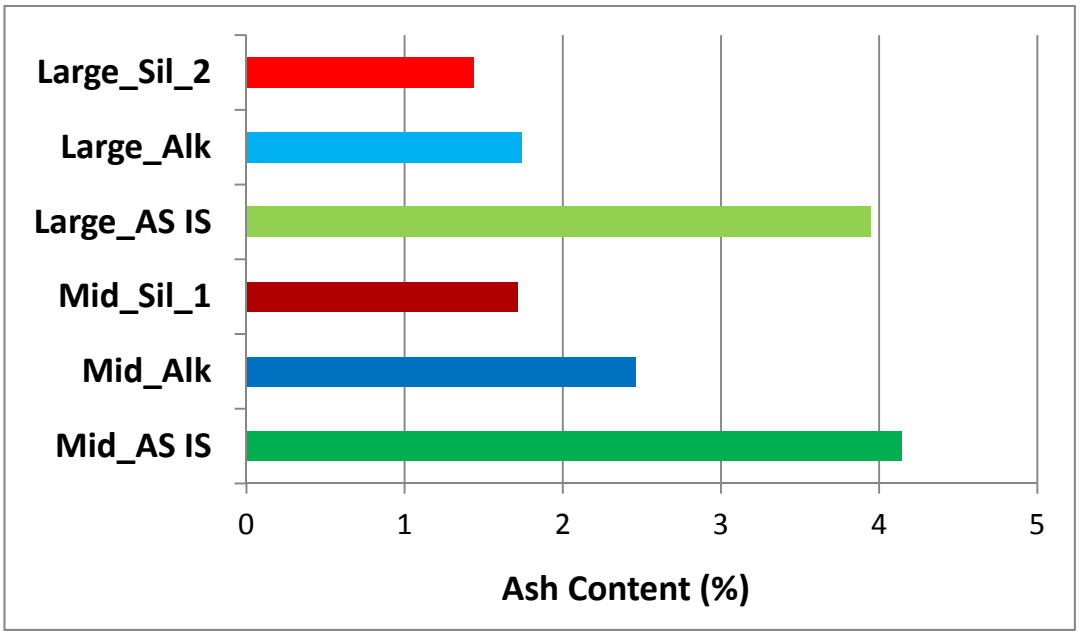

Figure 152: Ash content percentage (mass left at 600 °C under air atmosphere) for WS samples.